Investigating Calcium Channel Blockers as Antimalarials

May Rajab

School of Environment and Life Sciences
University of Salford
Salford, UK

Submitted in Partial Fulfilment of the Requirements for the Degree of Doctor of Philosophy, March 2018

Declaration

I certify that this thesis, submitted to the University of Salford in partial fulfilment of the requirements for a Degree of Doctor of Philosophy, is a presentation of my own research work and has been funded by the University of Salford's Pathway to Excellence studentship. The content of this thesis has not been submitted for any degree or other purpose at this or any other university.

Although the author has carried out most experiments and analysis of this research, some parts of this thesis were carried out in collaboration with other colleagues. Wherever contributions of others are involved, every effort is made to indicate this clearly with due reference to the literature and acknowledgment of collaborative research and discussions. Dr Steve Rossington carried out the synthesis of some of the fendiline analogues which have been clearly stated within the thesis.

Table of contents

List of figures

List of tables

Acknowledgments

Many people have made this research possible and I would like to take the time to thank everyone. I would like to acknowledge the University of Salford's Pathway to Excellence studentship that funded this research and the PGR Fund to attend conferences. Initial thanks go to my supervisor Niroshini. Without you this research simply would not have been possible. Thank you for choosing me to do this project and for your guidance along the way.

Jim, where do I begin. I could dedicate the entire acknowledgements section to you for all your support, help, encouragement and, most importantly, your belief in me. The past nine years have been a rollercoaster ride; from telling you I was leaving to do a degree in Physics in 2009 to standing in your office complaining about how much I hated the forever-breaking flow cytometer a few months ago. Your patience and diplomacy are astounding. You never doubted me, and for that I can't thank you enough. I've said this before and I truly mean it, I will forever be in your debt.

Steve, without you this research surely would not have happened. I owe a lot of my lab skills to you. You're a generous man with a good heart, even though most people think you are a phantom!

Gemma Lace, you're an absolute star! You have done right by me many times over the years. I won't forget your words of advice or your encouraging comments, nor will I forget the little diagram you drew showing me how far I had come in my academic life. That really did put it all into perspective.

A big thank you to Basmah Allarakia, Maria Morlan-Mairal and Matthew Jones for the advice and suggestions with the calcium experiments.

The technicians; Mark, Sally, Tony, Cath, Manisha, Marian, Andrew, Nicki, Andy and Abby, if it weren't for you I'd still be wondering around Cockcroft looking for random bits of glassware, machinery, reagents and my sanity! You're an amazing team. Your hard work, compassion and endless supply of biscuits never went unnoticed. Thank you for always telling me I could do it!

Manisha you will always be a dear friend. You once said that you would carry me through to the end of my PhD if that's what it took. Little did you know it was that comment that got me through a very dark time.

To my lab colleagues, Basmah, Muna, Priyanka and Matthew, it's been a journey. We've had our ups and downs. At times it felt like more downs than ups, but we got through it and that's the main thing. I wish you every success in your future.

To my fellow postgraduate friends (Jess Hall, Dr Laura Brettell, Dr Maria Morlan-Mairal, Dr Paz-Aranega Bou, Dr Kamila Schmidt, Dr Ana Cubas Atienzar and Natalie Barnes) thanks for listening to my never-ending rants, for your advice (in more areas than just science!) and for all the laughter. Most importantly though thank you for the lovely adventures up Ben Nevis, Scafell, Snowdon, Mam Tor, our walk along the Tolkein trail and the amazing holidays in Barcelona and Benicassim. It was these times that made the PhD journey worthwhile.

To my Uncle Peter, thank you for being my professional proof-reader. My placement in Uganda would not have been possible if it weren't for you and Aunty Marti. An adventure that has been a turning point in my life.

Hazel and Graham, thank you for giving me a home, for providing me with an endless supply of teacakes and for putting up with a very moody me while writing my thesis. My gratitude, respect and love for you is endless.

Dave, my partner in crime and my confidant. I admire the dedication and perfection you give to any project you have, even though that comes with a high level of stubbornness. I should really learn some lessons from you. You have stood by me day in and day out, through thick and thin and never once gave up faith or belief in me. I love you dearly and totally understand if you never want to hear the words fendiline, calcium and flow cytometry again!

Last but not least, my family. I am who I am today because of you. Grandad, we love you very much even though we are constantly nagging you. Hanni, thanks for being the best brother I could have wished for, in spite of all the tormenting. Dad, my inquisitiveness and love for science no doubt came from you. For that and for so many other things I will always be grateful. Mum, if I become half the woman you are in strength and selflessness then I have succeeded in life. I dedicate this thesis to you.

Abbreviations

2-APB	2-aminoethyl diphenylborinate
ACT	Artemisinin combination therapy
AM	Acetoxymethyl
ART	Artemether
ATQ	Atovaquone
BAPTA	1,2-Bis(2-aminophenoxy)ethane-tetraacetic acid
BIPY	2,2'-bipyridyl
CaMK	Calmodulin kinase
CCB	Calcium channel blocker
CDPK	Calcium-dependant protein kinase
CI	Combination index
CM	Complete media
CQ	Chloroquine
DDE	Delayed-death effect
DDT	Dichlorodiphenyltrichloroethane
DHFR	Dihydrofolate reductase
DHPS	Dihydropteroate synthase
DIL	Diltiazem
DMSO	Dimethyl sulfoxide
dTMP	Deoxythymidine monophosphate
DV	Digestive vacuole
DOX	Doxycycline
EC_{50}	Half maximal effective concentration

ED	Effective dose
EDTA	Ethylenediamine tetraacetic acid
EGTA	Ethylene glycol tetraacetic acid
ELISA	Enzyme-linked immunosorbent assay
ER	Endoplasmic reticulum
FDA	Food and drug administration (USA)
FHCl	Fendiline hydrochloride
FIC	Fractional inhibitory concentration
FSC	Forward scatter
Fu	Fraction unaffected
G6PD	Glucose-6-phosphate dehydrogenase
GSK	GlaxoSmithKline
hERG	human ether-à-gogo-related gene
IC_{50}	Half maximal inhibitory concentration
ICAM-1	Intercellular adhesion molecule-1
IP_3	Inositol 1,4,5-trisphosphate
IP_3R	Inositol-1,4,5-trisphosphate receptor
IPT	Intermittent preventative treatment
IRS	Indoor residual spraying
LLINs	Long-lasting insecticidal nets
LTCCs	L-type calcium channels
MDA	Mass drug administration
mdr1	Mammalian multi-drug resistant gene
MEF	Mefloquine
MTT	Methylthiazol tetrazolium assay
NIC	Nicardipine

NMDA	*N*-methyl-*D*-aspartate
NMDAR	*N*-methyl-*D*-aspartate receptor
*p*ABA	*para*-aminobenzoic acid
PBS	Phosphate-buffered saline
PCT	Parasite clearance time
PfCHA	*P. falciparum* Ca^{2+}/H^{+} antiporter
PfCRT	*P. falciparum* chloroquine resistance transporter
PfEMP1	*P. falciparum* erythrocyte membrane protein 1
PfHRP	*P. falciparum* histidine-rich protein
PfMDR1	*P. falciparum* multi-drug resistant protein-1
PfMRP	*P. falciparum* multidrug resistance-associated protein
PG	Proguanil
PMCA	Plasma membrane Ca^{2+} ATPase
PRR	Parasite reduction ratio
PV	Parasitophorous vacuole
PVM	Parasitophorous vacuole membrane
RBCs	Red blood cells
RFU	Relative fluorescence units
rt	Room temperature
RTCCs	R-type calcium channels
RYR	Ryanodine receptor
SEC	Single exposure chemoprotection
SERCA	Sarco/endoplasmic reticulum Ca^{2+} ATPase pumps
SG	SYBR Green I
SOCE	Store-operated calcium entry
SMC	Seasonal malaria chemoprevention

SR	Sarcoplasmic reticulum
SSC	Side scatter
TPC	Two-pore channels
TRP	Transient receptor potential channels
VP	Verapamil
WHO	World Health Organisation
WM	Wash media

Abstract

The rise in resistance to current antimalarial drugs has led researchers to consider drug repositioning as a quicker alternative for drug development and discovery. Preliminary drug repositioning screens carried out at the University of Salford identified calcium channel blockers (CCBs) as potential antimalarial agents. A growing body of evidence has demonstrated the importance of calcium within the *Plasmodium* life cycle. Studies have shown CCBs and calmodulin inhibitors to exhibit antimalarial activity. The research carried out in this project aims to evaluate the antimalarial efficacy, safety profile, mode of action and drug interactivity of the commercially available CCB and calmodulin inhibitor fendiline, and a range of its synthetic analogues.

Initial screening of fendiline alone and in combination with commercially available drugs was carried out using a SYBR Green (SG) plate reader assay. Both CalcuSyn-based combination studies and a chloroquine potentiation assay were carried out. This was succeeded by the synthesis of fendiline analogues, which were carried out via a two-step synthetic route starting with a palladium catalysed coupling reaction followed by a reductive amination. Both the antimalarial activity and the cytotoxicity of the synthesised compounds were evaluated which led to a lead candidate to be selected (the hydroxy fendiline analogue, **4c**). Further investigations into the activity, stage specificity and the effect compound **4c** has on the hERG channel was carried out to develop a preliminary understanding of the mode of action of the compound. Finally, optimisation experiments to develop a flow cytometry-based assay that would detect fluctuations in calcium levels within infected red blood cells (RBCs) were performed.

The conducted research showed the commercially available fendiline to have activity towards the multi-drug resistant *Plasmodium falciparum* K1 strain within the micromolar range (IC_{50} = 3.74 ± 0.64 μM). CalcuSyn-based combinations studies showed fendiline to have either an antagonistic or additive effect with currently available drugs. Interestingly, fendiline was found to reverse chloroquine resistance, similar to verapamil, however at half the

concentration required for verapamil. Furthermore, the range of synthesised fendiline analogues identified several compounds that exhibited more activity towards the *P. falciparum* infected RBCs. The 2' hydroxyl fendiline analogue (**4c**) was 5.6-fold more potent than fendiline itself (IC_{50} = 0.67 ± 0.21 µM) on the *P. falciparum* K1 strain, with an almost one-hundred-fold difference between antimalarial activity and cytotoxicity. The compound was found to be slow acting that targets the schizont stages of the parasite blood stages. The hERG channel inhibition assay gave an IC_{50} of 4.03 ± 0.52 µM, which is within the range that most small compounds fall within (1-10 µM). Finally, the optimisation experiments showed the developed method was only sensitive to dramatic calcium changes within RBCs and not within the parasites themselves. Further work is required to improve the sensitivity of the assay.

In conclusion, the hydroxy fendiline compound provides an interesting candidate to investigate further as a combinatory partner with other antimalarials, and as a scaffold to synthesise other potentially more potent fendiline analogues.

Chapter 1
Introduction

1.1 Global impact of malaria

Malaria is a major infectious disease that has affected the human population for thousands of years (Hong, 2013). Despite efforts to treat and eradicate the disease it remains a major public health concern. According to the World Health Organisation (WHO), there was an average of 216 million malaria cases with an estimated 445,000 deaths in 2016, the majority of which were in sub-Saharan Africa. Approximately 70% of the deaths in that year occurred in children under the age of five (WHO, 2017c).

Despite ongoing efforts to treat the disease and control its spread, the situation remains problematic. According to Walker, Nadjm and Whitty (2018), in parts of Africa an average person can become infected with malaria four times a year, if not more. The WHO states that since 2010 there has been progress in reducing incidences of malaria worldwide (WHO, 2017c). Cases of malaria fell from 243 million in 2010 to 210 million in 2014. However, since then progress has stalled and, in fact, reversed somewhat in 2016, when the number of cases increased compared with the previous year (WHO, 2015, 2017c). The graphs in Figure 1.1 (A and B) show the number of malaria cases and deaths over a range of years between 2000 and 2015.

The effect of malaria is not solely limited to human health, mortality and morbidity, but also affects the economics, productivity, national growth and development of the areas worst hit by the disease, and frequently also the social aspects of life - an effect often overlooked (Jones and Williams, 2004; Ovadje and Nriagu, 2011; Hong, 2013).

The wide and unregulated use of effective drugs to treat infected people, as well as extensive use of insecticides to kill the mosquito vector, has led to one of the biggest problems faced with tackling this disease – resistance (Cobo, 2014). There are two types of resistance, the

first is the parasite's resistance to chemotherapy and the second is resistance of the mosquitoes to insecticide (Cobo, 2014).

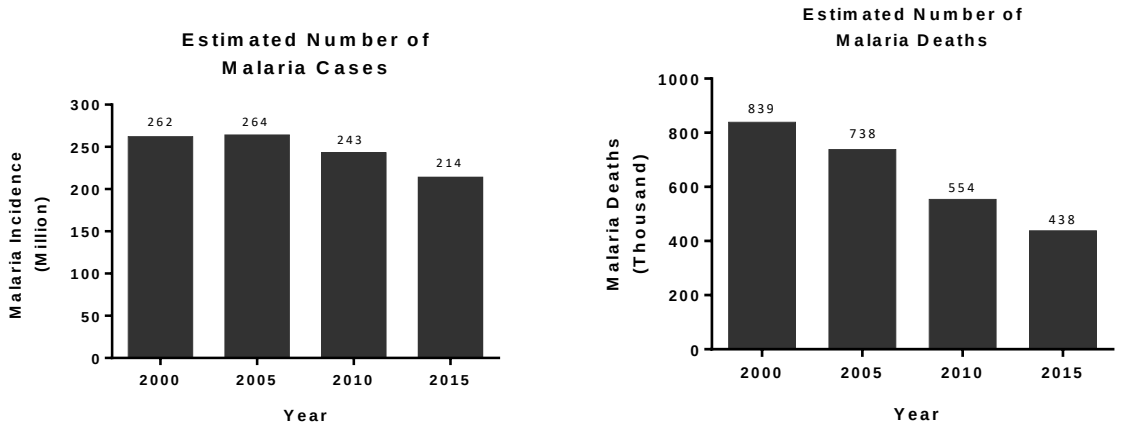

Figure 1.1 – Estimated number of malaria cases (A) and deaths (B) between 2000 and 2015. Source (WHO, 2015)

1.2 Biology of the parasite

Despite malaria being in existence for thousands of years, the causative *Plasmodia* protozoan was not identified until the 1880s (Aditya *et al.*, 2013). Amongst the 120 known species, *P. malariae, P. falciparum, P. ovale, P. vivax* and *P. knowlesi* are linked to human malaria. *P. malariae* and *P. knowlesi* are known to infect other animals as well as humans, whereas the other malaria causing parasites are believed to only infect humans (Aditya *et al.*, 2013; Singh and Daneshvar, 2013; Sutherland, 2016).

The parasite is transferred from one host to another *via* the *Anopheles* mosquito, which was found to be the vector of malaria in the 1890s (Urscher, Alisch and Deponte, 2011). Malaria occurs when an infected female mosquito injects the parasites into a human during a blood meal. The parasites at this stage are in the form of "sporozoites" and are found in the mosquito's salivary glands. Once inside the human the parasites travel to the liver and infect the hepatocytes, which develop into exoerythrocytic schizonts after an incubation period which can last anything from a few days, a few months or even years (Perlmann and Troye-Blomberg, 2002).

It is important to note that *P. vivax* and *P. ovale* are two strains that have the ability to hibernate in the liver for long periods of time in the form of hypnozoites before being reactivated and released into the bloodstream. It is this dormant stage in these species that cause relapses of the infection even after the initial blood stage infection is cleared (Perlmann and Troye-Blomberg, 2002; Sutherland, 2016).

Exoerythrocytic schizonts contain up to 30,000 merozoites which are released into the blood stream and invade red blood cells (RBCs) starting the erythrocytic cycle (Cobo, 2014; Leroy *et al.*, 2014). This is the asexual stage in the parasite's life cycle and the phase that results in the pathology associated with malaria (Leroy *et al.*, 2014). The parasites develop in the RBC through three main stages; ring, trophozoite and schizont. Initially the parasite digests haemoglobin present in the RBC during the ring stage; it cannot, however, digest the toxic heme part of haemoglobin and thus converts it to insoluble crystalline packages known as hemozoin. The build-up of hemozoin signifies the trophozoite stage (Grimberg, 2011). Finally, during the schizont stage the parasite begins DNA synthesis: it assembles and packages a copy of the genome into each merozoite and eventually the infected RBC ruptures and the cycle is repeated (Grimberg, 2011). A schematic of the life cycle is shown in Figure 1.2.

Within the RBCs the parasites can sometimes differentiate into sexually reproducing cells (gametocytes). If an *Anopheles* mosquito takes a blood meal when these cells are present the sexual stage of the parasite's life cycle begins (Marcus, 2009). Once inside the mosquito, the parasites are released from the RBC and travel to the midgut where fertilization occurs to form diploid zygotes. These then migrate to the intestine to undergo meisosis and form haploid cells (oocytes) (Wahlgren and Perlmann, 2003; Marcus, 2009). Up to ten oocytes can be carried by an infected mosquito that continue dividing and eventually travel to the mosquito's salivary glands in the form of sporozoites, which is where the cycle of human infection begins. It is important to note that thousands of sporozoites are released by each oocyte (Strickland and Hoffman, 1994).

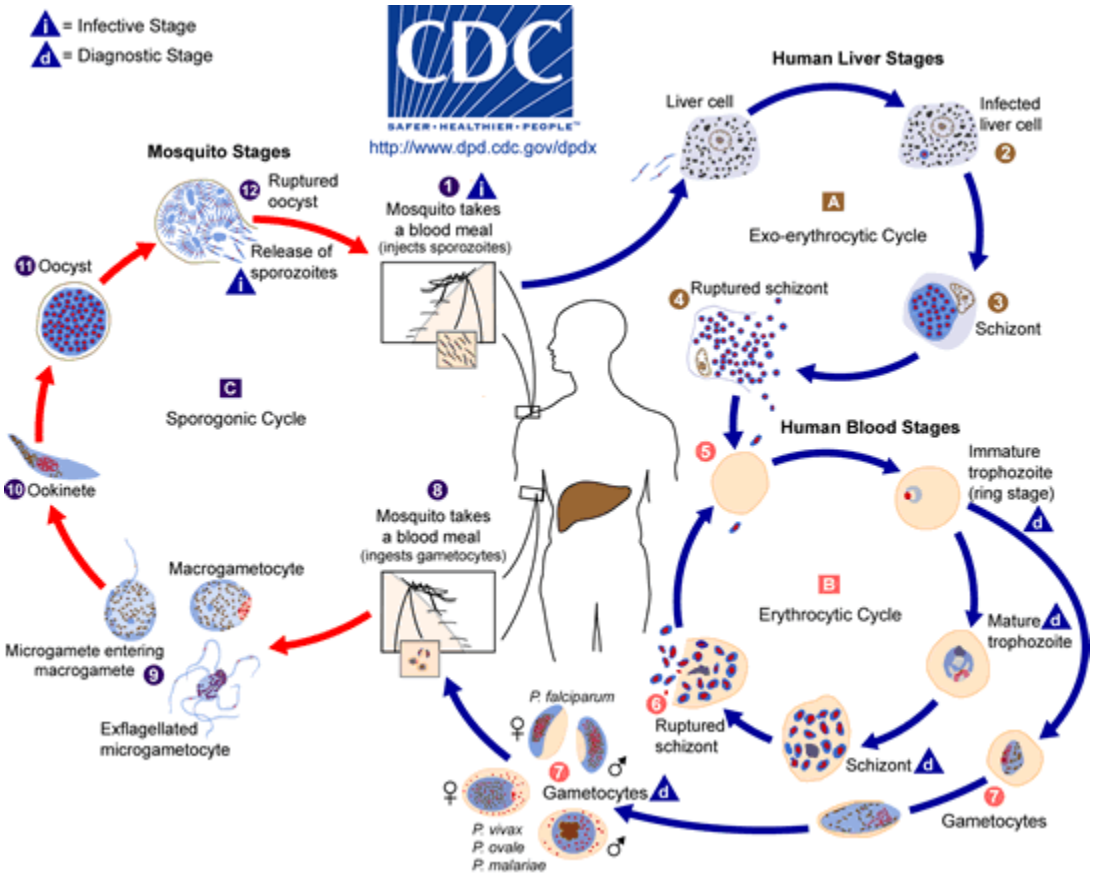

Figure 1.2 – A schematic showing the life cycle of the Plasmodium parasite.

Source: https://www.cdc.gov/malaria/about/biology/index.html

1.3 Clinical symptoms of malaria

Out of the malaria causing *Plasmodium* species, *P. falciparum* and *P. vivax* cause the most infections worldwide, with *P. falciparum* being the most deadly (Ovadje and Nriagu, 2011; Autino *et al.*, 2012). Clinical symptoms occur as a result of the asexual erythrocytic cycle of the parasite. Symptoms of uncomplicated malaria include general flu-like symptoms, encompassing headache, fever, vomiting, fatigue and dizziness. Whereas symptoms of severe malaria include high fever, respiratory failure, lactic acidosis, progressing anaemia, cerebral malaria and multiorgan dysfunction (Chen, Schlichtherle and Wahlgren, 2000; Trampuz *et al.*, 2003; Bartoloni and Zammarchi, 2012; Alister, Mustaffa and Pradeep, 2012; Eugene-Ezebilo and Ezebilo, 2014). Fatality often occurs due to severe anaemia or cerebral malaria (Autino *et al.*, 2012; Eugene-Ezebilo and Ezebilo, 2014).

Severe anaemia due to malaria is multifactorial and complex. Infected RBCs rupture for the release of schizonts therefore naturally reducing RBCs in circulation. Reduction of infected and non-infected RBCs by splenic removal or immune mediated lysis also contributes to anaemia. Other causes include reduced erythropoiesis, reduced erythropoietin, bone marrow suppression and inadequate reticulocyte production (Phillips and Pasvol, 1992; Chen, Schlichtherle and Wahlgren, 2000; Kai and Roberts, 2008; Haldar and Mohandas, 2009; Autino *et al.*, 2012; Alister, Mustaffa and Pradeep, 2012)

Mature parasitized RBCs can be removed from circulation and adhere to endothelial cells (cytoadhesion) within the microvasculature of organs, a process known as sequestration. They can adhere to the brain, lung, heart, kidney, liver and placenta (Autino *et al.,* 2012). It is thought sequestration helps infected RBCs avoid splenic removal. The *P. falciparum* erythrocyte membrane protein 1 (PfEMP1) and the *P. falciparum* histidine-rich protein (PfHRP) have long been attributed to the adhesion of infected RBCs to the host's blood vessels and tissues. Reports have suggested PfEMP1 interacts with human endothelial proteins CD36 and intercellular adhesion molecule-1 (ICAM-1) (Chen, Schlichtherle and Wahlgren, 2000; Autino *et al.*, 2012; Tuikue *et al.*, 2017).

Cytoadhesion along with rosetting, which is the adhesion of infected RBCs to non-infected RBCs, lead to vascular obstruction. These processes can result in local hypoxia, in addition to the localised release of parasite toxins to the area causing a focused inflammatory response which can lead to tissue damage (Chen, Schlichtherle and Wahlgren, 2000; Autino *et al.*, 2012; Alister, Mustaffa and Pradeep, 2012). Initially these effects were thought to be unique to *P. falciparum* infections but have since been extended to *P. vivax* and *P. knowlesi* infections (Carvalho *et al.*, 2010; Fatih *et al.*, 2012).

1.4 Malaria control and prevention

Many factors influence the development and spread of malaria, including the three main agents required for the disease to occur (humans, mosquitos and the parasites). Examples of other contributing factors include: climate, vector and human habitation, and most importantly for the purpose of this review – drugs.

An overview of the three main strategies to control the spread of malaria is shown in Figure 1.3.

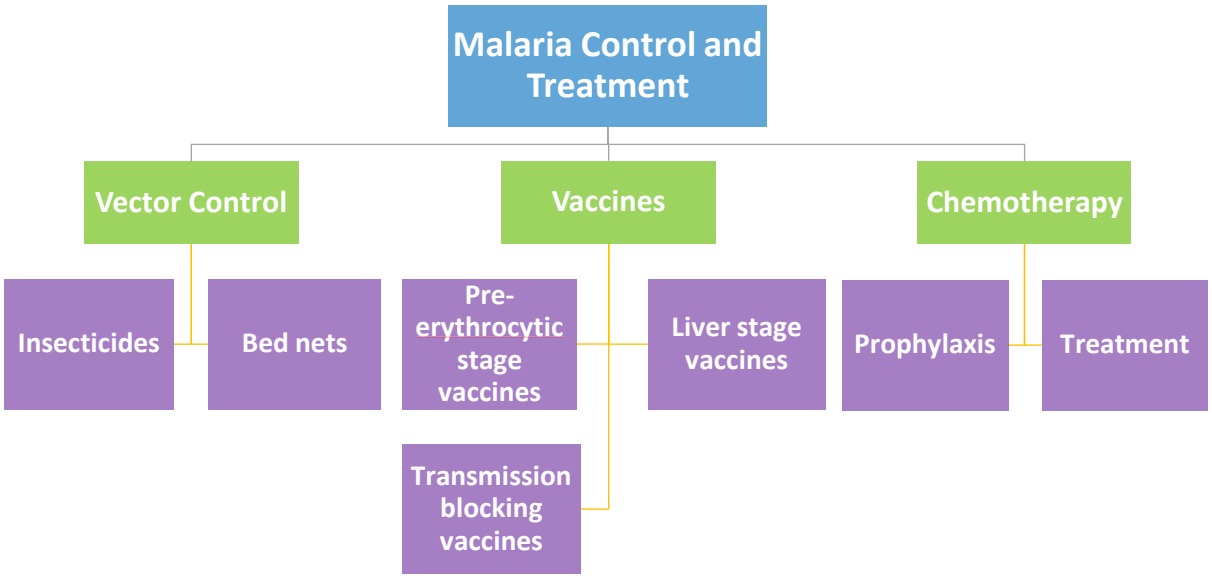

Figure 1.3 - An overview of the main areas of research that are ongoing to control the spread of malaria.

1.4.1 Vector control

The ability of malaria to spread is directly linked to the survival of the vector. Climate plays a major role in mosquito survival and although that cannot be influenced - environmental control measures, personal protective measures and use of effective insecticides are all methods that have been applied in order to constrain the mosquito and thus the spread of malaria (Ovadje and Nriagu, 2011).

A breakthrough in mosquito control occurred when the insecticidal properties of dichlorodiphenyltrichloroethane (DDT) were discovered, and the effects were large scale after WWII when the use of DDT was widely adopted (Oliva *et al.*, 2014). Despite the positive effect, DDT was banned in the 1970s in some countries due to its toxicity to the environment and was replaced by pyretheroids, but the emergence of mosquitos resistant to pyretheroids and the urgent need to reduce malaria incidences led to DDT being reintroduced specifically for Indoor Residual Spraying (IRS) (Van Dyk *et al.*, 2010; van den Berg *et al.*, 2012).

The use of IRS and long-lasting insecticidal nets (LLINs) (commonly known as bed nets) has helped greatly in reducing the incidences of malaria, particularly in some regions of Africa

(Pinder *et al.*, 2015). The spread of resistance to commonly used insecticides however has led researchers to explore alternative and novel vector control tools. Research is ongoing into developing novel insecticides and genetic modification of mosquitoes in addition to a variety of mosquito odour baits and traps (Takken and Knols, 2009; Barreaux *et al.*, 2017; Benelli and Beier, 2017). In the meantime, the WHO's core vector control recommendations are the use of insecticide-treated nets (namely LLINs) and IRS (WHO, 2017a).

1.4.2 Vaccines

The complexity of the disease and the complexity of immunity towards it creates a major hurdle in developing a vaccine for malaria (Drew and Beeson, 2015; Dunachie *et al.*, 2015). The WHO, along with Malaria Vaccines Funders Group, revised a strategic plan in 2013 under the title "The Malaria Vaccine Roadmap" with the aim of developing vaccine by 2015 that "has a protective efficacy of more than 50% against severe disease and death and lasts longer than a year" (WHO, 2014).

There are three broad types of vaccines in development for malaria; pre-erythrocytic vaccines to target the liver-stage sporozoites which would decrease, if not prevent, the amount of blood stage infection, blood stage vaccines which target infected blood cells by recognising antigens present on their surface, and transmission-blocking vaccines which would produce antibodies that target the sexual or mosquito stages of the parasite life cycle (Moorthy *et al.*, 2007; Ballou and Vekemans, 2017). The latter type of vaccine would reduce the spread of malaria, but would not prevent malaria developing in the vaccinated person (Ballou and Vekemans, 2017).

Despite the ongoing research, there is currently no registered malaria vaccine (Ballou and Vekemans, 2017). The only leading vaccine candidate, RTS,S/AS01 (Mosquirix^{TM}, GSK), has completed phase III clinical trials and will enter a Malaria Vaccine Implementation Program in three African countries (Malawi, Ghana and Kenya) this year (2018). This is a WHO-coordinated pilot program that will closely monitor and evaluate the safety and efficacy of the vaccine (WHO, 2017b). RTS,S/AS01 is based on a fragment of the *P. falciparum* circumsporozoite protein, which is coexpressed and fused with Hepatitis B virus surface antigen and combined with an adjuvant (RTS/S Clinical Trials Partnership, 2015). The

circumsporozoite protein is transmitted from the mosquito to the host during infection (Ballou and Vekemans, 2017).

Reports have stated that RTS,S/AS01 is a promising start for a malaria vaccine, although an ideal candidate would be a multi-antigen vaccine that would both protect individuals from infection and block transmission of multiple species and strains (Karunamoorthi, 2014; Drew and Beeson, 2015; Hemingway *et al.*, 2016; Ballou and Vekemans, 2017).

1.4.3 Prophylaxis

Malaria chemoprophylaxis is most commonly used for travellers to malaria endemic areas (Castelli *et al.*, 2010; Walker, Nadjm and Whitty, 2018). Ideally there would be a prophylaxis programme for people living in malaria endemic areas, but the reality is not so simple. The rise of resistant strains to cheap and readily available drugs (such as chloroquine) and the existence of parasite strains resistant to different drugs depending on the geographical location, are among the reasons why a single prophylactic drug is not available for malaria endemic countries (Fernando, Rodrigo and Rajapakse, 2011a).

The WHO does however recommend intermittent preventative treatment (IPT) for pregnant women and seasonal malaria chemoprevention (SMC) for children aged 3-59 months in malaria endemic countries. Sulfadoxine-pyrimethamine is the recommended drug combination for IPT, and sulfadoxine-pyrimethamine in addition to amodiaquine is recommended for SMC (WHO, 2017c). According to the WHO (2017c), as of 2015 no country had reported implementing an IPT strategy for pregnant women, whereas 15 million children in 12 countries were included in SMC programmes.

There have been previous occasions where antimalarial drugs have been given to whole populations (Mass Drug Administration, MDA) in attempts to eradicate malaria. For example, the Italian government in 1900 administered free quinine to be taken by the population as a prophylaxis and treatment. This did result in reduced malaria numbers and mortality, but transmission was not stopped and elimination of malaria did not occur until after WWII when strict DDT spraying, treatment and prophylaxis using quinine along with organised malaria diagnosis occurred (Alonso *et al.*, 2011).

Another example, albeit in a slightly different manner, was seen in the form of medicated salt. The method included the addition of antimalarial drugs, chloroquine or pyrimethamine, to salt used for cooking (Wernsdorfer, 1994; Greenwood, 2008; Alonso *et al.*, 2011). The method was carried out as part of a malaria eradication programme by the WHO. It was tested in Brazil between 1959 and 1961, and parts of Africa in the mid-1960s (da Silva and Hochman, 2011; Talisuna *et al.*, 2015). Although some reports stated reduction in the prevalence of malaria (Alonso *et al.*, 2011), the method was withdrawn and the overall results were inconclusive, if not somewhat negative (Greenwood, 2008; Talisuna *et al.*, 2015). The inability to control administration due to drug leakage and variation in dosage, as well as the rise of resistance, are among the reasons suggested for this method's failure (Alonso *et al.*, 2011; Talisuna *et al.*, 2015). In fact, an article published in 1988 suggested the rise of chloroquine resistant *P. falciparum* may largely be due to the medicated salt programme (Payne, 1988).

1.5 Malaria chemotherapy

Treating malaria by chemotherapy is one of the most important methods relied on to control the disease. For the purpose of this review, drugs used to treat malaria have been broadly grouped into four sections; quinoline derivatives, antifolates, artemisinins, and antibiotics and antiparasitic agents. A few examples of some of the major drugs used from each group are discussed in this section.

1.5.1 Quinoline derivatives

The use of natural products to treat malaria has been around for thousands of years. One of the oldest antimalarial drugs that has been used in treatment since the 17th century is quinine, a natural product derived from the bark of the *Cinchona* tree. Initially infusions of the bark of the tree were used in treatment, however in 1820 the active ingredient quinine was extracted from the *Cinchona* bark and soon after became the standardised malaria treatment (Saxena *et al.*, 2003; Achan *et al.*, 2011; Adebayo and Krettli, 2011).

According to a published review by Achan *et al.* (2011), alkaloids from the *Cinchona* tree that included quinine amongst others, were tested in one of the earliest recorded clinical trials between 1866 and 1868 and were all found to have antimalarial activity. The proportions of

quinine in the bark were higher than the other extracts, and thus it remained the main source of malaria treatment until the 1920s (Achan *et al.*, 2011).

It is thought the quinoline component of quinine is important for its antimalarial activity, thus several synthetic analogues of quinine have been made preserving this chemical moiety (Jones, Panda and Hall, 2015). Of the synthetic compounds, the most important was chloroquine which was synthesised in 1934 by Hans Andersag and his group at Bayer AG, though not used for malaria until 1947 (Thomé *et al.*, 2013; Mushtaque and Shahjahan, 2015). From then onwards chloroquine became the treatment of choice, in fact it was the only drug used for long periods of time in some areas in Africa due to it being cheap and effective with acceptable side effects (Saxena *et al.*, 2003; Thomé *et al.*, 2013; Mushtaque and Shahjahan, 2015).

Due to the great success of chloroquine at the time, along with the successful use of vector control using DDT, the eradication of malaria was highly anticipated (Mojab, 2012). Regrettably the expectation was diminished when resistance to both chloroquine and DDT developed in the 1960s, and by the 1980s strains of *P. falciparum* that were multi-drug resistant had appeared in several countries (Mojab, 2012).

Several theories have been proposed for the mechanism of action of quinoline-derived drugs. The most accepted of these is that it interferes with the digestion of haemoglobin in the digestive vacuole (DV). As previously described (section 1.2), the parasite cannot digest heme in haemoglobin and thus converts it to hemozoin crystals, which are toxic to the human host. It is thought that the basic drug diffuses into the acidic environment of the DV where it becomes protonated and is unable to diffuse out again. The drug prevents the conversion of heme to hemozoin by binding to heme resulting in a build-up of toxic heme which kills the parasite (Thomé *et al.*, 2013; Jones, Panda and Hall, 2015; Mushtaque and Shahjahan, 2015).

The accumulation of chloroquine in the DV is greatly reduced in chloroquine resistant strains; this is particularly seen in *P. falciparum* (Thomé *et al.*, 2013; Jones, Panda and Hall, 2015). The inability of the drug to be transported into the DV is believed to be the reason behind the resistance. There have been several theories offered to explain the reduced chloroquine levels, such as reduced influx, increased efflux and modified chloroquine binding site (Lakshmanan *et al.*, 2005). A single mutation found in the *P. falciparum* chloroquine resistance

transporter (*PfCRT*) gene is believed to be responsible for the resistance (Thomé *et al.*, 2013; Jones, Panda and Hall, 2015; Antony and Parija, 2016). A study carried out by Lakshmanan *et al.* (2005) showed that replacing the mutated *PfCRT* gene with the wild type gene resulted in the strains becoming chloroquine sensitive, thus supporting the theory. An important area of research involves synthesizing compounds that would reverse chloroquine resistance, with PfCRT protein being a potential target (Jones, Panda and Hall, 2015; Mishra *et al.*, 2017).

Reports of mutations found in the *P. falciparum* multidrug resistance protein 1 (*Pfmdr1*) gene and the *P. falciparum* multidrug resistance-associated protein (*Pfmrp*) gene have also been linked with resistance to chloroquine. However studies have suggested that mutations in these genes alone are not enough to cause the resistance (Djimde *et al.*, 2001; Mu *et al.*, 2003; Duraisingh and Cowman, 2005; Raj *et al.*, 2009; Antony and Parija, 2016).

A number of modifications have been made to the quinine skeleton which includes substituting the hydroxyl group, vinyl group, the quinoline and quinuclidine rings (Jones, Panda and Hall, 2015). Some of the modified compounds either replaced chloroquine or are given as second-line drugs, examples of which are amodiaquine, mefloquine, primaquine, ferroquine and halofantrine (Figure 1.4 shows the chemical structures of some of the analogues) (Duraisingh and Cowman, 2005; van Schalkwyk and Egan, 2006), but cross resistance to some of these drugs has developed (Duraisingh and Cowman, 2005).

The 8-aminoquinoline, primaquine (Figure 1.4), should be mentioned due to it being the only drug capable of clearing hypnozoites in early *P. vivax* and *P. ovale*. The drug however does have the adverse side effect of haemolytic anaemia in patients with glucose-6-phosphate dehydrogenase deficiency (G6PD). Screening patients before using the drug is therefore necessary and its use is prohibited for pregnant women and children (Ramos Junior *et al.*, 2010; Fernando, Rodrigo and Rajapakse, 2011b; Myint *et al.*, 2011; Andrews, Fisher and Skinner-Adams, 2014; Ashley, Recht and White, 2014). Research into developing primaquine analogues with reduced toxicity is ongoing, with the only prominent candidate to date being tafenoquine, which is cited to be less toxic than primaquine but should also not be administered to pregnant women (Zhu *et al.*, 2007; Mishra *et al.*, 2017). Another analogue, known as elubaquine or CDRI 80/53, has completed Phase II/III clinical trials, but has only been approved for marketing in India (Krudsood *et al.*, 2006; Mishra *et al.*, 2017).

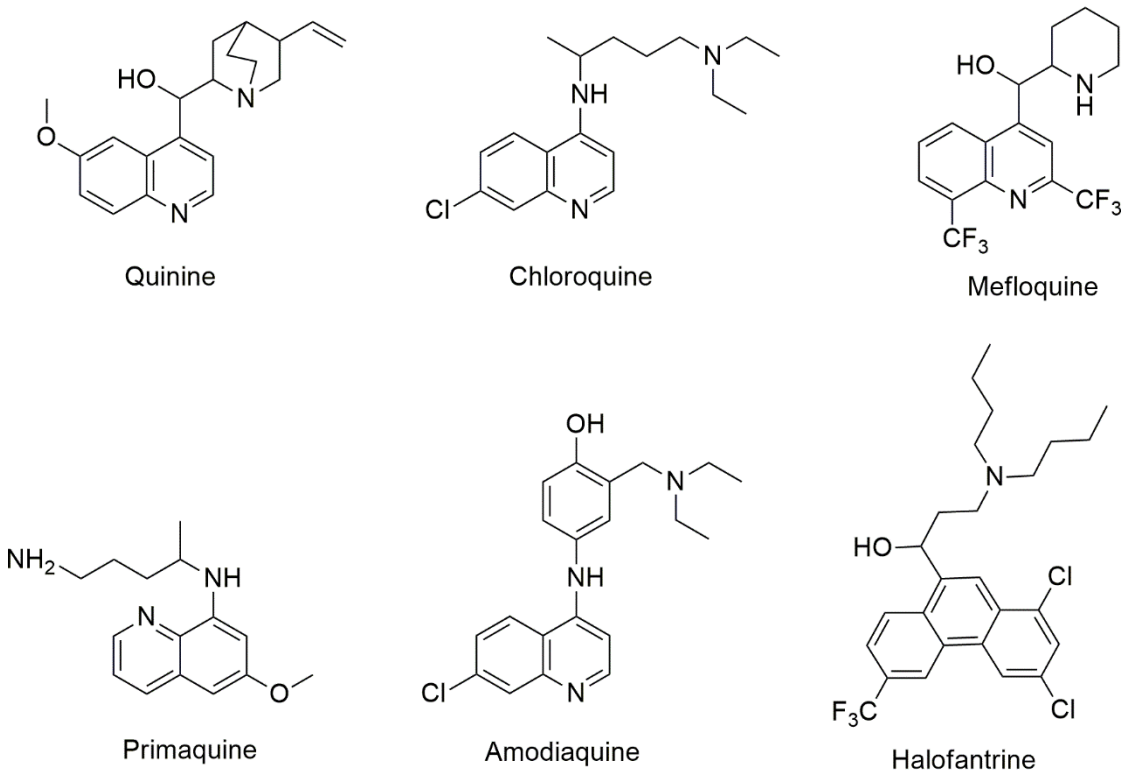

Figure 1.4 - Chemical structures of quinine and some of its analogues.

1.5.2 Antifolates

For the last 70 years, antifolates have been used to prevent cell proliferation in cancer, bacterial and parasitic infections such as malaria (Said, Jeffes and Weinstein, 1997; Salcedo-Sora and Ward, 2013; Kuhlmann and Fleckenstein, 2017). The term folate encompasses several folate derivatives which include, but are not limited to, folic acid, dihydrofolate and tetrahydrofolate (Nzila *et al.*, 2005).

Folic acid (vitamin B9) is essential in the folate pathway. In humans folic acid is obtained through diet, but organisms such as bacteria and parasites have the ability to synthesise it themselves (Litwack, 2008). Furthermore, folate derivatives are involved in providing one carbon units needed for the synthesis of purines, thymidylate and some amino acids (Nelson and Cox, 2008).

Both the conversion of the vitamins and the inhibition of synthesis are an attractive pathway for drug development (Nzila, 2006a). The two folate enzymes targeted by antimalarial drugs are dihydropteroate synthase (DHPS) and dihydrofolate reductase (DHFR). Agents that act as

DHPS inhibitors and DHFR inhibitors are often given together in combination. Figure 1.5 shows a simple schematic of the folate pathways, highlighting both enzymes.

In brief, DHPS is an enzyme involved in synthesising dihydropteroate - a precursor to dihydrofolate. Inhibiting DHPS activity ultimately results in reduced amounts of dihydrofolate, the substrate of DHFR. The decrease in substrate allows the activity of the DHFR inhibitors to increase, therefore blocking the pathway at two points results in a synergistic combination (Yuthavong, 2002; Gregson and Plowe, 2005; Nzila, 2006a).

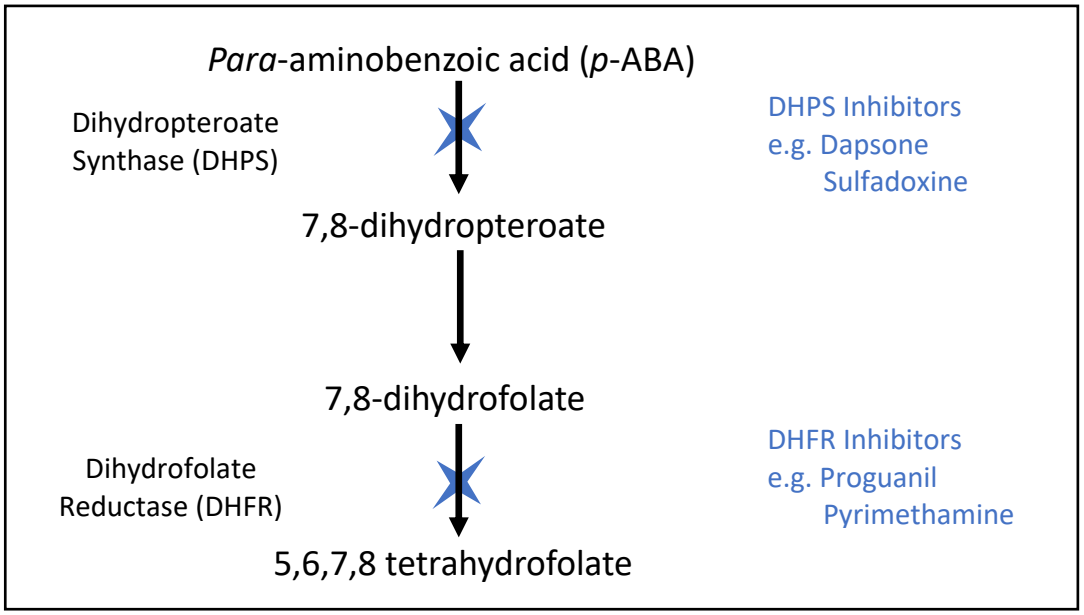

Figure 1.5 - A brief schematic of the folate pathway, highlighting the sites of action of the anti-folate drugs.

DHFR Inhibitors

Interest in agents that targeted this pathway occurred during WWII when the supply of quinine was reduced and research into synthetic antimalarials was becoming necessary (Gregson and Plowe, 2005). Around the same time cancer research showed that folic acid played a major role in the proliferation of leukaemia, and agents that block the folate pathway could reduce the spread of cancer (Nzila, 2006b; Müller and Hyde, 2013). The success of antifolates in cancer treatment led to the development of the prodrug proguanil in 1945, which was the first reported antifolate (DHFR Inhibitor) used for malaria (Nzila, 2006b).

The effectiveness of proguanil led to the development of analogues such as chlorproguanil. It also led to interest being taken in the 2,4-diaminopyrimidine family that identified pyrimethamine – which was according to (Nzila, 2006b) "the most widely used antifolate antimalarial agent". A diagram showing the three mentioned drugs can be seen in Figure 1.6. It is believed that the potency of these agents is in the chlorine(s) on the phenyl ring along with the additional bond between the phenyl and the diaminopyrimidine ring – which can be seen in the active form of proguanil and chlorproguanil (Nzila, 2006b).

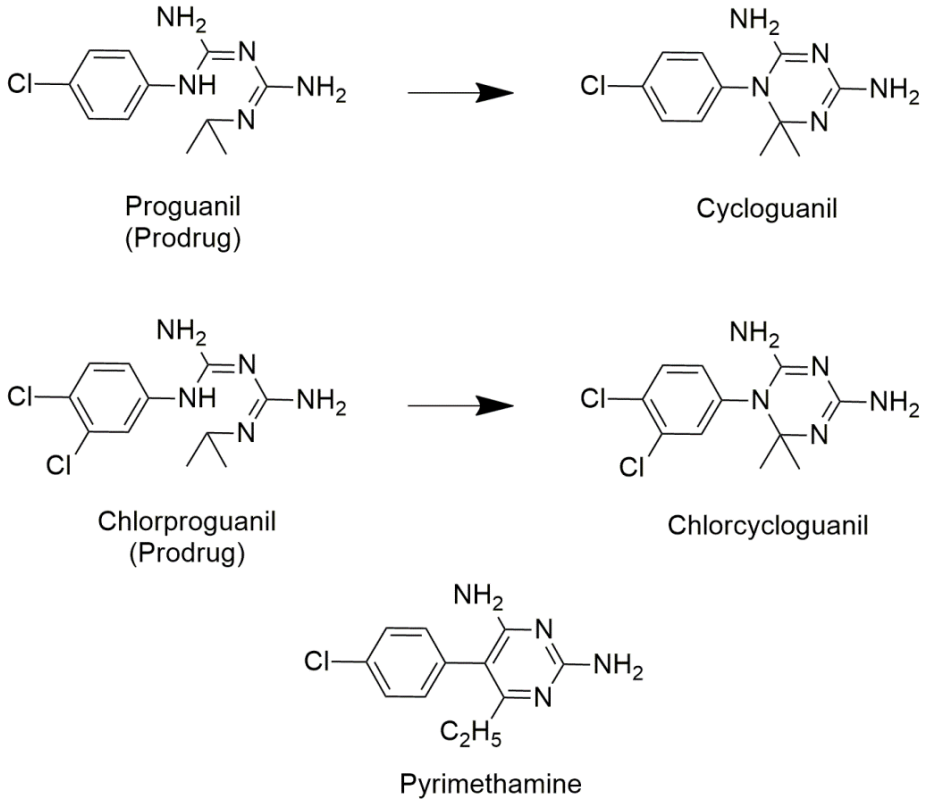

Figure 1.6 - Chemical structures of pyrimethamine and the two prodrugs proguanil and chlorproguanil along with their active forms.

As with other antimalarial agents, resistance also occurred with these DHFR inhibitors also. Resistance to proguanil was reported rapidly. This may have been due to its heavy use as a prophylactic drug in Southeast Asia in the 1940s and 1950s (Gregson and Plowe, 2005). Reports stated that a 100 mg dose in 1947 would have a 100% cure rate, whereas in 1949 failure rose to 25% after a 300 mg dose (Davey and Robertson, 1957). According to Gregson and Plowe (2005) both proguanil and pyrimethamine resistance were also reported during the conflict in Vietnam.

Despite the parasites' resistance to proguanil and pyrimethamine they are still used in combination with other drugs, although their use is strategically planned (WHO, 2017c; Walker, Nadjm and Whitty, 2018). For example, combination therapy that includes pyrimethamine along with sulfadoxine (DHPS inhibitor) and artesunate (discussed in section 1.5.3) is given as first line treatment in India (WHO, 2017c). Pyrimethamine combined with sulfadoxine is given as IPT for pregnant women in parts of Africa (WHO, 2017c). The combination of proguanil and atovaquone (Malarone®) is recommended as a prophylaxis drug for travellers to malaria endemic countries where resistance to chloroquine is high (Waller and Sampson, 2018).

DHPS Inhibitors

A major class of DHPS inhibitors are the sulphonamides. The basic structure of sulphonamides is similar to *para*-aminobenzoic acid (*p*ABA), a DHPS substrate (Katzung, Masters and Trevor, 2012). Although they are important drugs in the treatment of malaria, the parasite has the ability to salvage exogenous folate and *p*ABA thus reducing the efficacy of these drugs (Delfino *et al.*, 2002; Yuthavong, 2002; Gregson and Plowe, 2005; Salcedo-Sora and Ward, 2013; Talawanich *et al.*, 2015). As previously discussed, using them in combination with DHFR inhibitors results in a synergistic effect (Yuthavong, 2002; Nzila, 2006a).

Of the several DHPS inhibitors used dapsone is one of the more important agents. Although synthesised in 1908, its antimicrobial activity was not identified until the 1930s (Nzila, 2006b). It was administered with pyrimethamine in a drug known as Maloprim™ (Müller and Hyde, 2013) and with chlorproguanil known as Lapdap (Lang and Greenwood, 2003; Alker *et al.*, 2005).

Another DHPS inhibitor, sulfadoxine, is also used in combination with pyrimethamine (Fansidar™). Although this combination was used as a first line treatment in Africa for many years, the development of resistance to it and to many of the above mentioned antifolates led to them being replaced by other antimalarials. Resistance is identified by mutations in both *dhfr* and *dhps* genes (Kublin *et al.*, 2002; Alker *et al.*, 2005; Plowe, 2009; Deloron *et al.*, 2010; Nzila, Ma and Chibale, 2011).

1.5.3 Artemisinins

Artemisinin, a natural product extracted from the Chinese herb qinghaor (*Atermisia annua L*), is thought to have been used as a therapeutic to treat high fevers as far back as 2000 years ago (Ploypradith, 2004; Krungkrai *et al.*, 2010). The compound was isolated and its chemical structure determined in 1972 by Chinese scientists who gave it the name Qinghaosu (now known as artemisinin) (Engel and Straus, 2002; Ploypradith, 2004). The clinical importance of artemisinin to treat malaria was reported in 1979 by the Qinghaosu Antimalarial Coordinating Research Group. The compound was subsequently distributed to the rest of the world (Engel and Straus, 2002; Krungkrai *et al.*, 2010).

Since the discovery of its antimalarial activity, several synthetic derivatives of artemisinin have been produced which are more soluble than artemisinin, examples of which are dihydroartemisinin, artemether, arteether and artesunate (Engel and Straus, 2002) (chemical structures can be seen in Figure 1.7). All artemsinin-based drugs are converted *in vivo* to dihydroartemisinin, which is the metabolically active form (Eastman and Fidock, 2009).

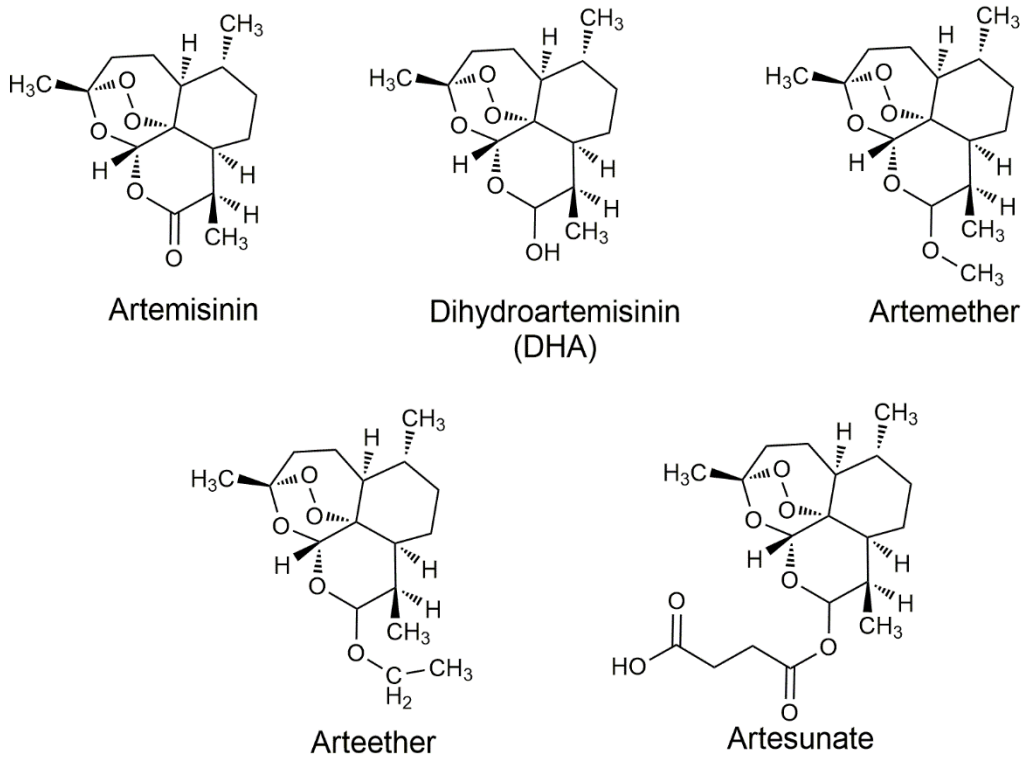

Figure 1.7 - Chemical structure of artemisinin and some of its synthetic analogues.

The artemisinin-based compounds are fast-acting drugs with a very short half-life of one to three hours (Liu, 2017). Due to their rapid elimination, the compounds cannot kill all parasites during a short three-day treatment resulting in recrudescence (Giao *et al.*, 2001; Liu, 2017; Wang *et al.*, 2017). The short half-life also eliminates their use for prophylaxis (Liu, 2017). In order to reduce the rate of recrudescence, and in a bid to slow down the rate of parasite resistance to artemisinin-based drugs, the WHO recommends the drug is not given as a monotherapy but as a combinatory therapy (artemisinin-based combination therapy, ACT), typically with a slower acting drug with a longer half-life (Giao *et al.*, 2001; Eastman and Fidock, 2009; Krungkrai *et al.*, 2010; Cheng, Kyle and Gatton, 2012; Tripathy and Roy, 2014; Severini and Menegon, 2015). According to Krungkrai *et al.* (2010) the WHO recommended ACT as the first line treatment for uncomplicated *P. falciparum* malaria in Africa in 2001. This remains the case to this day (WHO, 2018).

The mechanism of action of artemisinin and its derivatives is not fully understood, however compounds lacking the endoperoxide bridge lose their antimalarial activity thus highlighting its importance (Krungkrai *et al.*, 2010; Mojab, 2012). A chemically engineered artemisinin that allowed the fluorescent labelling of proteins covalently bound to the compound following incubation with the parasites was synthesised (Wang *et al.*, 2015). The proteins were then identified by mass spectrometry. The chemically engineered analogue was as effective as the unmodified artemisinin when tested on *P. falciparum* parasites. The results identified 124 protein targets, suggesting artemisinin has a diverse mechanism of action targeting several cellular activities. Furthermore the study also suggested that artemisinin is activated by heme within infected RBCs, which further supports previous suggestions that artemisinin's selectivity to infected RBCs is due to heme activation within the parasite (Klonis *et al.*, 2011; Klonis, Creek and Tilley, 2013). Other groups have since supported these findings (Ismail *et al.*, 2016; Zhang *et al.*, 2016; Zhou, Li and Xiao, 2016). Although studies have shown artemisinin to target hundreds of proteins, the contribution of each target to parasite death is unknown (Wang *et al.*, 2017).

It is also thought that the activation of artemisinin by heme within the parasitophorous vacuole (PV) triggers a series of reactions that result in the build-up of oxygen centred and/or carbon centred free radicals within the infected RBC which interfere with biomolecules

leading to parasite death (Olliaro *et al.*, 2001; Krishna, Uhlemann and Haynes, 2004; Saifi *et al.*, 2013; Severini and Menegon, 2015; Tilley *et al.*, 2016).

Efforts to slow the rate of resistance to artemisinin-based drugs were made by providing training for health care professionals in certain countries, both in diagnosis and in distinguishing between severe and uncomplicated malaria. The WHO also provided treatment guidelines and recommendations to protect their efficacy (Ndong *et al.*, 2015). Nevertheless, reports of delayed parasite clearance after treatment with artemisinin-based drugs has emerged. Initially this was reported in Cambodia but has since become widespread across Southeast Asia (Krungkrai *et al.*, 2010; Cheng, Kyle and Gatton, 2012; Tun *et al.*, 2015).

Initial studies by Ariey *et al.* (2014) showed mutations in the *kelch* gene (K13) to be associated with the delayed clearance. A study carried out by Nyunt *et al.* (2015) in Myanmar found K13 mutated parasites in the eastern side of the country. Myanmar provides the only route for the resistance to travel from Southeast Asia through to India and on to Africa, which is believed to be the trajectory of previous antimalarial drug resistance (Tun *et al.*, 2015).

Resistance to ACT threatens the world's effort to control and eradicate malaria (Ariey *et al.*, 2014; Paloque *et al.*, 2016), particularly as reports of artemisinin resistance spreading is outpacing the implementation of new control measures and the development of new drugs (Tun *et al.*, 2015).

1.5.4 Antibiotics and antiparasitic drugs

The spread of parasites resistant to chloroquine in the 1960s prompted investigations into alternative treatments, such as antibiotics (Tan *et al.*, 2011). One of the most important class of antibiotics used for malaria treatment are the tetracyclines, mainly doxycycline. Doxycycline is a broad-spectrum antibiotic synthetically derived from tetracycline which is produced by *Streptomyces* sp. As antimalarials, these drugs are slow acting. Infections take a week to clear following administration; this is known as delayed-death effect (DDE). Due to the delayed effect, the recommendation for both doxycycline and tetracycline is that they be given in combination with quinine as a second line treatment for uncomplicated malaria (Noedl, 2009; Tan *et al.*, 2011; WHO, 2017c; Walker, Nadjm and Whitty, 2018). Doxycycline can also be given as a prophylactic drug, especially to travellers to areas with chloroquine and

pyrimethamine-sulfadoxine resistant strains (Tan *et al.*, 2011; Walker, Nadjm and Whitty, 2018).

The malaria parasite has an apicoplast organelle which is a non-photosynthetic plastid that is essential for the parasite's survival and unique to apicomplexan parasites (Nzila, Ma and Chibale, 2011; Chakraborty, 2016). This organelle carries out metabolic pathways in a manner similar to that of prokaryotes. It has a circular genome, replicates DNA and carries out transcription and translation in a prokaryote-like manner (Chakraborty, 2016). It is believed that doxycycline targets the translation proteins of the apicoplast in the parasite, producing a progeny with dysfunctional apicoplasts. The dysfunctional apicoplasts eventually result in parasite death – hence the DDE (Nzila, Ma and Chibale, 2011; Chakraborty, 2016).

Clindamycin is another antibiotic used in malaria treatment. This drug is used as an antibiotic to treat anaerobic and gram positive bacterial infections, as an antiparasitic to treat toxoplasmosis and an anti-fungal to treat *Pneumocystis carinii* pneumonia (Obonyo and Juma, 2012). Clindamycin is another slow acting antimalarial believed to have a similar mechanism of action to doxycycline (Chakraborty, 2016) and is recommended to be given in combination with quinine to treat pregnant women with uncomplicated malaria (D 'alessandro *et al.*, 2018).

Another important class of drugs for malaria treatment are the naphthoquinones. These are a group of naturally occurring compounds with reported antibacterial, antiparasitic and antifungal activity (Riffel *et al.*, 2002). The most important compound from this group is atovaquone. Atovaquone is an analogue of ubiquinone, which is a lipophilic molecule found in the mitochondria of cells and is involved in the transfer of electrons in the mitochondrial respiratory chain (Riffel *et al.*, 2002; El Hage *et al.*, 2009; Müller and Hyde, 2010; Quinzii and Hirano, 2010). Atovaquone is reported to inhibit the cytochrome bc_1 complex in the parasite's mitochondria (Sutherland *et al.*, 2008; Siregar *et al.*, 2015). The effect of the drug is believed to result in the collapsing of the mitochondrial membrane potential and the inhibition of the parasite specific enzyme dihydroorotate dehydrogenase, which is involved in the synthesis of pyrimidine. The parasite is unable to salvage pyrimidine from the host, the drug therefore depletes the parasite from its pyrimidine pool preventing replication and eventually leads to parasite death (El Hage *et al.*, 2009; Gamo, 2014). Atovaquone is administered in combination

with the antifolate proguanil (Malarone®) as a standalone treatment and as a prophylactic drug for travellers (Kate *et al.*, 2016; WHO, 2017c; Walker, Nadjm and Whitty, 2018). Mutations in the parasite's *pfcyt-b* gene is believed to be linked with resistance to atovaquone (Fivelman *et al.*, 2002; Sutherland *et al.*, 2008; Siregar *et al.*, 2015).

1.6 Antimalarial drug discovery

1.6.1 Traditional drug development

The development of new antimalarial drugs is needed to combat the ongoing battle against resistance (Lotharius *et al.*, 2014). Despite the urgent need to develop new drugs, not only for malaria but for other diseases such as cancer and resistant bacterial infections, the number of new drugs being released on to the market has reduced over recent years (Proschak, 2013). According to Milardi and Pappalardo (2015), for every 10,000 new candidates only one gets through per year.

The strict and complex process needed to develop a drug, the increase in cost needed to discover and develop a candidate and the lack of efficacy in addition to undesirable side effects are among the various reasons that have led to the attrition in approval of new drugs (Williams, 2011; Proschak, 2013; Kenakin, 2014).

The drug development timeline of a single candidate can take anywhere between 10 to 17 years (Pronker *et al.*, 2011). Developing a target alone can take years of research (Hughes *et al.*, 2011). Once a target is identified, synthesising and identifying a lead compound, testing its activity, followed by a series of rigorous *in vitro* and animal testing in order to determine its pharmacological data takes a further several years (Peters *et al.*, 2012; Kenakin, 2014). After preclinical tests the compound enters clinical trials which include three phases and can last between six and seven years. These stages determine the efficacy, dosage, side effects and adverse reactions of the drug. Once a compound passes all three clinical stages it can then be submitted for approval from the Food and Drug Administration (FDA) (FDA, 2018).

The process to develop antimalarial drugs is compelled to follow the same lengthy pathway, however with further considerations: 1) drugs would ideally be taken orally to ease

administration in a non-health care setting; 2) drugs need to be well tolerated with minimal side effects due to the large number of people of different age groups that require antimalarials; 3) drugs need to be cheap due to the financial constraints in developing countries that are most affected by malaria; 4) duration of treatment should be minimal, for example three day therapy or less would be ideal, due to concerns with compliance and the development of resistance; 5) combination therapy is essential for malaria to delay the development of resistance which increases the number of drugs that require development (Rosenthal, 2003; Gelb, 2007; Alonso *et al.*, 2011).

Unfortunately, these factors have had a negative effect on producing new antimalarial drugs. According to Ekins *et al.* (2011) big pharmaceutical companies have historically not focused on diseases that only affect small groups of people in developed countries due to the difficulty in marketing the drug sufficiently to recover development costs. As a result, development for diseases such as malaria occurs in academic research institutions or smaller companies that are not ideal for drug discovery (Gelb, 2007; Ekins *et al.*, 2011). In order to encourage the development of drugs for neglected diseases such as malaria, the US government implemented a programme known as the "priority review voucher". Using this incentive scheme means if a drug is developed for a neglected disease or rare paediatric disease and is approved by the FDA then the developing company will be awarded a bonus priority voucher for another drug (Ridley, 2017). Additionally GlaxoSmithKline (GSK) have dedicated a research and development (R&D) facility in Spain to develop new treatments that affect people in the developing world (Tres Cantos Open Lab Foundation, 2014).

Furthermore Medicines for Malaria Venture (MMV) is an example of a product development partnership dedicated to malaria research. MMV brings together many organisations with the vision of developing new antimalarial drugs described under two Target Product Profiles (TPPs). The first, a Single Encounter Radical Cure and Prophylaxis which would be a single dose treatment that would be effective against resistant strains of malaria. The second TPP, a Single Exposure Chemoprotection (SEC) to protect non-infected people entering a malaria endemic area. The SEC would have different mechanism of action to the compounds used for treatment.

1.6.2 Drug repositioning

Researchers have been looking to adopt new methods to develop drugs in a cheaper and quicker manner (Baek *et al.*, 2015). An alternative route is drug repositioning/repurposing, which is when a compound has been developed for one condition but shows activity in another (Andrews, Fisher and Skinner-Adams, 2014; Lotharius *et al.*, 2014). Sources of repositioned drugs can be clinically/FDA approved drugs (Andrews, Fisher and Skinner-Adams, 2014; Lotharius *et al.*, 2014), drugs that were approved but are no longer used, or clinical investigational compounds that were developed but withdrawn prior to approval or did not achieve efficacy for their intended condition (Lotharius *et al.*, 2014; Sun, Sanderson and Zheng, 2016). Sometimes the drug of interest is used as a starting point to produce new compounds and therefore does not get repositioned directly into a new area, yet it still reduces time that would have been spent developing the first compound (Andrews, Fisher and Skinner-Adams, 2014; Jin and Wong, 2014).

Examples of repositioned drugs include sildenafil (Viagra) which was initially tested for hypertension and has been repositioned for erectile dysfunction (Ekins *et al.*, 2011; Jin and Wong, 2014) and thalidomide which, although the cause of birth defects when taken by pregnant women to alleviate nausea, has been repositioned to treat multiple myeloma (Ekins *et al.*, 2011). Some drugs have been repositioned for use in malaria; a primary example is the previously discussed antibiotic, doxycycline.

Another example is a programme supported by MMV which saw the high-throughput screening of approximately 4 million compounds by Novartis, GlaxoSmithKline (GSK) and St. Jude Children's Research Hospital in the late 2000s. The outcome of this programme deposited over 20,000 compounds that showed antimalarial activity into the public domain to be used by researchers as starting points for new antimalarial drugs (Guiguemde *et al.*, 2012; Fong, Sandlin and Wright, 2015). One of the main aims for drug discovery in malaria is to develop novel drugs with new mechanisms of action in order to avoid cross-resistance from existing drugs (Guiguemde *et al.*, 2012; Fan *et al.*, 2018).

The advantages associated with drug repositioning, in addition to reduced cost and time needed to develop the drug, are reduced risks of drug failure due to the fact that pre-clinical

toxicology data, pharmacokinetics and dose range is sometimes already known (Baek *et al.*, 2015). It is important however to point out the disadvantages as well. Repositioned drugs may have a new mechanism of action which can lead to potential failure of the compound for the new use (Baek *et al.*, 2015). Furthermore, legal issues can arise with regards to intellectual property of the drug (Witkowski, 2011).

1.7 Calcium and calmodulin

Calcium and calcium channels along with calmodulin (a calcium binding protein) play major roles in human cells (Bogdanova *et al.*, 2013) and within the *Plasmodium* parasite (Enomoto *et al.*, 2012; Furuyama *et al.*, 2014). Studies have shown that interfering with calcium levels can lead to parasite death (Enomoto *et al.*, 2012). Additionally, several antimalarial drugs are reported to have anti-calmodulin activity (Noori *et al.*, 2008). With this in mind the, importance of calcium, calmodulin and their inhibitors with regards to *Plasmodium* infections are explored.

1.7.1 Importance of calcium

Calcium is found in abundance in eukaryotic cells and plays a major role within them (Lin and Jan, 2002). Levels of calcium regularly fluctuate within a cell's cytosol affecting various cellular functions and activities, although the levels of fluctuation are tightly regulated (Clapham, 2007; Pandey *et al.*, 2016).

Calcium is an important tool in signal transduction. The addition and removal of calcium to a protein changes the shape and charge of the protein allowing cellular activity to occur (Clapham, 2007). This allows calcium to be involved in many important cellular functions such as metabolism, cell cycle, secretion and neuronal signalling (Enomoto *et al.*, 2012; Bogdanova *et al.*, 2013).

Studies have shown that parasite-infected RBCs have higher levels of calcium compared with non-infected RBCs (Desai *et al.*, 1996; Rohrbach *et al.*, 2005; Lourido and Moreno, 2015). Rohrbach *et al.* (2005) carried out a series of tests using confocal fluorescence microscopy which found levels of calcium in the infected erythrocyte between 289 nM and 352 nM. The variation was dependent on the strain of parasite tested. These levels are considerably higher

than calcium levels in non-infected RBCs, which is normally between 30 nM and 60 nM (Gazarini *et al.*, 2003; Bogdanova *et al.*, 2013).

According to Camacho (2003), eukaryotic cells require approximately 1 mM extracellular calcium in order to maintain cellular functions that require calcium. Therefore investigations into the parasite's ability to survive under the reduced calcium levels of the RBC was investigated by Gazarini *et al.* (2003). First of all however, it is important to note that the RBC membrane contains plasma membrane Ca^{2+} ATPase pumps (PMCAs) (Camacho, 2003). They are activated by calmodulin and are responsible for maintaining low levels of intracellular calcium by expelling it from the cytosol of cells (Ortega, Ortolano and Carafoli, 2007).

During the invasion of RBCs, merozoites are thought to shed surface proteins, they potentially also shed antibodies that have been attached to their surface by the host. It is believed this process is done to distract the host's immune response (Farrow *et al.*, 2011; Harvey, Gilson and Crabb, 2012). The merozoite then invades the RBC via endocytosis with the RBC plasma membrane which results in a membrane developing and forming a vacuole (the PV) around the parasite. The close interaction between the merozoite and the host plasma membrane is believed to allow an exchange of proteins and lipids between the host plasma membrane and the PV membrane (PVM) (Ward, Miller and Dvorak, 1993; Eksi and Williamson, 2011).

Gazarini *et al.* (2003) suggest that during the invasion some of the PMCAs on the RBC membrane are integrated into the PVM, however they are now facing inwards and thus allow calcium to enter the PV from the RBCs cytosol. This proposed method aligns with another method discussed in a review by Kirk (2001) that suggests there is a continuous flow of calcium in and out of RBCs - calcium is constantly being leaked into RBCs due to the high levels present in the extracellular medium, and then PMCA pumps expel the leaked calcium – allowing the parasite to draw enough calcium for it to survive.

Desai *et al.* (1996) suggest the parasite causes an increase in permeability of the infected RBC's membrane to calcium. The group suggest that the parasite inserts a calcium channel into the RBC membrane allowing a flow of calcium into the cell that is controlled by the parasite. Another suggestion was that the parasite inhibited the activity of the PMCA present on the RBC membrane, although this option was thought to be less likely due to the massive increase in calcium levels. However work carried out by Thomas *et al.* (2001) on chicken RBCs

infected with *P. gallinaceum* found there were no new channels present in infected cells. Instead they found an upregulation in the host cell's own pathways. Although the reasons are unknown the group suggested parasite activation of these channels or activation simply due to the host cell expanding in size with the growing parasite inside it.

Not only are there increased levels of calcium in infected RBCs but various studies have shown that blocking the flow of calcium in the erythrocytic stages of parasite infection leads to parasite death (Enomoto *et al.*, 2012). It is important to note that the endoplasmic reticulum (ER) has high levels of calcium; it is known to be one of several calcium stores in cells (both mammalian cells and *Plasmodium* parasites) (Lourido and Moreno, 2015). Inositol 1,4,5-trisphosphate (IP_3 or inositol trisphosphate) is a molecule present in cells that can bind to IP_3-gated calcium channels present on the ER, allowing the gates to open and a flow of calcium to be released into the cells (Nelson and Cox, 2008). There is evidence to suggest the release of calcium by IP_3 from calcium stores within the parasite (Alves *et al.*, 2011) although there is no molecular evidence of an IP_3 receptor (Brochet *et al.*, 2014).

Nonetheless, studies carried out by Enomoto *et al.* (2012) have shown that the flow of calcium can be blocked using an IP_3 receptor inhibitor, 2-aminoethyl diphenylborinate (2-APB), at stage-specific intervals during the erythrocytic cycle of the *P. falciparum* infection. The result of this blockage, particularly in the trophozoite stages, led to degeneration and eventual parasite death. The study also showed that 2-APB did not give these results due to degeneration of the RBCs themselves. This was tested by pre-treating RBCs with 2-APB, removing the drug from the RBCs and then infecting them with parasites. Under these conditions the parasites were able to grow normally, comparable with the controls. The study showed that the flow of calcium plays a major role in the parasites' life cycle and disrupting it has a negative, if not deadly, effect on the parasite's erythrocytic life cycle (Enomoto *et al.*, 2012).

There is evidence that highlights the importance of calcium during the invasion and development of the parasite within the RBC (Alleva and Kirk, 2001; Camacho, 2003; Gazarini *et al.*, 2003; Borges-Pereira, Campos and Garcia, 2014; Withers-Martinez *et al.*, 2014). Jean *et al.* (2014) cited that the interaction between the membranes of the parasite and the RBC during the invasion is calcium dependent. The parasite encodes calcium dependent protein

kinase (CDPK) - a group of proteins not found in the human genome. Dvorin *et al.* (2010) cited that the protein (*PfCDPK5*) is transcribed during the egression and invasion of RBCs, suggesting the protein is required for those stages in the parasite life cycle. It is believed that calcium controls cellular signals that are important not only in invasion but also in motility and protein secretion (Furuyama *et al.*, 2014).

The importance of calcium in *Plasmodium* parasites has been thoroughly documented; the presented points are only a brief summary of a few published reviews (Desai *et al.*, 1996; Garcia *et al.*, 1996; Alleva and Kirk, 2001; Kirk, 2001; Thomas *et al.*, 2001; Camacho, 2003; Gazarini *et al.*, 2003; Rohrbach *et al.*, 2005; Dvorin *et al.*, 2010; Enomoto *et al.*, 2012; Borges-Pereira, Campos and Garcia, 2014; Withers-Martinez *et al.*, 2014; Furuyama *et al.*, 2014; Jean *et al.*, 2014; Lourido and Moreno, 2015).

1.7.2 Importance of calmodulin

Calmodulin is a ubiquitous calcium binding protein found in all eukaryotic cells (Berchtold and Villalobo, 2014). It has remained largely conserved over 1.5 billion years of evolution as noted by Clapham (2007) and in humans calmodulin is transcribed from three genes found on different chromosomes (Toutenhoofd *et al.*, 1998; Clapham, 2007).

As previously discussed, many cellular proteins are activated by calcium. Some proteins cannot bind to calcium themselves, instead a calcium-adaptor complex is formed first, such as a calcium-calmodulin complex, which then binds to the protein. Thus calmodulin acts as a mediator for various calcium signals (Vetter and Leclerc, 2003). As with other calcium binding proteins, calmodulin is formed of a pair of EF hands. An EF hand motif is when a protein forms a helix-loop-helix structure; the conformation resembles “the extended thumb and index finger of a hand” (Vetter and Leclerc, 2003) as shown in Figure 1.8. Calmodulin’s EF hands have high affinity for calcium which is often increased when bound to the target protein (Clapham, 2007).

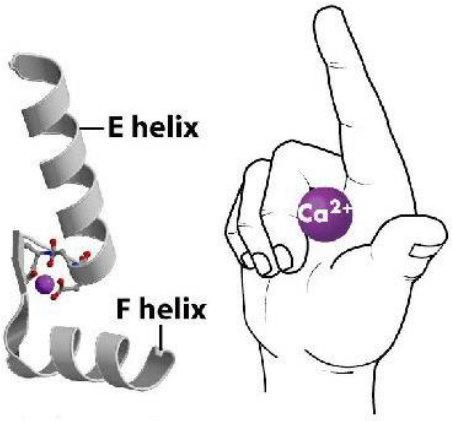

Figure 1.8 – A schematic showing the EF hand motif of calmodulin.

Source: http://chemistry.umeche.maine.edu/CHY431/EF-Hand.jpg

Saucerman and Bers (2012) suggest that a cell has two pools of calmodulin, dedicated and promiscuous. The former are found bound to their targets, even when not activated – such as L-type calcium channels (LTCCs) - and the latter are free calmodulin that bind to calcium molecules in the cell and thus activate and interact with other cellular proteins (Saucerman and Bers, 2012; Berchtold and Villalobo, 2014). Moreover, Nunomura *et al.* (2000) cited that there are high levels (micromolar) of calmodulin in RBCs; 5% is involved with PMCAs and the remaining 95% interact with other proteins.

A study carried out by Scheibel *et al.* (1987) showed that levels of calmodulin in *P. falciparum* infected RBCs was higher than that in non-infected cells. Non-infected RBCs contained 11.2 ng of calmodulin per 10^6 cells, whereas ring stage *P. falciparum* infected RBCs contained 17.8 ng and schizont stage contained 23.3 ng. During the same study calmodulin was found randomly scattered in the trophozoite and schizont stages, whereas it was concentrated in the apex of the merozoites (Scheibel *et al.*, 1987). The apex is the site of interaction between the merozoite and a RBC during invasion (Preiser *et al.*, 2000).

There have been several reports of important antimalarial drugs such as quinine, chloroquine, artemisinin and dihydroartemisinin having anti-calmodulin activity (Scheibel *et al.*, 1987; Robson, Gamble and Acharya, 1993; Noori *et al.*, 2008, 2010). In fact Noori *et al.* (2008) showed that artemisinin had more anti-calmodulin activity than Cyclosporin A – a known calmodulin inhibitor.

Furthermore, calmodulin inhibitors (such as trifluoperazine, calmidazolium and W-7) have shown antimalarial activity by inhibiting RBC invasion and parasite maturation in blood stages (Scheibel *et al.*, 1987; Tanabe *et al.*, 1989). Thus reinforcing the results seen by Scheibel *et al.* (1987) where calmodulin was found in the apex of the merozoite which is involved in RBC invasion.

The importance of calmodulin cannot be underestimated; it is known to interact with several hundred different proteins (Berchtold and Villalobo, 2014) and can form a minimum of three different conformations thus adding to its complexity (Hoeflich and Ikura, 2002). However this also highlights the potential risk of developing drugs that specifically target calmodulin (Berchtold and Villalobo, 2014).

1.8 Calcium channels and their blockers

1.8.1 Voltage-gated calcium channels

There are various ways in which cells regulate calcium flow, one of these methods being voltage-gated calcium channels. These channels consist of four subunits; α_1, $\alpha_{2\delta}$, β and γ that are encoded by different genes. The main α_1 subunit is approximately 190-250 kDa (Ertel *et al.*, 2000), belongs to three separate subfamilies and exists in 10 different isoforms each encoded by a different gene (Catterall *et al.*, 2005; Chandra and Ramesh, 2013; Striessnig *et al.*, 2014). The α_1 subunit contains the ion conduction pore and the gating structure and is the known site for drugs to interact with and regulate the channel's activity (Ertel *et al.*, 2000; Chandra and Ramesh, 2013). The β subunit is intracellular and interacts with the cytoplasmic part of the channel, whilst the $\alpha_{2\delta}$ subunit interacts with the extracellular domain. Finally γ subunits have only been found in skeletal muscle calcium channels (Ertel *et al.*, 2000; Striessnig *et al.*, 2014). Figure 1.9 shows a schematic of the different subunits within the calcium channel and where they are positioned with regard to the cell membrane and each other.

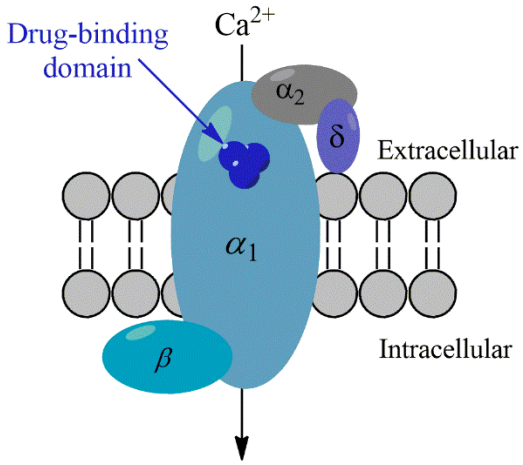

Figure 1.9 – Schematic of a voltage gated calcium channel and its subunits within a cell membrane.
(Adapted from: Striessnig et al. 2014)

Figure 1.10 shows a diagram taken from Striessnig *et al.* (2014) who have used crystallographic data from potassium and sodium channels to show the different domains found within the α_1 subunit. There are six segments found within the α_1 subunit: four of the segments form the voltage sensing domains and the two other segments, attached by linkers, are the pore forming domains (Catterall *et al.*, 2005; Striessnig *et al.*, 2014). There are several of these gated ion channels located next to each other within a cell membrane (Striessnig *et al.*, 2014). According to Catterall *et al.* (2005) it requires three amino acid changes in the pore forming domain (segments 5 and 6) to convert the selectivity of the channel from sodium to calcium.

According to Sadava *et al.* (2011) regardless of the signal that causes a calcium channel to open the result is a massive increase in cellular calcium; sometimes this can be a "one hundred fold increase within a fraction of a second" (Sadava *et al.*, 2011). As reviewed by Christel and Lee (2012) calcium influx into cells via calcium channels (particularly LTCCs) is regulated by calmodulin via a feedback system. Interestingly, Striessnig *et al.* (2014) state in another review that calmodulin can be considered as another subunit for LTCCs as it is bound to the C-terminus of the transmembrane protein. As calcium binds to calmodulin, conformational changes occur that affects the influx of calcium into cells (Ben *et al.*, 2013).

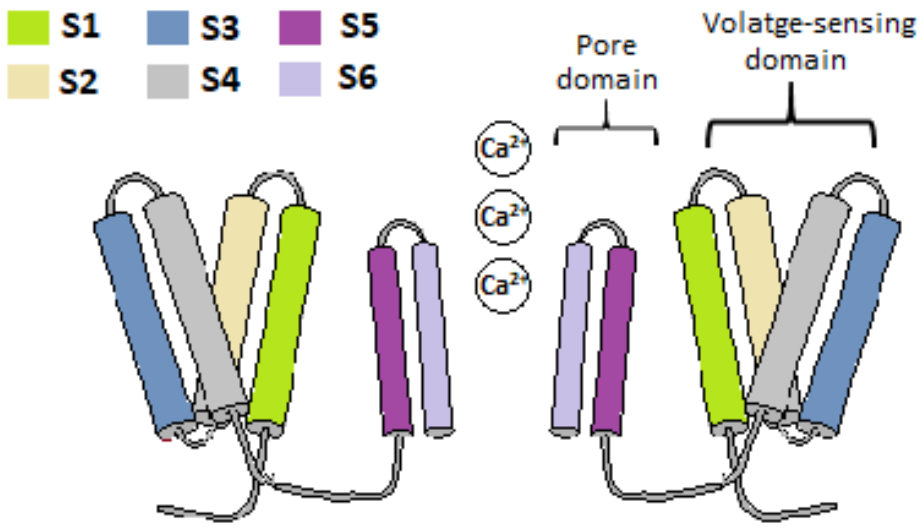

Figure 1.10 - Schematic showing the different segments within the α1 subunit of voltage gated ion channels.
The image is based on crystallographic data from soium and potassium channels.
(Adapted from: Striessnig et al. 2014)

Despite the crucial role of calcium channels in biological processes, interest and research into them was slow to develop (Tsien and Barrett, 2005). According to Tsien and Barrett (2005) one of the first reports of voltage gated calcium channels was in 1953 by Fatt and Katz, but it was not until the 1970s that interest fully developed and until the 1980s for patch clamping work to be carried out on calcium channels.

1.8.2 Calcium channel blockers

Despite there being several types of calcium channels (L, N, T, P, Q and R) there is a lot of interest in the LTCCs due to the fact that they are one of the main targets for the majority of calcium channel blockers (CCBs) (Bangalore *et al.*, 1994; Nawrath *et al.*, 1998; Chandra and Ramesh, 2013; Whyte, Buckley and Dawson, 2016).

CCBs are a group of drugs used to treat a variety of disorders which include “hypertension, angina pectoris, coronary artery spasm, supraventricular arrhythmias and migraine” (Olson *et al.*, 2005). There are three broad types of CCBs which are grouped based on their chemical structure; dihydropyridines (e.g. nicardipine), phenylalkylamines (e.g. verapamil) and benzothiazepines (e.g. diltiazem) (Nawrath *et al.*, 1998). Once bound, CCBs reduce the frequency in which channels open thus blocking the movement of calcium across cell membranes (Katzung, Masters and Trevor, 2012). This in turn reduces heart contractions and

reduces hypertension (Fleckenstein, 1983; Michiels *et al.*, 2014; Chiba *et al.*, 2015). A recent study by Tang *et al.* (2016) using crystallographic analysis showed that dihydropyridines (amlodipine) bind to the external lipid-facing surface of the calcium channel at the interface of two subunits, whereas phenylalkylamines interact with the central cavity of the pore, blocking the channel pathway.

In addition to targeting calcium channels, reports have stated that some CCBS such as verapamil, nicardipine and fendiline bind to and inhibit calmodulin and act as calcium channel and calmodulin antagonists (Hidaka and Hartshorne, 1985; Bayer and Mannhold, 1987). The different types of CCBs have varying selectivity to different tissues and binding sites which may explain the clinical differences seen between the different groups of CCBs (Nathan, Pepine and Bakris, 2005).

There have been several reports over the years of some CCBs and calmodulin antagonists having antimalarial activity (Scheibel *et al.*, 1987; Tanabe *et al.*, 1989; Alleva and Kirk, 2001; Kirk, 2001). A study carried out on fresh chloroquine-resistant *P. falciparum* strains isolated in Brazil found antimalarial activity in CCBs such as verapamil, nifedipine and dilitiazem within their therapeutic cardiovascular concentrations (Menezes *et al.*, 2003). These reports align with results produced at the University of Salford where two patent-expired drug libraries, ENZO and LOPAC (Library of Pharmaceutically Active Compounds), were screened for antimalarial candidates (Matthews, 2015). The screen showed that 2 (niguldipine and nicardipine HCl) out of the 60 most potent compounds were CCBs. At a concentration of 2.5 µM, the percentage of inhibition was 63.92 and 62.35 for niguldipine and nicardipine HCl respectively.

Synergistic relations between CCBs and antimalarial drugs have also been reported (Adovelande, Deleze and Schrevel, 1998; van Schalkwyk and Egan, 2006). Studies have shown that CCBs and chloroquine work synergistically against chloroquine resistant strains by reversing chloroquine resistance (Martin, Oduola and Milhous, 1987; Basco and Le Bras, 1991; Ye and Van Dyke, 1994; Adovelande, Deleze and Schrevel, 1998). Studies have however shown that verapamil does not reduce the concentration of calcium in the parasite. It is thought that the resistance reversal by verapamil may be associated with the PfCRT mutation (van Schalkwyk and Egan, 2006).

1.8.3 Fendiline

The CCB fendiline (Figure 1.11), is a commercially available yet "clinically obsolete" (van der Hoeven *et al.*, 2013) drug that is safe for human use (van der Hoeven *et al.*, 2013; Voigt, Riddle and Napier, 2014). Fendiline was used to treat angina and hypertension and has been reported to inhibit both smooth muscle LTCCs and calmodulin (Bayer and Mannhold, 1987; Tripathi, Schreibmayer and Tritthart, 1993).

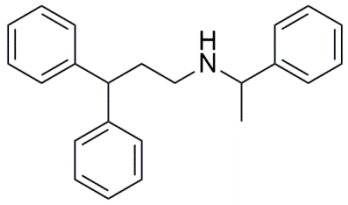

Figure 1.11 - Molecular structure of fendiline.

Tests of fendiline on calcium channels of guinea pig ventricular myocytes showed an IC_{50} value of inhibition of 17 μM (Tripathi, Schreibmayer and Tritthart, 1993). Other tests carried out by Wilkinson *et al.* (2007a) on the vasodilatory effect of fendiline (*S* and *R* enantiomers separately) on mesenteric and coronary rat arteries gave comparable results, with EC_{50} values of 17.1 μM and 26.7 μM for *R*-fendiline and *S*-fendiline respectively for mesenteric arteries. This test was also carried out on synthetic analogues of fendiline (2'-hydroxy-fendiline, molecular structures shown in Figure 1.12) and showed that the hydroxy analogues (Compounds 1 and 2) were more potent vasodilators than the fendiline isomers, with EC_{50} values of 0.16 μM for both compounds on mesenteric arteries (Wilkinson *et al.,* 2007a).

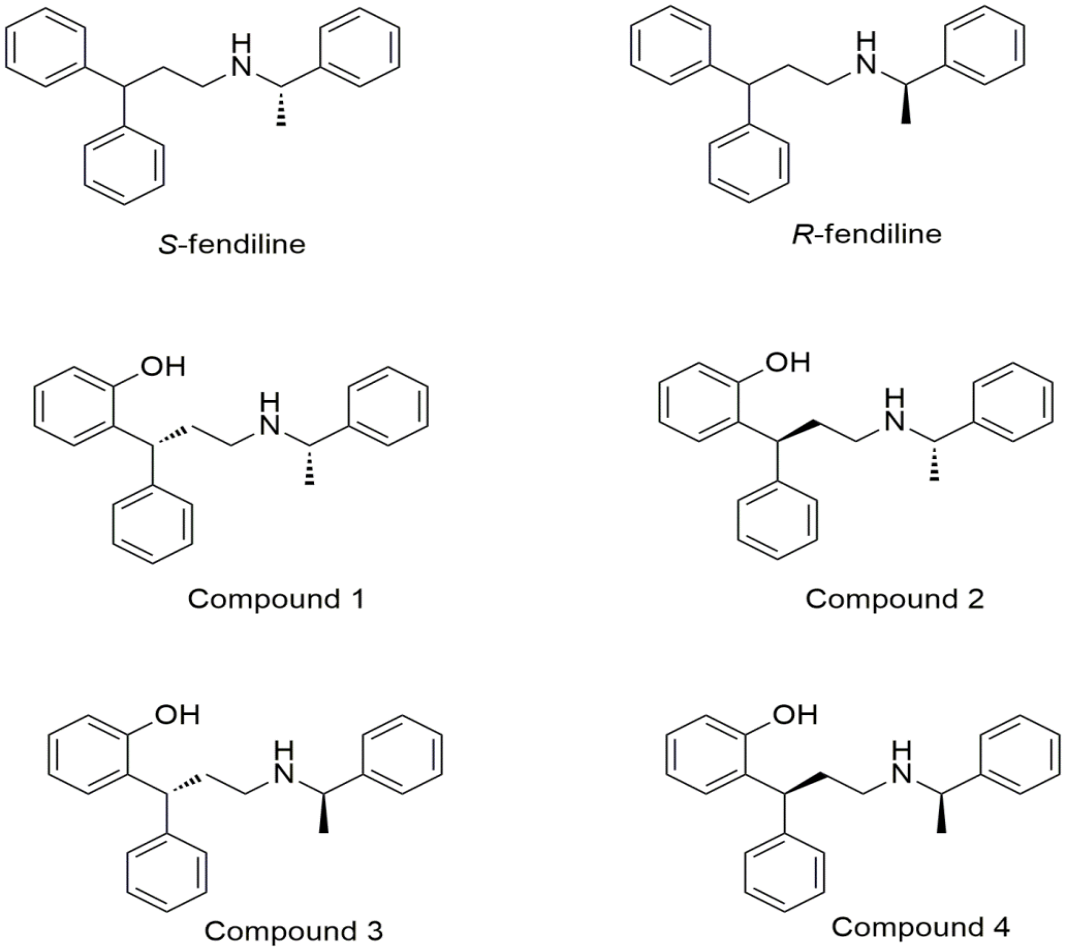

Figure 1.12 - Molecular structures of S- and R-fendiline along with four hydroxy analogues. *Compounds 1, 2, S- and R-fendiline were tested on rat arteries. All 6 compounds were tested on K562 leukaemic cells (Wilkinson et al. 2007a, 2007b).*

Wilkinson *et al.* (2007b) also tested the fendiline isomers along with four synthetic analogues seen in Figure 1.12 on K562 leukaemia cells. All six compounds showed anti-leukaemic activity, with the highest IC_{50} value being 6.1 µM. However the two lowest IC_{50} values were 2.5 µM and 2.9 µM for compounds 2 and 3 respectively. The hydroxy fendilines were seen again to be more biologically active than the original fendiline isomers (Wilkinson *et al.*, 2007b).

More recently, van der Hoeven *et al.* (2013) have shown that fendiline interferes with and prevents K-Ras signalling. Ras GTPases are a family of proteins involved in cell proliferation. Mutations in Ras are found in approximately 15% of human tumours, particularly K-Ras, making it an important target in cancer research. The results found that fendiline disrupted various signalling pathways downstream of K-Ras. The IC_{50} value reported for K-Ras inhibition

was 9.64 µM (van der Hoeven *et al.*, 2013). The group also found that the isomer *R*-fendiline was more potent in certain assays than *S*-fendiline. However data from the study suggests that activity of fendiline on K-Ras was not related to calcium channel inhibition, leading to the assumption that fendiline may have biological activity other than the previously reported calcium channel/calmodulin antagonism (van der Hoeven *et al.*, 2013).

Furthermore, investigations into the antiprotozoal effect of four CCBs found fendiline to have anti-leishmanial activity within the micromolar range (Reimão *et al.*, 2016). In another study, a high-throughput screening of drugs to treat the opportunistic fungal infection caused by *Cryptococcus neoformans* found fendiline hydrochloride as a potential candidate (Samantaray *et al.*, 2016). Alveolar macrophages in the body are the first line of defence against the fungus, although the fungus survives within the macrophage (Samantaray *et al.*, 2016). The study found that fendiline hydrochloride did not kill the fungus; instead it is thought that fendiline increased levels of calcium in the cell by releasing it from intracellular stores such as the ER thus disrupting the macrophage, which eventually lead to the fungus death (Samantaray *et al.*, 2016). This aligns with results of tests carried out in human hepatoma cells (HA/22) which showed fendiline increased levels of intracellular free calcium by releasing calcium from the ER (Cheng *et al.*, 2001). However the study suggested that the effect was not due to calmodulin inhibition (Cheng *et al.*, 2001).

Although clinically superseded, investigations into fendiline as a pharmacologically interesting compound are still being reported, with studies suggesting fendiline having more activity than the originally reported calmodulin and calcium channel antagonism.

1.9 Aims and Objectives

The need to develop new drugs for the treatment of malaria, preferably with new mechanisms of action, due to the rise of resistance to current treatment has been stated (Guiguemde *et al.*, 2012; Fan *et al.*, 2018). The traditional drug discovery process is long and costly therefore alternatives such as drug repositioning presents an attractive and promising alternative. The importance of calcium and calmodulin in the parasites' life cycle in addition to the potentially deadly affect interfering with either of these factors could have on the malaria parasite (Scheibel *et al*., 1987; Tanabe *et al*., 1989; Enomoto *et al*., 2012; Furuyama

et al., 2014), makes targeting them an attractive strategy. Subsequently an interesting class of drugs to investigate are CCBs and calmodulin inhibitors especially due to reports of them having antimalarial activity (Scheibel *et al.*, 1987; Robson, Gamble and Acharya, 1993; Noori *et al.*, 2008, 2010). More importantly, the CCB and calmodulin inhibitor fendiline has shown interesting biological activity with studies suggesting it affects more than one target. Analogues of fendiline are shown to be more potent than fendiline itself both as vasodilators and toxicity on leukaemic cells, thus further piquing interest into these compounds. With these statements in mind the main aims of this research are to:

1. Investigate the antimalarial efficacy of fendiline on the multi-resistant *P. falciparum* K1 strain.
2. Carry out combination assays with fendiline and other currently used antimalarial drugs to look for a synergistic partner.
3. Synthesise and evaluate the antimalarial activity of a range of fendiline analogues in an effort to produce a more active lead compound.
4. Evaluate the toxicity of the tested compounds on human cells.
5. Determine the stage specificity and killing profile of the lead compound(s) in order to develop an understanding of the mode of action.
6. Optimise and develop a flow cytometry-based method to detect calcium fluctuations within infected RBCs with the objective of determining the effect fendiline has on calcium levels within the parasite infected cell.

Chapter 2
Materials and methods

2.1 *In vitro* cultivation of *P. falciparum*

Parasites were cultured following the previously described method by Read and Hyde (1993). Experimental work was carried out in the pathogen laboratory at the University of Salford within a sterile hood (ESCO Infinity Class II Biosafety cabinet). Virkon (2%, VWR, UK) was used to disinfect waste material prior to autoclaving and disposal.

2.1.1 Parasite strains:

All cultures and experiments were carried out with the K1 *P. falciparum* strain which is reported to be chloroquine, pyrimethamine and sulfadoxine resistant (Rahman, 1997).

2.1.2 Complete media:

Parasites were cultured in complete media which consisted of RPMI-1640 supplemented with L-Glutamine and 25 mM HEPES (Gibco, Life Technologies, UK). Four ingredients were added to the RPMI, the final concentrations were 0.5% (w/v) lipid rich bovine serum albumin (Albumax II, Gibco, Life Technologies, UK), 360 µM hypoxanthine (Sigma, UK), 104 µM gentamicin (Sigma, UK) and 0.1 % D-Glucose (Dextrose anhydrous, Sigma, UK). The supplemented RPMI was stored between 2-8 °C for up two weeks.

2.1.3 Wash media:

Wash media consists of RPMI-1640 with L-Glutamine and 25 mM HEPES (Gibco, Life Technologies, UK) without any further additives. This was used to wash blood and was stored between 2-8 °C.

2.1.4 Processing human RBCs for parasite culture

Fresh human O+ whole blood was obtained from the National Health Service (NHS) blood bank and used to culture the *P. falciparum* parasites. Buffy coat and plasma were removed by centrifugation for 5 minutes at 3,400 rpm. The RBCs were then washed three times, twice with wash media and once with complete media, centrifuging at 3,400 rpm for 5 minutes each time. Following the final wash, 100% haematocrit blood was brought to 50% haematocrit by adding an equal volume of complete media. The 50% haematocrit washed blood was stored between 2-8 °C.

2.1.5 Maintaining parasite culture

Parasites were cultured in 25 cm^3 flasks in a final volume of 10 ml at a 5% haematocrit. This meant that for every 10 ml of complete media there would be 1 ml of 50% haematocrit blood.

The cultures were checked approximately every 48 hours; this was done by carefully removing the old media without displacing the blood layer formed at the bottom of the flask, estimating parasitaemia (see section 2.1.6) and then diluting the parasitized blood with washed blood (50% haematocrit) to maintain approximately 1% parasitaemia. Complete media was then added to the flask to obtain a 5% haematocrit culture. Finally, the flask was gassed with 5% CO_2, 5% O_2 and 90% N_2 (BOC Limited, UK) and incubated at 37 °C in a LEEC Culture Safe Touch 190s CO_2 incubator.

2.1.6 Estimating parasitaemia

A thin blood smear was performed on a microscope slide. The slide was air dried, fixed with 100% methanol and then stained for approximately 20 minutes in freshly prepared Giemsa stain. The stain used was a 1:10 dilution of Giemsa stain solution (TCS Biosciences, UK) in Giemsa buffer. Giemsa buffer consisted of one Buffer tablet pH 6.4 (BDH/VWR, UK) dissolved in 1 litre of freshly distilled water.

Following staining, the slide was washed with tap water, air dried and then viewed under the microscope (oil immersion, x100). Parasitaemia was estimated by counting the number of total RBCs and infected RBCs per field of view under the microscope. In total three fields of

view or approximately 500 RBCs were counted, and an average of infected RBCs was calculated.

2.1.7 Preservation of parasites in liquid nitrogen

Preservation in liquid nitrogen was carried out on a majority ring stage culture of approximately 10-20% parasitaemia. The culture was centrifuged at 3,400 rpm for 5 minutes, the complete media supernatant was discarded, and the pellet re-suspended in an equal volume of fresh warm complete media to obtain a 50% haematocrit. Then in a 2 ml cryotube, 0.5 ml of the mixture was added to 0.5 ml of 20% dimethyl sulfoxide (DMSO) (sterile filtered DMSO, Sigma-Aldrich, UK) in Ringer's solution (9g NaCl, 0.42g KCl and 0.25g of $CaCl_2$/Litre). The cryotube was then snap frozen in liquid nitrogen immediately.

2.1.8 Thawing of parasites from liquid nitrogen

Cryopreserved parasite vials were thawed in an incubator at 37 °C for several minutes, transferred to a sterile microcentrifuge tube and then centrifuged at 13,400 rpm for 90 seconds. The supernatant was discarded and the pellet was washed three times. First wash was in 1 ml of 10% (w/v) sorbitol solution in phosphate buffered saline (PBS), the second wash was in 1 ml of 5% (w/v) sorbitol solution in PBS, and the final wash was in 1 ml of complete media. The blood pellet was then re-suspended in complete media and added to a flask containing 0.5 ml of washed blood (50% haematocrit) and 10 ml of complete media (as described in section 2.1.5).

2.1.9 Culture synchronisation

Predominantly ring stage cultures were centrifuged for 5 minutes at 3,400 rpm for pellet recovery. A 5% (w/v) sorbitol solution in distilled water was prepared and filtered through a 0.22 μm filter and then added to the culture pellet. For every 1 ml of culture 9 ml of 5% sorbitol was added. The resuspended mixture was left at room temperature for 5 minutes and then centrifuged as previously described, the supernatant was discarded and the pellet was washed three times with complete media. Finally, the parasitized pellet was re-suspended in complete media to obtain a 50% haematocrit and a new culture was set up as previously described (section 2.1.5).

2.1.10 Percoll purification

Purifying late-stage parasites from the *in vitro* culture was carried out using a Percoll gradient centrifugation method adapted from Miao & Cui (2011). A 90% Percoll solution was obtained by adding 18 ml of Percoll (Percoll®, Sigma-Aldrich, UK) to 2 ml of 10xPBS solution. The solution was then filtered through a 0.22 μm filter. From this, 65% and 35% Percoll solutions were prepared with wash media.

A Percoll gradient was set up by layering 3 ml of 65% Percoll solution, then 3 ml of 35% Percoll and finally 3 ml of 5% haematocrit infected RBCs in a 15 ml Falcon tube. The layers were added very gently on top of one another. The solution was centrifuged at 14,000 rpm for 15 minutes. The top layer (media and debris) and the 35% Percoll solution were discarded. The late-stage parasites were recovered from the 35%/65% Percoll interface and transferred to a sterile microcentrifuge tube, washed three times with PBS - each time centrifuging at 1,200 rpm for 5 minutes - before experimental use.

2.2 Drug susceptibility assays

Although the gold standard for detecting and estimating malaria infection in RBCs is the microscopic examination of blood smears (Grimberg, 2011), less tedious and labour intensive methods were utilised during this study. The use of the fluorescent DNA dye SYBR Green (SG) was used in dose-response assays, relying on the lack of DNA present in RBCs and therefore fluorescence was attributed to parasitic DNA (Smilkstein *et al.*, 2004). Both a SG flow cytometer method and SG plate reader method has been previously optimised at the University of Salford laboratories (Matthews *et al.*, 2013), however further optimisation of the plate reader method was carried out.

2.2.1 Optimising the haematocrit levels of SG plate reader assay

The initial optimisation experiment carried out was to determine the effect two factors have on the SG plate reader assay; the haematocrit level and the medium used for the assay. Therefore an experiment was set up with two different haematocrit levels (5% and 2.5%) using two mediums (wash media and complete media).

The parasitaemia of a continuous culture was determined by blood smear (parasitaemia of ≥ 3% was required). The infected blood was centrifuged at 13,400 rpm for 90 seconds, the supernatant was removed and the blood re-suspended in either wash media or complete media at either 5% or 2.5% haematocrit.

Infected blood was then serially diluted in a 96-black well plate (flat bottom) with non-infected blood. Briefly 200 µl of infected RBCs was added to well 1 of the 96 well plate, a two-fold serial dilution was carried out leaving 100 µl per well (columns 1-10). Negative controls were also prepared and consisted of non-infected blood in both wash media and complete media.

One hundred microliters of SG solution (5x in PBS) was then added to each well. This gave a final volume of 200 µl per well and an adjusted SG concentration of 2.5x. The plate was then incubated in the dark at room temperature for 45 minutes prior to measuring the fluorescence intensity on a TECAN GENios Multifunction Fluorescence, Absorbance and Luminescence Microplate Reader. The plate reader was set to measure the fluorescence from the top, with gain set to 70 and excitation and emission wavelengths set to of 485 nm and 535 nm respectively.

2.2.2 Optimisation of media levels for SG plate reader assay

A second optimisation experiment was set up to determine whether reducing the final amount of media in the plate would reduce the interference in the fluorescence. A final haematocrit of 2.5% only was tested during this experiment.

As previously described a two-fold serial dilution of infected RBCs (parasitaemia ≥ 3%) and blood controls were added to the 96 well plate. However this time once the serial dilution was carried out, 100 µl of media (wash and complete) was then added to each well - not SG, which gave a final volume in each well of 200 µl and final haematocrit of 2.5% (only).

The 96 well plate was centrifuged for 5 minutes at 1000 rpm and then 150 µl of media was removed very carefully from each well without disturbing the blood at the bottom of the plate. This was then replaced by 150 µl of 3.33xSG in PBS - which gave a final concentration

of 2.5xSG in each well. The plate was then incubated in the dark for 45 minutes prior to measuring fluorescence by the plate reader as previously described.

Following the plate reader analysis, the samples were then analysed using the previously optimised flow cytometer method which is described in detail elsewhere (section 2.2.5). For the purpose of this experiment the flow cytometry method began with the fixation with formaldehyde step. Briefly, 100 µl from each well was placed in an Eppendorf tube with 250 µl of 0.37% formaldehyde in PBS and incubated at 4 °C for 15 minutes. The samples were then washed three times with PBS and then re-suspended in 1 ml of PBS prior to analysis on the flow cytometer.

2.2.3 Dose-response assay

For the dose-response experiments 96 well (flat bottom) plates were used, specifically black 96 well plates were used for the plate reader assay. Predominantly ring stage cultures were used for 72-hour incubation experiments.

Initially, 100 µl of drug solution (double the final concentration required) in complete media was added to each well. For dose-response experiments where two drugs were combined 50 µl of each drug was added to each well and concentrations were adjusted accordingly. This was followed by the addition of 100 µl of infected blood at 5% haematocrit and 1% parasitaemia. For both positive and negative controls 100 µl of complete media only was added to each well followed by 100 µl of 5% haematocrit infected blood for the positive controls and non-infected blood for the negative controls. This brought the total volume per well to 200 µl and final haematocrit level to 2.5%. The 96 well plate was placed in a humidifying chamber, gassed with 5% CO_2, 5% O_2 and 90% N_2 and incubated at 37 °C for 72 hours.

2.2.4 Adopted SG plate reader method

Based on the results of the optimisation experiments, the final version of the plate reader method was modified slightly in comparison with Matthews *et al*. (2013). Following the incubation of a dose-response experiment, 150 µl of media was removed from each well and

replaced with 150 µl of 3.33xSG in PBS. The plate was then incubated in the dark for 45 minutes prior to measuring fluorescence by the plate reader as previously described.

2.2.5 SG flow cytometer method

Following incubation with the drugs, 100 µl of 2.5% haematocrit culture was removed from each well and washed with 1 ml of PBS, centrifuged at 13,400 rpm for 90 seconds. Pellets were re-suspended in 1 ml of 2.5xSG in PBS and incubated in the dark at room temperature for 20 minutes. Samples were then centrifuged as previously described, supernatant was discarded and samples were re-suspended in 250 µl of 0.37% formaldehyde in PBS (Formaldehyde 36.5%, Sigma-Aldrich, UK). Finally, samples were washed three times in PBS prior to resuspension in 1 ml of PBS to be analysed using the FITC (Fluorescein isothiocyanate) channel of a BD FACs Verse flow cytometer system.

Fifty thousand events were recorded for each sample on the flow cytometer. The BD FACs suite software automatically produced a density plot of forward scatter (FSC) versus side scatter (SSC). The data was obtained using the FITC channel, blue laser excitation laser line 488 nm (BD Biosciences, 2015) by creating a dot plot consisting of FITC fluorescence versus FSC. Gating settings were conducted as described by Karl *et al.* (2009) and Matthews *et al.* (2013). Percentage parasitaemia for dose-response curves was calculated by obtaining the fluorescent events from within the gated regions against total number of events recorded.

2.2.6 Validating the SG plate reader method

In order to validate the reliability and reproducibility of both plate reader and flow cytometer methods, three dose-response experiments were set up using two antimalarial drugs (artemether and mefloquine) in addition to emetine dihydrochloride (emetine). Although not an antimalarial, emetine has shown interesting antimalarial activity (Matthews *et al.*, 2013). Results of the experiments were analysed using the traditional Giemsa-stained microscope slide method along with both SG flow cytometer and the adopted plate reader methods. Finally the obtained IC_{50} values were compared to published results.

2.3 Plate reader optimisation results

2.3.1 Optimising the haematocrit levels of SG plate reader assay

Results of the initial optimisation experiment are shown in Figure 2.1. The graphs show the parasite dilution on the x-axis and the relative fluorescence units (RFU) on the y-axis. Results before (A and B) and after (C and D) subtracting the background fluorescence (negative controls) are shown in the graphs. The results, particularly from the 5% haematocrit in complete media, echoes previous findings which reiterate the assumption that high haematocrit levels as well as Albumax present in complete media interfere with fluorescence measurements (Matthews *et al.*, 2013).

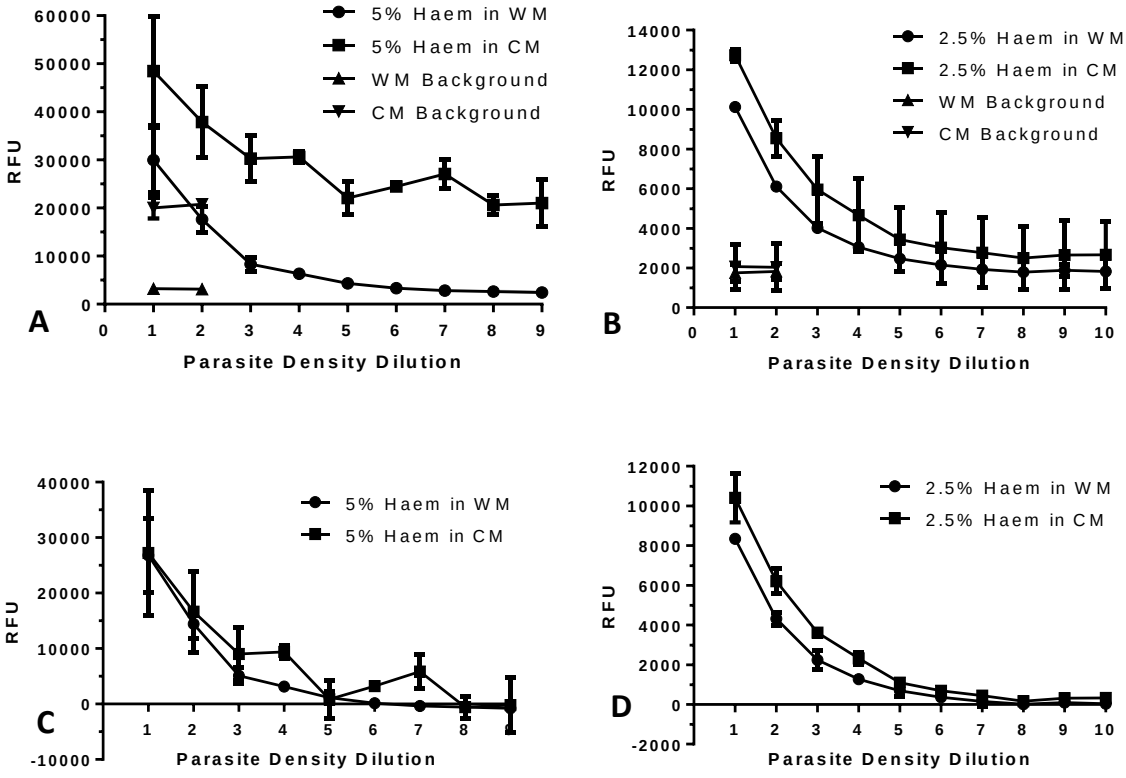

Figure 2.1 - Initial optimisation results of infected RBCs diluted in different mediums with varying haematocrit levels. *A and B) infected RBCs before subtracting the background fluorescence (negative control) at 5% haematocrit and 2.5 haematocrit levels, respectively; C and D) results after subtracting the background fluorescence at 5% haematocrit and 2.5 haematocrit levels, respectively. WM: wash media and CM: complete media. Error bars represent duplicate data points.*

2.3.2 Optimisation of media levels for SG plate reader assay

As a result of the initial optimisation experiment, a second experiment was set up and maintained at 2.5% haematocrit in both wash and complete media. This time however, more media (150 µl) was removed from each well and replaced with SG in PBS. The aim was to attempt to reduce the fluorescence interference that arises from complete media. The results were also analysed using the flow cytometer. The graphs in Figure 2.2 show the results from both plate reader and flow cytometer in wash media and complete media. The fluorescence results were transformed into percentages, with the first dilution (highest parasite density) being 100% and the rest relative to it.

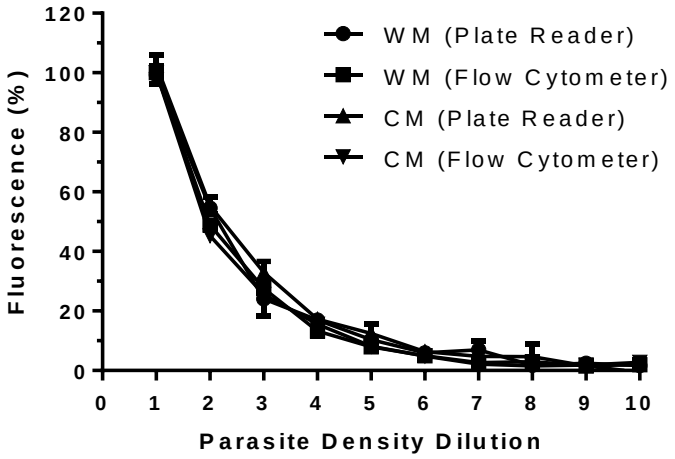

Figure 2.2 – Comparison between the plate reader results and the flow cytometer data.

The data suggests that by carrying out this method, enough media has been removed from each well to reduce background fluorescence to a negligible level. The results obtained from both types of media are comparable with each other and with the results obtained from the flow cytometer.

2.3.3 Validating the SG plate reader method

In order to confirm the validity of the plate reader method dose response experiments were set up and results were analysed using the adopted plate reader method, the flow cytometer

method and Giemsa-stained microscope slides method (Figure 2.3). The IC_{50} values obtained from each method were compared to results found in the literature (Table 2.1).

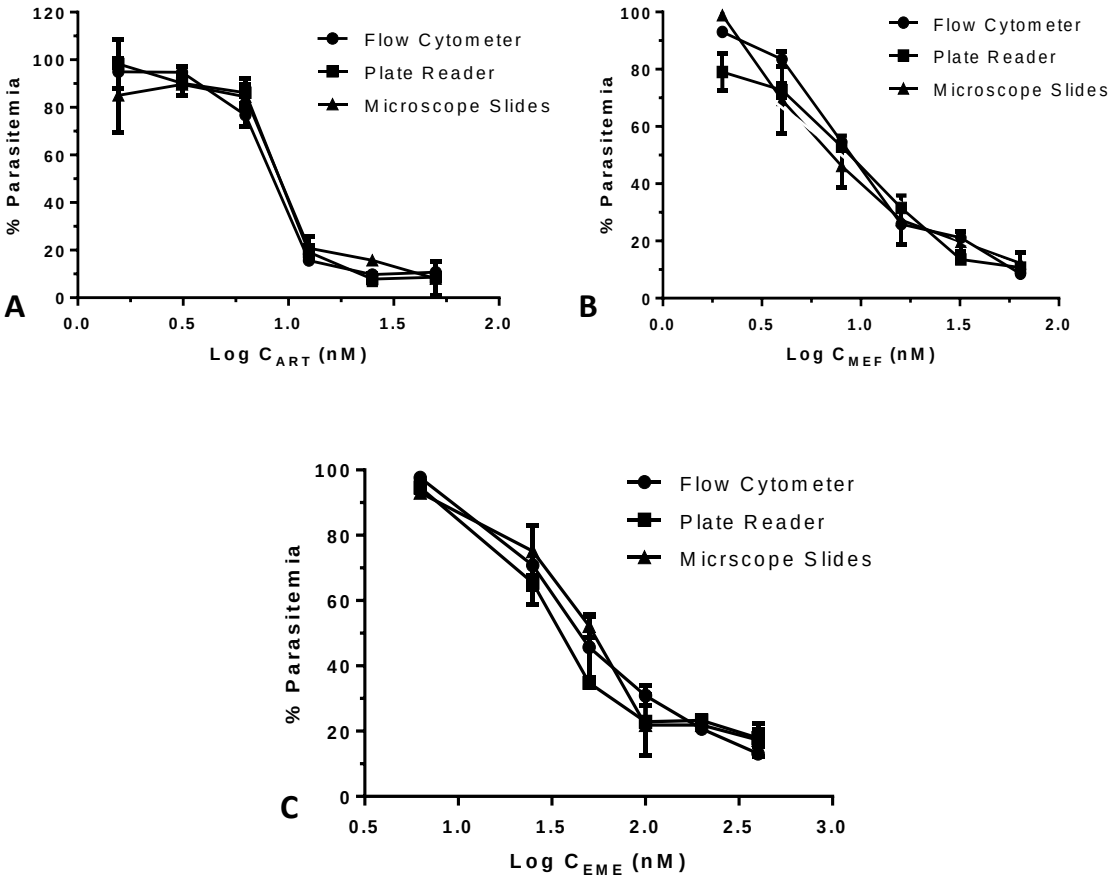

Figure 2.3 – Comparison of results obtained using flow cytometry, plate reader and Giemsa-stained microscope slides. *The results of artemether (ART), mefloquine (MEF) and emetine (EME) are shown in graphs A, B and C respectively.*

Drug	IC_{50} Values (nM)			
	Plate Reader	Flow Cytometer	Microscope Slides	Literature
Artemether (ART)	8.3 ± 4.2	7.6 ± 4.7	9.3 ± 4.3	7.6 (Otoguro *et al*. 2002) 1.8 (Akoachere *et al*. 2005)
Mefloquine (MEF)	7.9 ± 1.2	9.4 ± 1.8	8.1 ± 2.1	8.6 (Fivelman *et al*. 2002) 7.8 (Akoachere *et al*. 2005)
Emetine (EME)	47.8 ± 1.6	48.0 ± 6.8	47.1 ± 3.3	47.0 (Matthews *et al.* 2013)

Table 2.1 - Comparison of three IC_{50} values obtained using different methods.

The results obtained from the three different methods showed comparable results, with the obtained IC_{50} values being similar to published data. Therefore this was the adopted method used to carry out dose response experiments throughout this research.

2.4 Cytotoxicity test on mammalian cells

The cytotoxicity of the drugs was tested on the mammalian HepG2 (hepatocellular carcinoma) cells (Bokhari *et al.*, 2007).

2.4.1 Cell culture media

The media used to culture HepG2 cells consisted of RPMI-1640 supplemented with L-Glutamine and 25 mM HEPES (Gibco, Life Technologies, UK). Added to this was; 10% (v/v) foetal bovine serum (FBS, Gibco, Life Technologies, UK), 1% (v/v) non-essential amino acids (NEAA, Sigma-Aldrich, UK) and 1% penicillin streptomycin (Pen-strep, Sigma-Aldrich, UK).

2.4.2 Cultivation of HepG2 cells

As with the parasite cultures, cell culture work was carried out inside an ESCO Infinity Class II Biosafety cabinet. HepG2 cells were cultured in 25 cm^3 flasks in a final volume of 5 ml. The cells were sub-cultured every 48 or 72 hours. In brief, media was discarded from the flask, cells were washed with 3 ml of PBS and then incubated with 0.5 ml of Trypsin-EDTA (Sigma-Aldrich, UK) at 37 °C for approximately 5 minutes. Cells were monitored under the microscope to confirm they had detached. The cells were then re-suspended in 4.5 ml of fresh cell culture media, centrifuged for 5 minutes at 3,400 rpm and supernatant was discarded, cells were re-suspended in a further 5 ml of cell culture media and then split into new flasks at an approximately 1:3 dilution. Cells were incubated at 37 °C with 5% CO_2 in a LEEC Culture Safe Touch 190s CO_2 incubator.

2.4.3 MTT (Methylthiazol tetrazolium) assay

The MTT assay was used to determine the cytotoxicity of the compounds on human HepG2 cells. The assay was repeated several times as initial drug concentrations (same as the ones tested on parasites) were too low and did not attain IC_{50} values. Cells were plated onto a 96

well plate, 100 µl of cells in media were added to each well at a concentration of 5,000 cells/well. The plate was then incubated at 37 °C and 5% CO_2 overnight in order for cells to adhere to the wells.

For each compound tested 100 µl of drug solution was added to the wells, making the final volume per well 200 µl. The drugs were diluted in cell culture media, the final tested range was between 10-160 µM in a two-fold series dilution. For the control wells 100 µl of cell culture media was added. Additionally, a control drug (cisplatin) was tested with a two-fold series range between 0.39-25 µM. This was carried out in order to confirm the validity of the assay.

After the addition of the drug, the plate was incubated for 5 days at 37 °C and 5% CO_2. Following the incubation, 50 µl of MTT solution (3 mg/ml in PBS) was added to the wells and then incubated for a further three hours.

Following the three-hour incubation, solution from each well was carefully aspirated without disturbing the purple crystals formed at the bottom of the wells. The crystals were then dissolved in 200 µl of DMSO and the absorbance of the wells was read using two measurements 540 nm and 690 nm on a Multiskan Ascent plate reader. The absorbance figures were presented on the "Ascent software for Multiskan Ascent version 2.4.2". The absorbance at 690 nm is a background reference and was deducted from the 540 nm measurement to obtain the final results.

2.4 Drug Stocks

Commercially obtained compounds were reconstituted following the manufacturer's instructions, aliquoted into sterile vials at two concentrations (5 mM and 20 mM) and maintained at -20 °C unless stated otherwise. Artemether (Sigma-Aldrich, UK, MW: 298.37 g/mol), atovaquone (Sigma-Aldrich, UK, MW: 366.84 g/mol), doxycycline (Sigma-Aldrich, UK, MW: 480.90 g/mol), emetine hydrochloride (Sigma-Aldrich, UK, MW: 553.56 g/mol), fendiline hydrochloride (Alfa Aesar, UK, MW: 351.91 g/mol), FPL 64176 (Biotechne Ltd, UK, MW: 347.41 g/mol), mefloquine hydrochloride (Sigma-Aldrich, UK, MW: 414.77 g/mol) and nicardipine hydrochloride (Alfa Aesar, UK, MW: 515.99 g/mol) were dissolved in DMSO. Bay K8644 (Biotechne Ltd, UK, MW: 356.30 g/mol) and verapamil hydrochloride (Sigma-Aldrich, UK, MW:

491.06 g/mol) were dissolved in ethanol. Chloroquine diphosphate (Sigma-Aldrich, UK, MW: 515.86 g/mol) was prepared on the day of use, dissolved in sterile water and sterile filtered through a 0.22 µM filter prior to use. Diltiazem hydrochloride (Alfa Aesar, UK, MW: 450.98 g/mol) was dissolved in water and sterile filtered through a 0.22 µM filter prior to storing at -20 °C. Proguanil hydrochloride (Sigma-Aldrich, UK, MW: 290.19 g/mol) was dissolved in acetonitrile: water (60: 40). For dose response experiments all drugs were diluted in complete media and filtered through 0.22 µm filter before use.

2.5 Calculation of IC_{50} values

All data was initially tabulated using Microsoft Excel. For dose-response experiments on parasites, infected blood controls were set at 100% parasitaemia in order to calculate parasite reduction and determine IC_{50} values. Similarly for the MTT toxicity assays, the non-treated controls were set at 100% growth and used for determining cell reduction and IC_{50} value determination.

Subsequent analysis was performed on GraphPad Prism 6.0 by transforming drug concentrations to logarithmic scale and plotted against the dose response. IC_{50} values were calculated using non-linear regression (log (inhibitor) vs. normalized response).

Chapter 3
Investigating the antimalarial efficacy of fendiline and combinatorial regimes with commercially available drugs

3.1 Introduction

Chemotherapy, along with chemoprophylaxis, is at the forefront of reducing morbidity and mortality caused by malaria (Pradines *et al*. 2002b). Various approaches are being investigated to overcome the emergence of resistance. Of these approaches, one is to prolong the shelf life of existing antimalarials through combinatorial regimes. Another approach is to investigate mechanisms permitting resistance reversal to enable further use of existing compounds. Both these approaches are explored in this study.

3.1.1 Combination therapy

The complexity of biological systems means they are more susceptible to a combination of drugs rather than a single entity. The concept of combination therapy has been in practice for many years, dating back to traditional Chinese medicines, where mixtures of up to 20 herbs could be combined to treat an illness (Yuan and Lin, 2000). Advances in drug discovery and cell biology have heavily influenced and progressed drug combinations in modern medicine (Chou, 2006).

Combination therapy is believed to increase the therapeutic effect, overcome toxicity linked to high dose of a single entity and impede the development of resistance (Chou, 2006; Foucquier and Guedj, 2015; Jaeger *et al.*, 2017). Drug combinations are well established in several diseases such as cancer, diabetes, AIDs and others as well as malaria (Zimmermann, Lehár and Keith, 2007; Bulusu *et al.*, 2016). However there have been inconsistencies due to

the numerous methods and theories surrounding the set up and interpretation of drug combination experiments over the last century (Bell, 2005; Chou, 2010).

Despite the variation in approaches there is an accepted concept amongst scientists: when a combination of two or more compounds is administered simultaneously the results could be synergistic, additive or antagonistic. An additive effect is when the outcome of the combination is similar to the expected outcome of each drug individually. Whereas if the outcome is either better or worse than the additive effect it is said to be synergistic or antagonistic, respectively. Thus a unanimously accepted definition of "additive effect" is essential in order to have a unified definition of synergy and antagonism (Chou, 2006).

In a comprehensive review by Chou (2006) the common hazards and errors in drug combinations are discussed. For example, two compounds A and B are considered, when given alone drug A has an effect whereas drug B has none. When given in combination however, if the outcome is greater than the effect of drug A alone the interaction would not be synergistic, it would be classed as enhancement or potentiation (discussed in section 5.1.2). Furthermore, it is too naive to state that synergy is when A+B>A or A+B>B. Baeder *et al*. (2016) echoed this by stating that the growth of a pathogen decreases in a sigmoidal manner rather than a linear one and thus the additive effect of a drug cannot be simply added mathematically. That is to say if both drugs inhibited 60% of growth, the added effect could not be 120% (Chou, 2006).

As discussed by Foucquier & Guedj (2015) commonly used methods for testing drug combinations can be divided into two sections, *effect-based* methods and *dose-effect* based methods. Although there have been several approaches over the years, the two most popular are the Bliss Independence approach (*effect-based* method) and Loewe Additivity approach (*dose-effect* based method).

The *Bliss Independence* method assumes that drugs have different mechanisms of action and do not interact with one another, all the while achieving a common result. Using this method, the additivity for two drugs, A and B, administered in combination would equate to 1-[(1-A)(1-B)]. Therefore if both drugs had an effect of 50%, additivity would be 1-[(1-0.5)(1-0.5)] = 0.75 (Yeh *et al.*, 2009). In other words, when combined an effect of 75% is classed as additive. Combination results above or below this are classed as synergy or antagonism respectively

(Chou, 2006; Feng *et al.*, 2009; Yeh *et al.*, 2009; Foucquier and Guedj, 2015; Matthews *et al.*, 2017). This method however does not consider the shape of the curve (for example sigmoidal), which consequently could lead to contradictory conclusions from the combinatory effect of drugs (Chou, 2006; Yeh *et al.*, 2009; Foucquier and Guedj, 2015).

Loewe Additivity on the other hand advocates that a drug cannot interact with itself. If a drug is given in combination with itself the effect is always additive. Using this method a combination of two drugs is compared to the effect each drug has individually (Feng *et al.*, 2009; Yeh *et al.*, 2009; Yu *et al.*, 2015; Baeder *et al.*, 2016; Bulusu *et al.*, 2016).

This approach also considers the slope of the curve. Baeder *et al*. (2016) discussed that at both low and high concentrations of drug the slope is small, whereas the concentrations in between have a high slope value. Thus, when maximal effect has already been reached (small slope) adding a second drug will not produce a better overall effect. Using the Loewe Additivity approach this would not be classed as an antagonistic effect (Baeder *et al.*, 2016).

It is assumed using this approach that if the combination is additive then there are several ratios from each drug that can be administered in combination to exhibit a similar effect. Examples of these ratios would be; 0.5 of both drugs, 0.25 of drug A and 0.75 of drug B or 0.33 of drug A and 0.67 of drug B (Bulusu *et al.*, 2016).

By measuring each drug individually, the dose required to produce a given effect can be plotted on a graph. Whereby, concentration from drug A is plotted on the x-axis with the y-axis coordinate being zero, and vice versa for the concentration of drug B. Once this is complete, the two points can be connected by a line to present a line of additivity (isobole). Combination results are indicated on the same plot, depending whether the results fall below, on or above the isobole determines whether the combination is synergistic, additive or antagonistic respectively (Yeh *et al.*, 2009; Zhao, Au and Wientjes, 2010; Tallarida, 2012). Figure 3.1 gives a basic representation of the described isobologram.

The isobologram method gives a graphical approach to the Loewe additivity method. The combination index (CI) approach on the other hand provides an algebraic method to complement the isobologram (Foucquier and Guedj, 2015). To calculate the CI, the dose required to produce the IC_{50} effect in combination is divided by the dose required alone.

Therefore, CI = $\frac{a}{A} + \frac{b}{B}$ were *a* and *b* are the doses required in combination and *A* and *B* are the doses required to produce the same effect alone. If the combination is additive the CI would equal 1, values below or above 1 mean a synergistic or antagonistic effect, respectively (Chou, 2006; Yin *et al.*, 2014; Foucquier and Guedj, 2015; Bulusu *et al.*, 2016).

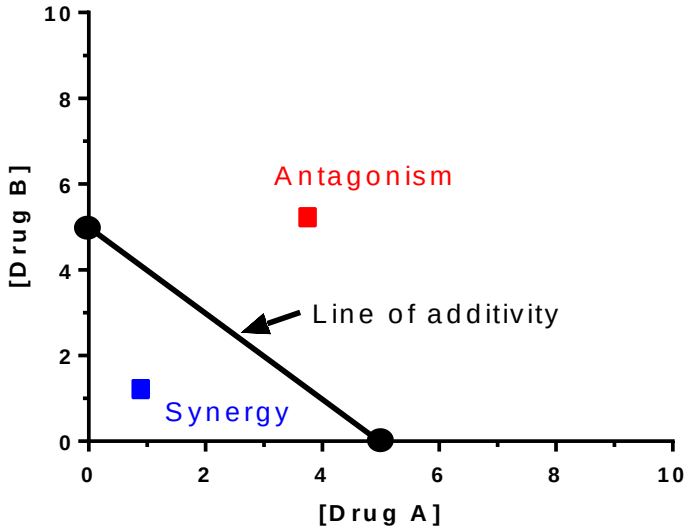

Figure 3.1 – Example of an isobologram. *Points on the axes represent the single dose of each drug (A and B) required to achieve effect (X). The single doses are used to connect the line of additivity. The combination results to produce the same effect (X) are plotted on the graph. Depending where they lie with respect to the line of additivity can be translated into synergy, antagonism or additivity.*

The lack of consistency in testing drug combinations is evident by the variety in published experiments and the differences in presentation of results (Bell, 2005; Harasym, Liboiron and D, 2010). Numerous published studies have reported antimalarial combination analysis using the Fractional Inhibitory Concentration (FIC) and sum of FIC (ΣFIC) (Canfield, Pudney and Gutteridge, 1995; Fivelman, Adagu and Warhurst, 2004; Bell, 2005; Gorka, Jacobs and Roepe, 2013; Desgrouas *et al.*, 2014). The ΣFIC is analogous to the CI method, with ΣFIC values equal to 1 meaning additive effect, and above or below 1 are antagonistic or synergistic respectively. According to Bell (2005) when ΣFIC values are much less than 1 there is no difficulty in assuming a synergistic interaction. When results are not as straightforward though, stating synergy or antagonism is more complicated. For this reason a cut-off value has been commonly used, which is ΣFIC < 0.5 is synergistic, ΣFIC > 2 or 4 is antagonistic and value in between as having no interaction (Bell, 2005; Vivas *et al.*, 2008; Co *et al.*, 2009; Tahar

et al., 2011). These values are arbitrary however (Bell, 2005; Meletiadis *et al.*, 2010) and are not used by all researchers (Ohrt *et al.*, 2002).

Discrepancies in setting up, analysing and interpreting drug combinations led to research by Chou and Talalay to devise a unified method for drug combinations. The outcome of years of work was the revised median effect equation, which is the unified form of four separate equations; the Michaelis-Menten equation, the Hill equation, the Henderson-Hasselbalch and Scatchard equations (Chou, 2006). Moreover, Chou and Talalay produced commercially available software programs (such as CalcuSyn and CompuSyn) which incorporate a series of complex algorithms and equations including the median effect equation, the combination index equation, the equation for the isobologram amongst others for dose-effect analysis (Chou, 2006).

By inputting the doses used and the fraction unaffected (fu), or fraction of live cells, the software produces a median effect plot. This is a transformation of the dose-effect curve into a linear regression line by plotting the log value of doses against the log value of the ratio of dead/live cells. The linear correlation coefficient (R), also produced by the software, gives an estimate to the conformity of the overall regression. This is carried out for each drug individually and in combination. The software takes into account the shape of the curve of each drug for the analysis (Chou, 2010).

Due to the emergence of resistance to current antimalarial drug combinations, the complicated process of drug discovery and the limited number of new drugs being approved, ideally, a novel combination with an already existing antimalarial would be attained. The availability of software programmes such as the ones produced by Chou and Talalay has provided a unified platform for scientists across the world to analyse combination data in an automated and unbiased manner.

3.1.2 Chloroquine reversal drugs

Reversal of drug resistance by other drugs was first reported by Tsuruo *et al*. (1981) where verapamil was found to enhance the efficacy of the anticancer drugs vincristine and vinblastine both *in vitro* and *in vivo*. Slater *et al*. (1982) also showed verapamil to enhance the anticancer drug daunorubicin. Soon after Martin *et al*. (1987) reported verapamil to reverse

chloroquine resistance in two *P. falciparum* chloroquine-resistant strains, however no effect was seen on chloroquine-sensitive strains. Since then, there have been several reports of drugs reversing chloroquine resistance *in vitro* on different *P. falciparum* strains such as; other CCBs – amlodipine, diltiazem and gallopamil (Basco and Le Bras, 1991; Ye and Van Dyke, 1994), the histamine H1 receptor antagonists chlorpheniramine and promethazine (Sowunmi *et al.*, 1997; Oduola *et al.*, 1998, 2004; Gbotosho *et al.*, 2008), the tricyclic antidepressant desipramine (Bitonti *et al.*, 1988) and the antipsychotic drugs chlorpromazine and prochlorperazine (Basco and Le Bras, 1992).

As previously discussed (Chapter 1, section 1.5.1), it is thought that chloroquine resistance in *P. falciparum* is associated with mutations in the membrane protein (PfCRT) of the digestive vacuole (DV). The physiological role of PfCRT is still not understood (Bakouh *et al.*, 2017), however, deleting the gene is not possible and thus it is believed to be essential in parasite growth (Sherlach and Roepe, 2014). Research has suggested it consists of 10 transmembrane domains and belongs to drug/metabolite transporter superfamily (Tran and Saier, 2004). The main mutation occurs at position 76 (K76T) in the first transmembrane helix which is located near the DV-end of the N-terminal (Peyton, 2012; Pulcini *et al.*, 2015). The location of this residue allows it to interact with drugs (and possibly other molecules) within the DV. Thus it is thought that losing the positively charged lysine residue allows the protonated chloroquine to leak out of the DV (Peyton, 2012; Pulcini *et al.*, 2015). Research by Juge *et al.* (2015) showed verapamil (and quinidine) to be competitive inhibitors of PfCRT which prevented transport of chloroquine, regardless of sensitivity of PfCRT to chloroquine.

Moreover, previous research carried out by (Bhattacharjee *et al.*, 2002) concluded that the pharmacophore of a chloroquine resistance reversal agent would consist of two aromatic rings and an aliphatic hydrogen bond acceptor (preferably a nitrogen). The majority of the above-mentioned chloroquine reversal agents fit into the description outlined by Bhattacharjee *et al.* (2002). Furthermore fendiline, a CCB like verapamil, diltiazem and other CCBs that have shown chloroquine reversal activity, also fits the description of Bhattacharjee *et al.* (2002). Therefore, the chloroquine reversal activity of fendiline was investigated during this study.

3.1.3 Aims

The aim of this study was to carry out novel combination studies between fendiline and clinically available antimalarial compounds and CCBs on *P. falciparum* parasites using the CalcuSyn-based combination assay. The objective was to find a synergistically active antimalarial combinatorial partner for fendiline. Additionally, a chloroquine potentiation assay was carried out in a bid to investigate fendiline's potential in reversing chloroquine resistance.

3.2 Methods

3.2.1 Dose-response assay for IC_{50} determination

Prior to carrying out combination studies, the IC_{50} values of the individual compounds were established using the SG plate reader method (see Chapter 2, section 2.2.4). The compounds tested were fendiline hydrochloride, the antimalarial compounds; artemether, atovaquone, chloroquine diphosphate, doxycycline, mefloquine, proguanil and the CCBs verapamil, diltiazem and nicardipine.

3.2.2 CalcuSyn combination assay for malaria

To confirm the validity of the CalcuSyn-based combination assay for malaria, a control experiment was carried out with an already existing synergistic combination: atovaquone and proguanil (Malarone®). Subsequently a series of combination experiments were set up between fendiline and existing antimalarial drugs and existing CCBs.

The CalcuSyn combination experiments were set up in such a way that seven concentrations were tested for each drug (alone and in combination). Two-fold serial dilutions were carried out with the middle concentration being the previously determined IC_{50} value of the drug. Thus three values above and below each IC_{50} were tested. Co-administration of drugs was carried out as a dilution series of a constant ratio (IC_{50}: IC_{50}). Experiments were set up using the SG plate reader method. Triplicate data from a minimum of two independent experiments

was converted to an average percentage and analysis carried out using the CalcuSyn software. The interpretation of the CI values followed the method outlined in Table 3.1.

Range of CI	Symbol	Description
<0.1	+++++	Very strong synergism
0.1-0.3	++++	Strong synergism
0.3-0.7	+++	Synergism
0.7-0.85	++	Moderate synergism
0.85-0.90	+	Slight synergism
0.90-1.10	±	Nearly additive
1.10-1.20	–	Slight antagonism
1.20-1.45	– –	Moderate antagonism
1.45-3.3	– – –	Antagonism
3.3-10	– – – –	Strong antagonism
>10	– – – – –	Very strong antagonism

Table 3.1 - Interpretation of the CI values that are produced by the CalcuSyn software. *(CalcuSyn manual, Biosoft, 2006).*

3.2.3 Chloroquine potentiation assay

To investigate whether fendiline would reverse chloroquine resistance in the K1 *P. falciparum* strain, a dose-response experiment was set up with chloroquine alone and chloroquine in the presence of fendiline at sub-inhibitory concentrations. Verapamil was also tested as a control. A two-fold serial dilution of chloroquine ranging from 12.5-1000 nM was used. Fendiline was added at two constant concentrations 1000 nM and 500 nM, whereas verapamil was tested at 1000 nM. The SG plate reader method was used for this experiment.

3.2.4 Cytotoxicity assay

The chloroquine potentiation experiment was repeated, however this time on human HepG2 cells using the MTT assay to determine the cytotoxicity of the concentrations used. Details of carrying out the MTT assay are described elsewhere (Chapter 2, section 2.4.3).

3.3 Results

3.3.1 Dose-response assay

The IC_{50} values of fendiline, the current antimalarial compounds and CCBs were established and are summarised in Table 3.2 along with values reported in the literature. The values obtained were comparable to the published data.

Drug	Mechanism of Action	IC_{50} Value (nM)	Literature IC_{50} Value (nM)	References
Fendiline hydrochloride	**CCB**	3740 ± 640	N/A	N/A
Artemether	**Antimalarial**	8.24 ± 1.13	7.60 1.76	(Otoguro *et al.*, 2002) (Akoachere *et al.*, 2005)
Atovaquone	**Antimalarial**	2.21 ± 0.98	2.41 1.30	(Fivelman *et al.*, 2002) (Cohen *et al.*, 2015)
Chloroquine diphosphate	**Antimalarial**	147.79 ± 20.43	133.29 357.00 500.00	(Fivelman *et al.*, 2002) (Otoguro *et al.*, 2002) (Cohen *et al.*, 2015)
Doxycycline	**Antimalarial & Antibiotic**	9,935 ± 2761	5000 6000	(Cohen *et al.*, 2015) (Gellis *et al.*, 2016)
Mefloquine	**Antimalarial**	7.35 ± 0.69	8.55 7.80	(Fivelman *et al.*, 2002) (Akoachere *et al.*, 2005)
Proguanil	**Antimalarial**	15,740 ± 3163	10240 34266	(Fivelman *et al.*, 2002) (Fivelman *et al.*, 2004)
Diltiazem	**CCB**	20,310 ± 6210	11995 on W2[a] strain 24549 on D6[b] strain	(Kyle *et al.*, 1990) (Kyle *et al.*, 1990)
Nicardipine	**CCB**	2830 ± 951	~ 800 - 1000	(Matthews, 2015)
Verapamil	**CCB**	10,700 ± 3413	28,530 on K1 strain 13200 on W2[a] strain	(Wirjanata *et al.*, 2017) (Pradines *et al.*, 2002b)

Table 3.2 - IC_{50} values of current antimalarial drugs and CCBs against P. falciparum K1 strain parasites, along with the published values. *Where values for the K1 strain were not found in the literature other P. falciparum strains were reported; [a]W2 strain is resistant to chloroquine, quinine, pyrimethamine, cycloguanil and sulfadoxine (Rathod, McErlean and Lee, 1997) and [b]D6 strain is reported to be sensitive to common antimalarials (Rathod, McErlean and Lee, 1997). (n ≥ 2).*

3.3.2 CalcuSyn combination assay for malaria

The combination results were analysed using the CalcuSyn software which generates data based on the effective dose (ED_{50}). ED_{50} is a term synonymous with IC_{50}. Therefore throughout the results and discussion section of the CalcuSyn-based experiments the terms will be used interchangeably.

Validating the combination assay using an ATQ-PG control

Atovaquone-proguanil, a known synergistic antimalarial combination, was tested as a positive control for the CalcuSyn-based experiments, results are presented in Figure 3.2 and Table 3.3. The compounds were tested at a constant ratio (ED_{50}:ED_{50}) and the results obtained by the CalcuSyn software show synergy at all three points (ED_{50}, ED_{75} and ED_{90}) with the results at ED_{50} and ED_{75} levels of inhibition showing strong synergy.

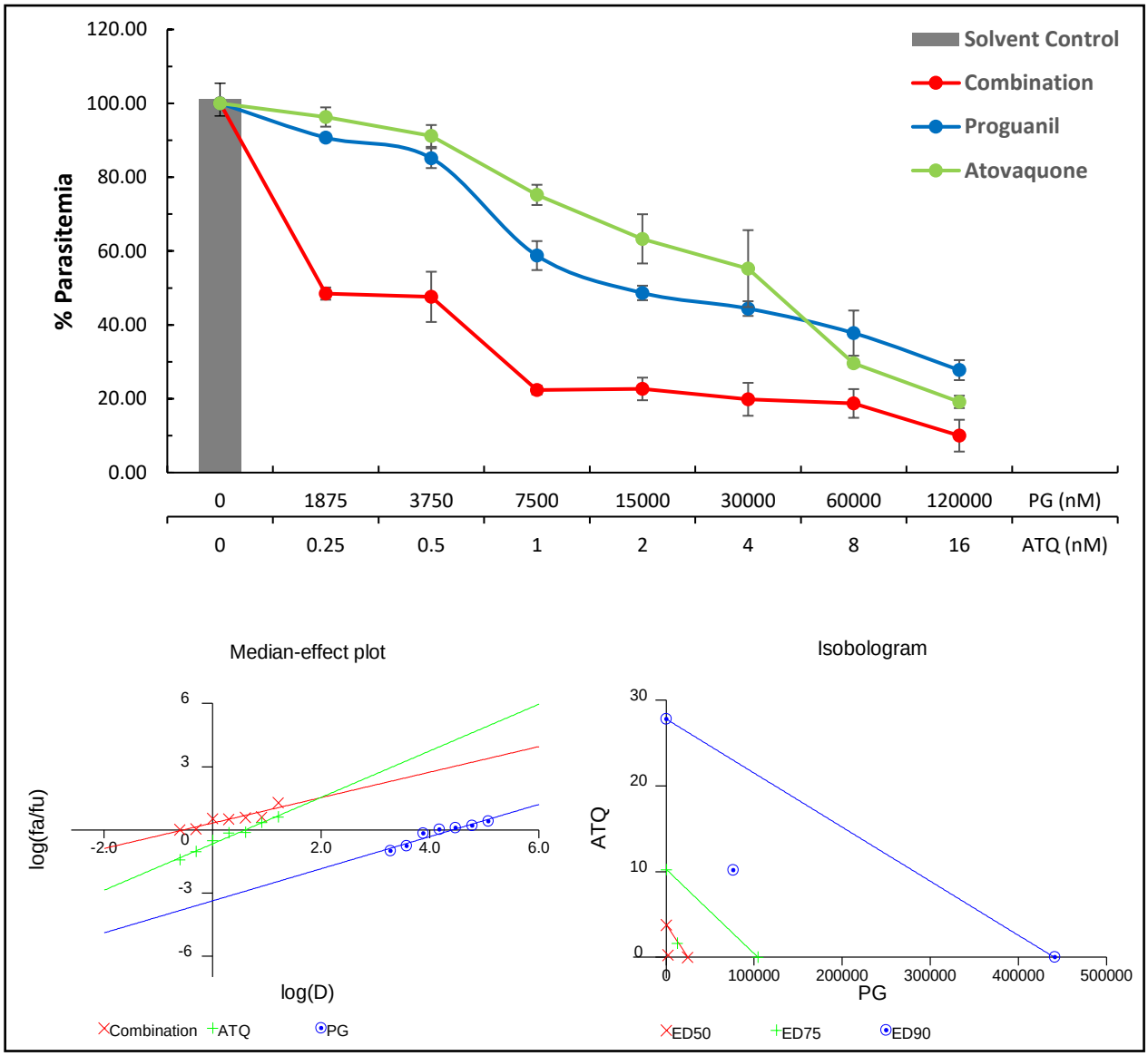

Figure 3.2 – Results of the positive control combination assay between atovaquone (ATQ) and proguanil (PG), incubated at a constant ratio (1: 7500). *The image shows, A) the raw data of the combination assay along with the CalcuSyn output B) median effect plot and C) isobologram.*

Drug	CI Values at			Dm	m	R
	ED_{50}	ED_{75}	ED_{90}			
ATQ	N/A	N/A	N/A	3.789	1.102	0.986
PG	N/A	N/A	N/A	24643	0.761	0.953
ATQ + PG (1: 7500)	0.152	0.279	0.540	0.268	0.604	0.914

Table 3.3 - The Combination Index (CI) values for the control experiment between atovaquone and proguanil. *The tabular data compliments the graphs in Figure 3.2 which was generated by the CalcuSyn software. Dm is the median effect dose (ED_{50}), m represents the sigmoidicity of the curve (were m = 1, > 1 or < 1 indicates hyperbolic, sigmoidal or negative sigmoidal respectively) and R is the linear correlation coefficient of the median effect plot.*

Combination of fendiline with existing antimalarial drugs

The combination of fendiline with six existing antimalarials was carried out and analysed using the CalcuSyn software (Figures 3.3-3.8 and Tables 3.4-3.9). For each experiment seven concentrations were tested, two-fold serial dilutions were carried out with the IC_{50}s for each drug falling in the midpoint of the dilution. The combinations were maintained at a constant ratio.

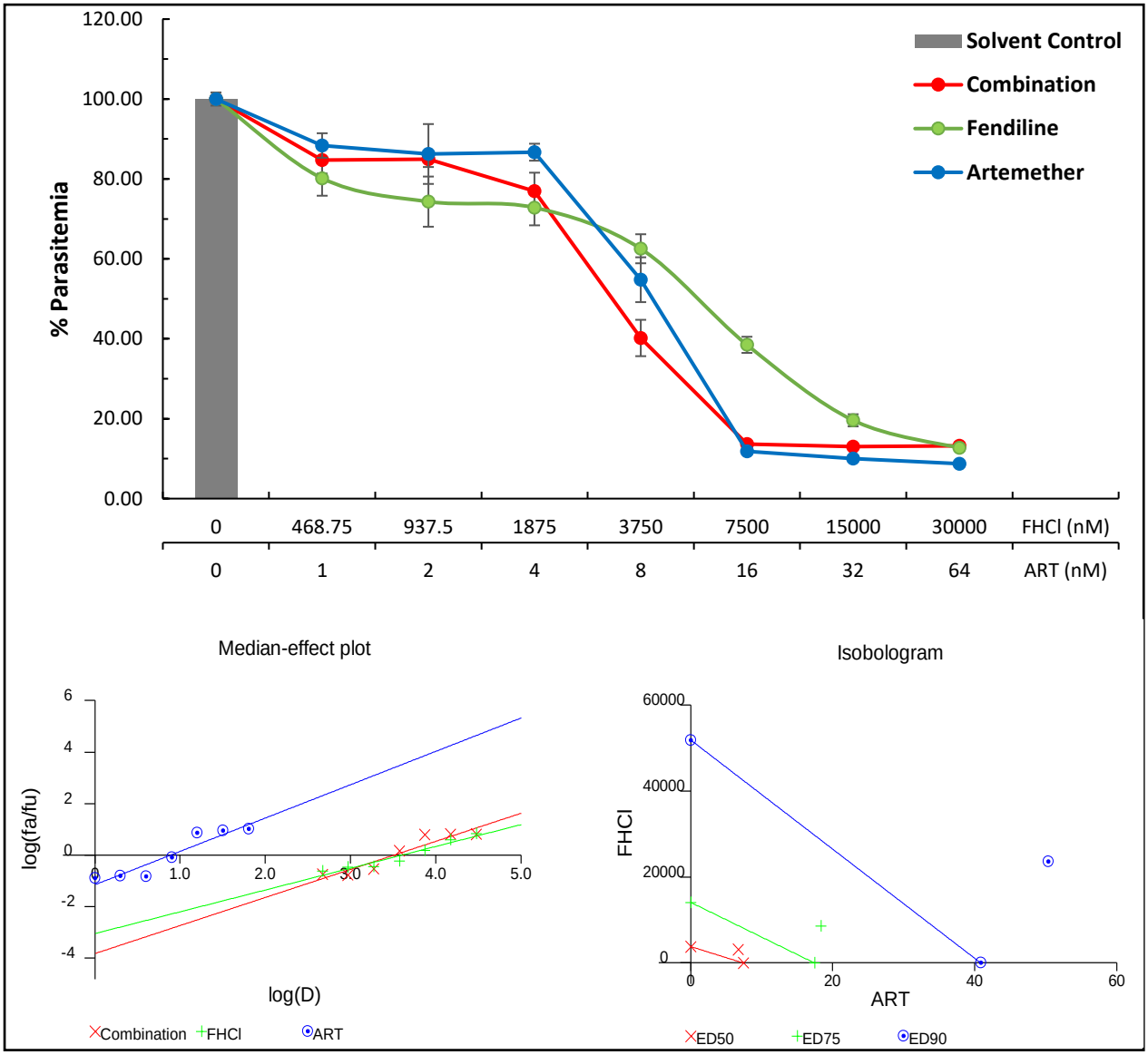

Figure 3.3 - The CalcuSyn-based combination assay between fendiline (FHCl) and artemether (ART). *Combinations were carried out at a constant ratio (468.75: 1). Graphs show the raw data (A), the CalcuSyn generated median effect graph (B) and the isobologram (C).*

Drug	CI Values at			Dm	m	R
	ED_{50}	ED_{75}	ED_{90}			
FHCl	N/A	N/A	N/A	3844.138	0.844	0.967
ART	N/A	N/A	N/A	7.468	1.292	0.941
FHCl + ART (468.75: 1)	1.709	1.658	1.686	3130.770	1.088	0.944

Table 3.4 - The CI values determined by the CalcuSyn software for the combination of fendiline and artemether. *The Dm, m and R values generated by the CalcuSyn software are also shown.*

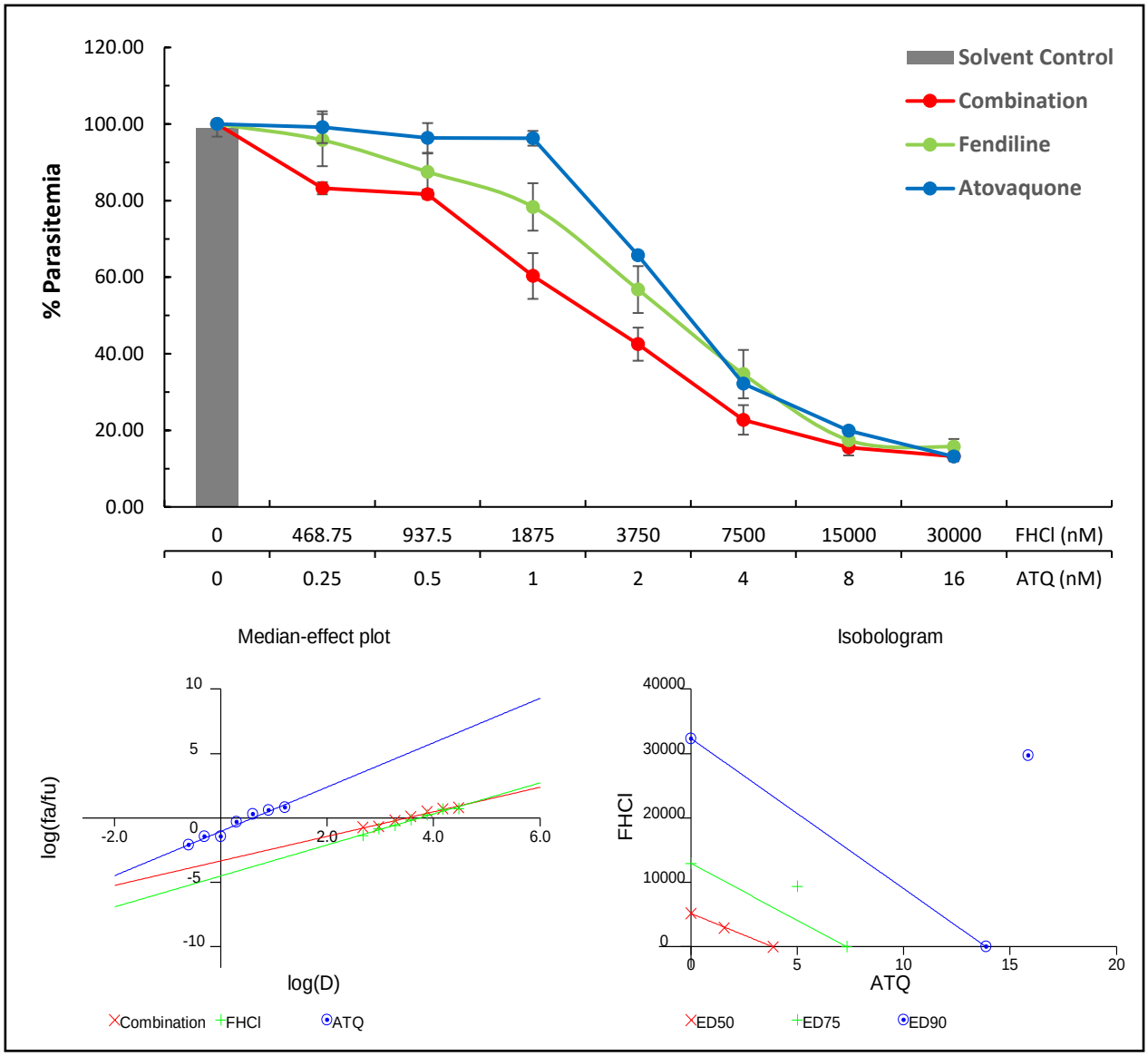

Figure 3.4 - The CalcuSyn-based combination assay between fendiline and atovaquone (ATQ). *Combinations were carried out at a constant ratio (1875: 1). Graphs show the raw data (A), the CalcuSyn generated median effect graph (B) and the isobologram (C).*

Drug	CI Values at			Dm	m	R
	ED_{50}	ED_{75}	ED_{90}			
FHCl	N/A	N/A	N/A	5207.005	1.203	0.990
ATQ	N/A	N/A	N/A	3.870	1.719	0.976
FHCl + ATQ (1875: 1)	0.975	1.404	2.061	2955.041	0.952	0.983

Table 3.5 - The CI values determined by the CalcuSyn software for the combination of fendiline and atovaquone.

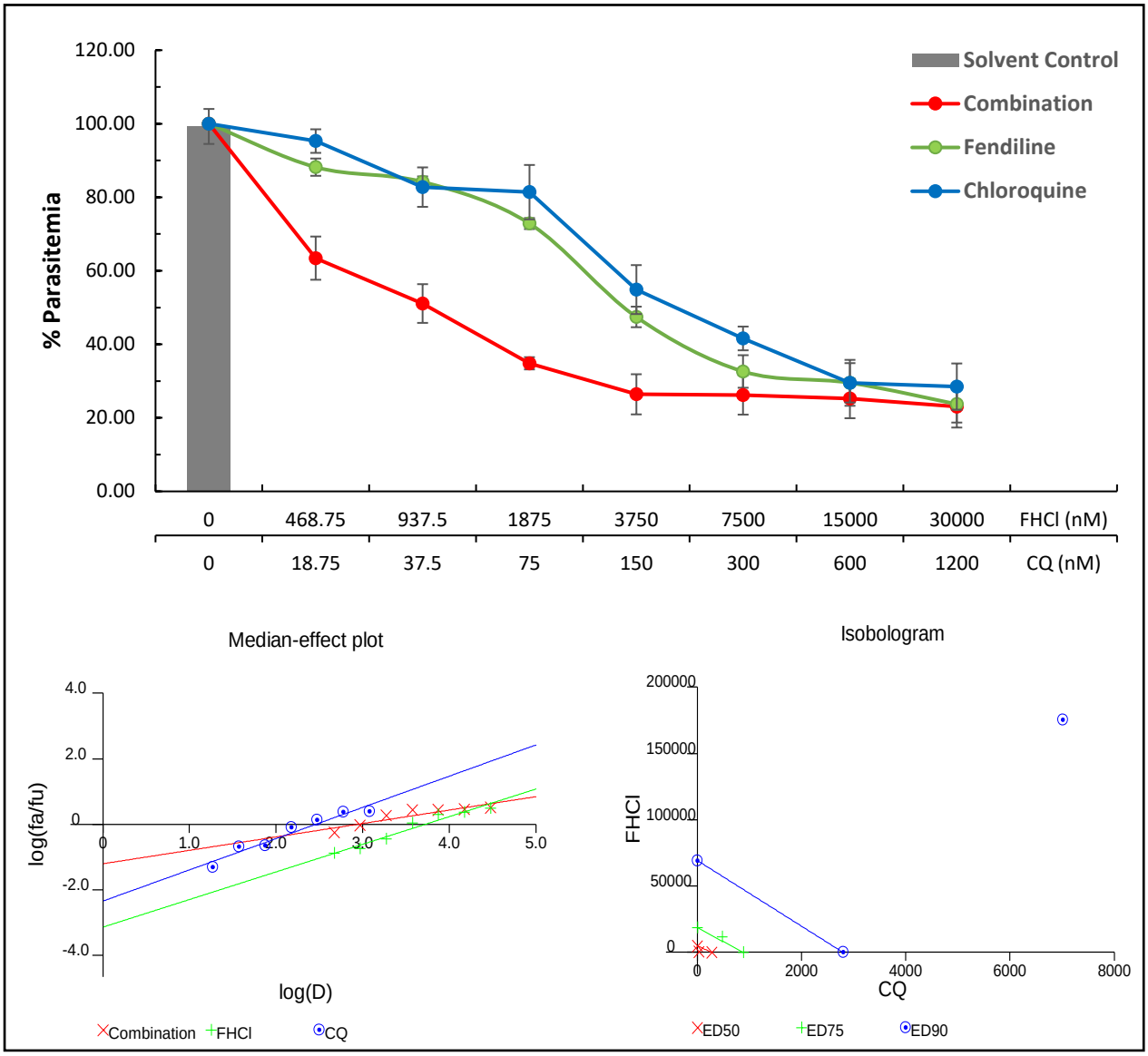

Figure 3.5 - The CalcuSyn-based combination assay between fendiline and chloroquine (CQ). *Combinations were carried out at a constant ratio (25: 1). Graphs show the raw data (A), the CalcuSyn generated median effect graph (B) and the isobologram (C).*

Drug	CI Values at			Dm	m	R
	ED_{50}	ED_{75}	ED_{90}			
FHCl	N/A	N/A	N/A	5091.999	0.841	0.976
CQ	N/A	N/A	N/A	278.217	0.951	0.968
FHCl + CQ (25: 1)	0.276	1.174	5.031	811.027	0.409	0.911

Table 3.6 - The CI values determined by the CalcuSyn software for the combination of fendiline and chloroquine.

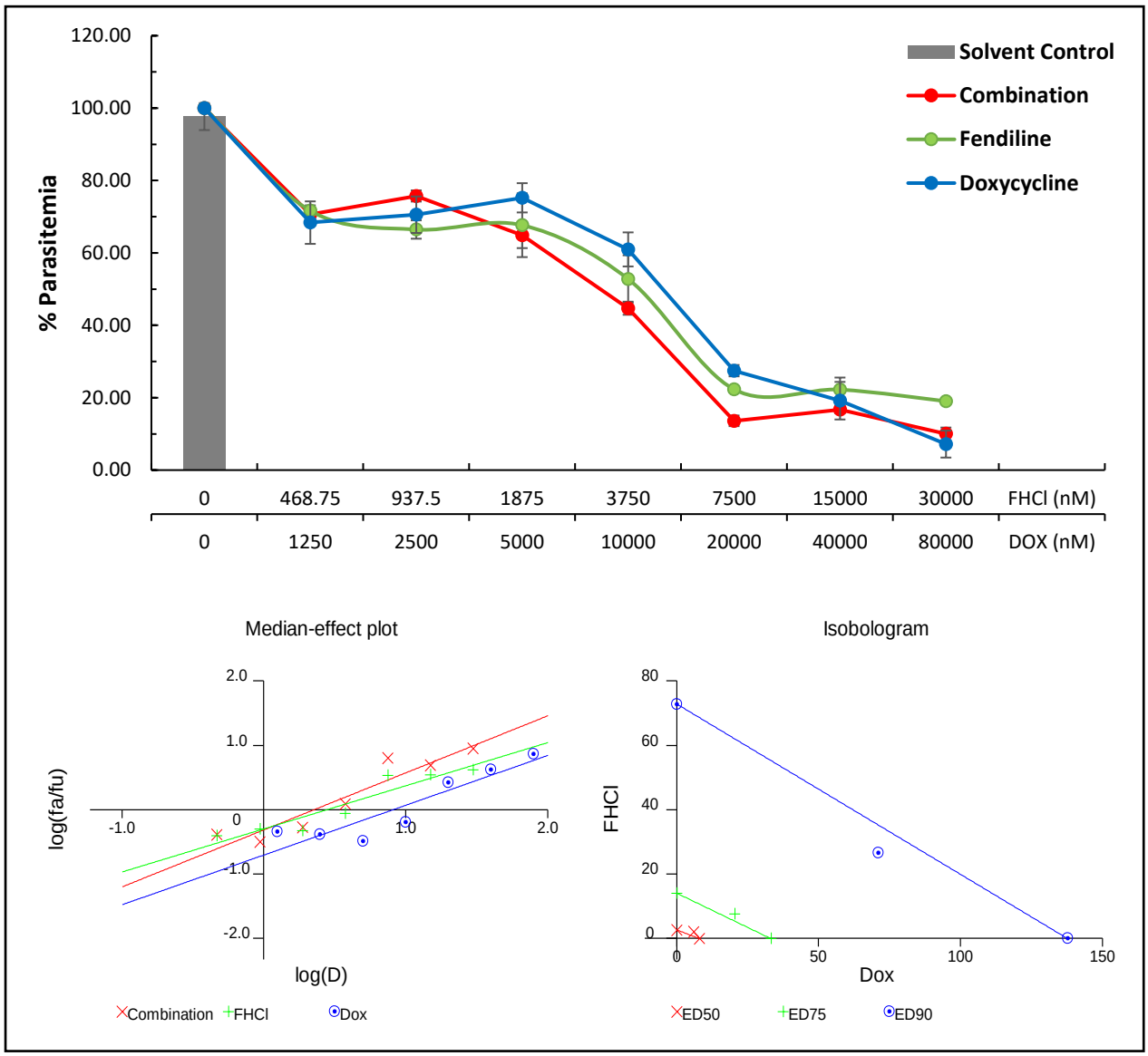

Figure 3.6 - The CalcuSyn-based combination assay between fendiline and doxycycline (DOX). *Combinations were carried out at a constant ratio (1: 2.67). Graphs show the raw data (A), the CalcuSyn generated median effect graph (B) and the isobologram (C).*

Drug	CI Values at			Dm	m	R
	ED_{50}	ED_{75}	ED_{90}			
FHCl	N/A	N/A	N/A	2729.320	0.670	0.942
DOX	N/A	N/A	N/A	8009.520	0.772	0.916
FHCl + DOX (1: 2.67)	1.557	1.165	0.882	2224.660	0.885	0.944

Table 3.7 - The CI values determined by the CalcuSyn software for the combination of fendiline and doxycycline.

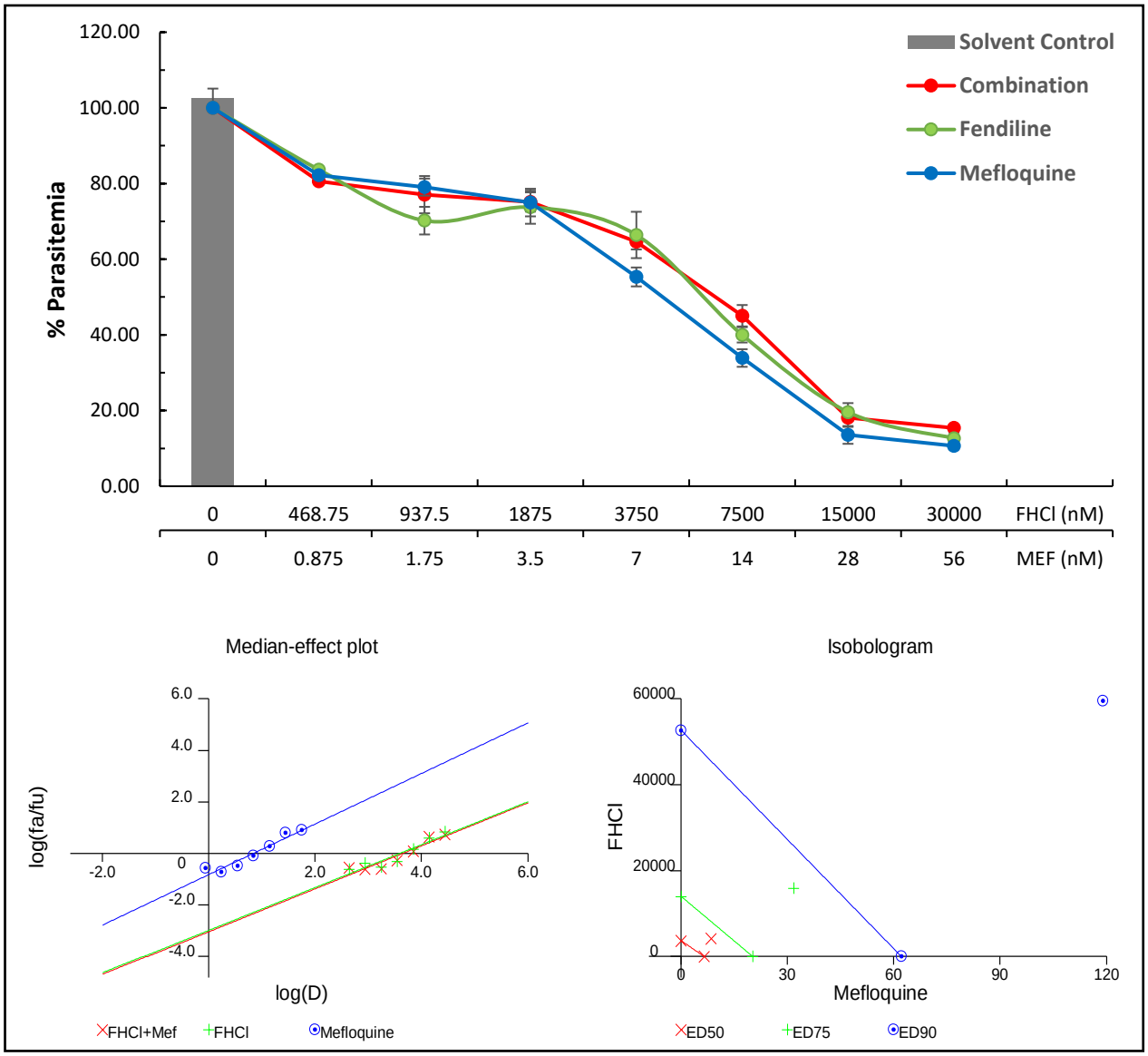

Figure 3.7 - The CalcuSyn-based combination assay between fendiline and mefloquine (MEF). *Combinations were carried out at a constant ratio (535.71: 1). Graphs show the raw data (A), the CalcuSyn generated median effect graph (B) and the isobologram (C).*

Drug	CI Values at			Dm	m	R
	ED_{50}	ED_{75}	ED_{90}			
FHCl	N/A	N/A	N/A	3744.982	0.831	0.942
MEF	N/A	N/A	N/A	6.613	0.980	0.960
FHCl + MEF (535.71: 1)	2.429	2.706	3.044	4265.842	0.834	0.937

Table 3.8 - The CI values determined by the CalcuSyn software for the combination of fendiline and mefloquine.

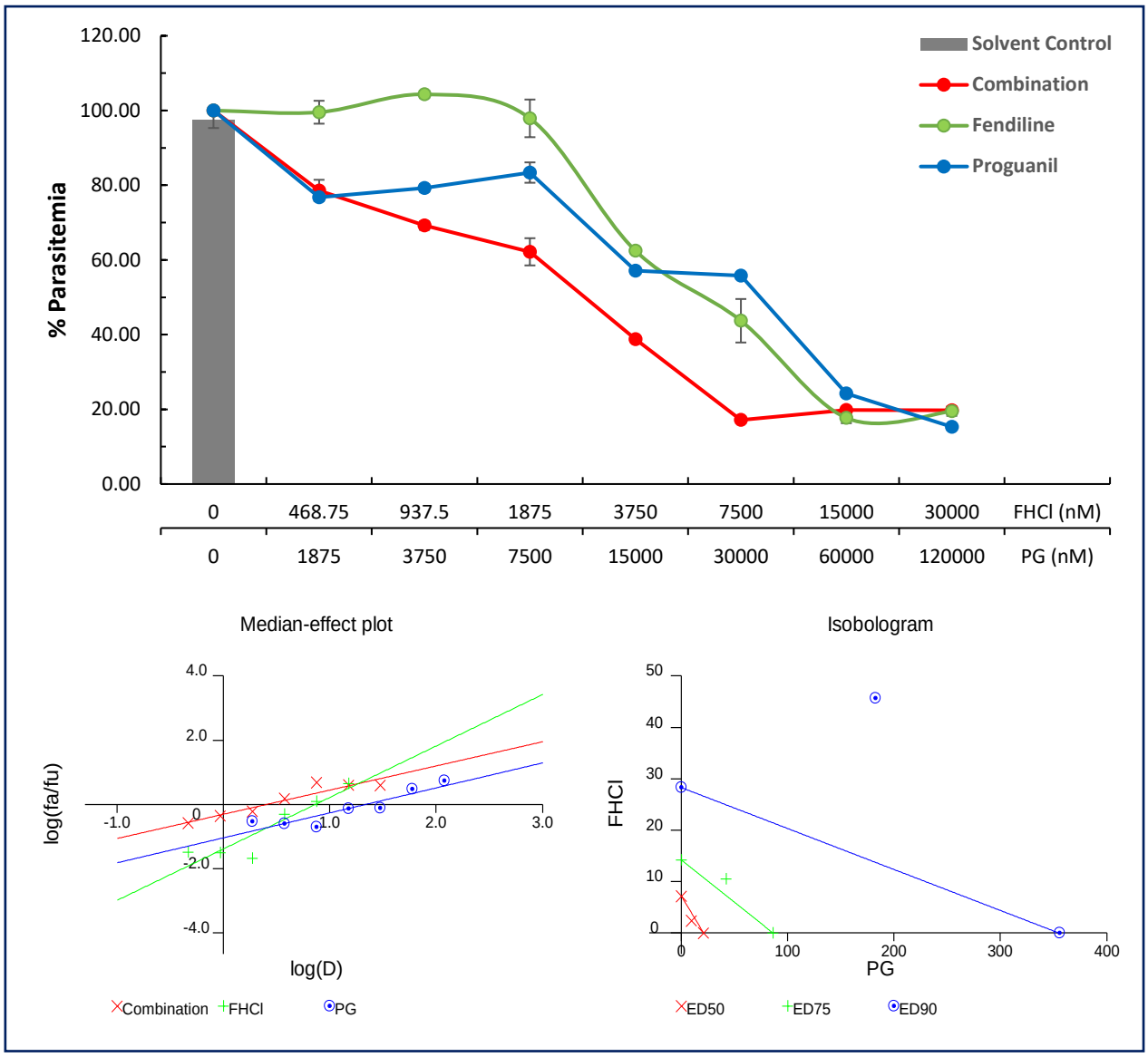

Figure 3.8 - The CalcuSyn-based combination assay between fendiline and proguanil (PG). *Combinations were carried out at a constant ratio (1: 4). Graphs show the raw data (A), the CalcuSyn generated median effect graph (B) and the isobologram (C).*

Drug	CI Values at			Dm	m	R
	ED_{50}	ED_{75}	ED_{90}			
FHCl	N/A	N/A	N/A	7176.180	1.600	0.915
PG	N/A	N/A	N/A	20990.670	0.776	0.913
FHCl + PG (1: 4)	0.811	1.233	2.125	2457.890	0.752	0.946

Table 3.9 - The CI values determined by the CalcuSyn software for the combination of fendiline and proguanil.

The combination of fendiline with existing antimalarial drugs showed either an additive or antagonistic effect. The results of fendiline-proguanil and fendiline-doxycycline showed the combinations to have slight synergistic interaction at ED_{50} and ED_{90} levels respectively, whereas remaining combinations showed either nearly additive or antagonistic effects with CI values ranging from 0.975-3.044. The exception to this was fendiline-chloroquine; at ED_{50} level the interaction between the two compounds showed strong synergism with the CI value being 0.276. However above ED_{50} level the drug interactions showed less positive outcomes, with both ED_{75} (CI = 1.174) and ED_{90} (CI = 5.031) showing moderate and strong antagonistic interactions respectively.

Combination of fendiline with existing calcium channel blockers

CalcuSyn-based combination experiments were set up between fendiline and three existing CCBs. As with the previous experiments, a constant ratio dose was applied using the previously established IC_{50} values. The results are presented in Figures 3.9-3.11 and Tables 3.10-3.12.

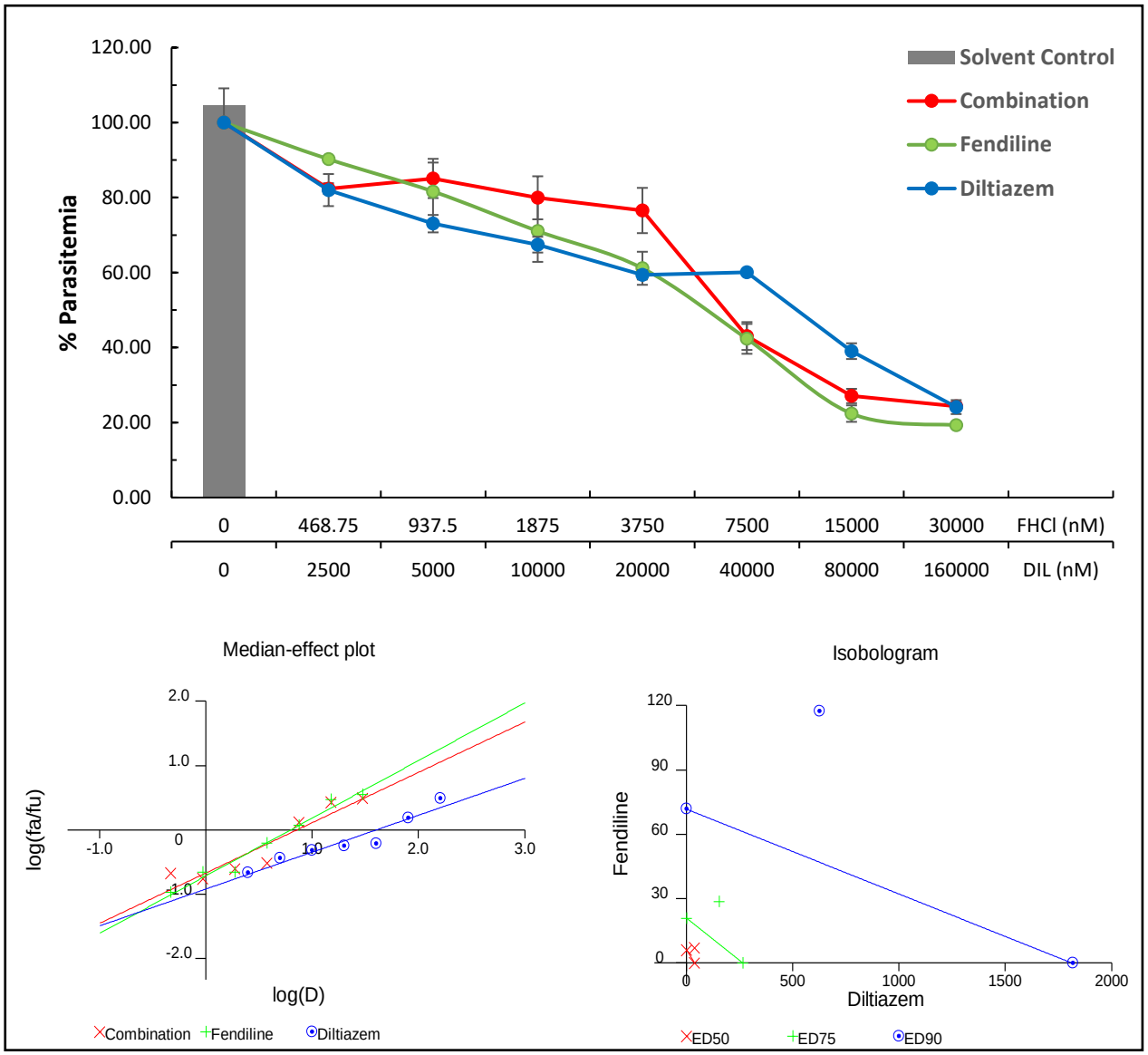

Figure 3.9 - The CalcuSyn-based combination assay between fendiline and diltiazem (DIL). *Combinations were carried out at a constant ratio (1: 5.33). Graphs show the raw data (A), the CalcuSyn generated median effect graph (B) and the isobologram (C).*

Drug	CI Values at			Dm	m	R
	ED_{50}	ED_{75}	ED_{90}			
FHCl	N/A	N/A	N/A	6157.264	0.894	0.985
DIL	N/A	N/A	N/A	39111.743	0.572	0.954
FHCl + DIL (1: 5.33)	2.104	1.943	1.979	7045.617	0.781	0.936

Table 3.10 - The CI values determined by the CalcuSyn software for the combination of fendiline and diltiazem.

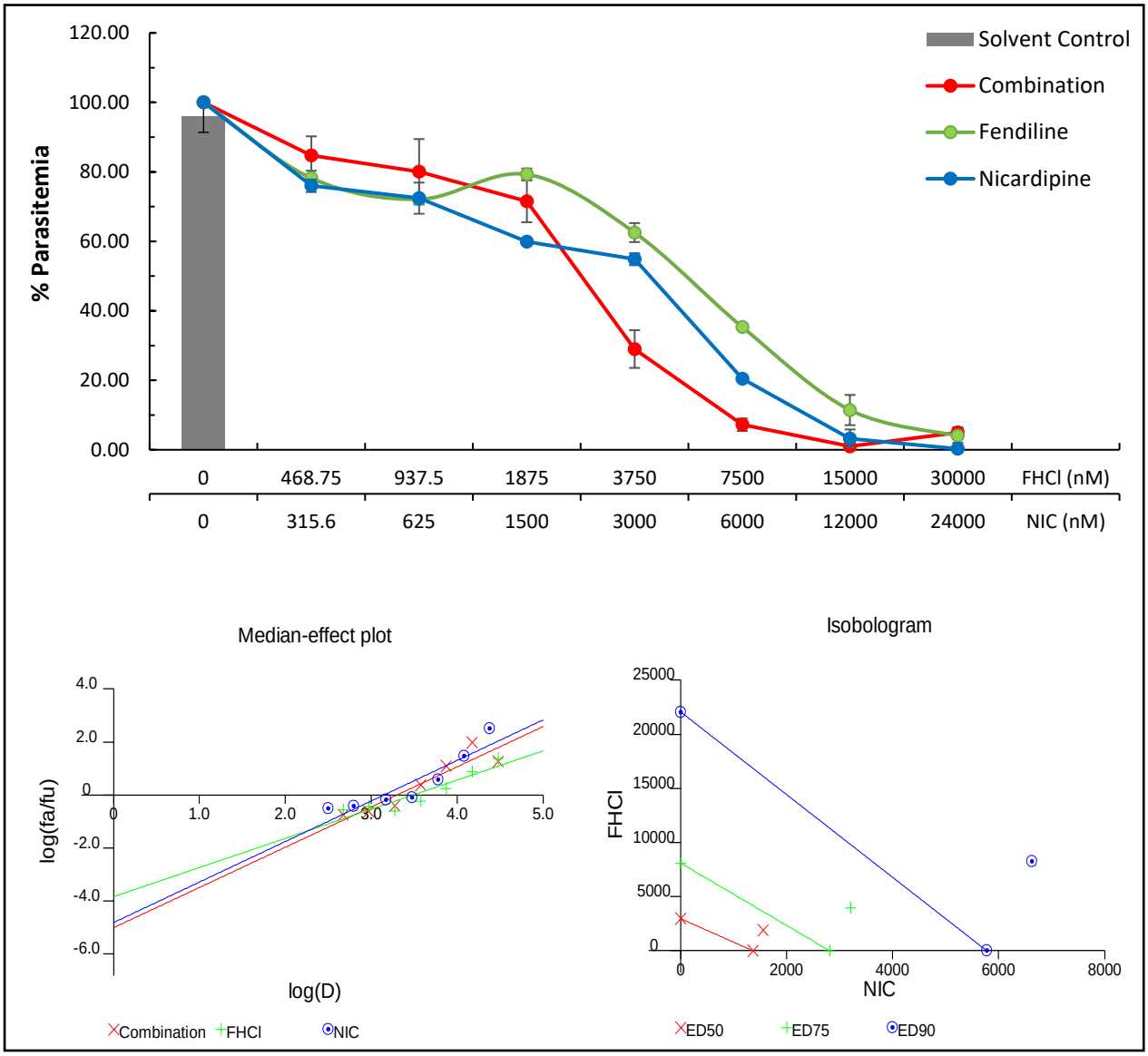

Figure 3.10 - The CalcuSyn-based combination assay between fendiline and nicardipine (NIC). *Combinations were carried out at a constant ratio (1.25: 1). Graphs show the raw data (A), the CalcuSyn generated median effect graph (B) and the isobologram (C).*

Drug	CI Values at			Dm	m	R
	ED_{50}	ED_{75}	ED_{90}			
FHCl	N/A	N/A	N/A	2985.111	1.098	0.928
NIC	N/A	N/A	N/A	1371.585	1.527	0.919
FHCl + NIC (1.25: 1)	1.784	1.634	1.521	1942.951	1.527	0.928

Table 3.11 - The CI values determined by the CalcuSyn software for the combination of fendiline and nicardipine.

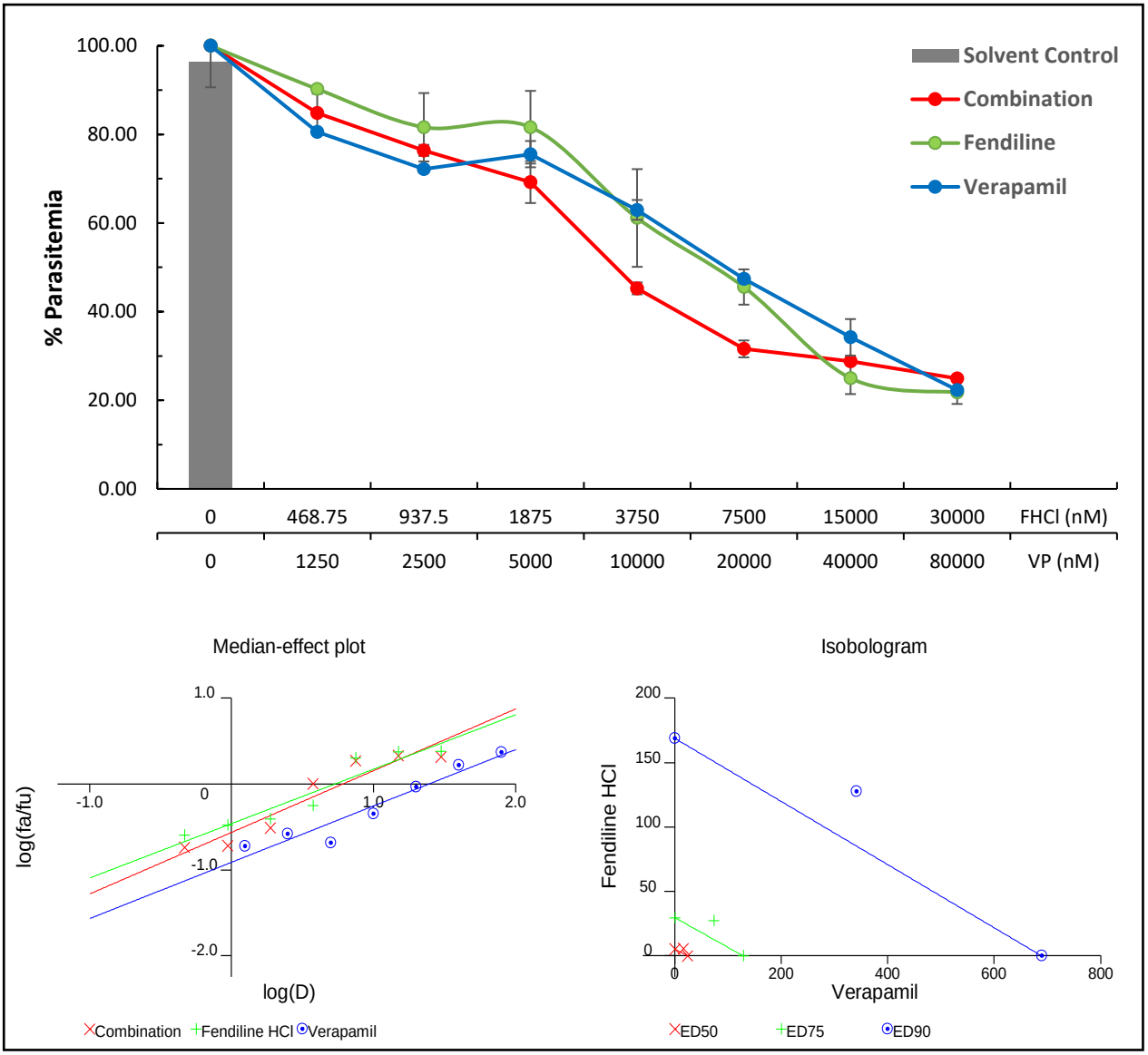

Figure 3.11 - The CalcuSyn-based combination assay between fendiline and verapamil (VP). *Combinations were carried out at a constant ratio (1: 2.67). Graphs show the raw data (A), the CalcuSyn generated median effect graph (B) and the isobologram (C).*

Drug	CI Values at			Dm	m	R
	ED_{50}	ED_{75}	ED_{90}			
FHCl	N/A	N/A	N/A	5245.450	0.633	0.953
VP	N/A	N/A	N/A	24137.550	0.655	0.961
FHCl + VP (1: 2.67)	1.802	1.501	1.252	5979.900	0.717	0.950

Table 3.12 - The CI values determined by the CalcuSyn software for the combination of fendiline and verapamil.

The combination of other CCBs with fendiline did not show synergistic effect against *P. falciparum* parasites. The results all gave an antagonistic effect with combination indices ranging from 1.252-2.104.

An overall summary of the tested fendiline combinations highlighting the combination indices and their interpretation at the ED_{50} and ED_{75} level of inhibition can be seen in Table 3.13.

Combination of fendiline with:	CI at:		Interpretation
	ED_{50}	ED_{75}	
Antimalarial agents:			
Chloroquine	0.28	1.17	Strong synergism/ Slight antagonism
Proguanil	0.81	1.23	Slight synergism/Slight antagonism
Atovaquone	0.98	1.40	Nearly additive/Moderate antagonism
Artemether	1.71	1.66	Antagonism
Doxycycline	1.56	1.17	Antagonism
Mefloquine	2.42	2.71	Antagonism
CCBs:			
Diltiazem	2.10	1.94	Antagonism
Nicardipine	1.78	1.63	Antagonism
Verapamil	1.80	1.50	Antagonism

Table 3.13 - Summary of the CI values of all combination assays carried out between fendiline and existing antimalarials and CCBs.

3.3.3 Chloroquine potentiation assay

The results from the chloroquine potentiation assay are presented in Figure 3.12. Fendiline showed similar activity to verapamil at reducing the IC_{50} value of chloroquine significantly at both concentrations, 1000 and 500 nM. Verapamil reduced chloroquine IC_{50} by 5.9-fold, fendiline reduced the IC_{50} by 6.37 and 6.88-fold at 500 nM and 1000 nM respectively (Table 3.14). The results show triplicate data from three independent experiments.

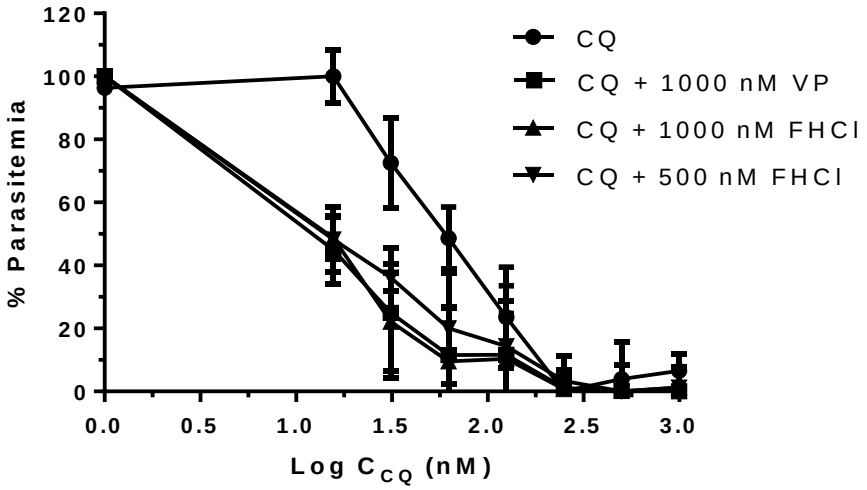

Figure 3.12 – Results of the chloroquine potentiation assay of verapamil and fendiline.

Drug	IC_{50} (nM)
CQ	143.37 ± 6.17
CQ + 1000 nM VP	24.09 ± 5.87
CQ + 1000 nM FHCl	20.85 ± 0.72
CQ + 500 nM FHCl	22.49 ± 2.05

Table 3.14 - IC_{50} values of chloroquine alone and in combination with verapamil or fendiline.

3.3.4 Cytotoxicity assay

The MTT cytotoxicity assay was carried out on HepG2 cells to determine whether the doses used for the potentiation assay have a toxic effect on human cells. This was done as an initial experiment to determine the safety of using fendiline and chloroquine in combination using these doses. Figure 3.13 shows the graph of the results obtained. The doses required to reverse chloroquine resistance with fendiline exhibited no cytotoxic effect on the human HepG2 cells, with approximately 100% growth detected at the highest concentration of chloroquine used.

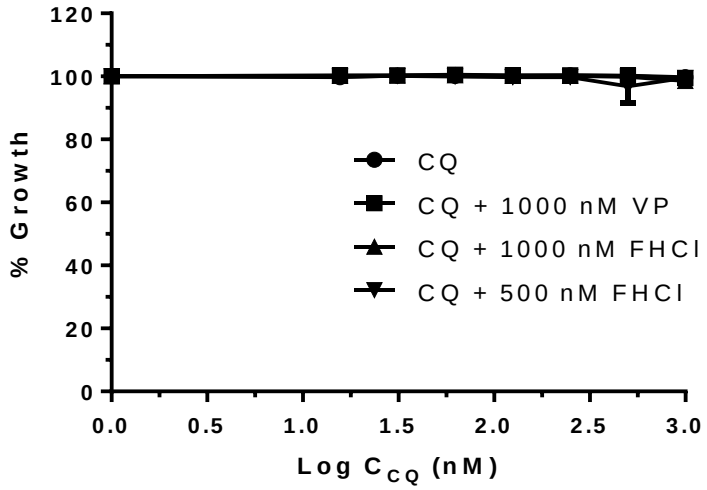

Figure 3.13 - Results of the MTT assay of chloroquine in combination with either verapamil or fendiline at a constant concentration.

3.4 Discussion

3.4.1 CalcuSyn combination assay

The search for novel, safe and cheap therapies to treat malaria is a priority for malaria endemic countries. This has driven researchers to consider alternative routes to develop and introduce novel drugs into the market such as; drug repositioning or prolonging the efficacy of existing drugs by combining them with non-toxic, cheap resistance reversal agents (Crandall, Charuk and Kain, 2000).

Moreover, CCBs as a class of drugs have demonstrated various biological activities in addition to their clinical use of hypertension and angina. Studies have shown CCBs to possess interesting activity with osteoarthritis (Takamatsu *et al.*, 2014), Parkinson's disease (Ritz *et al.*, 2010), Alzheimer's disease (Corbett, Williams and Ballard, 2013) and Ebola infections (Johansen *et al.*, 2015) to mention a few. Therefore the aim of this study was to investigate the efficacy of fendiline, a previously developed CCB on the *P. falciparum* parasite and carry out drug interaction experiments in a bid to discover a novel synergistic combination.

The CalcuSyn-based combination assay presented in this study relies on predetermining accurate IC_{50} values of the component drugs. The antimalarial activity of fendiline on the K1

P. falciparum strain resulted in an IC_{50} value of 3.74 ± 0.64 µM. At the time of this report, there had been no published study of the antimalarial effect of fendiline. However recent research on fendiline found it to have antifungal (Samantaray *et al.*, 2016) and antileishmanial (Reimão *et al.*, 2016) activity both within the micromolar range. Therefore the value obtained for its antimalarial parasitic activity appears to be in keeping with its biological activity on other organisms.

Often during combination studies, the interaction at IC_{50} level is considered a good indicator of the outcome of the combination, whereas some argue that interactions at the IC_{90} or IC_{99} are more accurate indicators. It is thought that high doses correspond to plasma concentrations that the parasite population would be susceptible to *in vivo* (Fivelman, Adagu and Warhurst, 2004). On the other hand, it can be argued that when using fluorescent dyes to carry out dose-response experiments a margin of error should be allowed. Background noise is inherent when carrying out fluorimetric and colorimetric based assays (Johnson *et al.*, 2007). Fluorescence from the media, haematocrit levels or even some drugs can slightly affect the values obtained when measuring parasite growth, particularly when reaching high levels of drug activity such as IC_{90} and IC_{99} levels where differences in parasitaemia are less detectable (Smilkstein *et al.*, 2004; Matthews *et al.*, 2017).

Although the CalcuSyn software calculated the CI at ED_{50}, ED_{75} and ED_{90} levels, in the summarised table of results (Table 3.13) the ED_{50} and ED_{75} levels of inhibition were selected only. The CI values were interpreted following the Chou-Talalay method outlined in Table 3.1, briefly CI values <, = or > 1 denote synergistic, additive or antagonistic interaction.

The combination study of fendiline with existing antimalarial drugs and CCBs showed an overall majority of antagonistic interactions. Combinations with proguanil and atovaquone showed slight synergism and nearly additive interactions at the ED_{50} level, however the remaining levels were antagonistic. The exception to this was chloroquine, a strong synergistic effect was seen at the ED_{50} level yet as with other samples the higher concentrations showed an antagonistic effect.

Combining fendiline with existing antimalarial drugs and CCBs has not been reported in the literature therefore a direct comparison could not be drawn. However, Reimão *et al*. (2016) carried out combination assays using the FIC method between fendiline and current antileishmanial drugs which resulted in a similar outcome of indifferent and antagonistic interactions.

It is possible that CCBs as a whole, and for this study fendiline specifically, interact with several targets within a cell and thus interfere with the activity of other drug targets leading to an antagonistic relationship. Investigations by Eastman *et al.* (2016) into the combination of dihydroartemesinin and a selection of four commercially available CCBs and a Na^+ blocker resulted in either additive or antagonistic interactions also. The study was carried out on two *P. falciparum* strains, Dd2 and HB3. The Dd2 strain is resistant to chloroquine, mefloquine and pyrimethamine whereas HB3 parasites are resistant to pyrimethamine but not chloroquine and mefloquine (Sun *et al.*, 2014). The conclusion of the study by Eastman *et al.* (2016) suggested CCBs and Na^+ blockers shared transport pathways or mode of action with dihydroartemesinin derivatives. The research suggested that the parasites genetic information such as PfCRT and PfMDR1, and mutations within these genes, could affect the combination outcomes (Eastman *et al.*, 2016).

3.4.2 Chloroquine potentiation assay

The fendiline-chloroquine combination results were interesting, the synergistic interaction at low dose warranting further investigation. Especially as chloroquine potentiation has been reported when using low concentrations of the reversing agent (Martin, Oduola and Milhous, 1987; Martiney *et al.*, 1995; Wirjanata *et al.*, 2017). These results in addition to the fact that other CCBs have also acted as reversing agents led to the chloroquine potentiation assay being carried out.

The results of the assay showed chloroquine reversal properties similar to those reported in the literature. The 5.95-fold reduction in chloroquine IC_{50} in the presence of verapamil (1000 nM) is comparable to the 5.65-fold difference reported by Wirjanata *et al.* (2017) on the K1 strain. Likewise Martiney *et al*. (1995) showed verapamil to reduce chloroquine IC_{50} by an average of 73 ± 6% in chloroquine resistant (Dd2) strain. Martiney *et al*. (1995) also proposed

that the reversal of chloroquine resistance and the antimalarial mechanism of action of verapamil were not related.

Fendiline was more effective at reducing chloroquine's IC_{50} than verapamil, 6.37-fold compared to 5.95, at half the concentration (500 nM). When fendiline was used at 1000 nM, it reduced the IC_{50} by 6.88-fold. These concentrations of fendiline showed no toxicity on human HepG2 cells.

Research carried out by Juge *et al.* (2015) showed that verapamil and quinidine both inhibited chloroquine transport by PfCRT from both chloroquine sensitive and resistant strains. The authors suggested that verapamil and quinidine were competitive inhibitors of PfCRT (Juge *et al.*, 2015). Moreover, research by Bellanca *et al.* (2014) studied interactions between quinine, chloroquine and verapamil with PfCRT from Dd2 *P. falciparum* strains. The results indicated mixed-type inhibition, in other words the binding of one drug to the PfCRT reduced the affinity, however did not fully inhibit the binding of a second drug. The study showed in the presence of verapamil the PfCRT complex transported chloroquine at a rate that was 30-fold lower than in the absence of verapamil. Thus reiterating the theory that some mutations, such as K76T, that result in chloroquine resistance allow the protein to interact with a variety of structurally diverse compounds (Bellanca *et al.*, 2014).

Fendiline, like verapamil, is an LTCC blocker. Comparison between the two drugs has been carried out using patch-clamp tests on rat ventricular cardiomyocytes. The study by Nawrath *et al.* (1998) showed fendiline to be a weaker CCB than verapamil under physiological conditions. This was due to the fact that fendiline inhibits channels in the open state more favourably than the closed state. In contrast, verapamil acted on the closed state. Under physiological conditions, channels are 90% more likely to be closed than open, hence the difference in potency between the two drugs (Nawrath *et al.*, 1998).

Despite the differences in activity, both fendiline and verapamil are believed to target the α_1 subunit of the LTCC (Nawrath *et al.*, 1998). The present finding could suggest that fendiline acts in a similar manner to verapamil; reversing chloroquine resistance by binding to the PfCRT protein. Both compounds are believed to have similar mechanisms of action on calcium channels, they fit the pharmacophore described by Bhattacharjee *et al.* (2002) of a

chloroquine reversal agent. Additionally, the strain used in this study (K1) has been reported to have the K76T mutation (Ojurongbe *et al.*, 2007) thus further supporting the hypothesis.

It is important to note however, although the concept of chloroquine reversal agents is interesting and does provide a positive aspect to the malaria resistance issue, according to Ye, Van Dyke and Rossan (2013) several of the *in vitro* tested chloroquine reversing agents were not successful *in vivo*. An example of this was seen in a study carried out by Warsame *et al*. in 1992, where 53 patients divided into two groups received either chloroquine alone or chloroquine in combination with desipramine (a tricyclic antidepressant). The outcome showed no difference in parasite clearance between the groups and thus did not complement the *in vitro* studies of chloroquine potentiation using desipramine (Bitonti *et al.*, 1988). The group suggested higher desipramine concentrations may be effective however toxicity would be a major concern (Warsame, Wernsdorfer and Björkman, 1992).

There are several potential explanations for the lack of success of reversing agents *in vivo*, primarily the complexity of biological systems in the absorption, distribution, metabolism and excretion of a drug combination in comparison with the *in vitro* testing. Additionally as discussed by Pereira *et al.* (2011), the concentration required to potentiate chloroquine activity with these agents *in vivo* is often within the concentration required for their own pharmacological activity, thus concerns for toxicity are a major obstacle. Ye, Van Dyke and Rossan (2013) conclude that the dose required for verapamil to reverse chloroquine resistance in humans would exhibit cardiac toxicity thus making it an unrealistic combinatory agent.

It is noteworthy however that half the concentration of fendiline is required to exert a similar effect to verapamil *in vitro*, in addition to the fact that under physiological conditions fendiline is less active against rat cardiomyocytes (Nawrath *et al.*, 1998). These outcomes would potentially favour fendiline to verapamil as a reversal agent candidate and thus warrant further investigation.

There have been alternatives suggested for chloroquine resistance reversing agents. One example is the study carried out by Burgess *et al.* in 2006 where hybrid compounds consisting of a chloroquine-like moiety linked to a reversing agent were synthesised. The rationale for synthesising such a compound would be that the chloroquine-like compound and the

reversing agent would be delivered at a one-to-one ratio to the site of action, it would reduce the risk of drug-drug interactions, simplify the pharmokinetics and subsequently reduce the dose required compared to when both drugs are given separately (Burgess *et al.*, 2006; Boudhar *et al.*, 2016). More recently, Boudhar *et al.* (2016) reported synthesising and testing the biological activity of a range of hybrid compounds maintaining the chloroquine scaffold. The study went on to test the solubility and permeability of the lead candidate, however *in vivo* toxicology studies are yet to follow. Despite the potential of such compounds, the likelihood of a candidate reaching the market and becoming a successful antimalarial drug is still a long way off. According to Agarwal, Gupta and Awasthi (2017) there is no report of hybrid compounds in either clinical trials or preclinical development. Additionally, the group comment that the majority of published papers have not carried out control experiments were a fixed dose combination assay between the two individual drugs has been carried out alongside the hybrid compound. Furthermore, the group point out that hybrid compounds would be bulkier compounds in general compared to individual compounds thus hindering the passage into the parasite (Agarwal, Gupta and Awasthi, 2017). Therefore, despite there being alternatives to combining reversal agents with existing drugs they are a long way from becoming the routinely prescribed drugs to treat malaria.

3.4.3 Conclusion

The CCB fendiline exhibited low micromolar activity on the *P. falciparum* multi-resistant K1 strain. Combination studies with current antimalarial and CCB drugs showed mainly additive and antagonistic effects except for the combination with chloroquine which resulted in a strong synergistic interaction at the IC_{50} level of inhibition. The obtained results prompted further investigation into the chloroquine resistance reversal properties of fendiline, which showed it to significantly reduce chloroquine's IC_{50} level using half the concentration required for verapamil. Further investigations into the mechanism of action of fendiline's chloroquine potentiation properties is required. The idea of restoring chloroquine's activity against resistant parasites without the need to develop a new drug entity has the potential to be an effective strategy.

Chapter 4
Synthesis and evaluation of fendiline analogues

4.1 Introduction

4.1.1 Historical perspective

In a rudimentary sense, medicinal chemistry has been in practice for thousands of years. Man has foraged for substances to treat illness by eating herbs, barks or other plant extracts for a very long time. There are records that go back 5100 years by the Chinese Emperor Shen Nung that describe herbs used to relieve fever (Chen, 2012). The prescription of these natural products was largely based on folklore and tradition rather than scientific evidence. Despite the fact that many of these medications are believed to have worked by placebo effect rather than being pharmacologically active, in some instances, such as quinine (cinchona tree) for malaria and digitalis (foxglove plant) to treat heart failure, the chosen product turned out to be an effective treatment (Smith, 1992; Silverman and Holladay, 2014).

Around 100-150 years ago the pharmacologically active constituents of natural products started to become known and natural products continue to be an important source of drugs to this date. In fact, between the early 1980s and early 1990s 40% of approved drugs were natural products (Silverman and Holladay, 2014).

Quite often natural products are chemically modified before administration; these become known as semi-synthetic agents. This is carried out for various reasons such as to make the compound more active, more soluble or to improve its pharmacokinetic and safety profile (Smith, 1992). Newman and Cragg (2016) state that 21% of all new approved drugs between the years 1981 to 2014 were natural product derivatives. The natural product artemisinin has

had several semi-synthetic derivatives produced in order to overcome its poor solubility (Engel and Straus, 2002; Medhi *et al.*, 2009; Li, 2012).

Artemisinin can be reduced by sodium borohydride to obtain dihydroartemisinin which can then produce artesunate by reacting with succinic anhydride (cited by: Wu *et al.* 2001; Huang & Aslanian 2012; Guo 2016). Artemether can also be derived from dihydroartemisinin by reacting with methanol benzene in the presence of BF_3-etherate as a catalyst (cited by: Huang & Aslanian 2012; Guo 2016). The mentioned derivatives are all available as drugs and are only a few examples of artemisinin derivatives; the chemical structures can be seen in Figure 4.1 with the modifications highlighted in red.

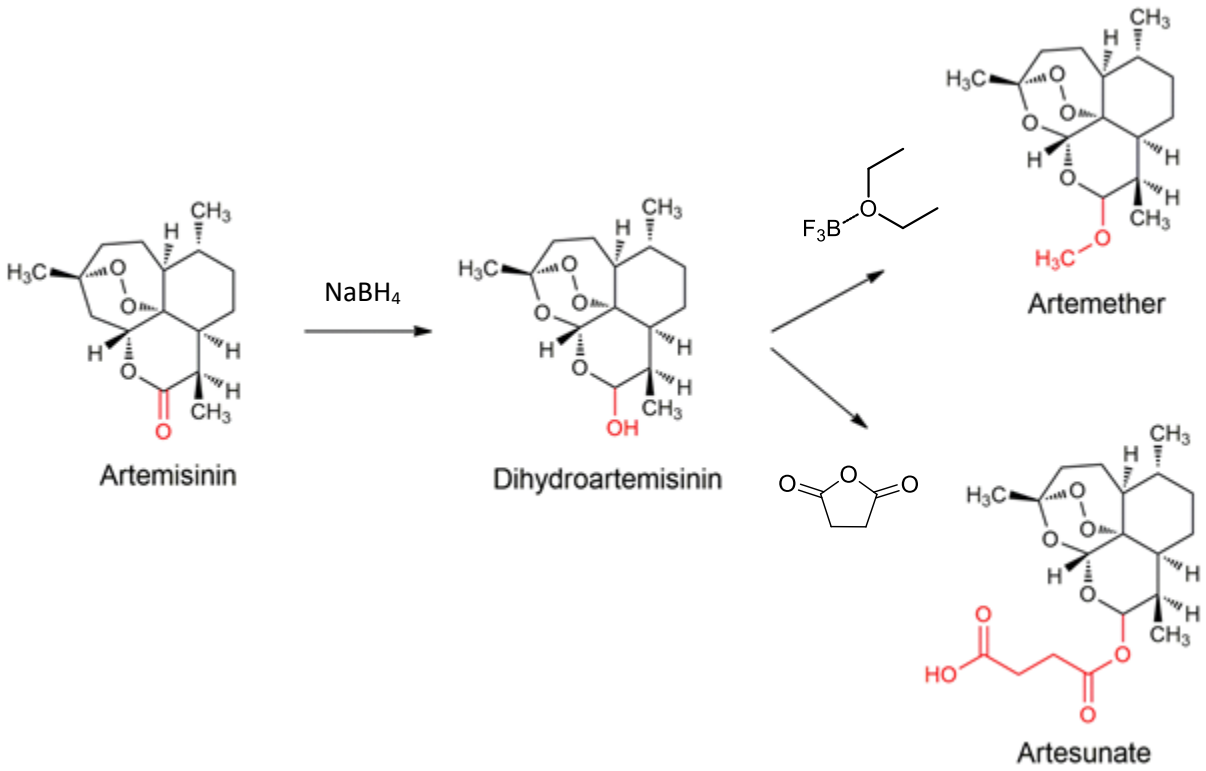

Figure 4.1 - Example of semi-synthetic artemisinin derivatives.
Alterations have been to the lactone moiety with the differences highlighted in red.

For a large part of the twentieth century synthetic chemists were producing as many novel compounds as possible in a bid to produce new drugs (Patrick, 2015), particularly after the making of the first fully synthetic (sulfa) drugs in the 1930s (Smith, 1992). However advancements in chemical and biological techniques have allowed drug design to reach new levels (Smith, 1992; Silverman and Holladay, 2014; Patrick, 2015). Better understanding of

how drugs work and being able to propose theories as to why some compounds are more active than others, allowed for rational drug design to come into play.

Medicinal chemistry is at the heart of a multitude of events that occur in the development of new pharmaceutical candidates (Karpf, 2011). Often a high throughput screening of compounds identifies a hit with interesting biological activity. When a compound is identified as active, research is then focused on producing analogues of the compound as a means of producing a safer and more effective entity.

Despite technological development and advancement in drug design, a large number of analogues – sometimes hundreds - still need to be synthesised and tested before a potential candidate is found that is worthy of being fully investigated (Karpf, 2011; Silverman and Holladay, 2014). The two main reasons behind synthesising analogues are the identification of important functional groups responsible for the drug's activity and the production of a structure with improved activity that can be economically synthesised (Patrick, 2015).

Modification of the lead compound should be done in stages, making only simple changes on one functional group at a time. By doing this, changes in activity can quickly be ascribed to the particular modification (Rick, 2009; Patrick, 2015). An example of how this is carried out can be shown with the modification of artemisinin as changes to the peroxide moiety resulted in loss of antimalarial activity (Krungkrai *et al.*, 2010; Mojab, 2012; Guo, 2016). An example of one of the produced analogues is shown in Figure 4.2 (Guo, 2016).

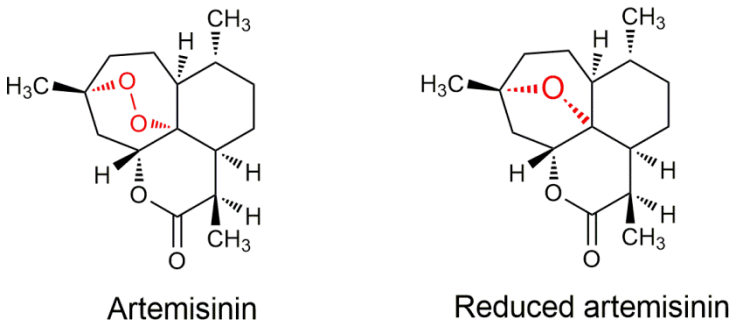

Figure 4.2 - An example of one of the artemisinin analogues that were synthesised modifying the peroxy group. *Differences are highlighted in red.*

Investigations of the antitumour activity of artemisinin led researchers at the Shanghai Institute of Materia Medica to modify the lactone moiety with different groups than ones previously reported. Li (2012) discusses the different analogues synthesised in detail, however Figure 4.3 shows two simple examples of analogues produced. The research showed the newly modified compound that preserved the peroxy group resulted in good activity towards P388 and A549 cell lines, whereas altering the peroxy group resulted in loss of activity (Li, 2012).

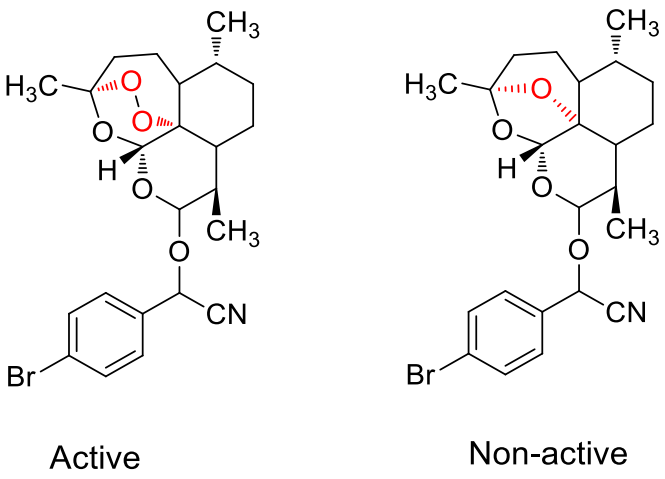

Figure 4.3 - Two artemisinin derived compounds tested against cancer cells. *Li (2012) discusses these and other investigated analogues in more detail.*

Another point discussed by Patrick (2015) with regard to synthesising analogues, particularly with fully synthetic molecules - although it could also apply to semi-synthetic agents – is that easily made or commercially available building blocks should be used in the synthesis. For example, an easily obtained precursor molecule should be made or purchased and from that different building blocks can be added to it creating a diverse library of analogues. Using a common precursor molecule that can be produced on a large-scale, speeds up the process dramatically, rather than each analogue being synthesised individually from the beginning.

It is important to note, however, that the yield and quantity of the synthesised analogues is not the focus of a medicinal chemist; the synthesis of milligrams of new compounds to test for biological activity is the focus (Karpf, 2011). Once initial parameters such as efficacy, toxicity and stage-specificity are established, compounds are progressed as potential drug

leads. It then becomes the focus of process chemists, usually within pharmaceutical/commercial companies, to scale up the production of the compound with better yield and minimal waste (Karpf, 2011).

Prior to entering the scale-up process which is carried out alongside the preclinical studies and the rigorous drug development testing process, it is important and advantageous to discover possible safety issues that may arise from a potential drug. Therefore screening panels of kinases and ion channels for off-target activity is a regular occurrence in drug development (Priest, Bell and Garcia, 2008). One important example is to screen the effect a compound has on the voltage-gated potassium channel coded by the human ether-à-gogo-related gene (hERG). The hERG channel plays an essential role in regulating cardiac rhythm by repolarising the cardiac action potential (Priest, Bell and Garcia, 2008; van den Berg *et al.*, 2012; Zhang, Yang and Li, 2014). Structurally diverse and functionally unrelated small molecules and drugs have been found to interfere with and inhibit the channel. This can cause prolonged QT intervals, which leads to long QT syndrome, *torsade de pointes* and sudden cardiac death (Sanguinetti *et al.*, 1995; Zhang, Yang and Li, 2014). Thus the concern over drug induced prolongation of QT intervals is a major one (Nogawa and Kawai, 2014) and the FDA has a compulsory regulation that drugs being developed do not target the hERG channel (Zhang, Yang and Li, 2014).

4.1.2 Synthesis of fendiline analogues

With regards to finding new antimalarial drugs, Flannery and coworkers (2013) discuss that upon finding a promising scaffold for a potential drug, the efficacy, toxicity and novelty, along with the cost and ease of synthesis, are taken into consideration for further selection. Additionally, analogues of the parent compound are often synthesised and their efficacy tested in order to identify a lead compound (Flannery, Chatterjee and Winzeler, 2013).

Gelb (2007) discusses that there are reports of interesting compounds targeting the blood stages of malaria with IC_{50} levels within micromolar range, however the activity of well-established antimalarial drugs such as quinine and artemisinin is within the nanomolar range.

Thus Gelb (2007) argues that for a candidate to be considered as an interesting lead the antimalarial activity should ideally be within the nanomolar range (Gelb, 2007).

The commercially obtained fendiline has an IC_{50} level of 3.74 ± 0.64 µM on *P. falciparum* parasites. As previously discussed (Chapter 1, section 1.8.3), published work carried out on some fendiline analogues showed approximately a one-hundred-fold increase in potency against rat mesenteric arteries compared with the parent compound - fendiline (Wilkinson *et al.*, 2007a). Another study using fendiline analogues found one analogue to be more than two-fold more active against leukaemia cells than fendiline itself (Wilkinson *et al.*, 2007b). Taking this into consideration, the objective of the following study is to synthesise a series of fendiline analogues in a bid to produce a more potent compound against malaria.

Fendiline, and its analogues, are synthesised by producing an intermediate aldehyde which is then reacted with a benzylamine derivative to form the final compound in a reductive amination step. Two synthetic routes were utilised to produce the intermediate aldehyde in this study, both are discussed briefly below (overall synthetic scheme is shown in Figure 4.4). However, it is important to note that some of the analogues were synthesised by Dr Steven Rossington and full experimental details can be found in the literature (Rossington, 2004; Wilkinson *et al.*, 2004; Wilkinson *et al.*, 2006).

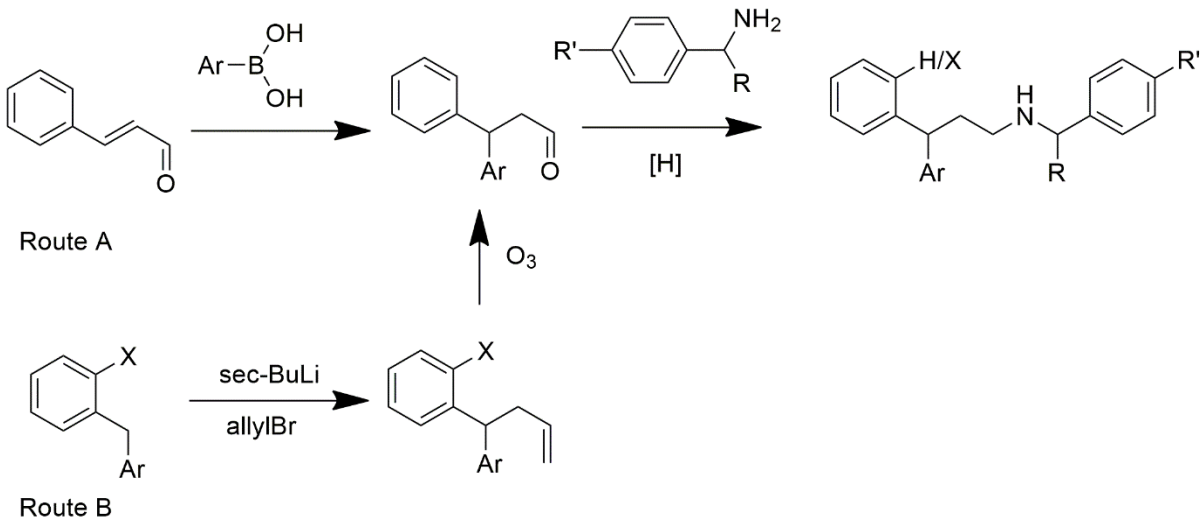

Figure 4.4 – The two synthetic routes utilised to produce the fendiline analogues.

Organolithium chemistry and ozonolysis

The method followed by Dr Rossington (Rossington, 2004; Wilkinson *et al.*, 2004; Wilkinson *et al.*, 2006) to form the aldehyde was a two-step process. First an allyl compound is formed which then undergoes ozonolysis to form the aldehyde. The first step utilises organometallic chemistry in forming a C-C bond (Clayden *et al.*, 2001).

The carbon in organolithium compounds is more electronegative than the lithium, making it a nucleophilic centre and allowing it to react with other molecules (Clayden *et al.*, 2001). Due to the fact that they are highly reactive nucleophiles the reactions are usually carried out under inert atmosphere and at low temperatures (Clayden *et al.*, 2001). The addition of water/dilute acid to a reaction results in the formation of the corresponding hydrocarbon, so this is usually done at the end once the reaction is complete (Clayden *et al.*, 2001).

The second step, the ozonolysis, makes use of the very unstable ozone molecule that reacts with the alkene forming a slightly more stable ozonide intermediate. However, the addition of dimethyl sulphide attacks the intermediate molecule releasing dimethyl sulfoxide, formaldehyde and the desired aldehyde (Clayden *et al.*, 2001).

An overview of the reaction carried out by Dr Rossington to produce one of the aldehydes can be seen in Figure 4.5. Briefly, starting with commercially available reagents (2-benzylphenol, 1-benzyl-2-methoxybenzene, 1-benzyl-2-ethoxybenzene or 1-benzyl-2-(2-methoxyethoxy)benzene) the aldehydes were formed by stirring with *sec*-Butyllithium (*sec*-BuLi) for several hours before cooling the reactions to -78 °C and adding allyl bromide. The reactions were then brought to room temperature and stirred for a further 18 hours before washing with acid. Following the work up, the non-purified products were dissolved in DCM and at -78 °C ozone was bubbled through for 1 hour and 20 minutes. The reactions were purged with argon and treated with dimethyl sulphide and then allowed to warm up to room temperature, stirring for 16 hours.

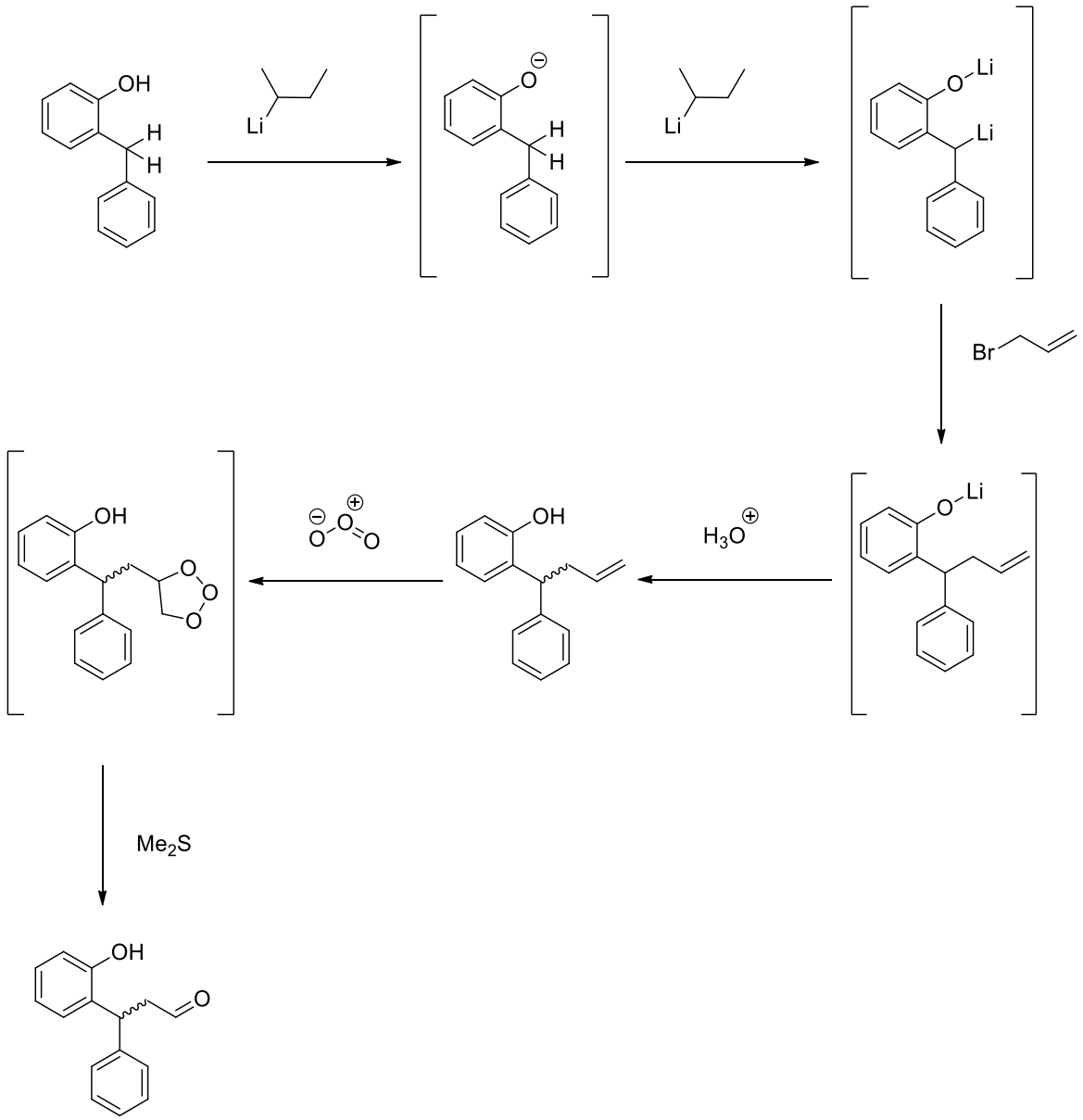

Figure 4.5 – Schematic of the synthetic route followed by Dr Rossington in the synthesis of the intermediate aldehyde. *The scheme is adapted from (Clayden et al., 2001) and from personal communication (Jim Wilkinson, July 22, 2016). (Me_2S: dimethyl sulphide).*

Current procedure: Palladium coupling

The procedure followed to synthesise fendiline and its analogues during this study utilises a different pathway from the one mentioned above. The aldehyde is formed using the conjugate addition of a boronic acid to an α,β-unsaturated carbonyl compound (in this case *trans*-cinnamaldehyde) in the presence of a palladium catalyst (palladium acetate $Pd(OAc)_2$) and 2,2'-bipyridyl (BIPY).

The α carbon, in an α,β-unsaturated carbonyl compound, refers to the carbon next to the carbonyl carbon and β is the one further down. Conjugate additions by nucleophiles usually occur on the β carbon (Clayden *et al.*, 2001).

The proposed mechanism of the reaction is shown in Figure 4.6. Briefly, in the presence of BIPY, transmetallation occurs between Pd(OAc)2 and the arylboronic acid. The addition of the *trans*-cinammaldehyde forms the palladium enolate, protonolysis then releases the product and regenerates the initial palladium species (Lu and Lin, 2005; Holder *et al.*, 2015). The method was reported by Lu & Lin (2005) who found that the presence of $Pd(OAc)_2$ and BIPY are essential for the reaction to occur and produce a high yield.

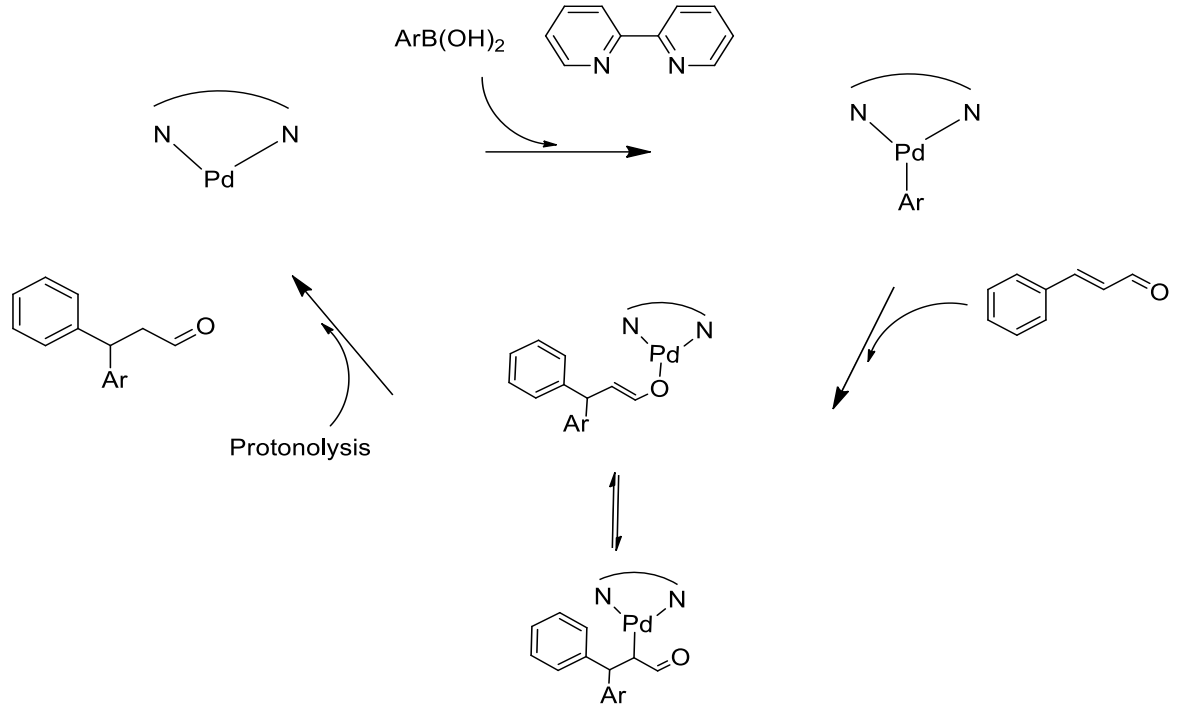

Figure 4.6 - The proposed mechanism of the palladium coupling reaction. *This scheme is adapted from Lu & Lin (2005) and Holder et al. (2015).*

Reductive amination

The formation of an amine from a carbonyl compound occurs via a reductive amination. Briefly an imine is formed by combining the carbonyl and an amine which is then followed by a borohydride reduction to form the secondary amine (Lane, 1975; Clayden *et al.*, 2001).

The reductive amination step to form fendiline can be seen in Figure 4.7. Although sodium borohydride can be used for a reductive amination, it readily reduces both imines and carbonyl compounds (Lane, 1975). The formation of the imine is a reversible process, thus using sodium borohydride will reduce the aldehyde from starting material as well as the imine (Lane, 1975). However sodium cyanoborohydride ($NaBH_3CN$) is a more selective reducing agent. Borch *et al.* (1971) found that selectivity is pH dependant; carrying out the reaction at pH 6 reduces the imine quicker than the carbonyl compound and therefore $NaBH_3CN$ is the agent used.

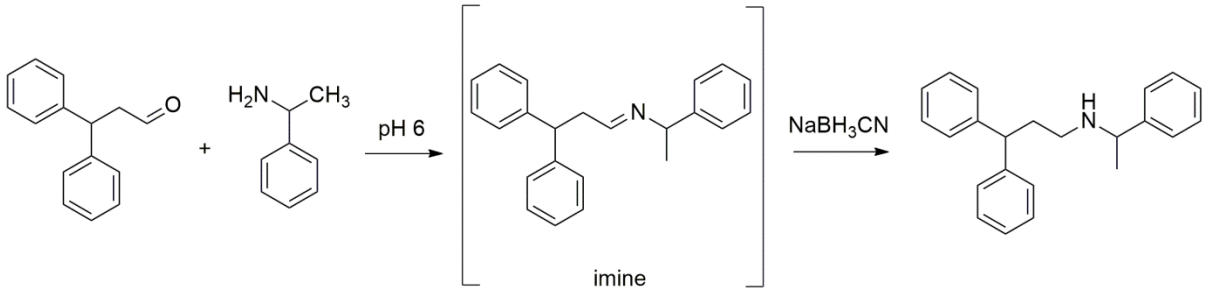

Figure 4.7 - The reductive amination reaction for the synthesis of fendiline.

4.1.3. Aims

The aim of this study was to synthesise a series of fendiline analogues using a modified synthetic pathway to the one utilised by Dr Rossington. The analogues would then be screened against *P. falciparum* infected RBCs and against human HepG2 cells for cytotoxicity with the objective of finding a more potent antimalarial compound. Furthermore, an investigation of the lead compound as a potential drug by testing the effect it has on the hERG channel and determining its stage specificity on the malaria parasite would follow.

4.2 Methods

4.2.1 General Experimental

Proton NMR (^1H) were recorded on a Bruker Ultrashield 400 MHz spectrometer. The chemical shifts (δ) are quoted in parts per million (ppm) downfield of tetramethylsilane (TMS). The abbreviations used are; s, singlet; bs, broad singlet; d, doublet; dd, double doublet; t, triplet; q, quartet; m, multiplet; and Ar, aromatics. All NMR data was processed offline on TopSpin®

processing software package. Mass spectra were recorded on an Agilent LCMS 6120b instrument under electrospray ionisation with MeOH (99.9 %) and formic acid (0.1 %). All reagents used for the synthesis were purchased from Sigma Aldrich, UK.

4.2.2 Synthesis of the aldehyde *via* Palladium coupling

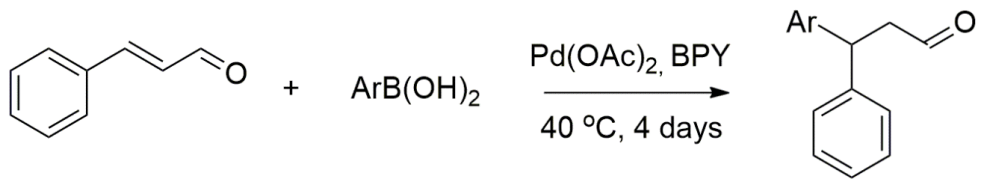

The method used for this reaction was adapted from Lu & Lin (2005). Trans-cinnamaldehyde (0.132 g, 1 mmol, 1 eq), phenylboronic acid (0.366 g, 3 mmol, 3 eq), 2,2'-bipyridyl (0.0254 g, 0.2 mmol) and palladium acetate (0.01 g, 0.05 mmol, 0.05 eq) were dissolved in acetic acid (3 ml), THF (1.5 ml) and water (0.9 ml) and left to stir at 40 °C for four days under argon. The reaction mixture was then filtered through celite, washed with $NaHCO_3$, dried with $MgSO_4$ and concentrated *in vacuo* to afford a brown oil. The product was purified by flash column chromatography using petroleum ether: ethyl acetate (pet.ether: EtOAc) (20: 1) to yield a colourless oil (compound **1**) which was analysed by ^{1}HNMR.

The method described is for the coupling of the trans-cinnamaldehyde with phenylboronic acid, the remainder of the coupling reactions followed the same procedure, for each equivalent of *trans*-cinammaldehyde, three equivalents of the relevant boronic acid was used. Although several boronic acids were tested (Table 4.1), only two successfully produced the relevant aldehyde: 3,3-diphenylpropanal (compound **1**) and 3-(2-naphthyl)-3-phenylpropanal (compound **2**) as shown in Figure 4.8.

$ArB(OH)_2$	Product	FCC eluent system	Yield (%)
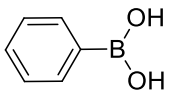	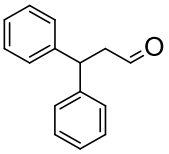	Pet.ether: EtOAc (20: 1)	92.6
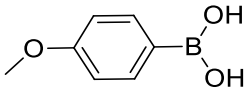	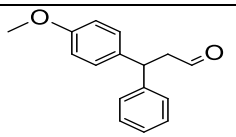	N/A	0
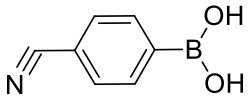	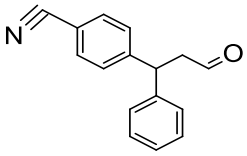	N/A	0
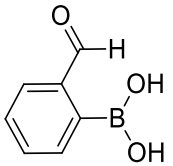	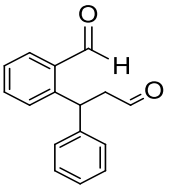	N/A	0
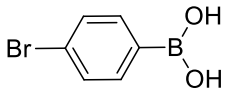	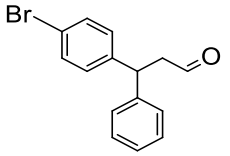	N/A	0
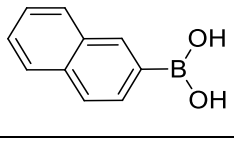	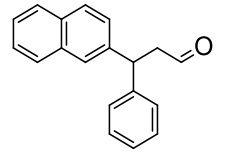	Hexane: EtOAc (10: 1)	72.0

Table 4.1 - $Pd(OAc)_2$ catalysed conjugate additions of arylboronic acids to trans-cinnamaldehyde.

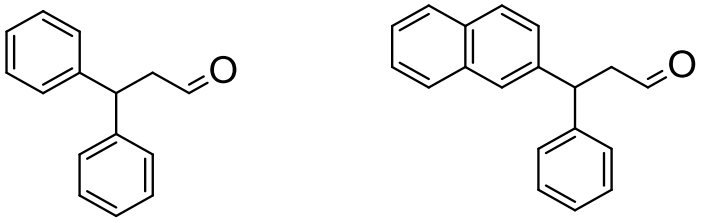

1 **2**

Figure 4.8 - Products obtained from the palladium coupling reactions.

δ ^{1}H NMR (400 MHz, $CDCl_3$) **1** are; 9.8 (1H, t, *J*=1.9 Hz, C*H*=O), 7.18-7.35 (10H, m, Ar*H*), 4.60 (1H, t, *J*=7.7 Hz, PhC*H*Ph), 3.27 (2H, dd, *J*=7.71, 1.9 Hz, CH_2).

δ ^{1}H NMR (400 MHz, $CDCl_3$) **2** are, 9.7 (1H, t, *J*=1.8 Hz, C*H*=O), 7.05-7.75 (12H, m, Ar*H*), 4.72 (1H, t, *J*=7.8 Hz, ArC*H*Ph), 3.20 (2H, dd, *J*=7.8, 1.8 Hz, CH_2).

4.2.3 Reductive amination

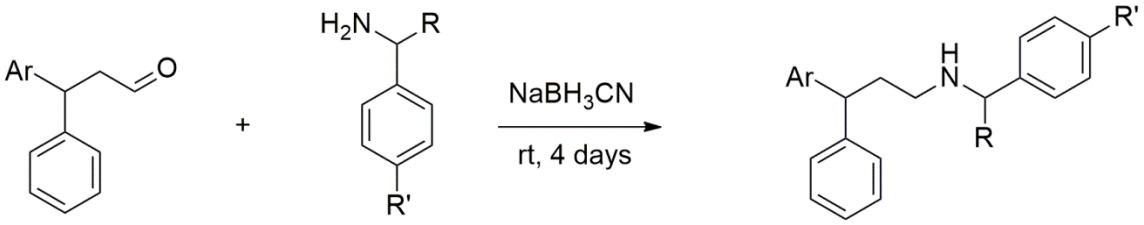

The method described here was taken from Rossington (2004). α-methylbenzylamine (0.048 g, 0.4 mmol, 1 eq) was dissolved in methanol (2 ml) and the pH was adjusted to 6 by adding 50% methanolic acid (methanol: hydrochloric acid, 1: 1) dropwise. 3,3-diphenylpropanal (compound **1**, 0.084 g, 0.4 mmol, 1 eq) was then dissolved in methanol (2 ml) and added to the reaction mixture dropwise. This was followed by the addition of sodium cyanoborohydride (0.044 g, 0.7 mmol, 1.75 eq) and the reaction was left stirring at room temperature for four days.

Methanol was then evaporated, water (5 ml) was added to the mixture and the pH was adjusted to 14 with the addition of solid potassium hydroxide. The product was extracted into chloroform (5 x 5ml), dried with $MgSO_4$ and concentrated *in vacuo* to afford a yellow oil. Purification was carried out by flash column chromatography using chloroform: methanol ($CHCl_3$: MeOH) (96: 4) to yield a colourless oil. Analysis of the product was carried out by ^{1}HNMR.

The described method used α-methylbenzylamine, however the remaining reactions followed the same procedure with one-to-one ratios of the aldehyde and benzylamine derivative.

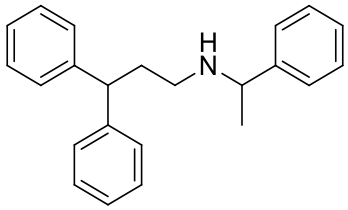

Compound 3a

Compound **3a**; 17.7 % yield; δ ^{1}H NMR (400 MHz, $CDCl_3$); 7.15-7.40 (15H, m, Ar*H*), 4.00 (1H, t, *J*=7.9 Hz, PhC*H*Ph), 3.62 (1H, q, *J*=6.6 Hz, C*H*CH_3), 2.40-2.55 (2H, m, $CHCH_2CH_2$), 2.25-2.30 (2H, m, $CHCH_2CH_2$), 1.45-1.65 (1H, br, N*H*), 1.33 (3H, d, *J*=6.6 Hz, CH_3). m/z 316.2 (MH^+), MH^+ found 316.2, $C_{23}H_{25}N$ requires 315.5.

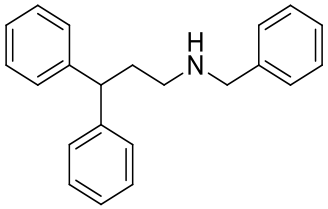

Compound 3b

Compound **3b**; 28.6 % yield; δ ^{1}H NMR (400 MHz, $CDCl_3$); 7.15-7.40 (15H, m, Ar*H*), 4.09 (1H, t, *J*=7.7 Hz, PhC*H*Ph), 3.75 (2H, s, CH_2Ar), 2.65 (2H, t, *J*=7.0 Hz, $CHCH_2CH_2$), 2.32 (2H, q, *J*=7.5 Hz, $CHCH_2CH_2$), 1.50-1.62 (1H, br, N*H*). m/z 302.2 (MH^+), MH^+ found 302.2, $C_{22}H_{23}N$ requires 301.4.

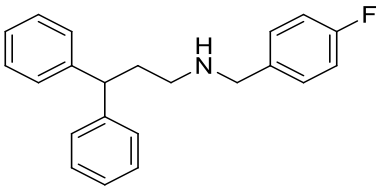

Compound 3c

Compound **3c**; 18.6 % yield; δ ^{1}H NMR (400 MHz, $CDCl_3$); 6.85-7.25 (14H, m, Ar*H*), 3.95 (1H, t, *J*=7.8 Hz, PhC*H*Ph), 3.62 (2H, s, CH_2Ar), 2.50-2.55 (2H, m, Hz, $CHCH_2CH_2$), 2.25-2.35 (2H, m, $CHCH_2CH_2$). m/z 320.1 (MH^+), MH^+ found 320.2, $C_{22}H_{22}FN$ requires 319.4.

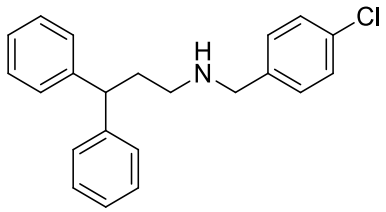

Compound 3d

Compound **3d**; 15.1 % yield; δ ^{1}H NMR (400 MHz, $CDCl_3$); 7.15-7.45 (14H, m, Ar*H*), 4.05 (1H, t, *J*=7.8 Hz, PhC*H*Ph), 3.72 (2H, s, CH_2Ar), 2.63 (2H, t, *J*=7.0 Hz, CHCH$_2$CH_2), 2.30 (2H, q, *J*=7.6 Hz, CHCH_2CH$_2$), 1.50-1.75 (1H, br, N*H*). m/z 336.1 (MH^+), MH^+ found 336.1, $C_{22}H_{22}ClN$ requires 335.8.

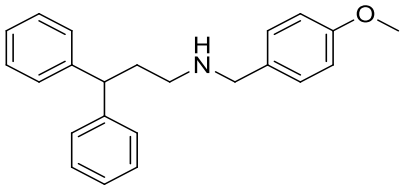

Compound 3e

Compound **3e**; 21.3 % yield. δ ^{1}H NMR (400 MHz, $CDCl_3$); 6.85-7.40 (14H, m, Ar*H*), 4.05 (1H, t, *J*=7.8 Hz, PhC*H*Ph), 3.85 (3H, s, CH_3), 3.69 (2H, s, CH_2Ar), 2.65 (2H, t, *J*=7.5 Hz, CHCH$_2$CH_2), 2.30 (2H, q, *J*=7.5 Hz, CHCH_2CH$_2$). m/z 332.1 (MH^+), MH^+ found 332.1, $C_{23}H_{25}NO$ requires 331.5.

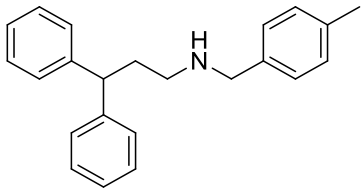

Compound 3f

Compound **3f**; 17.6 % yield; δ ^{1}H NMR (400 MHz, $CDCl_3$); 6.95-7.3 (14H, m, Ar*H*) 3.95 (1H, t, *J*=7.8 Hz, PhC*H*Ph), 3.60 (2H, s, CH_2Ar), 3.40 (3H, s, CH_3), 2.55 (2H, t, *J*=7.8 Hz, CHCH$_2$CH_2), 2.25-2.40 (2H, m, CHCH_2CH$_2$). m/z 316.2 (MH^+), MH^+ found 316.2, $C_{23}H_{25}N$ requires 315.5.

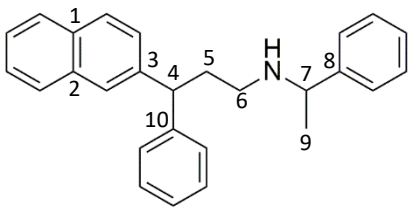

Compound 3g

Compound **3g**; 69.1 % yield; δ ^{1}H NMR (400 MHz, $CDCl_3$); 7.15-7.55 (17H, m, Ar*H*), 4.25 (1H, t, *J*=7.6 Hz, ArC*H*Ph), 3.72-3.80 (1H, m, C*H*CH_3), 2.50-2.65 (2H, m, $CHCH_2CH_2$), 2.30-2.49 (2H, m, $CHCH_2CH_2$), 1.35 (3H, dd, *J*=1.4, 6.6 Hz, C*H*$_3$). δ ^{13}C NMR; 145.1 (C-10), 145.0 (C-8), 142.0 (C-3), 133.5 (C-1), 132.5 (C-2), 125.1-128.8 (17 x ArC), 58.5 (C-7), 48.9 (C-4), 46.0 (C-6), 35.3 (C-5), 24.0 (C-9). m/z 366.2 (MH^+), MH^+ found 366.2, $C_{27}H_{27}N$ requires 365.5.

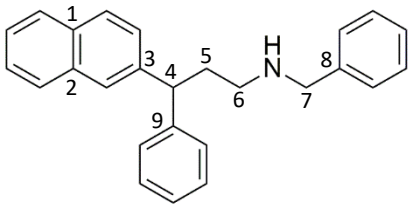

Compound 3h

Compound **3h**; 59.1 % yield; δ ^{1}H NMR (400 MHz, $CDCl_3$) **3h**; 7.10-7.40 (17H, m, Ar*H*), 4.15 (1H, t, *J*=7.6 Hz, ArC*H*Ph), 3.65 (2H, s, C*H*$_2$Ar), 2.60 (2H, t, *J*=7.2 Hz, $CHCH_2CH_2$), 2.30-2.45 (2H, m, $CHCH_2CH_2$), 1.25-1.45 (1H, br, N*H*). δ ^{13}C NMR; 144.5 (C-9), 142.5 (C-3), 140.0 (C-8), 133.5 (C-1), 132.2 (C-2), 128.2-120.5 (17 x ArC), 53.2 (C-7), 48.8 (C-4), 47.5 (C-6), 35.2 (C-5). m/z 352.1 (MH^+), MH^+ found 352.2, $C_{26}H_{25}N$ requires 351.5.

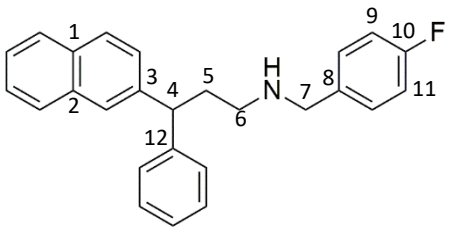

Compound 3i

Compound **3i**; 74.1 % yield; δ ^{1}H NMR (400 MHz, $CDCl_3$) **3i**; 6.98-7.51 (16H, m Ar*H*), 4.25 (1H, t, *J*=8.0 Hz, ArC*H*Ph), 3.72 (2H, s, CH_2Ar), 2.71 (2H, t, *J*=7.2 Hz, $CHCH_2CH_2$), 2.35-2.50 (2H, m, $CHCH_2CH_2$), 1.55-1.65 (1H, br, N*H*). δ ^{13}C NMR; 163.1 (C-10), 144.9 (C-12), 142.2 (C-3), 135.9 (C-8), 131.1 (C-1), 132.3 (C-2), 130.5-125.0 (14 x ArC), 115.0 (2 x C, C-9, C-11), 53.1 (C-7), 48.6 (C-4), 47.3 (C-6), 35.3 (C-5). m/z 370.2 (MH^+), MH^+ found 370.2, $C_{26}H_{24}FN$ requires 369.5.

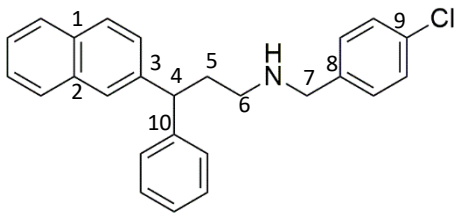

Compound 3j

Compound **3k**; 54.8 % yield; δ ^{1}H NMR (400 MHz, $CDCl_3$) **3j**; 7.05-7.45 (16H, m, Ar*H*), 4.25 (1H, t, *J*=7.8 Hz, ArC*H*Ph), 3.60 (2H, s, CH_2Ar), 2.55 (2H, t, *J*=7.1 Hz, $CHCH_2CH_2$), 2.28-2.40 (2H, m, $CHCH_2CH_2$), 1.15-1.30 (1H, br, N*H*). δ ^{13}C NMR; 144.6 (C-10), 142.0 (C-3), 138.9, (C-8), 133.5 (C-9), 132.0 (C-1), 132.5 (C-2), 129.7-121.2 (16 x ArC), 52.7 (C-7), 48.8 (C-4), 47.5 (C-6), 34.9 (C-5). m/z (MH^+), MH^+ found 386.1, $C_{26}H_{24}ClN$ requires 385.9.

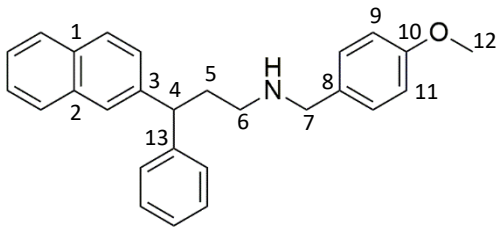

Compound 3k

Compound **3k**; 54.8 % yield; δ ^{1}H NMR (400 MHz, $CDCl_3$) **3k**; 6.80-7.50 (16H, m, Ar*H*), 4.22 (1H, t, *J*=7.8 Hz, ArC*H*Ph), 3.85 (3H, s, CH_3), 3.75 (2H, s, CH_2Ar), 2.65 (2H, t, *J*=7.2 Hz, $CHCH_2CH_2$), 2.30-2.45 (2H, m, $CHCH_2CH_2$). δ ^{13}C NMR; 161.2 (C-10), 144.5 (C-13), 142.0 (C-3), 136.9 (C-8), 133.1 (C-1), 132.2 (C-2), 128.0-121.2 (14 x ArC), 114.4 (2 x C, C-9, C-11), 55.5 (C-12), 52.1 (C-7), 48.8 (C-4), 46.5 (C-6), 34.0 (C-5). m/z 382.2 (MH^+), MH^+ found 382.2, $C_{27}H_{28}NO$ requires 381.5.

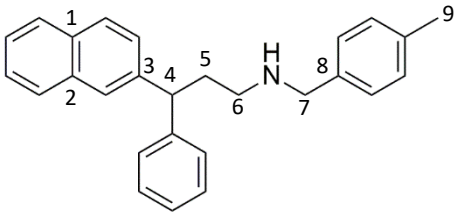

Compound 3l

Compound **3l**; 67.2 % yield; δ ^{1}H NMR (400 MHz, $CDCl_3$) **3l**; 7.00-7.50 (16H, m, Ar*H*), 4.20 (1H, t, *J*=7.7 Hz, ArC*H*Ph), 3.60 (2H, s, CH_2Ar), 2.55 (2H, t, *J*=7.1 Hz, $CHCH_2CH_2$), 2.40-2.55 (2H, m, $CHCH_2CH_2$), 2.35 (3H, s, CH_3). m/z 366.2 (MH^+), MH^+ found 366.3, $C_{27}H_{28}O$ requires 365.5.

^{13}C NMR and high-resolution mass spectra data was obtained for the novel compounds only (**3g**-**3l**). The exception was compound **3l**, only high-resolution mass spectra was obtained due to there being insufficient amount of product to produce the ^{13}C NMR spectra.

4.2.4 Antimalarial activity

The *in vitro* antimalarial activity of the compounds was tested against the K1 *P. falciparum* parasites. A two-fold serial dilution of the compounds was carried out (1-16 µM). Dose-response experiments were set up and analysed using the SG plate reader method as described earlier (Chapter 2, sections 2.2.3 and 2.2.4). The chemical structures of the panel of compounds tested are detailed in Table 4.4.

4.2.5 Cellular toxicity

The cellular toxicity of the compounds was tested using the MTT assay described elsewhere (Chapter 2, section 2.4.3). An initial screening using the same dose range used for the antimalarial activity was carried out (1-16 µM), however no reduction in growth occurred. Therefore a two-fold serial dilution using a higher concentration range (5-160 µM) was set up to determine the IC_{50} of the compounds on HepG2 cells.

4.2.6 hERG channel inhibition assay

The compound with most antimalarial activity and reasonable toxicity against HepG2 cells, **4c** (Table 4.4), was chosen for further investigation, and the effect it had on the hERG channel was assessed using the hERG inhibition assay. The hERG channel plays an essential role in regulating cardiac rhythm and the results of this experiment would indicate whether the compound targets receptors on this channel.

Chinese hamster ovary (CHO) cells transfected with hERG were used for this experiment. CHO cells were plated on a 384 well plate and placed in an IonWorks™ automated patch clamp instrument. This is an automated machine that is set up in a way that applies a vacuum below the cells, allowing the cells to be sealed to a hole in the bottom of each well. The cells are positioned between two isolated fluid chambers. The medium above the cell resembles extracellular solution (consisting of Dulbecco's PBS with calcium and magnesium) and the section below the cell is common to all the patched cells and resembles intracellular solution (pH 7.2 with HEPES). Following clamping, amphotericin B was added to the intracellular fluid section in order to form pores in the cell membrane, creating an electrical pathway. An electrode set up above the cells holds a negative potential of -80 mV for 15 seconds.

Depolarisation of the channel is achieved by applying a potential of +40 mV for 5 seconds followed by repolarisation at a potential of -50 mV for 4 seconds. This allows the hERG channel to change from a closed state to an open state, followed by inactivation. An electrode located below the cells records the ionic current.

Following measurement of the initial current, the drug was added (concentration ranged from 0.016-50 μM), incubated for 300 seconds and then the current was measured again.

The IonWorks™ automated patch clamp instrument is located at Cyprotex, (Macclesfield, Cheshire) where this experiment was carried out.

4.2.7 Time-course analysis

Investigations into the antimalarial activity of **4c** followed the toxicity tests. The IC_{50} of the compound at different time points (24, 48 and 72 hours) was obtained in order to determine whether it is a slow or fast acting drug. Unsynchronised cultures were incubated with different concentrations of the compound. Untreated controls were also set up and analysed in parallel to the treated cultures. Analysis was carried out using the SG plate reader method.

4.2.8 Stage-specificity assay

An experiment was set up to determine the stage-specificity of the compound (**4c**). The procedure followed for this experiment was adapted from Le Manach *et al.* (2013). In order to obtain tightly synchronised cultures, two sorbitol synchronisation steps were carried out (for sorbitol synchronisation details see Chapter 2, section 2.1.9). To obtain a late trophozoite/early schizont culture, the second sorbitol synchronisation step was carried out six hours after the first; the cultures were then left for approximately 18 hours before incubating with the drug. However, to obtain cultures with a majority ring population, the second synchronisation was carried out 31 hours after the first, the cultures were then incubated with the drug immediately after the second synchronisation. Giemsa-stained microscope slides were prepared from both cultures to confirm the stage of the parasite prior to the addition of drugs.

Each culture was set up in a separate 96 well plate and incubated with the drugs for 24 hours. The procedure followed to set up the experiment was the same as the previously described dose-response assay (Chapter 2, section 2.2.3). Two-fold serial dilutions of the control drug

(atovaquone, IC_{50} 2.21 nM) and **4c** were carried out with concentrations ranging from 1.6-100 times the determined IC_{50} for each drug. Following the 24 hours incubation, the plates were washed four times in complete media, centrifuging each time at 1,500 rpm for five minutes before further 24 hours incubation in complete media. Finally, the results were obtained following the SG plate reader method.

4.3 Results

4.3.1 Screening

The first series of synthesised compounds using the palladium coupling method are shown in Table 4.4 along with their antimalarial activity and cytotoxicity effect. The activity of the commercially obtained fendiline is also shown. The biological activity results are an average of three independent experiments each repeated in triplicate. The graphs for the dose-response experiments can be seen in Appendix II and III.

Compound	Structure	*P. falciparum* K1 IC_{50} (µM)	HepG2 Cells IC_{50} (µM)	SI
	Fendiline Hydrochloride (Commercially obtained)	3.74 ± 0.64	13.00 ± 0.83	3.48
3a	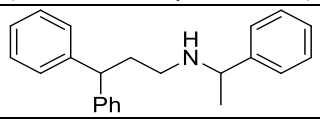	2.40 ± 0.42	15.68 ± 2.00	6.53
3b	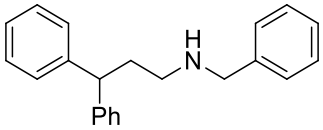	12.69 ± 2.43	29.35 ± 4.60	2.31
3c	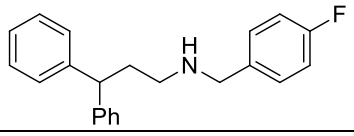	14.37 ± 2.70	39.22 ± 1.44	2.73
3d	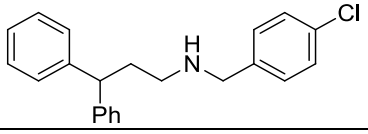	17.20 ± 1.28	31.75 ± 5.40	1.85
3e	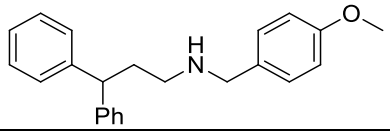	8.13 ± 1.94	55.56 ± 0.78	6.83
3f	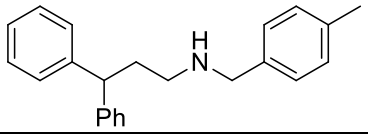	> 40	> 160	N/D
3g	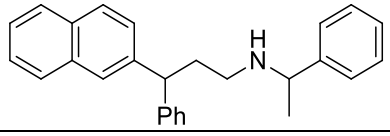	1.80 ± 0.42	9.72 ± 3.46	5.40
3h	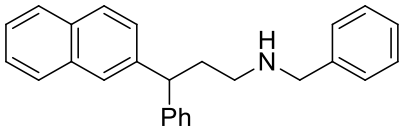	1.40 ± 0.31	6.74 ± 0.86	4.81
3i	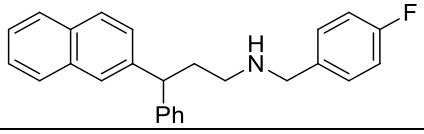	3.02 ± 0.61	10.03 ± 1.03	3.32
3j	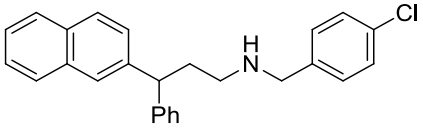	3.63 ± 0.96	14.61 ± 3.63	4.02
3k	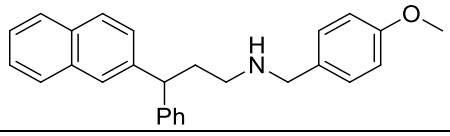	11.70 ± 1.54	57.89 ± 3.33	4.95
3l	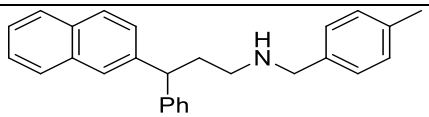	8.86 ± 0.47	61.19 ± 6.83	6.91

Table 4.4 - Yields, anti-plasmodial activity (P. falciparum K1 strain) and HepG2 cytotoxicity of the first series of fendiline analogues. *SI: selectivity index (IC_{50} HepG2/IC_{50} P. falciparum), (n=3). The IC_{50} value of the control drug cisplatin on HepG2 cells was 3.89 µM.*

The second series of fendiline analogues synthesised by Dr Steven Rossington along with their biological activity are shown in Table 4.5. Three independent experiments with each concentration repeated in triplicate was carried out.

Compound	Structure	*P. falciparum* K1 IC_{50} (µM)	HepG2 Cells IC_{50} (µM)	SI
4a	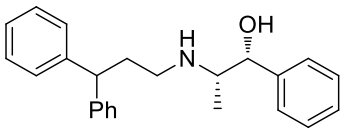	1.14 ± 0.48	27.81 ± 0.93	24.40
4b	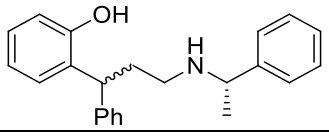	1.50 ± 0.26	125.30 ± 22.20	83.53
4c	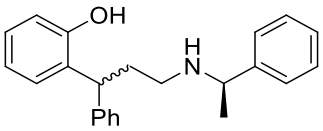	0.67 ± 0.21	62.26 ± 6.22	92.93
4d	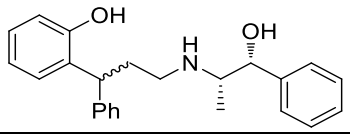	2.66 ± 1.82	27.75 ± 0.46	10.43
4e	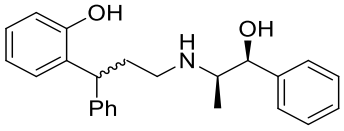	0.83 ± 0.25	58.17 ± 1.32	70.08
4f	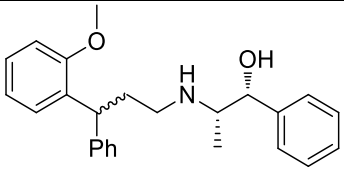	0.88 ± 0.32	55.39 ± 0.49	62.94
4g	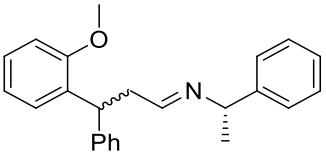	21.63 ± 1.97	87.21 ± 1.76	4.03
4h	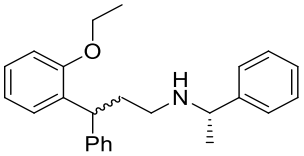	6.21 ± 1.19	29.02 ± 0.61	9.04
4i	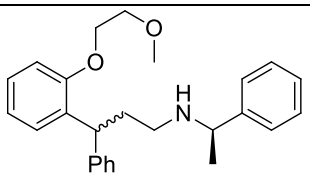	13.59 ± 2.19	64.94 ± 0.93	4.78
4j	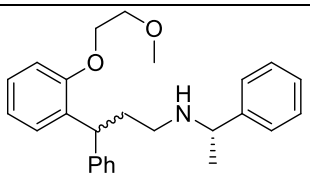	31.96 ± 0.93	51.12 ± 1.81	1.59

Table 4.5 - Antimalarial activity and HepG2 cytotoxicity of the second series of fendiline analogues. *SI: selectivity index (IC_{50} HepG2/IC_{50} P. falciparum), (n=3).*

4.3.2 hERG channel inhibition assay

The analogue with most antimalarial activity and acceptable toxicity on HepG2 cells was taken forward for further analysis. The effect compound **4c** (Figure 4.9) had on the hERG channel was assessed using an IonWorks™ automated patch clamp instrument. The results can be seen in Figure 4.10. The IC_{50} value obtained was 4.03 ± 0.52 μM.

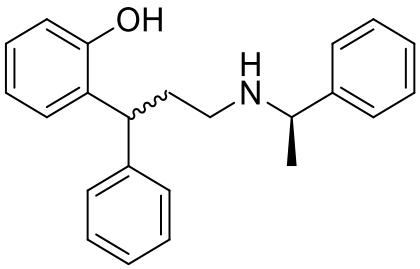

Figure 4.9 – The fendiline analogue (4c) taken forward for further investigation.

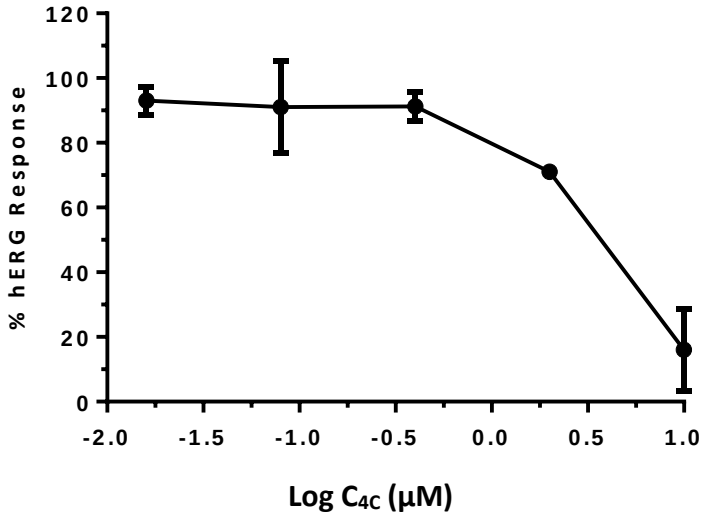

Figure 4.10 - Graph showing the results of the hERG inhibition assay.

4.3.3 Time-course analysis

The IC_{50} value of compound **4c** tested at different time intervals (24, 48 and 72 hours) was obtained. Figure 4.11 shows the dose-response curves and the IC_{50} values are presented in Table 4.6.

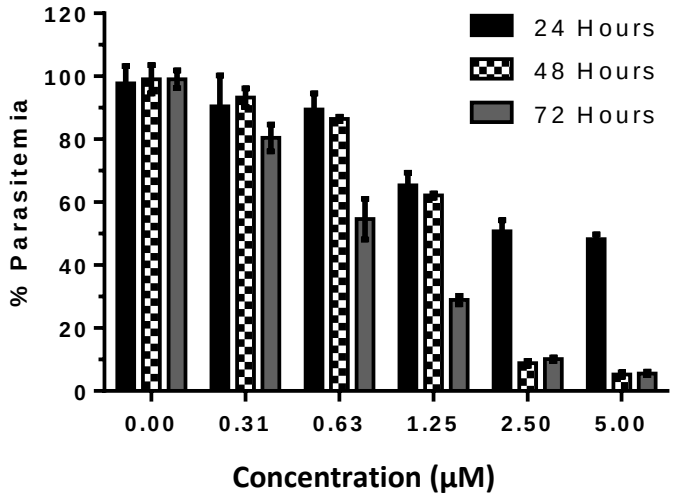

Figure 4.11 – Dose-response of compound 4c. *Data was obtained at different time points. Error bars represent results repeated in duplicate. (n=2)*

Time Points (Hours)	IC_{50} (µM)
24	3.48 ± 1.10
48	1.40 ± 0.11
72	0.72 ± 0.05

Table 4.6 – IC_{50} values of compound 4c obtained at three different time points.

4.3.4 Stage-specificity assay

A stage-specificity assay was carried out on the lead compound to gain insight into its mechanism of action. The assay was carried out on a control drug (atovaquone) as well as the compound of interest and the results were corroborated with current literature (Le Manach *et al.*, 2013). The results can be seen in Figures 4.12 (A and B) for atovaquone and **4c** respectively.

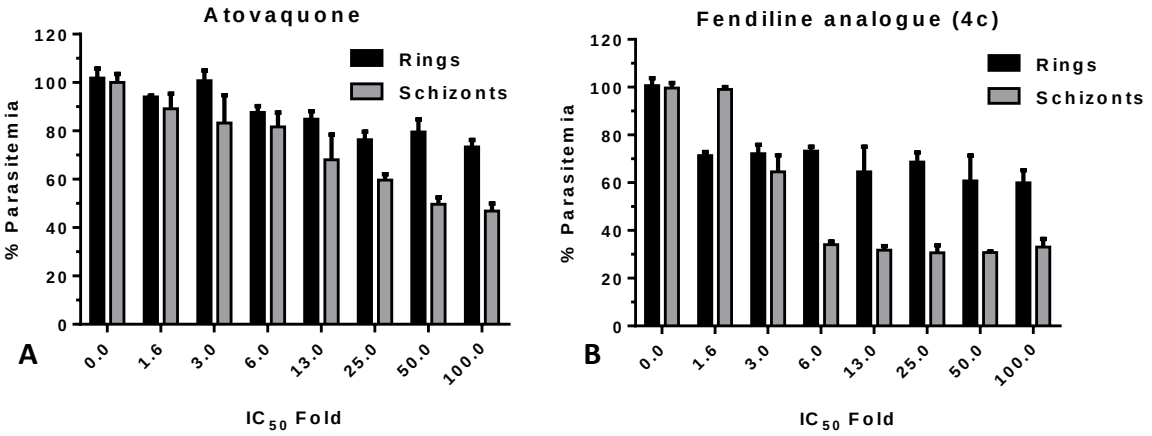

Figure 4.12 - Results of the stage-specificity assay. *A) Shows results of atovaquone and B) shows the results obtained with compund 4c. Error bars represent triplicate results.(n ≥ 3).*

4.4 Discussion

4.4.1 Synthesis of fendiline analogues

When a compound with interesting biological activity for a particular target is identified, the development of analogues in order to produce a more efficacious compound usually follows. Interesting antimalarial activity seen with fendiline on malaria led to the synthesis of more analogues in an attempt to produce a more potent antimalarial compound.

Producing analogues of fendiline loosely followed two processes discussed by Patrick (2015). Initially, a precursor molecule was synthesised in a one-step reaction (the aldehydes, compounds **1** and **2**, Figure 4.8) then a selection of commercially available building blocks (benzylamine derivatives) were used to form the diversity of the analogues. Secondly only simple changes were made to the compound, thus fendiline itself was synthesised then functional groups were added or removed in the hope that the active functional group within the compound could be identified.

The initial procedure followed to synthesise the compounds was different from the previously published method (Wilkinson *et al.*, 2004; Wilkinson *et al.*, 2006). Utilising $Pd(OAc)_2$ as a catalyst to form the conjugate addition of an arylboronic acid to an aldehyde has proven to be a promising method, giving 92.6% and 72.0% yields with phenylboronic acid and 2-naphthylboronic acid respectively, all the while reducing the number of steps and different reaction conditions (sub-zero temperature) required using the organolithium method.

The ^{1}H NMR spectra of the reactions carried out with the cyano electron-withdrawing group and 4-bromophenylboronic acid showed no reaction had occurred. Whereas 2-formylphenylboronic acid showed some product formation, the reaction did not go through to completion. This could be a result of the palladium catalyst reacting with both aldehyde groups, although no investigation was carried out to confirm this. Optimising the reaction conditions might improve the results, but this has not been carried out.

The reaction with 4-methoxyphenylboronic acid also showed some product formation with the reaction not going through to completion. This result resembles that seen by Lu & Lin (2005) who suggest the electron donating methoxy group in the *para*-position reduces the efficiency of the reaction.

Reductive amination using sodium cyanoborohydride successfully produced the final compounds. Purifying the basic molecules proved difficult even with the addition of trimethylamine to the solvent mixture. An improved purification system should be optimised if more synthesis is to be carried out in the future, particularly for compounds **3e**, **3f**, **3k** and **3l.**

4.4.2 Screening

The antimalarial activity and toxicity of fendiline and its analogues was carried out on *P. falciparum* K1 strain parasites and on human HepG2 cells. According to Mahmoudi *et al.* (2006) an antimalarial drug is considered interesting if it has an IC_{50} value below 10 μM, however Gelb (2007) suggested for a compound to be considered an interesting antimalarial lead the IC_{50} should be within nanomolar range. The phenyl derivatives of fendiline (**3a**-**3f**, Table 4.4) in general appeared to be less active against *P. falciparum* parasites than the naphthyl compounds (**3g**-**3l**, Table 4.4). Both the commercially obtained and the synthesised fendiline (**3a**) along with the methoxybenzylamine derivative (**3e**) were the only compounds of the phenyl derivatives to obtain an IC_{50} below 10 μM. In fact, the majority of the naphthyl derivatives obtained an IC_{50} below 10 μM, except for methoxybenzylamine derivative (**3k**) which obtained an IC_{50} of 11.70 ± 1.54 μM. Four out of the six naphthyl compounds had an IC_{50} value below 4 μM.

The second series of compounds tested (synthesised by Dr Rossington) that were substituted in the *ortho* position showed a range of activities. In general, compounds containing an OH group (2'-hydroxy fendiline compounds and the ephedrine derivates, **4a**-**4f**, Table 4.5) showed good activity with IC_{50} values ranging from 0.67-2.66 µM. Indeed only one (**4d**) of the six compounds resulted in an IC_{50} value above 1.50 µM. The methoxy, ethoxy and methoxyethoxy derivatives however all showed poor activity with IC_{50} values over 10 µM, with the exception of compound (**4h**) which had an IC_{50} of 6.21 ± 1.19 µM.

The 2'-hydoxy fendiline analogue (**4c**) has proven to be the most potent antimalarial compound. Interestingly, Wilkinson *et al.* (2007a) found that the 2'-hydroxy fendiline analogues were more active vasodilators on coronary and mesenteric arteries than the fendiline isomers. Additionally, the hydroxyl compounds also had increased anti-leukaemic effect compared to fendiline and other analogues modified at the 2' position (Wilkinson *et al.* 2007b).

The results from the MTT assay for the first series of analogues showed a similar trend, with compounds **3a**-**3f** being less active towards HepG2 cells than the naphthyl series (**3g**-**3l**). In both series, the methoxy (**3e** and **3k**) and methyl (**3f** and **3l**) derivatives were the least active compounds with IC_{50} values over 50 µM. It is important to note that the least active compounds **3e**, **3f**, **3k** and **3l** are the compounds with highest level of impurities. This highlights the importance of further purifying these compounds in order to determine whether the impurities are affecting their activity. The results overall show that the compounds containing the naphthyl group are largely more biologically active towards *P. falciparum* infected RBCs and HepG2 cells than the phenyl compounds.

Unlike the first series of compounds, the biological activity of the *ortho* analogues didn't follow a trend. The toxicity these compounds exhibited on HepG2 cells was low with all analogues having an IC_{50} value above 25 µM. Most importantly, the 2'-hydoxy analogue (**4c**) showed an approximate one-hundred-fold difference in IC_{50} values between HepG2 cells and parasites by having a cytotoxicity IC_{50} value of 62.26 ± 6.22 µM.

From the preliminary screen, modifications to the diphenyl moiety of fendiline by means of substituting a hydrogen with a hydroxyl group in the *ortho* position on the benzene ring, or by replacing a benzene with a naphthyl group, has shown improved antimalarial potency.

Furthermore, substituting the alkylamine region of fendiline with an ephedrine also appeared to improve activity towards the parasite. However further investigation would need to be carried out by screening a wider range of analogues to support such a premise.

Out of the tested compounds, **4c** was the most potent analogue with good selectivity towards the human cell line and thus was selected for further investigation.

4.4.3 hERG channel inhibition assay

A diverse range of molecules and drugs have been found to interfere with and inhibit the hERG channel leading to long QT syndrome and *torsade de pointes;* a condition which can potentially lead to sudden death. The off-target effect that drugs have on this channel has caused drugs to be withdrawn from the market and others to fail at a late stage of the development route when significant amount of resources had already been spent on the candidate compound (Sanguinetti *et al.*, 1995; Fenichel *et al.*, 2004; Priest, Bell and Garcia, 2008; Danker and Möller, 2014; Zhang, Yang and Li, 2014). Trefenadine, astemizole (H1 receptor agonists) and grepafloxacin (an antibacterial compound) are some examples of drugs that have been withdrawn from the market due to their effects on the hERG channel (Fenichel *et al.*, 2004; Priest, Bell and Garcia, 2008; Danker and Möller, 2014).

It is believed that some drugs interfere with hERG by blocking potassium from passing through the pore; others reduce hERG function by interfering with the production of the hERG channel, thus resulting in less channels being present within the cell membrane (Ficker *et al.*, 2004). Whereas some drugs are able to cause both effects (Rajamani *et al.*, 2006).

According to Fenichel *et al.*, (2004) the number of *torsade de pointes* cases resultant of a drug is usually minute in comparison with the hundreds of thousands, if not millions, of people receiving a drug. Consequently, this effect can go unnoticed during clinical trials where only several thousand patients are exposed to the drug. Moreover, once in the market it is more difficult to attribute *torsade de pointes* to a particular drug, and even more so if patients are taking several drugs at once (Fenichel *et al.*, 2004). It has therefore become common practice to screen a compound's activity towards the hERG channel early in a drug development program (Danker and Möller, 2014) especially as the FDA has an obligatory regulation for drugs being developed not to target the hERG channel (Zhang, Yang and Li, 2014).

According to Guth & Rast (2010) the majority of tested compounds have some effect on the hERG channel, although it is rare to come across compounds that are classed as potent channel inhibitors (IC_{50} values in low nM range). Most small molecules have an IC_{50} value of 1-10 μM for hERG channel inhibition. However it is more preferable for a compound to fall within the higher end of the range (Guth and Rast, 2010).

The results obtained from compound **4c** (4.03 ± 0.52 μM) falls within the range of most small molecules. The result means there is an approximate six-fold difference between IC_{50} value for the hERG assay and IC_{50} value for antimalarial activity. Pollard *et al.* (2010) state that in several reviews there is a recommendation for a 30-fold safety margin to be in place. However Pollard *et al.* (2010) also discuss that during the early lead optimisation the likely exposure of a patient to a drug is not known and therefore there is no rational way to decide on the progress of a compound simply by obtaining the hERG channel inhibition IC_{50} value. With the results of the hERG assay in mind, further investigation into the antimalarial activity of compound **4c** was carried out.

4.4.4 Time course analysis and stage-specificity assay

Upon finding a potential candidate, several experiments need to be carried out initially to establish the basics of the compound's activity. Once potency is determined against the parasite the next steps are to determine the speed of activity and the stage at which the compound acts on the parasite (Burrows *et al.*, 2013). Therefore, initially a time course analysis to determine the rate of action of **4c** was carried out. IC_{50} values were obtained at three different time points (24, 48 and 72 hours). The results show that the IC_{50} values decrease almost by half at every time point, from 3.5 μM to 0.7 μM from 24 to 72 hours respectively, which would suggest the compound is slow acting.

According to Burrows *et al.* (2013) ideally new antimalarial drugs would be fast acting. However, from a combinatorial perspective, there is some scope for new candidates to be slow acting. Due to the fact that any antimalarial treatment would consist of a combination of at least two drugs, it is advantageous for there to be both fast acting and slow acting drugs to clear residual parasites in any given combination (Biamonte, Wanner and Le Roch, 2013; Burrows *et al.*, 2013).

A stage-specificity assay was carried out with compound **4c** on tightly synchronised cultures following the procedure described by Le Manach *et al.* (2013). Either ring or schizont staged cultures were incubated for 24 hours with the drugs (**4c** and control drug atovaquone). A two-fold serial dilution of the drugs was carried out. The concentrations used were between 1.6 to 100 times the previously obtained IC_{50} values from a 72 hour assay. Following the 24 hour incubation, the drug was washed away from the infected RBCs and they were then incubated with media for a further 24 hours prior to analysis. The rationale for this assay was to further determine the stage specificity and rate of activity of compound **4c**.

The results obtained by the control drug atovaquone corroborates published findings by Le Manach *et al.* (2013); minor differences in results could be explained due to the different strains of parasite used. Overall, atovaquone was seen to be more active towards the schizont stages of the *P. falciparum* parasite.

Compound **4c** showed a clear preference for the schizont stages of the parasite. This is seen by the approximate 30% activity towards rings and 70% towards schizonts (Figure 4.12). The activity towards schizonts could potentially explain the slow activity of the compound seen from the time course analysis, as the parasites would go through almost a full cycle before being affected by the drug.

Although the two assays carried out indicate **4c** as a slow acting drug, the assays have not measured the viability of the parasites. Sanz *et al.* (2012) describe a method that allows the measurement of the number of parasites able to survive drug treatment and continue productive growth after drug removal. Carrying out an assay like this would allow the calculation of the parasite reduction rate (PRR) and parasite clearance time (PCT) which would give more in-depth detail of a compound's killing profile.

The results obtained here are interesting, especially as several reports have discussed the importance of calcium during the egression and invasion stages of the parasite (Dvorin *et al.*, 2010; Furuyama *et al.*, 2014; Jean *et al.*, 2014). Additionally, Scheibel *et al.* (1987) showed calmodulin to be concentrated in the apex of the merozoite, which is the point of interaction between the merozoite and the RBC during invasion (Preiser *et al.*, 2000).

As previously stated, fendiline is thought to interact with several cellular activities, although it is mainly thought to interfere with calcium levels within a cell. Some reports indicate it acts by reducing cellular calcium levels through inhibiting LTCCs (Nawrath *et al.*, 1998) whereas other reports state it increases cellular calcium by activating LTCCs (Lo *et al.*, 2001). Studies have also suggested fendiline acts by releasing calcium from the ER store, thus causing a calcium imbalance (Cheng *et al.*, 2001; Samantaray *et al.*, 2016). Although no definite mechanism of action for fendiline has been determined, a general theme appears to be persistent amongst many reviews, which is that fendiline acts by disrupting calcium levels within a cell (Nawrath *et al.*, 1998; Cheng *et al.*, 2001; Lo *et al.*, 2001; Samantaray *et al.*, 2016). Additionally, reports have cited fendiline to also inhibit calmodulin (Luckhoff *et al.* 1991; Wilkinson *et al.* 2007a).

With this in mind, although no investigation has been carried out, an interesting hypothesis would be that compound **4c** acts by interfering with the calcium levels of the parasite, which could explain its preference for acting on the schizont stages of the life cycle. This could be either by inhibiting the calcium channels, inhibiting calodulin, releasing calcium stored within calcium stores, or a combination of methods. All of the suggested options would potentially disrupt the fine calcium balance that the parasite maintains (Alleva and Kirk, 2001).

4.4.5 Conclusion and future work

In conclusion, the palladium coupling followed by reductive amination successfully led to the synthesis of fendiline and 11 analogues. If more compounds were to be synthesised purification steps should be optimised in order to obtain purer compounds with improved yields.

Of the 22 fendiline analogues screened, the 2'-hydroxy fendiline (compound **4c**) was the most potent antimalarial compound with good selectivity against human HepG2 cells (selectivity index 92.93). The compound was shown to be a slow acting drug targeting the schizont stages of the *P. falciparum* erythrocytic cycle. Finally, the IC_{50} value obtained from the hERG inhibition assay was 5.7 times higher than that for parasites; although the value was not very high (4.03 μM) it is still within the range that most small molecules fall within (Guth and Rast, 2010).

Future work would ideally follow two directions, firstly synthesis of new fendiline analogues that would incorporate both the naphthyl and hydroxyl groups in a bid to produce an even more potent antimalarial compound, and secondly, further determination of the current candidate's mode of action by establishing its PRR and PCT.

Chapter 5
Optimising a flow cytometry-based calcium fluctuation assay

5.1 Introduction

5.1.1 Calcium regulation in mammalian cells *vs* malaria parasites

Changes in calcium levels within eukaryotic cells can be responsible for a variety of physiological processes (Patel and Docampo, 2010). An intricate system of calcium pumps, channels and buffering proteins allows changes in cellular calcium levels to be precisely controlled (Berridge, Lipp and Bootman, 2000). The concentration of calcium is maintained at low levels within the cytosol, approximately 100 nM. However cells contain more calcium than that, the majority of which can be found stored within organelles such as the ER, mitochondria and other calcium stores or bound to proteins and membranes (Docampo and Moreno, 2013).

Channels located on cell membranes regulate calcium influx and efflux. Examples of influx channels are; voltage-gated channels, receptor-operated channels such as *N*-methyl-*D*-aspartate receptors (NMDARs) (Makhro *et al.*, 2013), store-operated calcium entry (SOCE) channels which become activated upon depletion of internal calcium stores (Smyth *et al.*, 2010) and calcium/sodium exchanger channels (Docampo and Moreno, 2013). Plasma membrane Ca^{2+} ATPases (PMCAs) also located on the plasma membrane are involved in efflux of cytosolic calcium out of the cell.

Upon entering a cell, calcium can bind to calcium-binding proteins or be sequestered into organelles. Calcium binding proteins such as calmodulin have highly conserved motifs for calcium to bind (Docampo and Moreno, 2013). The ER (or sarcoplasmic reticulum, SR, in muscle cells) is the most studied calcium store within cells (Patel and Docampo, 2010). Calcium is released from the ER by several channels such as the inositol-1,4,5-trisphosphate

receptor (IP_3R) and ryanodine receptor (RYR). The sarco-endoplasmic reticulum ATPase (SERCA) pumps transport calcium from the cytosol into the ER's calcium store (Berridge, Lipp and Bootman, 2000; Patel and Docampo, 2010; Docampo and Moreno, 2013). Other calcium stores like the Golgi complex, acidocalcisomes, vacuoles, endosomes and lysosomes have mechanisms to regulate calcium such as calcium pumps, exchanger channels, two-pore channels (TPC) and transient receptor potential channels (TRP) (Patel and Docampo, 2010). The image in Figure 5.1 shows a schematic of some of the discussed channels and calcium stores found within a cell.

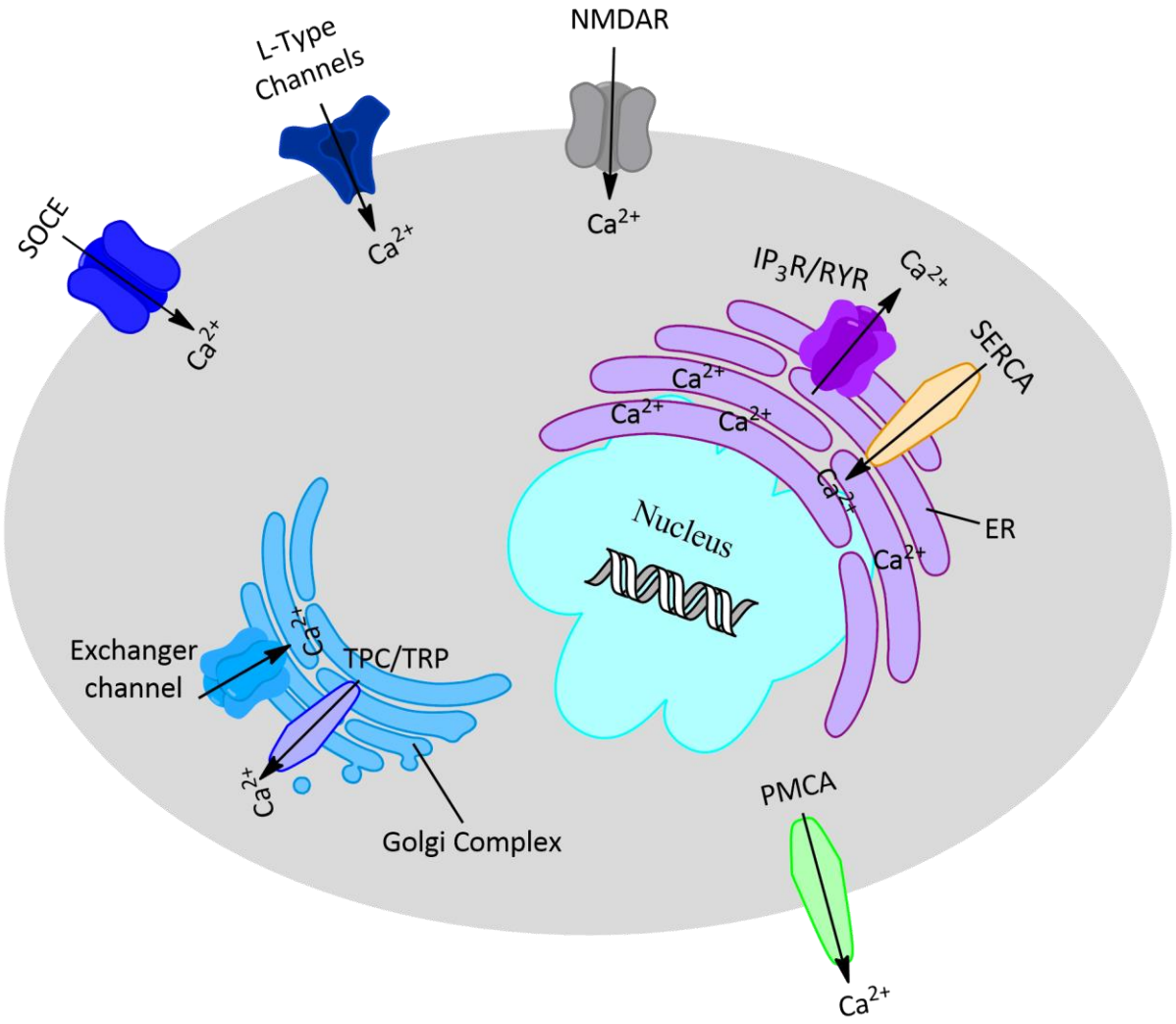

Figure 5.1 - Schematic of the different calcium channels that can be found within a mammalian cell. *Adapted from Clapham (2007) and Satheesh and Büsselberg (2015).*

Although RBCs lack organelles and calcium stores that are found in other cells, they maintain the ability to regulate their calcium levels through channels found on the membrane such as PMCAs (Camacho, 2003; Gazarini *et al.*, 2003; Romero *et al.*, 2006; Clapham, 2007; Docampo and Moreno, 2013; Bazanovas *et al.*, 2015; Pandey *et al.*, 2016). Additionally Makhro *et al.* reported the importance of *N*-methyl-*D*-aspartate (NMDA) and its receptor NMDAR in regulating RBC calcium levels consequently maintaining the cell's volume, stability and oxygen carrying ability (Makhro *et al.*, 2013; Makhro, Kaestner and Bogdanova, 2017). As previously discussed, studies have shown increased calcium levels in malaria infected RBCs thus piquing interest into the parasites' calcium regulation pathway (Desai *et al.*, 1996; Rohrbach *et al.*, 2005; Lourido and Moreno, 2015).

Regulation of calcium in malaria parasites appears to differ significantly in comparison with mammalian cells (Docampo and Moreno, 2013). The results of a study carried out by Prole and Taylor (2011) where genes from mammalian calcium channels were screened for homologues in genomes of fully sequenced pathogenic parasites, showed no homologues with *Plasmodium* species for voltage gated calcium channels, store-operated calcium channels, IP_3R or RYR channels and no NMDA channel homologues. The lack of IP_3R was echoed by Brochet *et al.* (2014) who stated release of calcium via IP_3 in malaria blood stages is evident although there is no genetic evidence for an IP_3 receptor. Earlier work published by Beraldo, Mikoshiba and Garcia in 2007 suggested presence of store operated calcium channels in *P. falciparum* however Prole and Taylor found no homology in the *Plasmodium* genome with the mammalian gene. The study did find some homology with TRP channels, however this was only identified due to homology with *T. gondii*, the homology between *Plasmodium* species and mammalian TRP was weak (Prole and Taylor, 2011).

The SERCA pump is highly conserved amongst various species and although vertebrates possess three serca genes, the *P. falciparum* genome possesses only one (Kimura *et al.*, 1993). The protein consists of ten transmembrane helices, three domains within the cytoplasm and luminal loops. The whole structure undergoes complex conformational changes which lead to the opening of the channel (Jambou *et al.*, 2010). The malarial SERCA pump has different sensitivities to eukaryotic SERCA inhibitors such as thapsigargin (Arnou *et al.*, 2011).

Rotmann *et al.* (2010) discuss the presence of a Ca^{2+}/H^{+} exchanger, PfCHA, in the *P. falciparum* genome which resides on the mitochondrial membrane and facilitates proton-coupled calcium, manganese and possibly magnesium exchange. Work carried out by Uyemura *et al.* (2000) proposed the potential for the uptake of calcium into mitochondria of *P. berghei* parasites. Suggestions that the mitochondria along with other organelles such as the ER, the food vacuole and acidocalcisomes act as calcium stores have been made (Uyemura *et al.*, 2000; Biagini *et al.*, 2003; Gazarini and Garcia, 2004; Rotmann *et al.*, 2010; Moreno, Ayong and Pace, 2011; Docampo and Moreno, 2013).

Approximately 30 proteins with potential calcium binding domains have been identified in the *Plasmodium* species, with 20 proteins encoding the conserved EF hand motif for calcium binding (Brochet and Billker, 2016). Only one calmodulin has been identified in the parasite genome. Generally, once calcium has bound to calmodulin, the complex binds to the catalytic domain of calmodulin kinases (CaMK) (Swulius and Waxham, 2008). CaMK are commonly found in eukaryotic cells, however only one class of these kinases was found in the *Plasmodium* species (Zhao *et al.*, 1992; Kato *et al.*, 2008; Brochet and Billker, 2016). Alternatively the parasite's genome encodes a diverse family of seven calcium dependent protein kinases (CDPKs). CDPKs are characterised by having a kinase catalytic domain along with EF motif calcium binding domains (Ward *et al.*, 2004). Furthermore there are several calcium effectors found within the parasites such as protein phosphatases (Brochet and Billker, 2016).

According to Brochet and Billker (2016), 60% of parasite genes have not been functionally annotated. This, in addition to the difficulty in genetically manipulating the AT-rich DNA of *Plasmodium* parasites and the inability to identify calcium channels and transporter systems due to the lack of homology with mammalian cells, have all played a part in hindering the study of calcium signalling pathways in the *Plasmodium* parasites over the years (Brochet and Billker, 2016).

5.1.3 Methods to detect intracellular calcium

Not surprisingly, considering the importance of calcium, an array of techniques have been and continue to be developed to measure calcium levels and calcium fluxes within cells.

Choosing the appropriate probe to detect and measure calcium levels for the particular cell type of interest is crucial but can be problematic. In 1928 (Pollack) reported using the dye alizarin sulfonate in ameba which would precipitate calcium ions as purple crystals that could be seen under the microscope. It was later determined that alizarin sulfonate was not specific for calcium and thus not a reliable dye (Kramer, 2015). An alternative to alizarin sulfonate was reported in the 1960s. Aequorin, extracted from jellyfish, is a light emitting protein activated by calcium or strontium (Shimomura and Johnson, 1969). Due to its size however it could not cross membranes, and was limited to large cells were it could be microinjected (Kramer, 2015). Although the issues regarding the size were eventually overcome, the process required to use aequorin is lengthy and susceptible to error due to contamination with calcium found in buffers or even glassware and thus not practical (Borle and Snowdowne, 1986).

It took approximately 50 years from the initial reports of Pollack in 1928 to develop practical calcium indicators that could be used in mammalian cells. The calcium-sensitive fluorescent dye, Quin2, was reported by Tsien, Pozzan and Rink in (1982), this was followed with improved dyes such as Fura-2 and indo-1 several years later (Grynkiewicz, Poenie and Tsien, 1985). The rationale behind the newly developed calcium indicators was based on hybridising a calcium chelator such as EGTA or BAPTA with a fluorescent chromophore (Meldolesi, 2004; Grienberger and Konnerth, 2012). The fluorescent dyes are synthesised in such a way that makes them only temporarily membrane permeable. This is achieved by coupling the chelators to an acetoxymethyl (AM) ester derivative, which is cleaved by endogenous esterases trapping the chelators within the cell (Tsien, 1981).

Since the initial synthetic calcium indicators emerged a variety of fluorescent dyes have become available (Grienberger and Konnerth, 2012). Dyes can come in three forms salts, dextran conjugates or AM esters (Paredes *et al.*, 2009). The salt indicators cannot cross the cell membrane and thus require various loading techniques such as microinjection or lipotransfer using liposomes. Once across the membrane however, they are ready to be used for calcium measurement within minutes albeit for a short period of time, thirty minutes to one hour, due to compartmentalisation of the dye away from the cytosol (Paredes *et al.*, 2009). Dextran conjugates resolve the compartmentalisation issue, however, still require the invasive loading techniques to cross the membrane into the cell (Kreitzer *et al.*, 2000; Paredes *et al.*, 2009). Finally the AM esters, as previously discussed, are membrane permeable

therefore resolving the cell loading issues equated with the other forms, however compartmentalisation of these dyes is an important drawback (Silver, Whitaker and Bolsover, 1992; Paredes *et al.*, 2009; Kramer, 2015).

Following his success developing fluorescent calcium indicators, Roger Tsein among others in the 1990s, went on to introduce genetically modified proteins that bind calcium sensors (Miyawaki *et al.*, 1997; Persechini, Lynch and Romoser, 1997; Grienberger and Konnerth, 2012). Progress in this field has led to the development of recombinant proteins that can measure very sensitive (nanoscale) calcium fluctuations within a cell (Whitaker, 2010; Looger and Griesbeck, 2012; Kramer, 2015). In fact recently Pandey *et al.* (2016) carried out calcium measurement experiments with *P. falciparum* parasites transfected with a recombinant calcium sensing protein. The calcium sensitive indicator yellow cameleon-Nano (YC-Nano) was fused to calmodulin and yellow fluorescent protein was fused to M13 peptide. The M13 peptide is a 27-residue peptide that displays properties of a calmodulin-binding domain. It was derived from skeletal muscle myosin light chain kinase. According to Pandey *et al.* (2016) in the presence of calcium, calmodulin binds to the M13 peptide which shortens the distance between the two fluorescent proteins, thus increasing the amount of fluorescence.

Once a suitable calcium indicator is identified, a variety of techniques can be developed to study calcium fluctuations and buffering within a cell. Compounds that interfere with calcium homeostasis within a cell are used frequently in research to either raise or reduce the overall calcium levels within a cell or to inhibit or activate specific channels. Examples of these include the calcium chelator EDTA, the calcium ionophore A23187 that raises intracellular calcium, CCBs such as verapamil, calcium channel activators such as Bay K8644 and FPL 64176, and riluzole, an NMDAR inhibitor (Kamal *et al.*, 2015).

5.1.3 Aims

The aim of the work reported in this chapter was to develop a flow cytometry-based method that allowed detection and quantification of fluctuations in calcium within *P. falciparum* infected cells using a combination of calcium and DNA binding fluorescent dyes. Initially a series of optimisation experiments were carried out to develop a Percoll gradient separation method on infected RBCs which results in obtaining concentrated parasitized cultures. The

Percoll separated cultures were used in the initial fluorescence tests to determine positive identification of infected cells. Once the use of the dyes was fully optimised a sequence of experiments using different calcium interfering compounds was carried out to determine if calcium fluctuations could be detected.

5.2 Experimental

5.2.1 Optimisation of a Percoll separation method

Percoll is a medium used to separate cells by density centrifugation. Percoll purification was carried out to obtain a concentrated late-stage parasitized culture. Numerous optimisation steps were attempted prior to obtaining a working method.

All working Percoll solutions were made from 90% Percoll, which was obtained by diluting 100% Percoll (Sigma, UK) in 10xPBS solution. Modification of a previously published procedure was used to optimise a working method (Miao and Cui, 2011; Iqbal *et al.*, 2016). Three samples were tested to optimise this method, in each sample a Percoll gradient was prepared by layering 3 ml of 35% Percoll (v/v in wash media) over 3 ml of 65% Percoll (v/v in PBS). Subsequently 2 ml of either 50%, 10% or 5% haematocrit infected RBCs was added to the top of the gradient and centrifuged for 15 minutes at 14,000 rpm.

To isolate the parasitized layer of infected RBCs, The top two layers (media and 35% Percoll solution) were removed and then the RBC layer in the 65%/35% Percoll interface was carefully pipetted out and washed three times with PBS. The results from the three separations can be seen in Table 5.1. Although the 50% haematocrit level sample did result in some separation, the 10% and 5% samples resulted in better separation and thus the 5% was the chosen method to be used in further experiments. Giemsa-stained slides of the cultures before and after the Percoll separation which highlight the concentrated parasitized culture obtained from the middle layer (65%/35% Percoll interface) can be seen in Figure 5.2 A and B respectively.

Haematocrit	Separation After Centrifugation
50%	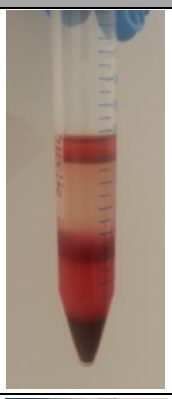
10%	
5%	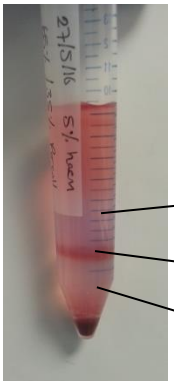

Table 5.1 - Results of the Percoll gradient separation.

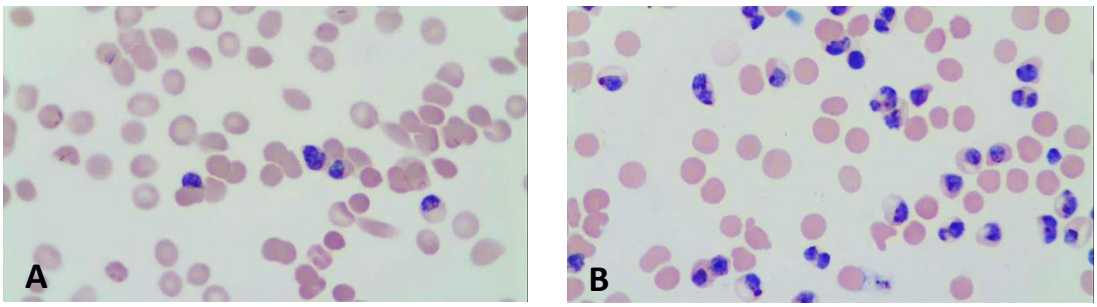

Figure 5.2 - Giemsa-stained microscope slide images of the cultures prior to (A) and after (B) Percoll gradient separation.

5.2.2 Fluo-8 staining of RBCs

In order to determine whether the use of the fluorescent dye Fluo-8 to detect calcium in infected RBCs is a viable option an experiment was set up. Two samples, infected and non-infected RBCs, were washed and incubated with Fluo-8 AM (Abcam, UK) in calcium-free Tyrode's buffer (140 mM NaCl, 10 mM glucose, 10 mM HEPES, 4 mM KCl, 1 mM $MgCl_2$, pH 7.4). Samples were incubated with Fluo-8 (0.5 µM) for 10 minutes in the dark at room temperature, they were then diluted further in 4 ml of Tyrode's buffer and incubated for 30 minutes prior to centrifugation for 5 minutes at 3,300 rpm. Finally, the pellet was washed and re-suspended in 1 ml of Tyrode's buffer and analysed on the flow cytometer using the FITC channel. Additionally, a sample of non-infected blood was washed and re-suspended in 1 ml of Tyrode's buffer without the addition of the fluorescent dye and was analysed in parallel. The density graphs in Table 5.2 show the difference between the three samples obtained by the BD FACs software.

Unstained blood	Non-infected blood loaded with Fluo-8	Infected blood loaded with Fluo-8
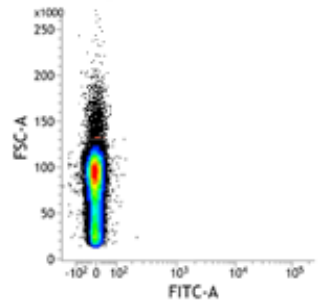	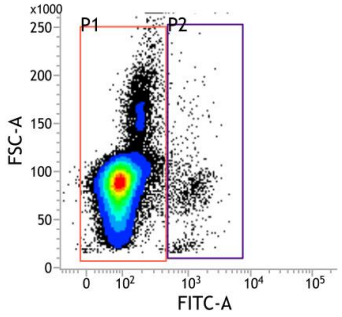	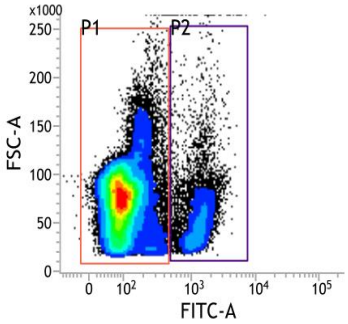

Table 5.2 - Comparison of unstained and Fluo-8 stained RBCs (infected and non-infected).

In the Fluo-8 loaded samples, the second population of cells (P2) is denser in the infected sample. The P2 population could potentially represent the population of parasites within the sample however further analysis was required to validate such an assumption.

5.2.3 Optimisation using long-wavelength DNA fluorescent dyes

Emissions from the SYBR Green (SG) dye and Fluo-8 dye are both on the FITC channel, therefore using the two dyes in combination would not be possible. Consequently, an alternative DNA binding dye was required to dual stain samples with calcium and DNA binding fluorescent dyes. The sensitivity of three long-wavelength nucleic acid stains (BOBO-3 Iodide, TOTO-3 Iodide and YOYO-3 Iodide) (Thermo Fisher, UK) were tested to detect parasitized RBCs. The staining was carried out following a modified version of a previously published method (Campo *et al.*, 2011). Briefly, 100 µl of 5% haematocrit RBCs (infected and non-infected) was washed with PBS, incubated with glutaraldehyde (0.25% in PBS) for 30 minutes at 4 °C and then centrifuged for 5 minutes at 3,500 rpm. Samples were incubated for a further 5 minutes with triton x-100 (0.25% in PBS) at room temperature, centrifuged again as previously described and then re-suspended in 0.5 ml of nucleic acid dye (0.5 µM in PBS) for 30 minutes at room temperature prior to analysis by flow cytometry. BOBO-3 was analysed on the PE channel, TOTO-3 and YOYO-3 on the APC-Cy7-A channel. The experiment was carried out in parallel to a SG control and results are presented in Table 5.3.

Dye	Non-infected RBCs	Infected RBCS	% Parasitaemia obtained by flow cytometer
SG	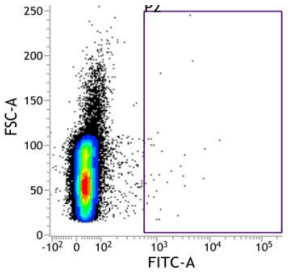	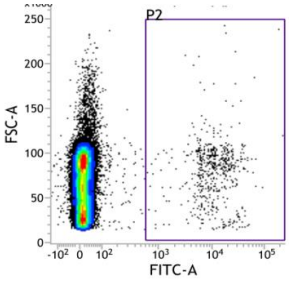	1.27
BOBO-3	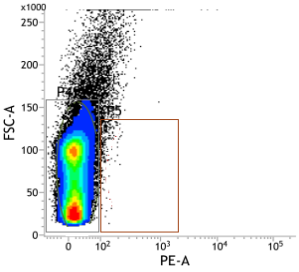	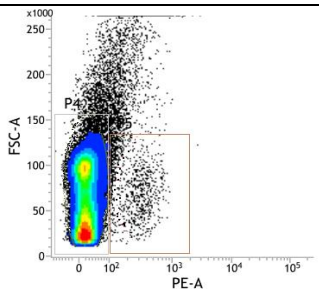	1.34
TOTO-3	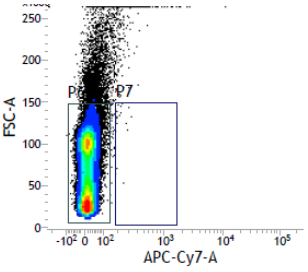	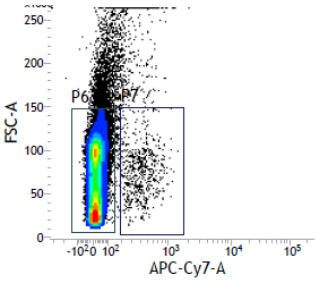	1.30
YOYO-3	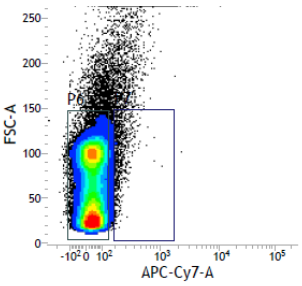	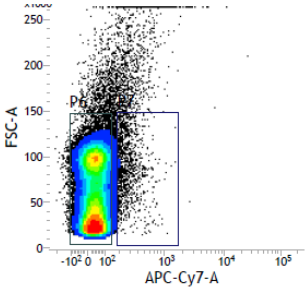	0.98

Table 5.3 - Comparison between SG and a range of long-wavelength DNA binding fluorescent dyes.

Good separation between the negative and positive cells (non-infected blood and infected blood populations) is advantageous in ensuring no overlap between the populations occurs. The infected population of the SG stained samples is far away from the non-infected population, showing no overlap between the two. The other tested dyes in this experiment did not show as good separation as observed with SG, however both BOBO-3 and TOTO-3 showed reasonable separation. Furthermore, the percentage parasitaemia estimated from all

three dyes were somewhat comparable to SG, again with BOBO-3 and TOTO-3 showing the best results. TOTO-3, was chosen as the long wavelength DNA binding fluorescent dye to use for subsequent experiments as it showed the best separation between the two populations.

5.2.4 Comparison between Fluo-8, TOTO-3 and SG *via* Percoll purification

An experiment comparing SG, TOTO-3 and Fluo-8 stained infected RBCs was carried out. Samples of infected RBCs were taken prior to and following Percoll treatment and stained with either SG, TOTO-3 or Fluo-8 and analysed in parallel using flow cytometry (Table 5.4). Non-infected blood and Giemsa-stained microscope slides were also analysed in parallel as controls (Figure 5.3).

Sample	SG	TOTO-3	Fluo-8
Non-infected Blood	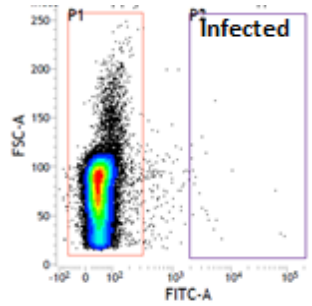	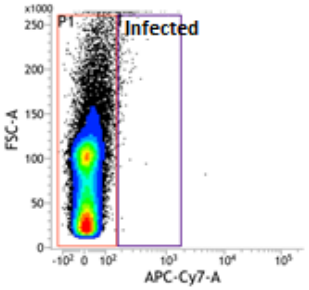	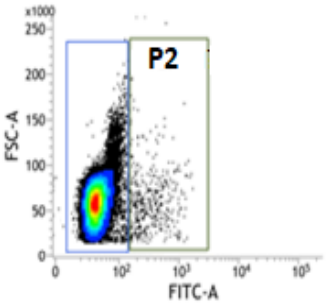
Infected Blood Before Percoll Purification	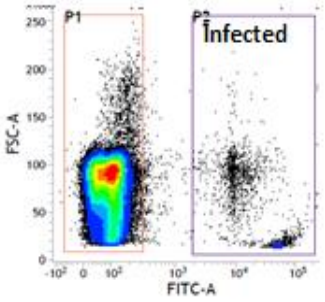	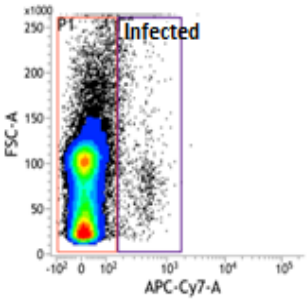	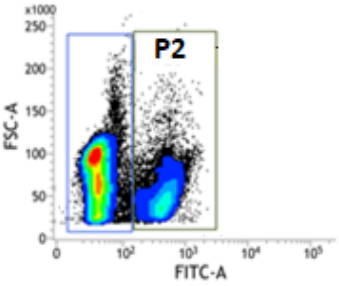
Infected Blood After Percoll Purification	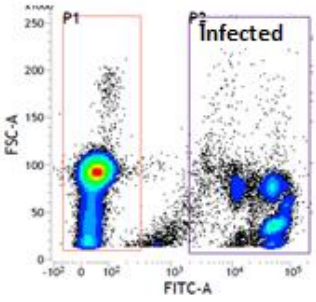	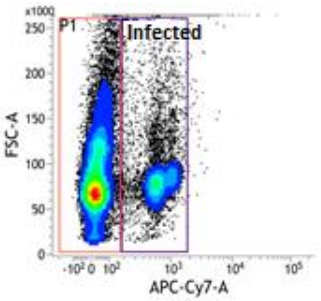	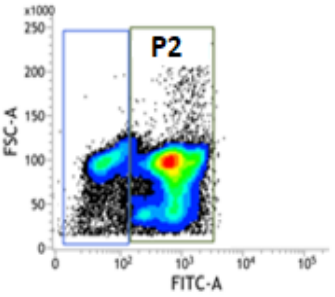

Table 5.4 – Density graphs showing SG, TOTO-3 and Fluo-8 stained infected RBCs before and after Percoll purification. *The population labelled (P2) in the Fluo-8 stained cells are the assumed infected population of cells.*

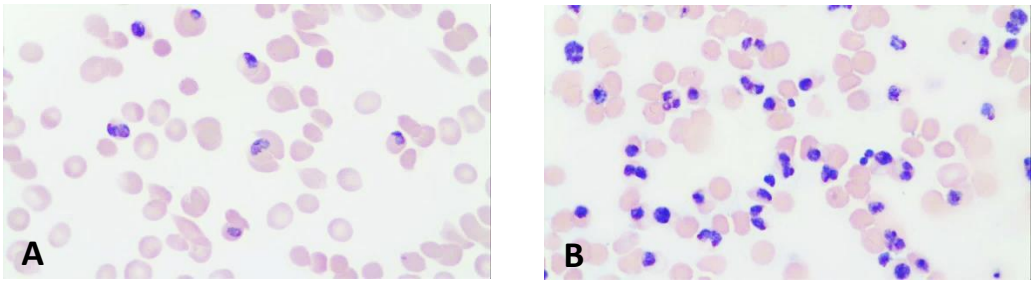

Figure 5.3 - Giemsa-stained slides of the cultures before (A) and after (B) Percoll purification.

The infected RBCs stained with SG and TOTO-3 in Table 5.4 show an increase in population size before and after Percoll treatment. A similar increase is seen in the presumed to be infected population (P2) loaded with Fluo-8. The images from the microscope slides show a concentrated parasite population after Percoll treatment supporting the results obtained by the flow cytometer.

Table 5.5 shows the fold increase in the infected population size obtained using flow cytometry and the increase in parasitaemia counted from the Giemsa-stained microscope slides. The presumed infected RBC population stained with Fluo-8 increased by 4.46-fold, which is comparable to the 4.85-fold average increase from the remaining samples. This further supports the hypothesis of the population being that of parasite infected cells.

Staining Dye Used	Fold Increase Post Percoll Treatment
SG	4.87 ± 0.15
TOTO-3	4.84 ± 0.08
Fluo-8	4.46 ± 0.01
Giemsa-stained Microscope Slides	4.83 ± 0.83

Table 5.5 – Comparison between different dyes of the fold-increase detected in parasite population before and after Percoll gradient separation.

5.2.5 Comparison between Fluo-8, TOTO-3 and SG in a serially diluted culture

To determine whether the higher Fluo-8 (calcium) fluorescence population is that of infected RBCs and to also test the compatibility of double staining a sample with Fluo-8 and TOTO-3 an experiment was set up with SG in parallel as a control. This time a four point two-fold serial dilution of infected blood was carried out. Triplicate samples were taken from each dilution and loaded with SG, TOTO-3, Fluo-8, or a dual stained with Fluo-8 and TOTO-3 then analysed using flow cytometry.

To achieve double staining with Fluo-8 and TOTO-3, the samples were loaded with Fluo-8 as previously described and then after the final wash the samples were stained with TOTO-3 following the previously explained method starting with the glutaraldehyde fixation step. TOTO-3 was diluted in Tyrode's buffer for this experiment and not PBS.

In order to compare the results obtained from each fluorescent dye, the values from the gated population (highlighted in Table 5.6) from the first sample (dilution 1) was set to 100% and subsequent dilutions were calculated as percentages relative to it. The results of the serial dilution can be seen in Figure 5.4.

SG	TOTO-3	Fluo-8
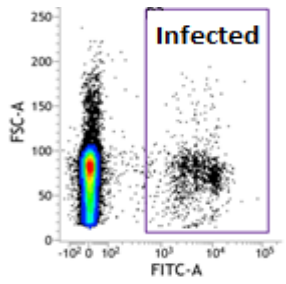	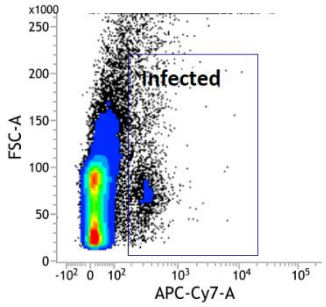	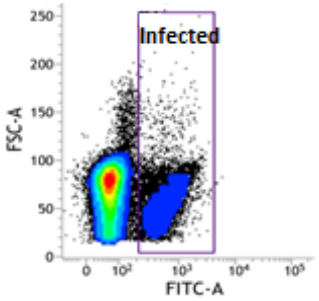

Table 5.6 – Image showing the gated population of infected cells (SG and TOTO-3) and the presumed to be infected population stained with Fluo-8 labelled (P2).

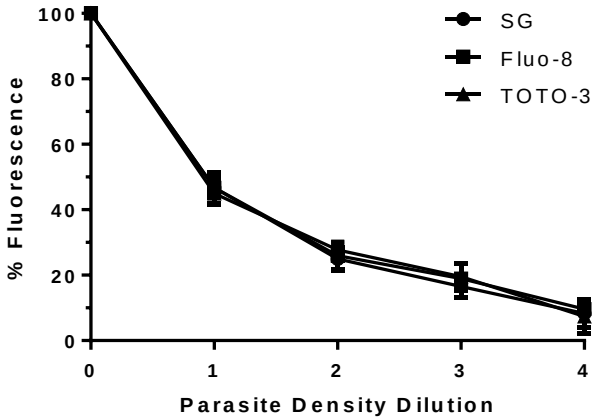

Figure 5.4 – Results of the serial dilution carried out using the three fluorescent dyes (SG, TOTO-3 and Fluo-8). The graph is presented as percentage fluorescence against dilution number. (n ≥ 3).

The Fluo-8 stained population of cells decreased in a similar manner to that of the infected populations stained with SG and TOTO-3. Once again the results further corroborate the premise that this population incorporates the infected cell population.

Samples dual stained with Fluo-8 and TOTO-3 dyes were also prepared for this experiment. However, once combined the signal from the Fluo-8 dye could no longer be detected in any of the samples and thus analysis could not be carried out on the dual stained samples.

5.2.6 DRAQ5 staining of RBCs

Due to the incompatibility between TOTO-3 and Fluo-8, an alternative long wavelength DNA binding dye was required, therefore DRAQ5 was tested. For DRAQ5 staining, 100 µl of 5% haematocrit RBCs was added to 1 ml of PBS, mixed and then centrifuged at 13,400 rpm for 90 seconds. The pellet was then re-suspended in 0.5 ml of DRAQ5 (Biostatus, UK; 5 µM in Tyrode's buffer) and incubated for 30 minutes at room temperature prior to analysis using flow cytometry.

In order to validate the use of DRAQ5 as an alternative to SG, a two-fold serial dilution of an ongoing culture was carried out. Samples from each dilution were taken and stained with either SG or DRAQ5, along with non-infected RBCs as controls. Analysis was carried out on the flow cytometer and the initial results can be seen in Figure 5.5.

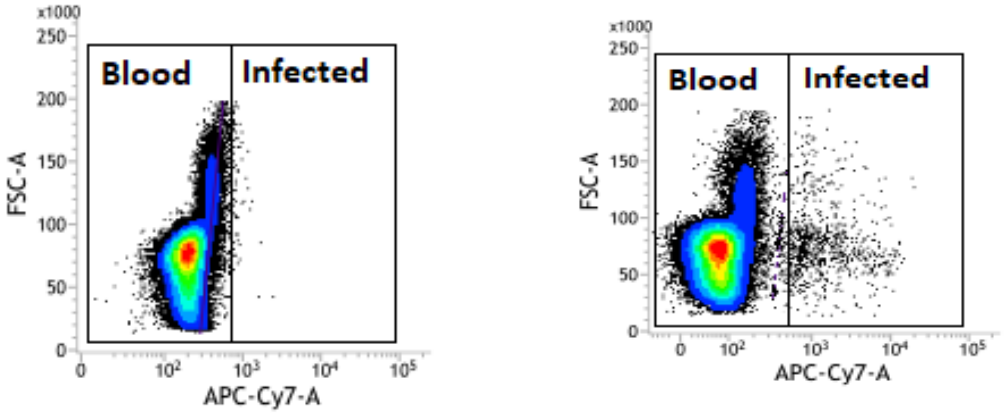

Figure 5.5 – Density graphs visualised on the APC-Cy7-A channel displaying infected and non-infected RBCs stained with DRAQ5.

Results of the serial dilution comparing SG and DRAQ5 can be seen in Figure 5.6. The experiment was carried out to validate the use of DRAQ5 as a long wavelength DNA fluorescent dye that can be used as an alternative to SG. Results from both dyes were comparable with one another and thus DRAQ5 was selected for combination with Fluo-8 in subsequent experiments.

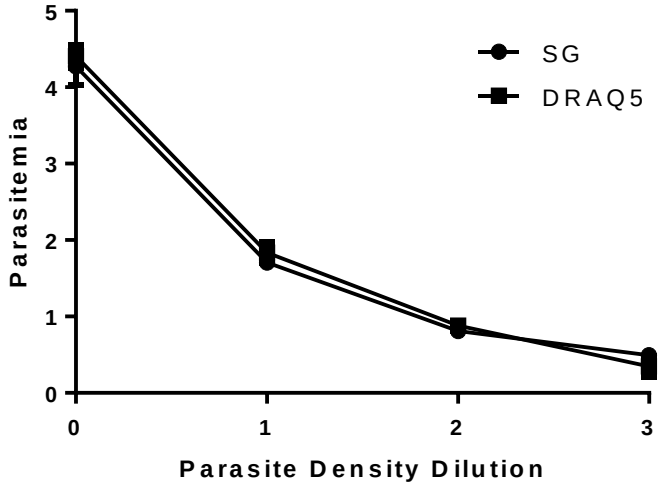

Figure 5.6 – Comparison of parasitaemia estimation between two DNA binding fluorescent dyes, SG and DRAQ5, via serial dilution. *(n = 2).*

5.2.7 Dual staining with Fluo-8 and DRAQ5

Dual staining of RBCs (infected and non-infected) was carried out by initially loading the sample with Fluo-8, following the incubation and washing steps, the samples were then incubated with DRAQ5 as previously described.

To test the compatibility of combining the dyes, dual staining was carried out on an ongoing culture prior to and following Percoll treatment. Fluo-8 only and DRAQ5 only samples were also prepared in parallel. All results were analysed using flow cytometry.

Fifty thousand events per sample were recorded on the flow cytometer. The data was obtained using the FITC channel and the APC-Cy7-A channel (laser excitation 650 nm, BD Biosciences, 2015). Density graphs consisting of APC-Cy7-A (DNA) fluorescence on the x-axis versus FITC (calcium) fluorescence on the y-axis were created and shown in Table 5.7. The

table shows images of the culture prior to and following Percoll treatment for single stained and dual stained samples. Images from the single stained samples show no overlap in emission from either dye further validating their use in combination.

Dye / Sample	Fluo-8	DRAQ5	Fluo-8+DRAQ5
Non-infected	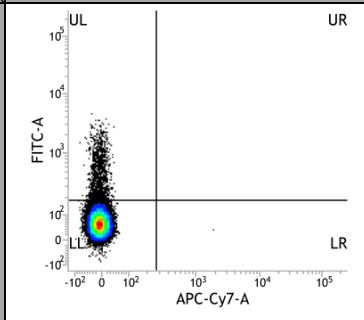	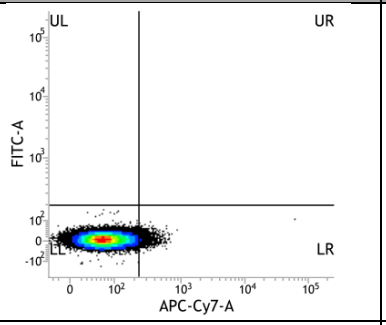	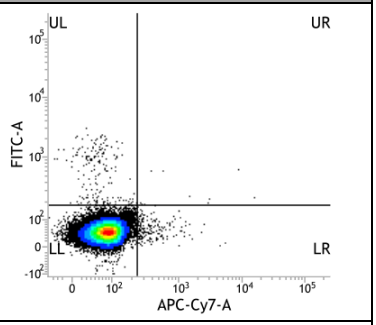
Infected Before Percoll	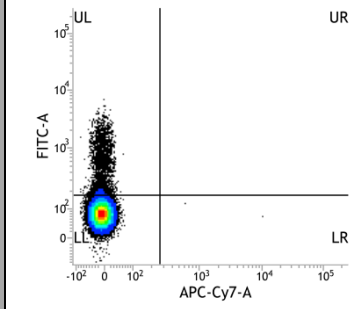	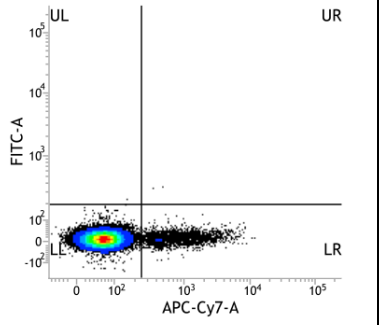	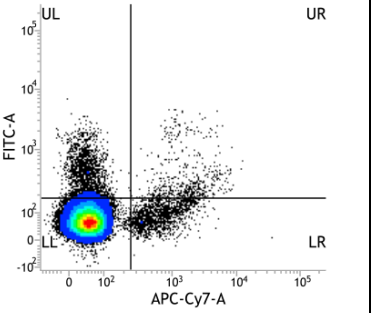
Infected After Percoll	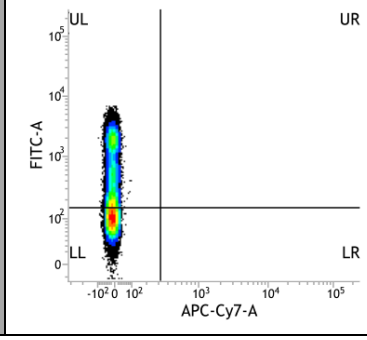	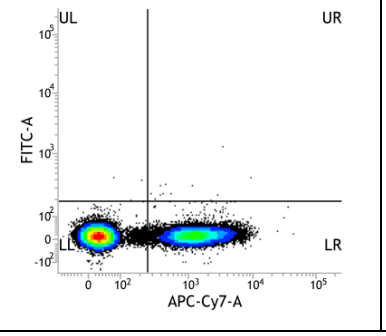	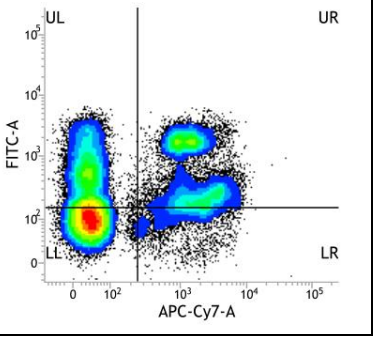

Table 5.7 - Flow cytometry produced denisty graphs displaying the APC-Cy7-A (DNA)/FITC-A(calcium) filters of an ongoing culture before and after Percoll treatment.

The results of combining Fluo-8 and DRAQ5 dyes implies that the infected population of cells does not lie solely within a high calcium fluorescence or low calcium fluorescence region. The population appears to spread from a low to a higher calcium fluorescence with increase in

DNA fluorescence. In fact, only after the Percoll treatment, which results in a concentrated late-stage parasite culture, does the infected population appear to shift slightly into the higher calcium region. Additionally, the infected cells are split into two populations, one of which is higher in calcium fluorescence. This could be two stages of parasites, for example late trophozoites and schizonts.

Furthermore, in the dual stained samples the results show a population of DNA negative cells with higher calcium fluorescence ($DNA^-/Calcium^+$), similar to the population of cells seen in the Fluo-8 only stained cells. Prior to introducing the DNA binding dye, the population of cells with higher calcium levels was presumed to be that of the infected cells. Following these results, the hypothesis is somewhat disproven, it is now assumed that only a portion of the higher fluorescence Fluo-8 population can be attributed to infected cells. The remainder being non-infected cells with a higher calcium content.

5.2.8 Stage-specific differences in intracellular calcium levels

Analysis of a dual stained, Fluo-8 and DRAQ5, synchronised culture was carried at three separate time points within the parasite blood cycle, namely ring, early trophozoite and late trophozoite/schizont stages. This was done to determine whether there was a difference in calcium levels between the different stages. Giemsa-stained microscope slides were also prepared to provide visual confirmation of parasite stages.

The gating strategy followed to select dual stained infected cells during this experiment and subsequent experiments is described in Figure 5.7. RBCs were initially gated, then the DNA positive population was identified and selected for calcium detection and measurement.

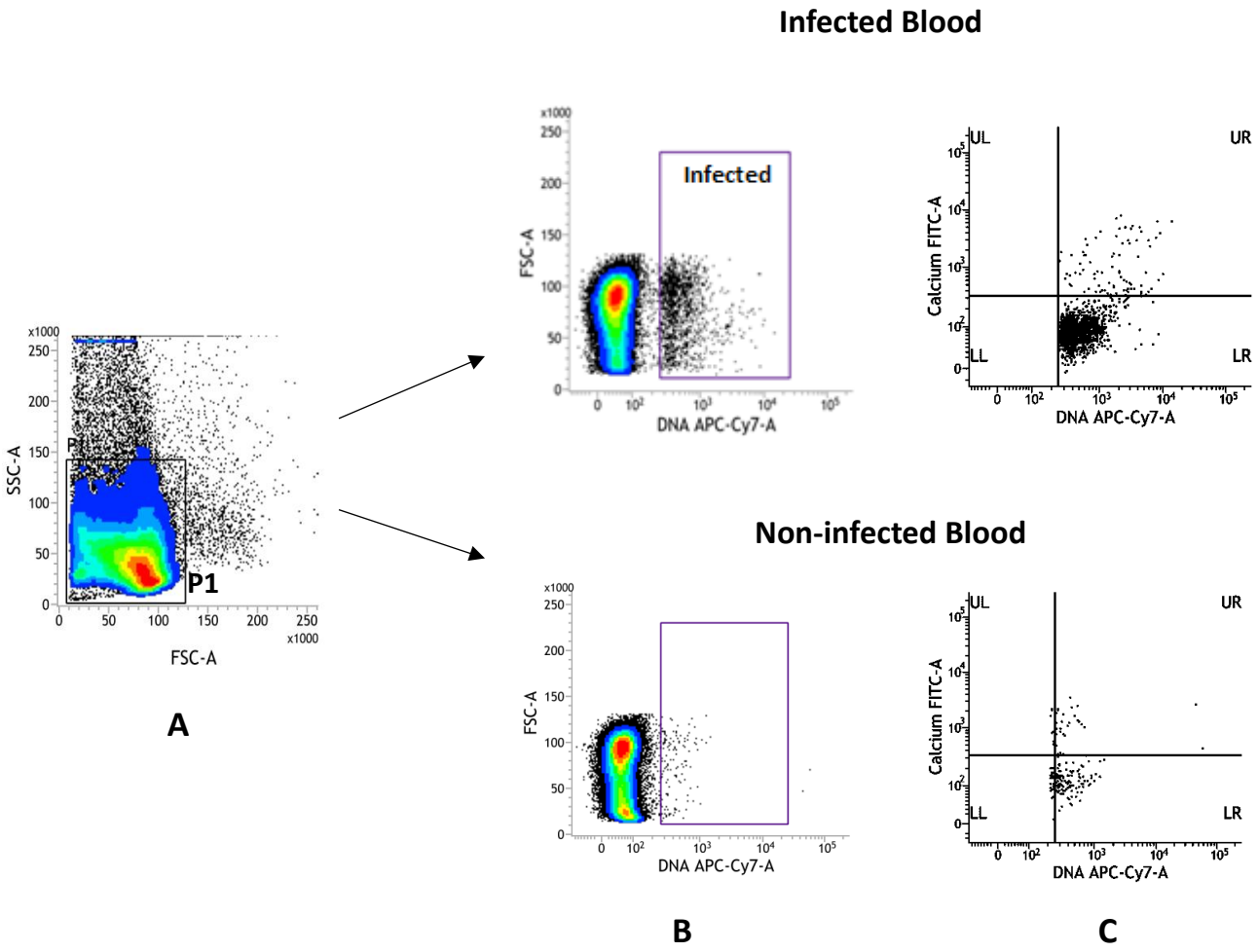

Figure 5.7 – Gating strategy used to visualise calcium changes within an infected culture.
A) The parameters used to select red blood cell population (P1), B) the P1 events are then displayed on the APC-Cy7-A/FSC-A density plot allowing the infected red blood cell population to be identified, C) the infected population events are then visualised on the APC-Cy7-A/FITC dot plot in order to visualise differences in calcium levels.

The images in Table 5.8 show the flow cytometry and microscopy results of the ongoing culture at three-time points of the parasite life cycle. The flow cytometry results are shown as APC-Cy7-A (DNA)/FITC (calcium) dot plot graphs of the infected only population. The results imply that late-stage parasites have higher calcium levels than in the early stages, this is determined due to the shift in the population into the higher FITC fluorescence region. This hypothesis is further corroborated with the results presented in Table 5.9 where the mean fluorescence values from both the FITC (calcium) channel and the APC-Cy7-A (DNA) channel were obtained from the BD FACs software. The results presented as relative fluorescence units (RFU) show ring stage parasites to have 1-fold higher calcium fluorescence than the early

trophozoite stage parasites, whereas the late-stage parasites had a 3.5-fold increase in fluorescence in comparison with the ring stages. The mean DNA fluorescence increased gradually through the parasite cycle, this further supports the stages of the parasites as DNA content increases with parasite maturity (Grimberg *et al.*, 2008).

Method	Ring	Early Troph	Late Troph/Schizont
Flow Cytmeter	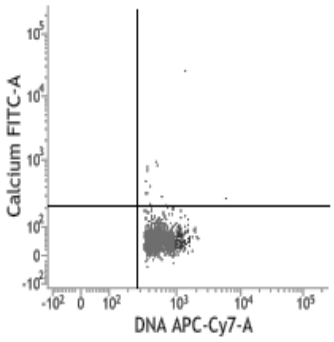	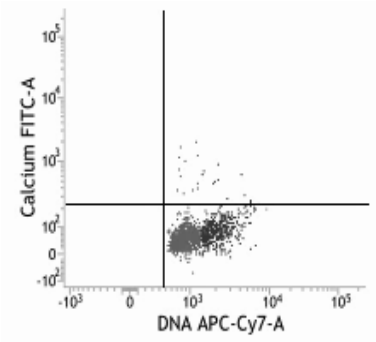	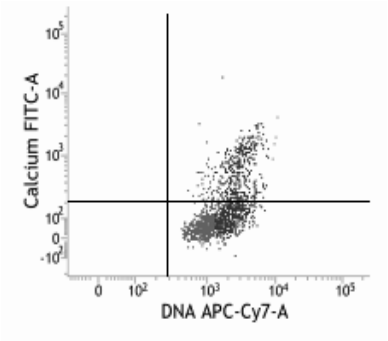
Microscope Slides	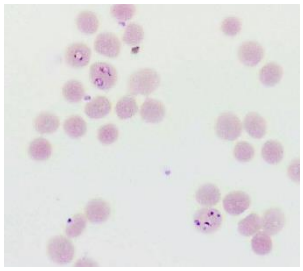	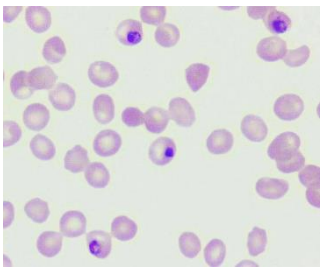	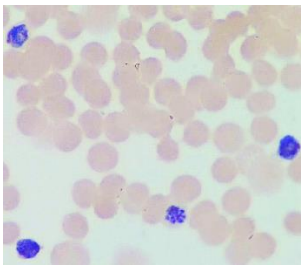

Table 5.8 - Flow cytometry produced images and Giemsa-stained slides of an ongoing culture at different time points.

Sample	Fluo-8 FITC Fluorescence (RFU)	DRAQ5 APC-Cy7-A Fluorescence (RFU)
Rings	74.05 ± 7.05	762.00 ± 6.50
Early Trophs	71.20 ± 2.20	1426.50 ± 8.50
Late Trophs/Schizonts	259.50 ± 4.50	2384.00 ± 8.00

Table 5.9 - Mean fluorescence values from the FITC and APC-Cy7-A channels from the different stages of parasites. *The figures are presented as relative fluoresnce units (RFU).*

5.2.9 Measuring variances in calcium concentrations

An experiment was set up to determine whether incubating a culture with varying concentrations of calcium would have a detectable effect using flow cytometry. Samples from an ongoing culture were dual stained with Fluo-8 and DRAQ5. Prior to analysis by flow cytometry, the samples were incubated with varying concentrations of $CaCl_2$ (0, 1, 10, 100 and 1000 nM) in Tyrode's buffer for 15 minutes. The flow cytometry gating strategy followed was the same as the one described previously in Figure 5.7. The data was analysed by obtaining the mean FITC fluorescence values from the BD FACs software. The control samples lacking calcium chloride (F_0) were given a base value of one and fluorescence from subsequent samples (F) were calculated relative to it (F/F_0).

The results of the experiment presented in Figure 5.8 show there was no difference in fluorescence following the addition of calcium chloride in comparison with the control samples which consisted of no calcium. The graph shows the log concentration of calcium chloride against fold-change in fluorescence.

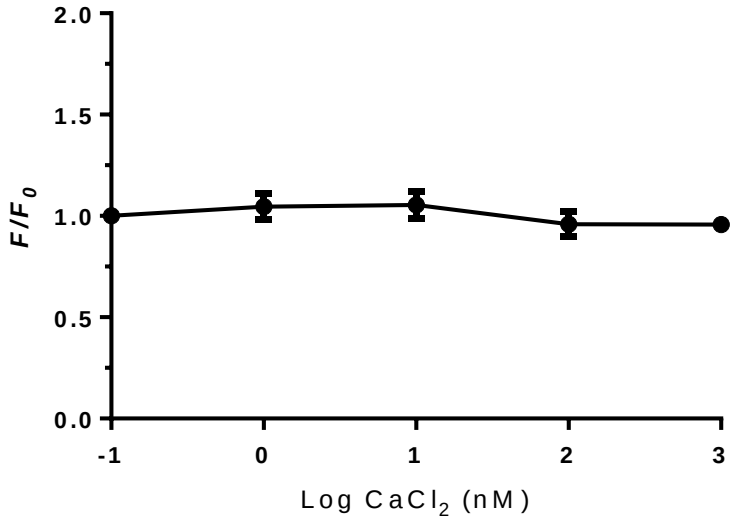

Figure 5.8- Analysis of varying calcium concentrations on infected RBCs. *The results are presented as the fold change of mean FITC fluorescence (F/F_0) against log concentration of $CaCl_2$. For the purpose of this graph, the result of the control sample with no calcium chloride is displayed at -1 (log $CaCl_2$ nM). (n = 2).*

5.2.10 Measuring calcium fluctuations using flow cytometry

A series of experiments were carried out to detect calcium dynamics in infected blood cells following exposure to various calcium interfering compounds. Two stages were selected to test each compound, ring and late trophozoite/schizont. Cultures were dual stained with Flou-8 and DRAQ5 as previously described in 1 mM $CaCl_2$ Tyrode's buffer. Experiments were carried out by exposing the parasites to either one or two calcium interfering compounds and measuring the effects at set intervals following the addition of the compound(s).

Following the dye loading, samples were analysed on the flow cytometer. Initially three readings per sample were carried out, this was used as a baseline for each sample. For the single drug samples, after the baseline readings, 50 µl of drug was added to the tube, mixed well and immediately analysed on the flow cytometer, nine subsequent readings were then taken at either 30 or 60 second intervals. For samples exposed to two compounds, following baseline recordings, 50 µl of the first drug was added, mixed and analysed once, this was followed by a four-minute interval and then on the fifth minute a further measurement was taken, followed by the addition of 50 µl of the second drug. After addition of the second drug, analysis resumed as with single drug samples with continuous measurements being carried out at 60 second intervals. Furthermore solvent (DMSO and ethanol) control experiments were also carried out in parallel.

Compounds used in these experiments were; the calcium ionophore A23187, EDTA, fendiline hydrochloride, verapamil hydrochloride, riluzole, and the LTCC activators FPL 64176 and Bay K8644. All stock compounds were diluted in Tyrode's buffer with $CaCl_2$ (1 mM) and each sample was exposed to a final concentration of 10 µM of each compound, except for EDTA which was added directly to the samples to a final concentration of 25 µM. Additionally solvent control experiments were also carried out in parallel.

The calcium ionophore A23187 that raises intracellular calcium (Vines, McBean and Blanco-Fernández, 2010) and the calcium chelator EDTA were used initially to show calcium levels increase or decrease within a population (Figure 5.9 A and B). Compound A23187 was used as a reference drug for each experiment, furthermore it was used to induce a raise in calcium

prior to and following the administration of EDTA (Figure 5.9 C and D), the L-type CCBs (fendiline and verapamil), and the NMDAR inhibitor riluzole (Figure 5.10 A-I).

Analysis of the results was carried as the previous experiment, where baseline readings (controls) were averaged and normalised to one (F_0), subsequent readings (F) were calculated as fold change relative to the controls (F/F_0). The addition of drug is indicated on the graphs by an arrow.

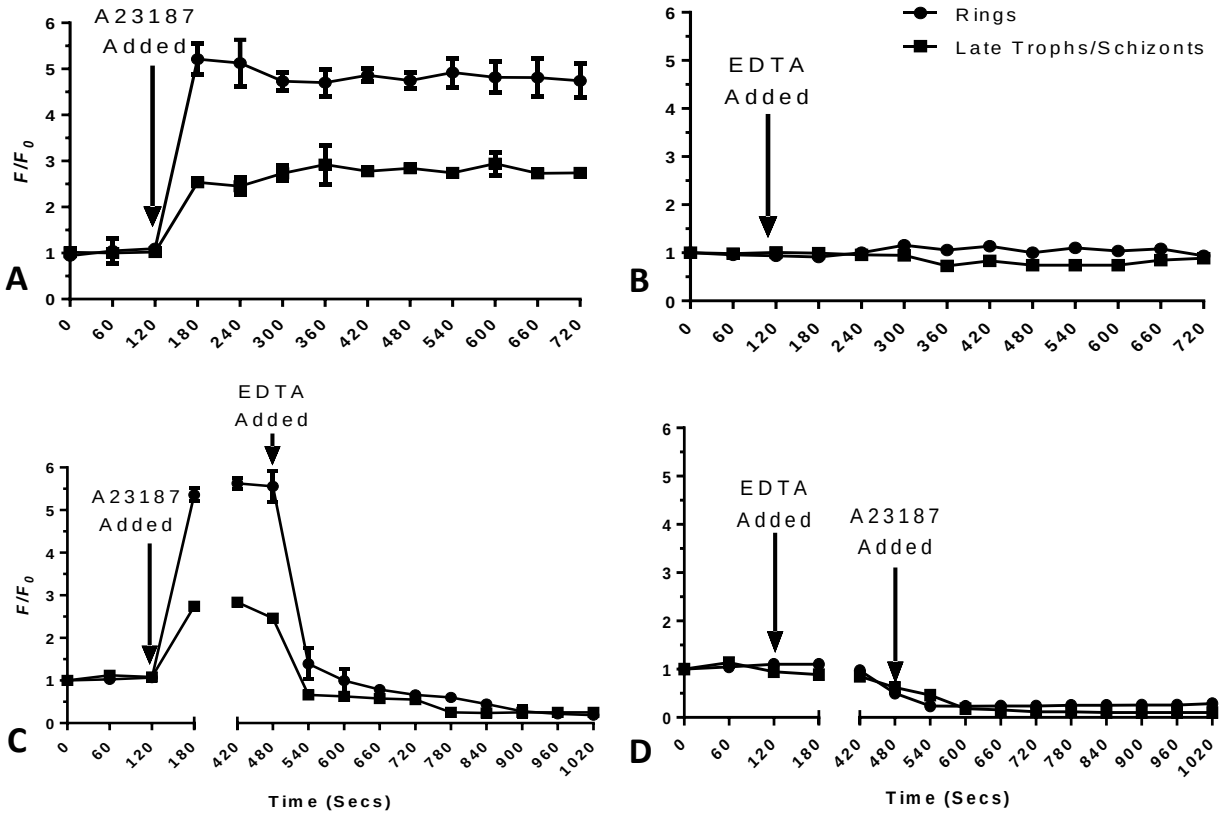

Figure 5.9 – Calcium flux experiments in response to the calcium ionophore A23187 and EDTA on infected RBCs. *Graphs are presented as the fold change of the mean Fluo-8 FITC fluorescence after exposure to the compounds (F/F_0) against time (Secs). Arrows indicate the administration of the compound. All experiments were carried out on ring (circles) and late trophozoite/schizont (squares) cultures; A) A23187 administered alone, B) EDTA administered alone, C) A23187 added initially and then followed by EDTA, D) EDTA administered first and then followed by A23187. (n ≥ 2)*

The graphs show compound A23187 to have a prominent increase on calcium levels of the infected RBCs (Figure 5.9 A). When administered alone EDTA (Figure 5.9 B) doesn't appear to have an effect on the calcium fluorescence of ring stage parasites. However in the late-stage parasites, the fluorescence is somewhat reduced following exposure to EDTA (Figure 5.9 B). Moreover regardless whether EDTA is administered prior to or after A23187, EDTA appears

to suppress the effect A23187 has on its own and reduces calcium fluorescence to almost zero.

The graphs also show that when ring stage cultures are exposed to A23187, the calcium fluorescence increases by approximately 5.5-fold whereas the increase is approximately 2.5-fold in the late-stage parasites.

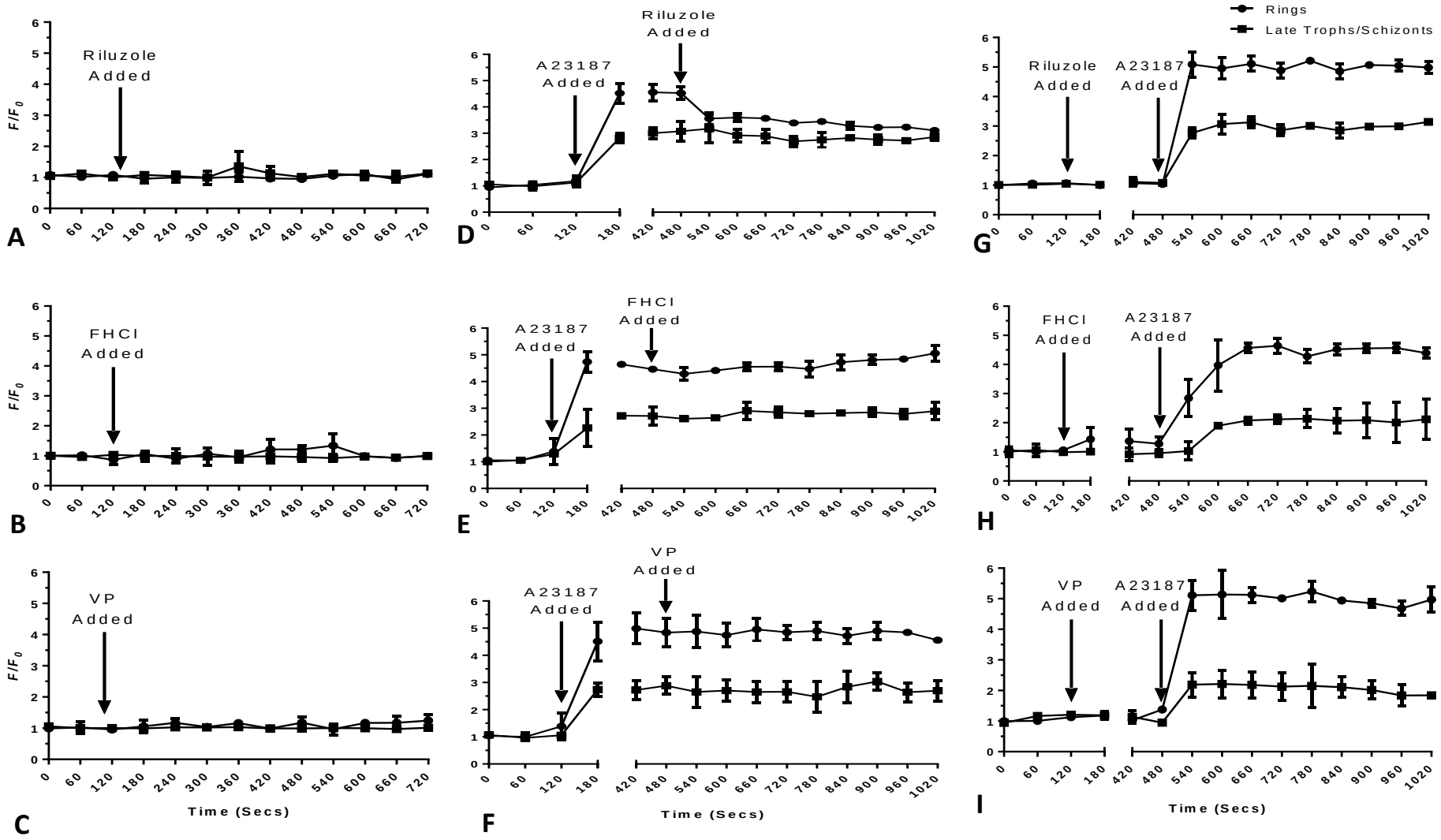

Figure 5.10 - Calcium fluctuation experiments carried out on P. falciparum infected RBCs at both ring (circles) and late trophozoite/schizont (squares) stages. *Each drug was tested alone, then the drugs were tested before and after the addition of the calcium ionophore A23187. Graphs A-C are of the drugs added alone, appearing in the order of riluzole, fendiline (FHCl) and then verapamil (VP) respectively, graphs D-F are of compound A23187 administered prior to the respective drugs, graphs G-I are of the individual drugs added first before the addition of A23187. Graphs are presented as mean FITC fluorescence change against time (Secs). (n ≥ 2)*

None of the compounds appear to have a detectable effect on calcium fluorescence when administered alone (Figure 5.10 A-C) using this method of detection.

Although riluzole itself did not affect calcium levels, Figure 5.10 D shows a culture being exposed to compound A23187; the cell's calcium levels were raised as seen with previous samples however once riluzole was administered the calcium fluorescence reduced by 0.8-fold. This effect is only seen in the results of the ring stage culture, not in the trophozoite culture.

Furthermore, the results of fendiline on the cultures did not present a noteworthy effect on the samples. The exception was following administration of fendiline, the effects of A23187 were slightly delayed (Figure 5.10 H).

Further calcium flux experiments were carried out on two l-type calcium channel activator compounds FPL 64176 and Bay K8644. The results presented in Figure 5.11 show that neither compound exhibited a detectable effect on the calcium levels using this method.

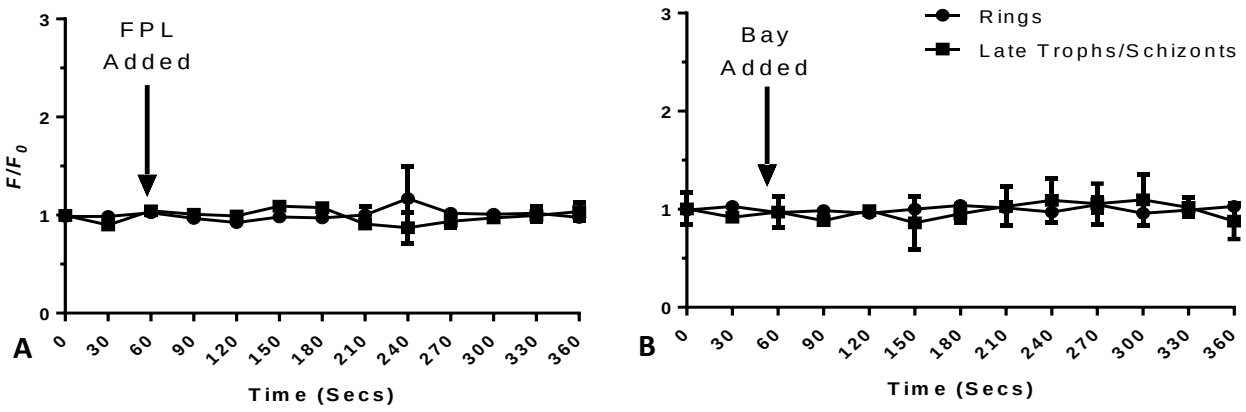

Figure 5.11 – Graphical analysis of calcium flux in response to both A) FPL 64176 (FPL) and B) Bay K8644 (Bay). *Graphs are displayed as fold change in fluorescence intensity against time. The addition of drug is represented by an arrow, experiments were carried out on ring (circles) and late trophozoite/schizont (squares) stage parasites. (n = 2).*

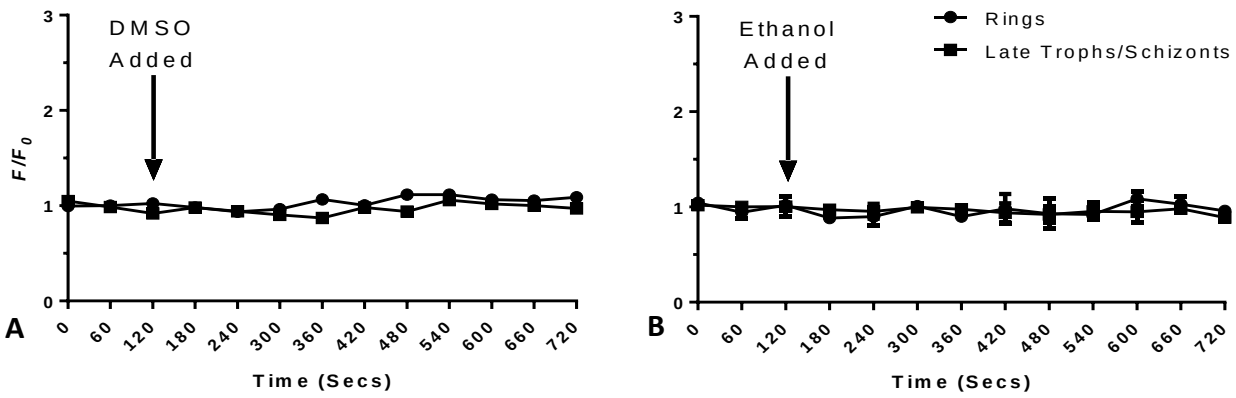

Figure 5.12 – Results of the solvent control experiments. *A) DMSO, B) Ethanol. The addition of solvent is represented by an arrow. (n = 2).*

The results obtained from the solvents used to reconstitute the compounds used in these experiments did not interfere with calcium levels as seen in the control experiments (Figure 5.12 A and B).

5.2.11 Measuring calcium fluctuations in non-infected blood

Out of the tested compounds, the calcium ionophore A23187 was the only calcium increasing compound to show a detectable effect. Therefore the effect it had on a blood only sample was carried out to determine whether a similar response would occur. Fluo-8 and DRAQ5 stained blood only samples were prepared as previously described. Initially base line recordings were taken, followed by the addition of the compound and subsequent measurements carried out at 60 second intervals. Recordings were carried out by flow cytometry as previously described and results are shown in Figure 5.13. Indeed, like the effect seen on ring stage infected RBCs, a 5.5-fold increase in calcium fluorescence was observed.

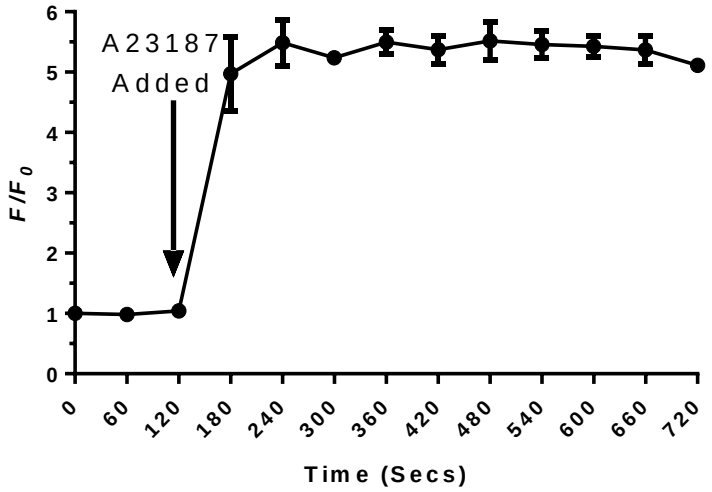

Figure 5.13 – Calcium flux experiments in response to the calcium ionophore A23187 on blood only samples. *(n=2)*

5.2.12 Measuring calcium fluctuations in saponin treated cultures

To determine whether the rise in calcium following exposure to A23187 is occurring within the RBC cytosol or within the parasite a further experiment was carried out on isolated parasites. In order to isolate parasites, unsynchronised infected blood was treated with 0.05% saponin in PBS for 10 minutes at room temperature. Samples were washed twice with PBS and then the typical Fluo-8 and DRAQ5 dye loading procedure followed. Each saponin treated sample was then exposed to compound A23187 and analysis proceeded as previously described using flow cytometry, results of which can be seen in Figure 5.14.

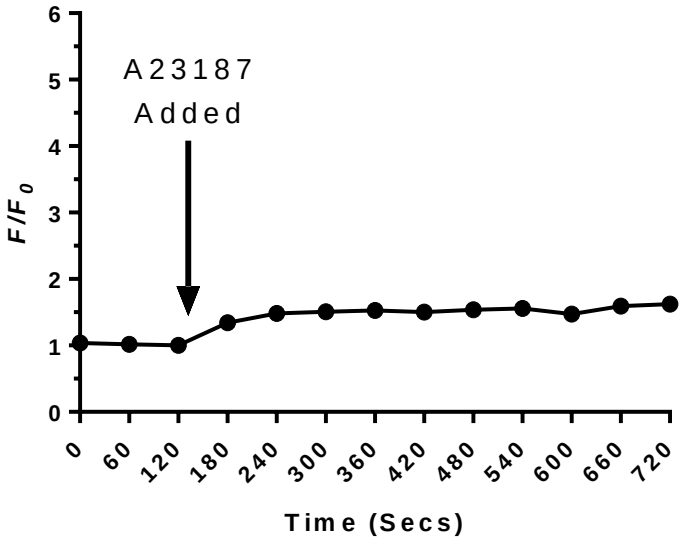

Figure 5.14 - Calcium flux experiments in response to the calcium ionophore A23187 on blood only samples.
Graphs are presented as mean FITC fluorescence change against time. (n=1)

The data seen in the graph suggests the increase previously seen following exposure to the calcium ionophore was an increase in RBC calcium levels. Following parasite isolation, the highest measured increase in fluorescence intensity is 1.6-fold.

5.3 Discussion

The aim of the research carried out in this chapter was to develop a method that allowed detection of calcium fluctuations within infected RBCs, particularly in response to calcium interfering compounds. Initially however a series of optimisation experiments were carried out, beginning with Percoll gradient separation, then optimising fluorescent dye loading and subsequently testing whether a viable calcium measuring method could be developed.

5.3.1 Percoll separation gradient

Percoll treatment of infected RBCs is a method that has been used in research for synchronisation and stage-specific enrichment of parasites. More importantly however, the procedure results in a reduced number of non-infected RBCs and a concentrated population of late-stage parasites (Miao and Cui, 2011; Mata-Cantero *et al.*, 2014). According to Mata-Cantero *et al.* (2014) the reason late-stage parasites accumulate in the middle interface in-

between the Percoll gradient is due to the fact that mature parasites are less dense than both ring stage parasites and non-infected blood cells.

Several methods were tested prior to successfully separating the infected blood. A main difference between the final method selected for further use and the previous unsuccessful attempts was the haematocrit level. All previous methods had used 50% haematocrit whereas the current adapted method uses 5% haematocrit.

5.3.2 Fluorescent dyes

Fluo-8 calcium dye

Fluo-8 was chosen as a relatively new calcium binding fluorescent dye, marketed as being brighter than the older Fluo-4 dye and has been tested on *P. falciparum* infected RBCs, albeit for confocal imaging and microplate assay analysis (Zipprer *et al.*, 2014).

The results of staining infected RBCs with Fluo-8 showed two separate populations, one was assigned to the non-infected RBCs and a second population with an increased Fluo-8 fluorescence (Table 5.2) was tentatively assigned to the infected population. When Fluo-8 was combined with a DNA binding dye however, a portion of DNA negative cells remained in the high calcium fluorescence region. This occurred in all double stained infected samples. Published reports have discussed the fact that ageing erythrocytes have increased intracellular calcium (Romero and Romero, 1999; Chia, Lee and Tan, 2017) therefore it is plausible that the DNA negative and high calcium population of cells could be that of ageing RBCs. The non-infected RBCs also have a population in the same region however the size of the population is smaller (see also Table 5.2). It is possible that the ageing population of cells is larger in the infected samples due to the fact that these cells have been incubated at 37 °C, whereas non-infected blood is stored at 4 °C thus slowing down the RBCs' metabolism (Sut *et al.*, 2017).

Bootman *et al.* (2013) also discuss that using single wavelength calcium fluorescent indicators can result in cells being loaded with unequal amounts of indicator thus resulting in cells showing different levels of fluorescence intensities. This therefore leaves the researcher

unsure whether the differences are due to different concentrations of calcium within the cells or whether it is due to variation in amount of indicator loading (Bootman *et al.*, 2013).

For the purpose of this study and to avoid interference, only the DNA positive population of cells were gated and selected for calcium measurements. Furthermore, also discussed by (Bootman *et al.*, 2013), relative changes in calcium can be measured using single wavelength indicators by presenting the fluorescence signal from an experiment relative to the basal or initial signal. This was the method followed during the calcium fluctuation experiments.

Long-wavelength DNA dye

Due to the limited excitation and emission filters available on the flow cytometer, a long wavelength fluorescent DNA dye was required to combine with Fluo-8 to avoid overlap on the FITC channel. TOTO-3 has high affinity for double stranded DNA (Henneberger *et al.*, 2011) and when used as a single dye gave comparable results to SG. However due to the fact it is cell-impermeable (Henneberger *et al.*, 2011), the required fixation step rendered TOTO-3 impractical for the use of this research. Therefore it was replaced with the cell-permeable DRAQ5. According to Smith *et al.* (2000) the ease in which DRAQ5 can be loaded into both live and fixed cells would allow it to be incorporated into multiparameter fluorescent and cytometric studies.

Staining infected RBCs with DRAQ5 gave comparable results to the control dye SG and indeed the use of DRAQ5 in combination with Fluo-8 proved to be successful and a better match than TOTO-3. Once infected cells were subjected to double staining, a rigid selection process was followed whereby DNA positive cells were gated and then that population was selected for further analysis on the calcium FITC channel (Figure 5.7).

5.3.3 Detecting calcium fluctuations

Following the successful double staining of samples, experiments to detect differences in calcium levels were initiated. Analysis carried out at different time points within the blood stages of the parasite life cycle showed an increase in calcium fluorescence of infected RBCs during the late trophozoite/schizont stage in comparison with the ring and early trophozoite stages. The mean relative fluorescence between the ring and early trophozoite stages were

comparable, with 74.05 and 71.20 RFUs respectively, whereas the fluorescence for the late-stage parasites was 3.5-fold higher at 259.50.

In 1982, Tanabe, Mikkelsen and Wallach, reported *P. chabaudi* infected RBCs were higher in calcium than non-infected cells and the greatest increase in calcium was in the post trophozoite stages. Adovelande *et al.* in (1993) reported using a variety of calcium fluorescent dyes to measure calcium levels of infected RBCs at different stages. The results obtained showed schizonts to have more calcium than trophozoites, they also found calcium concentration of rings to be similar to that of non-infected controls. Moreover work recently carried out by Chia, Lee and Tan (2017) using imaging flow cytometry showed schizonts to have higher Fluo-4 (calcium) fluorescence than trophozoites. Pandey *et al.* in (2016) also showed schizonts to be higher in calcium than trophozoites using a transgenic *P. falciparum* line encoded with fluorescent calcium biosensors. Contrary to the results obtained in this research and in other published data (Adovelande *et al.*, 1993), Pandey *et al.* (2016) found ring stage parasites to be higher in calcium than the schizont stage. The measurements obtained by Pandey *et al.* (2016) were from the parasite cytosol whereas such details are unattainable from the present study. All the above-mentioned studies, including the results presented here, conclude that calcium levels within the schizont stage are higher than that of the trophozoite stage, however the results are conflicting for the ring stages.

Research carried out by Biagini *et al.* in (2003), using Fluo-4 and confocal laser scanning microscopy, found a calcium pool in the DV of parasites almost 5-6-fold higher than the cytosol during the trophozoite stage. When the parasites matured into schizonts however, calcium was observed to leave the DV and enter the intermembrane space of the parasite. On the other hand, research carried out by Rohrbach *et al.* (2006), using Fluo-4 on confocal scanning fluorescence microscopy, showed Fluo-4 to compartmentalise and concentrate in the DV of the parasite, however levels of concentration differed amongst different *P. falciparum* strains. The variation in results concerning calcium levels within the different stages of the asexual cycle of the parasite is apparent. Differences in indicator, in detection method and in the strain of parasite all appear to have an impact on the results. Despite the variation however, there appears to be an intricate calcium-dependent process in the progression of the parasite through its life cycle (Biagini *et al.*, 2003).

Moreover, an experiment was carried out where cultures were incubated with different levels of calcium chloride, the results obtained in this research showed no detectable changes in calcium fluorescence. A similar experiment carried out by Pandey *et al.* (2016) using confocal microscopy on the transgenic parasites resulted in the detection of nanomolar increases in calcium levels within the parasitic cytosol.

Alleva and Kirk (2001) carried out a similar experiment which involved saponin isolated parasites being loaded with Fura-2, these were exposed to different concentrations of calcium chloride and then fluorescence was measured using a spectrofluorometer. The research showed detectable increase in calcium fluorescence with the increasing amounts of calcium chloride. During this study Alleva and Kirk (2001) proposed once an optimum amount of cytosolic calcium is reached, the parasite maintains that level regardless of the level of extracellular calcium.

Although the research by Alleva and Kirk showed more positive results than ones acquired in this research, it is important to note that their work was carried out on saponin isolated parasites. Whereas the results obtained here were on parasite infected RBCs. As previously discussed RBCs have the ability to regulate their calcium levels (Camacho, 2003; Gazarini *et al.*, 2003; Romero *et al.*, 2006; Clapham, 2007; Docampo and Moreno, 2013; Bazanovas *et al.*, 2015; Makhro, Kaestner and Bogdanova, 2017), it could be that calcium levels within the blood cells had been maintained and thus not having a major effect on the calcium levels of the parasites within them.

Possibly a more plausible explanation is that small changes in calcium levels cannot be detected using this method. Several published articles have discussed the inability of some fluorescent calcium indicators to detect low nanomolar changes in calcium (Bootman *et al.*, 2013; Lock, Parker and Smith, 2015; Pandey *et al.*, 2016). Furthermore, it is also plausible for Fluo-8 to be compartmentalised within the parasite, similar to the findings of Rohrbach *et al.* in (2006) where Fluo-4 was compartmentalised in the DV, resulting in small changes in cytosolic calcium levels to be undetected. The drawback of the compartmentalisation of AM dyes into cellular organelles has also been discussed by Silver, Whitaker and Bolsover (1992).

The addition of the calcium ionophore A23187 on infected RBCs resulted in a sharp increase in calcium fluorescence which is in alignment with published results obtained on parasite

infected RBCs and other mammalian cell types (Tsien, Pozzan and Rink, 1982; Leybaert, Sneyd and Sanderson, 1998; Przygodzki, Sokal and Bryszewska, 2005; Vines, McBean and Blanco-Fernández, 2010; Assinger, Volf and Schmid, 2015; Pandey *et al.*, 2016). The calcium chelator EDTA added both before and after A23187 reduced the calcium fluorescence following administration of A23187 to approximately zero. The administration of EDTA alone however did not result in any changes in calcium fluorescence. These results showed that alterations in calcium levels in the infected RBCs can be detected at least when the change is a dramatic one.

The difference in fluorescence intensity observed between the two stages of parasite could be due to the fact that the basal calcium levels of late-stage parasites are higher than the ring stages. It is possible that in the late-stage parasites saturation of the calcium dye occurred, hence the full increase in calcium level was not accurately measured. Dye saturation is a drawback that has been reported in the literature (Bootman *et al.*, 2013; Lock, Parker and Smith, 2015). This is further highlighted in the blood only sample exposed to A23187 (Figure 5.13). Similar to the ring stage infected blood (74.05 ± 7.05 RFU, shown in Table 5.9), the non-infected blood had a low basal calcium level (78.6 ± 0.70 RFU) and following exposure to A23187 a 5.5-fold increase was also detected. These results imply that there is a limit of calcium increase beyond which fluorescence cannot be measured, most probably due to dye saturation. Furthermore it is important to highlight the flow cytometry results of the late stage parasites showed two populations (Table 5.7), presumably one population represents late trophozoite parasites and the second population is that of schizonts. Future work would involve investigating the two populations further to determine whether more information could be extracted from the individual populations.

Following the results obtained with the calcium ionophore, experiments using NMDAR inhibitor (riluzole) and CCBs (verapamil and fendiline) were carried out to investigate their ability to reduce or block the rise in calcium following administration of A23187, and more importantly to ascertain whether such an effect could be detected using the current flow cytometry method.

The NMDAR inhibitor, riluzole, did not have an effect on the calcium levels of infected RBCs either when administered alone or with A23187. An exception to this was when A23187 was

administered prior to riluzole during the ring stage parasites. A decrease in calcium fluorescence occurred once riluzole was added and was maintained for subsequent samples. The calcium ionophore A23187 is reported to potentiate responses to NMDA (Terunuma *et al.*, 2010), furthermore the presence of both NMDA and its receptor are reported in RBCs (Makhro *et al.*, 2013; Makhro, Kaestner and Bogdanova, 2017). Therefore riluzole potentially inhibited the effects of NMDAR resulting in less calcium entering the infected RBC, hence the reduction in fluorescence. Surprisingly this effect was seen when riluzole was given after A23187 on ring stage parasites only and not during any of the other experiments.

Fendiline and verapamil, similar to riluzole, did not exhibit detectable changes in calcium following administration, neither alone nor when administered along with A23187. The exception to this was a slower and slightly reduced response to A23187 in infected cells that had already been exposed to fendiline. It is possible that fendiline directly inhibited the activity of a calcium channel, or acted indirectly by inhibiting calmodulin, which led to the cell's reduced uptake of calcium. As discussed in previous chapters and reported in several publications, fendiline potentially interferes with more than one target, several of which appear to impact on cellular calcium levels (Nawrath *et al.*, 1998; Cheng *et al.*, 2001; Lo *et al.*, 2001; Samantaray *et al.*, 2016). Furthermore research carried out by (Mott *et al.*, 2015) using single cell photometry examined calcium homeostasis in response to drugs. A variety of compounds were tested, including the CCB nicardipine. The results showed that following administration of nicardipine a release of calcium from the digestive vacuole accompanied with an increase in cytosolic calcium occurred (Mott *et al.*, 2015). Although the research was not carried out on verapamil or fendiline, a similar situation could be occurring after administration of either compound. Due to the lack of detail obtained using this method, where calcium fluctuations in individual organelles cannot be tracked, such a hypothesis cannot be confirmed. Neither can realistic explanations be derived as to what occurred with the fendiline samples.

Further calcium flux experiments were carried out using two LTCC activators; FPL 64176 and Bay K8644. The results from both compounds did not show a rise in calcium levels. The purpose of this experiment was to add LTCC activators in a bid to raise calcium levels within infected RBCs, the effects of which could then potentially be targeted using the LTCC blockers verapamil and fendiline. Although using Bay K8644 to raise cellular calcium levels enough to

be detected using flow cytometry has been successfully reported, this was carried out on human Jurkat T cells and not *Plasmodium* infected RBCs (Kotturi *et al.*, 2003) therefore comparisons between the two may not be appropriate. Both FPL 64176 and Bay K8644 have also been reported to raise intracellular calcium, however these results were obtained using patch clamp tests on rat ventricular myocytes (Rampe and Lacerda, 1991; Fan and Palade, 2002) thus also rendering a comparison between the studies unsuitable.

The care required while analysing fluorescence data was highlighted following exposing non-infected RBCs to A23187. The results showed the RBCs themselves to increase in calcium by 5.5-fold, an increase comparable to the one seen on ring stage infected RBC. This raised the question whether the observed increase in calcium in the infected population occurred within the RBC itself (outside of the parasite) or within the parasite. Indeed the same question could be asked about the effect seen with riluzole and fendiline; were the differences observed due to an interaction between the compounds and a target within the RBC, a target within the parasite or possibly both? The inability to distinguish between the RBC cytosol and the parasite in addition to the inability to identify organelles within the parasite made deriving theories and explanations a difficult task. This led to carrying out the experiment on saponin treated parasites, the results of which showed a 0.6-fold increase in comparison with the controls following A23187 exposure, implying the raise in calcium had all along been within the RBC itself and not the parasite.

Pandey *et al.* (2016) tested effects of A23187, in addition to other compounds, on parasite infected RBCs, saponin-treated parasites and streptolysin O (SLO) treated parasites. According to Pandey *et al.* (2016), SLO treatment permeabilises the RBC membrane only, whereas saponin treatment permeabilises the RBC membrane and the parasitophorous vacuole membrane (PVM) whilst leaving the parasite plasma membrane intact. The group's results showed a high increase in calcium levels with untreated blood cells which was reduced in SLO and saponin treated samples.

Although the results obtained on saponin treated samples implied that previous results on untreated RBCs should be analysed with care, it is also worth noting that saponin treatment is a harsh procedure, which renders some parasites within the population unviable therefore compromising results of experiments (Klonis *et al.*, 2011). Furthermore Elandalloussi and

Smith (2002) also discuss that strict criteria should be met following parasite isolation for biochemical experiments. The integrity and stability of the parasites and their subcellular constituents should ideally be maintained post treatment. It can be argued that experiments ran on saponin freed parasites would not necessarily resemble the physiological response of the parasites (Elandalloussi and Smith, 2002).

This research has highlighted the amount of caution that should be taken when carrying out fluorescence experiments due to the potentially misleading results. Several aspects need to be considered and resolved for future studies. First of all, although flow cytometry is a powerful tool, Vines, McBean and Blanco-Fernández (2010) discuss that the majority of alterations in intracellular calcium concentration can occur within a very short space of time, sometimes nanoseconds. Indeed, published work carried out on FPL 64176 and Bay K8644 recorded the results in milliseconds (Rampe and Lacerda, 1991; Fan and Palade, 2002). Therefore using a non-continuous measuring system for calcium fluctuations can result in lack of detail in the first few seconds following administration of the compound. The traditional pressurised flow cytometers, like the one used in this study, require measurement to be stopped while the compound is added to a sample, thus resulting in the loss of vital information in the initial few seconds following administration of a compound. Newer generations of flow cytometers are available that have replaced the pressurised pump with a peristaltic pump, this allows the addition of reagents or drugs to a sample while continually processing cells. Using a system such as this would allow the measurement of calcium fluctuations without disruption, theoretically recording responses that occur within the initial few seconds (Abu-Absi *et al.*, 2003; Vines, McBean and Blanco-Fernández, 2010).

Additionally, visualising the response of the parasites themselves following exposure to a compound is an equally important issue. Although carrying out the experiments using saponin isolated parasites could potentially give an idea of how the parasites react to a drug(s), the integrity of the results would be questionable for reasons mentioned previously regarding the viability and stability of the parasites once outside the RBC (Elandalloussi and Smith, 2002; Klonis *et al.*, 2011).

Using methods such as confocal microscopy provides valid alternatives to flow cytometry for measuring calcium fluctuations. The method allows visualisation of the parasite within the

RBC while continuously measuring changes that occur following administration of a drug. Examples mentioned previously from Biagini *et al.* (2003) and Rohrbach *et al.* (2006) both presented results where calcium levels were detected not only within the parasite, but specifically within the parasite's organelles. However potential compartmentalisation of the dye is an aspect that should not be ignored. Another major drawback of using microscopy for such studies is the small number of cells that can realistically be examined thus making microscopy a low throughput method (Vines, McBean and Blanco-Fernández, 2010; Chia, Lee and Tan, 2017).

Imaging flow cytometry is another potentially viable alternative to traditional flow cytometry for visualising the changes that occur within the parasite following exposure to a drug. According to Barteneva, Fasler-Kan and Vorobjev (2012) this technique "combines features of flow cytometry and fluorescent microscopy". Using imaging flow cytometry provides the user with real images of the processed cells and allows for a larger sample size to be analysed than using confocal or fluorescence microscopy (Barteneva, Fasler-Kan and Vorobjev, 2012). It would be possible to visualise calcium fluorescence within parasites (Chia, Lee and Tan, 2017) and thus detect fluctuations. However the resolution of the images is not as high as with traditional fluorescence or confocal microscopy, the machine is sometimes unable to focus on a cell resulting in images being excluded from the analysis (Barteneva, Fasler-Kan and Vorobjev, 2012). Unlike confocal microscopy where the response of a cell can be monitored for the duration of an experiment, with this method a single image is captured, thus not showing as much detail per cell. However, similar to traditional flow cytometry, the response of an entire population and subpopulation can be measured.

A third issue that should be considered for future studies is the type of indicator used. The issues regarding compartmentalisation and saturation of the dyes has previously been discussed. One suggestion would be to carry out experiments using two (or more) different indicators to identify differences in results and determine whether one dye is more sensitive in detecting small changes in calcium levels. This would help develop a more robust measuring system. Furthermore, the results seen by Pandey *et al.* (2016) using genetically modified transgenic parasites on confocal microscopy appeared to provide a great amount of detail regarding calcium levels within the nanomolar range. The use of a system similar to the one

described by Pandey *et al.* as a comparison to traditional synthetic dyes could also provide interesting results.

The above-mentioned suggestions are by no means the only potential solutions to the issues encountered during this research. They provide an example of alternative methods that could be tested to resolve the problems. Ideally however, as suggested by Borle (1990), the best approach to studying cell calcium levels is to try several methods in order to focus on a problem from different angles.

5.3.5 Conclusion and future work

In conclusion, infected RBCs were successfully dual stained with calcium fluorescent and DNA binding fluorescent dyes. Results showed that schizont stage parasites have higher levels of calcium in comparison to trophozoites and ring stages. Furthermore, results also showed non-infected RBCs to have a subpopulation with a higher calcium content. This could be due to ageing blood cells or uneven loading of dye. The calcium fluctuation assay carried out showed the method tested was not sensitive enough to detect fluctuations in calcium levels in parasites within RBCs. Future work should focus on developing a more robust method that would enable identification of the parasite itself to measure calcium fluctuations in response to drug exposure. Ideally more than one method would be tested and compared to one another to ensure reliability.

Chapter 6
General Discussion

6.1 General discussion

Malaria is a major public health concern, the socio-economic burden of which is a great cause for concern in malaria endemic countries. Despite ongoing research a viable vaccine is yet to be officially approved (Ballou and Vekemans, 2017), therefore, the main strategies to control malaria are by vector control using insecticides, and by chemotherapy drug treatment. Although the first line antimalarial drugs are very effective against susceptible parasites, wide-spread resistance has dictated the need to develop new drugs. Potent compounds with low toxicity and new mechanisms of action are urgently needed (Guiguemde *et al.*, 2012; Fan *et al.*, 2018).

There has been increasing interest in the role and importance of calcium within parasitic diseases in recent years (Camacho, 2003; Gazarini *et al.*, 2003; Moreno and Docampo, 2003; Prole and Taylor, 2011; Bansal *et al.*, 2013; Pace *et al.*, 2014; Lourido and Moreno, 2015). The complex life cycle of the malaria parasite dictates that diverse morphological states and varying internal environments with differing ionic conditions are encountered through the parasitic life cycle (Prole and Taylor, 2011). As a consequence, the need for calcium and the mechanism in which calcium is acquired differs significantly between different stages of a parasite's life cycle.

The work conducted for this project has been based on the growing body of evidence revealing the importance of calcium in the development of the malaria parasite within the RBC stages of infection. This further understanding of the calcium metabolism of the parasite has enabled a viable target pathway for antimalarial drug discovery. This project aims to investigate a commercially available calcium channel blocker (fendiline), and a range of its synthetic analogues for repurposing against the K1 *P. falciparum* strain. At the time of writing

the antimalarial effect of fendiline or any of the discussed analogues had not been reported in the literature.

The use of CCBs to treat malaria is a concept that should be approached with caution. This is due to reasons which have been previously highlighted with regards to malaria drug development. The drugs need to be well tolerated due to the large population of people that require malaria treatment, many of whom are children. This would be of concern with CCBs as they exhibit clinical effects. Sahney (2006) reported commonly used CCBs to be well tolerated in children aged ≥ 3 years for the management of paediatric hypertension. However data regarding toxicity of CCBs in children without medical indication can only be obtained retrospectively and is therefore limited (Belson *et al.*, 2000; Flynn and Pasko, 2000; Sahney, 2006; Hetterich *et al.*, 2014). The reduced activity of fendiline as a CCB has meant it has been clinically superseded by other more active CCBs, this could potentially be advantageous from a drug repositioning point of view.

Chapter 3 investigated the efficacy of fendiline alone and in combination with other commercially available antimalarials and CCBs. One of the aims of looking for a synergistic partner is to reduce the side effects of the compounds individually. The observed potentiating effect of fendiline on the activity of chloroquine on the resistant strain was interesting, particularly as it exhibited a similar effect to verapamil, a clinically active drug, at half the concentration. Further work would investigate if the concentration of fendiline could be reduced even further while maintaining the potentiating effect on chloroquine.

The importance of synthesising analogues of a compound with the aim of producing a more potent entity was highlighted in Chapter 4. Indeed some of the newly synthesised fendiline analogues were more potent, with the 2'-hydroxy fendiline analogue (**4c**) exhibiting most activity. Preliminary investigations into the mode of action of compound **4c** was carried out in this study. Future work would include the synthesis of more analogues incorporating the naphthyl and hydroxyl groups with the aim of producing a more active compound with better selectivity for the *P. falciparum* parasite. The compound would ideally have a reduced effect on the hERG channel in comparison with compound **4c**. Further work would also include combination studies with current antimalarial drugs, similar to the experiments carried out on fendiline, particularly the chloroquine potentiating effect of compound **4c**. The increased

activity of the compound as a CCB however is an aspect that should not be dismissed and thus should be investigated.

It is thought that the ideal combination therapy for malaria would incorporate both fast-acting and long-lasting blood stage schizonticidal agents in addition to drugs that would target either the liver stage and/or sexual stages (Delves *et al.*, 2012). Each drug within a combination should also ideally be able to kill a large population, if not all, of parasites within an infection (Wells, Huijsduijnen and Voorhis, 2015). A better understanding of the activity of compound **4c** could be gleaned from determining its schizonticidal effect by carrying out parasite viability assays. Such information would enable us to envisage how this compound, or a more potent analogue of it, would fit into a malaria treatment regime.

Investigations into the activity of fendiline and its more potent analogues on other *P. falciparum* strains with different resistance profiles would be interesting, particularly as parasites in different geographical areas confer resistance to different antimalarial drugs. Additionally, testing the chloroquine potentiation assay on chloroquine sensitive strains might shed some light on whether fendiline acts in a similar manner to verapamil. It is thought that verapamil may potentiate chloroquine activity by binding to the PfCRT protein in resistant strains (Bellanca *et al.*, 2014). Furthermore, testing the activity fendiline and its analogues have on other human infecting *Plasmodia* species would also be interesting to determine the effectiveness of these compounds for the wider treatment of malaria.

The work reported in Chapter 5 emphasised the amount of care that should be taken when analysing results obtained using flow cytometry. The aim was to develop a method that would allow high-throughput analysis of the calcium fluctuation within infected RBCs. Having a rapid assay that could determine calcium fluctuations could be advantageous in determining the mode of action of drugs. An important drawback faced during this research was the lack of a second method of detection to confirm or challenge the results obtained from the flow cytometer. A second drawback was the lack of sensitivity of the calcium binding dye used. Modifications to the method carried out using this research are required to optimise a more sensitive assay. Several calcium binding fluorescent dyes should be tested to find an optimal dye that detects small fluctuations in calcium using flow cytometry. Additionally, in order to draw credible conclusions, a larger number of calcium interfering compounds should be

tested to be able to determine the sensitivity of the assay and its limits. Moving forward the experiments should be carried out on both parasite infected RBCs and saponin-treated parasites on the flow cytometer, along with a second method of detection such as microscopy as previously discussed (Chapter 5, section 5.4.3). The inability to determine whether the fluctuation in calcium levels is occurring within the parasite itself or the RBC is a concern the author fears will remain an issue using flow cytometry even if the sensitivity issue is resolved.

Although the research carried out achieved the primary objectives of the project, there were technical limitations that should be noted. The calcium measurement assay was carried out using flow cytometry. This has proven to be a valid technique in mammalian cells using some of the same compounds utilised during this research (Kotturi *et al.*, 2003). As previously discussed, the continuous measurement of calcium fluctuations using microscopy would provide details that could not be attained by flow cytometry. Several attempts to use both fluorescence and confocal microscopy were made during this project. Limitations of the equipment however rendered these attempts unsuccessful and thus only the flow cytometry method was utilised.

In conclusion, the conducted research has further validated the use of a SG-based plate reader method for the high-throughput screening of compounds against *P. falciparum* parasites. The method is rapid and showed comparable results with published data. Within a three-year period, the project has shown the potential of drug repositioning as an alternative to the traditional drug development pathway. The results of this research have identified several areas in which fendiline can be further investigated for use in malaria treatment. Fendiline itself can be further investigated as a chloroquine potentiating agent or more importantly the basic scaffold of fendiline can be used as a base for further research to expand on.

The study has identified two fluorescent binding dyes, DRAQ5 and Fluo-8, to be compatible with each other in staining parasite infected RBCs. Although the outcome of calcium fluctuation assay was not the anticipated result, the use of the dyes in combination can be utilised for future assays. The outcome of the research has echoed previously published reports stating the complexity of tracking calcium within *P. falciparum* infected RBCs (Brochet and Billker, 2016). It has nonetheless created a platform from which further optimisation experiments can build from.

Appendix I

Compound **3a**

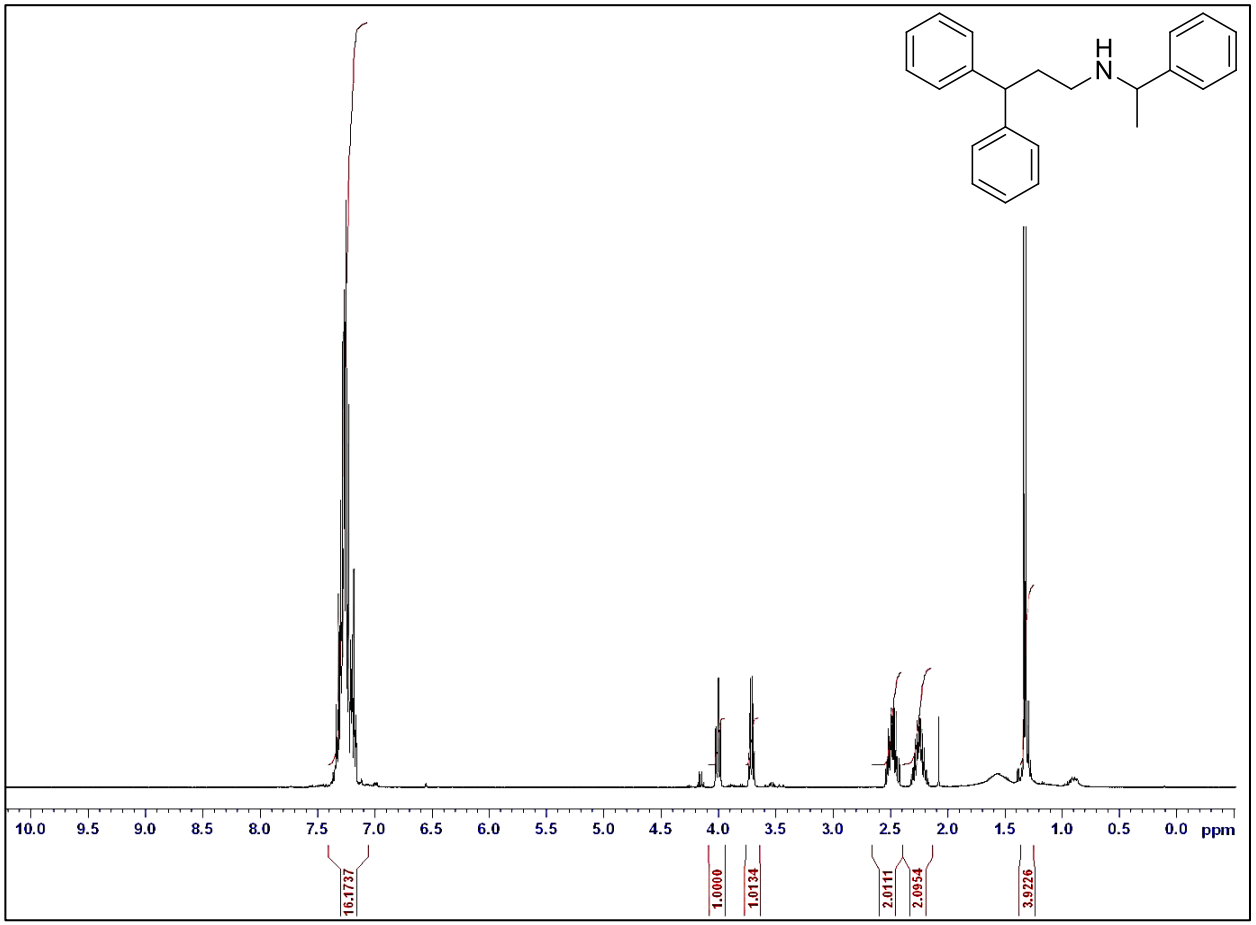

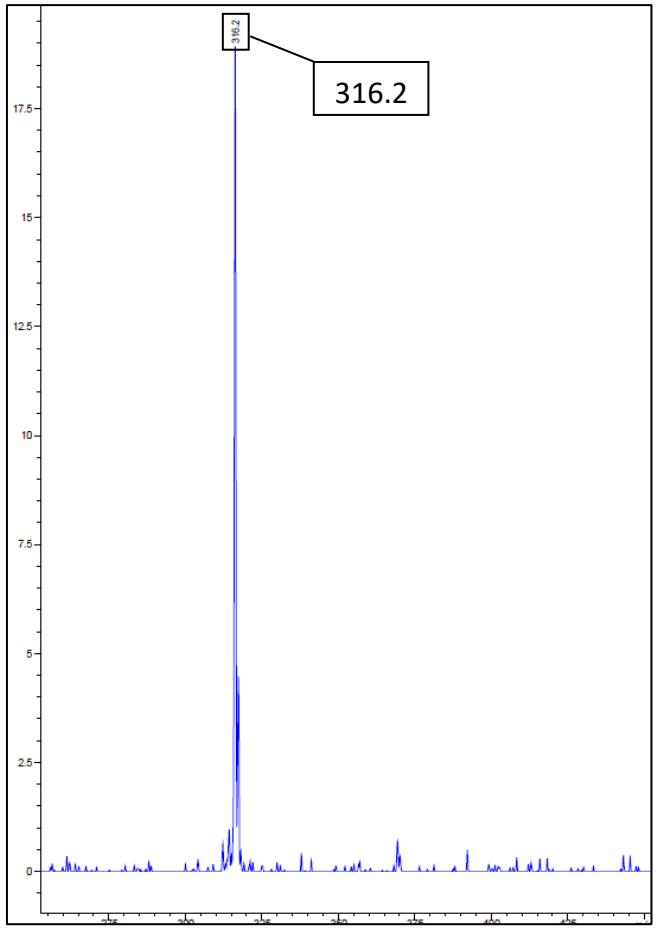

Compound **3b**

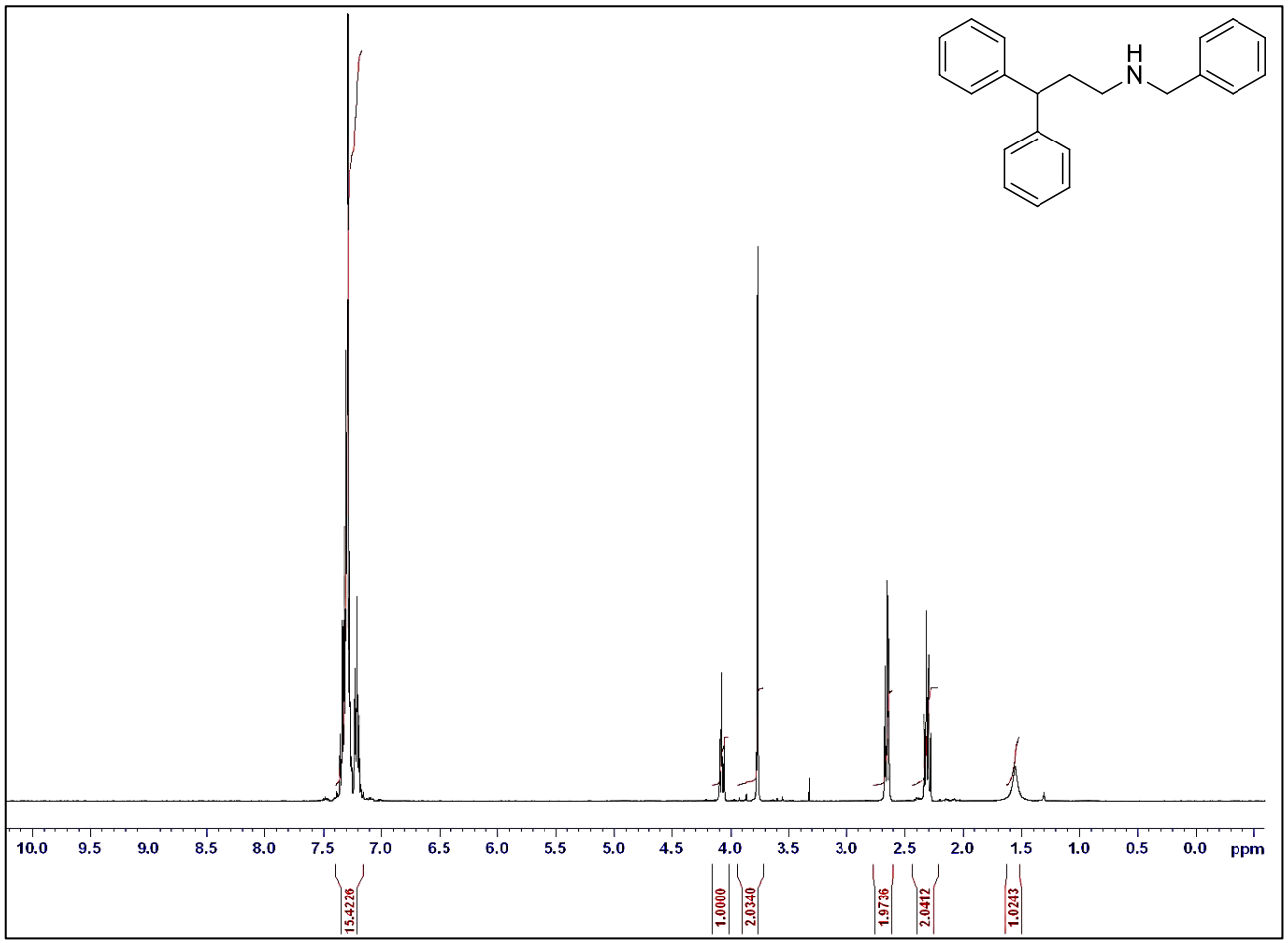
H
N
10.0
9.5
9.0
8.5
8.0
7.5
7.0
6.5
6.0
5.5
5.0
4.5
4.0
3.5
3.0
2.5
2.0
1.5
1.0
0.5
0.0
ppm
15.4226
1.0000
2.0340
1.9736
2.0412
1.0243

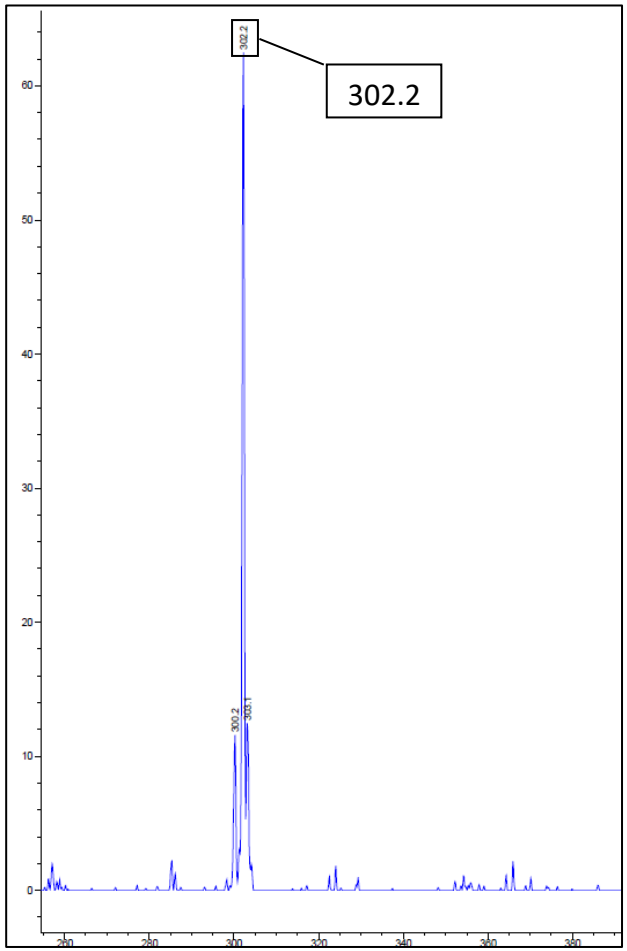
302.2
302.2
60
50
40
30
20
10
0

Compound **3c**

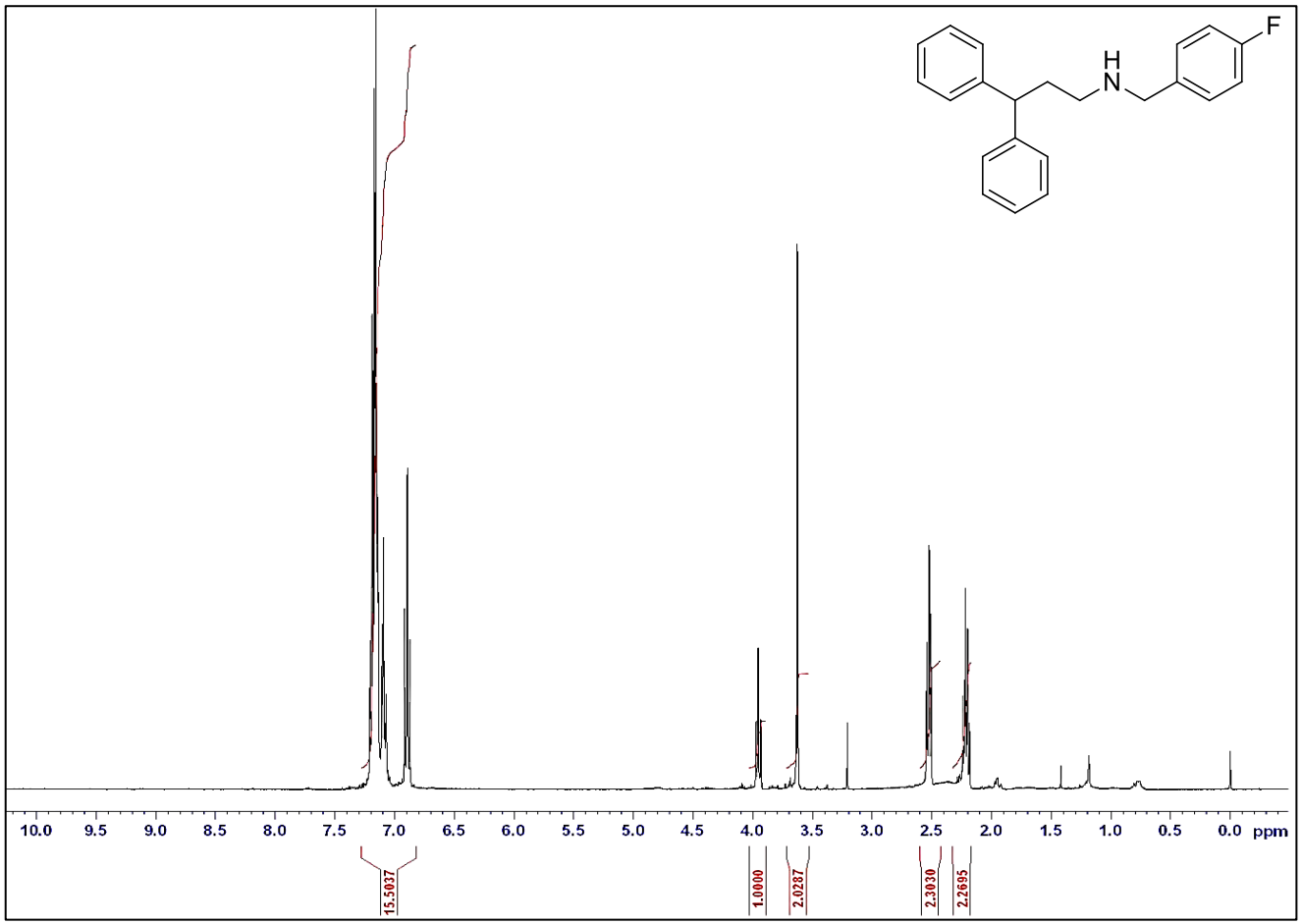
F
H
N
10.0 9.5 9.0 8.5 8.0 7.5 7.0 6.5 6.0 5.5 5.0 4.5 4.0 3.5 3.0 2.5 2.0 1.5 1.0 0.5 0.0 ppm
15.5037
1.0000
2.0287
2.3030
2.2695

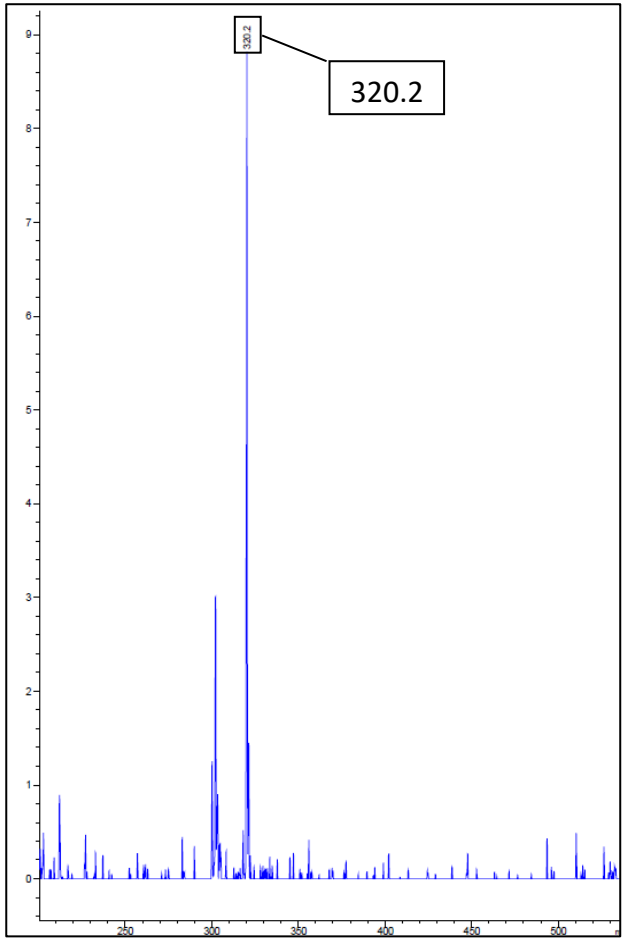
320.2
320.2

Compound **3d**

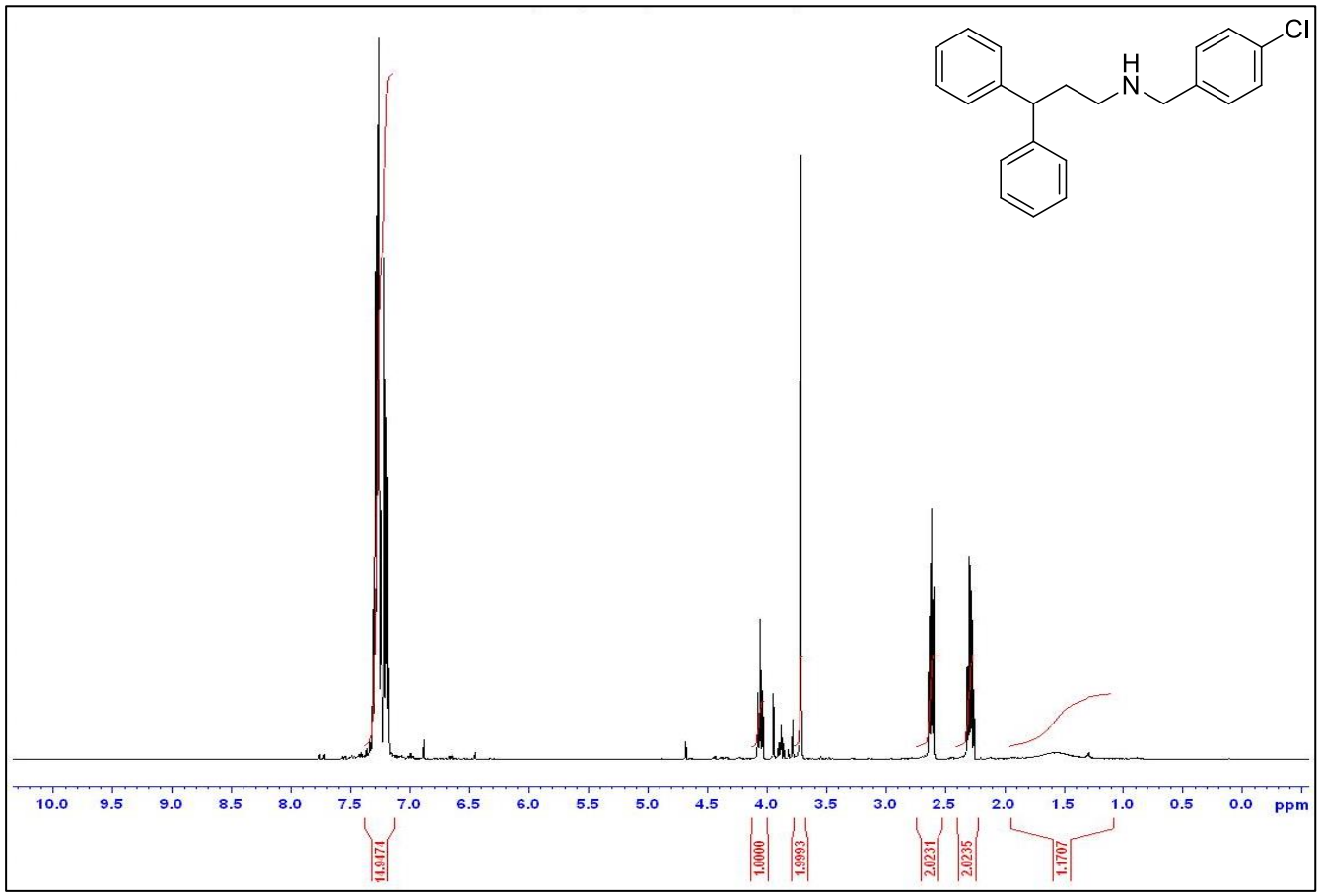
Cl
H
N
10.0
9.5
9.0
8.5
8.0
7.5
7.0
6.5
6.0
5.5
5.0
4.5
4.0
3.5
3.0
2.5
2.0
1.5
1.0
0.5
0.0
ppm
14.9474
1.0000
1.9993
2.0231
2.0235
1.1707

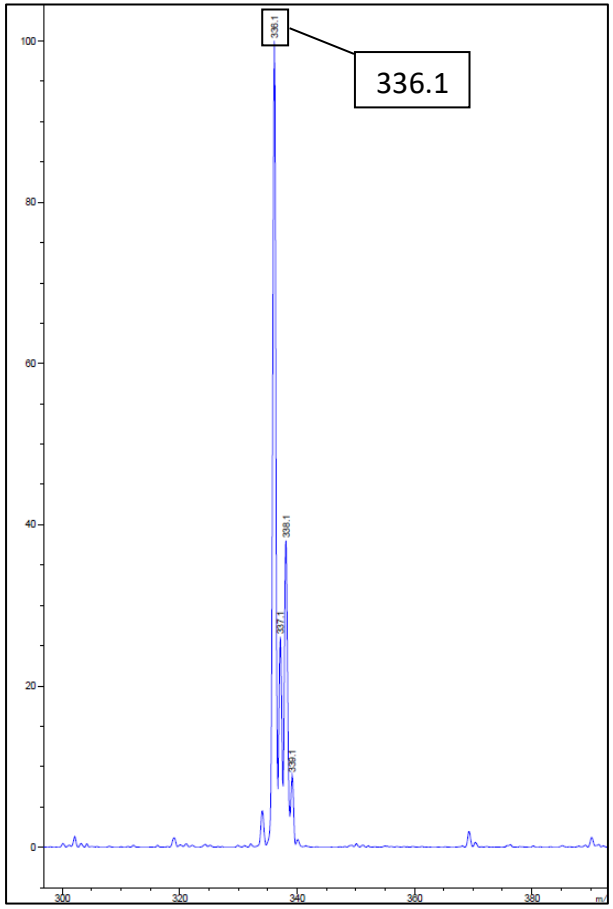
336.1
100
80
60
40
20
0
300
320
340
360
380

Compound **3e**

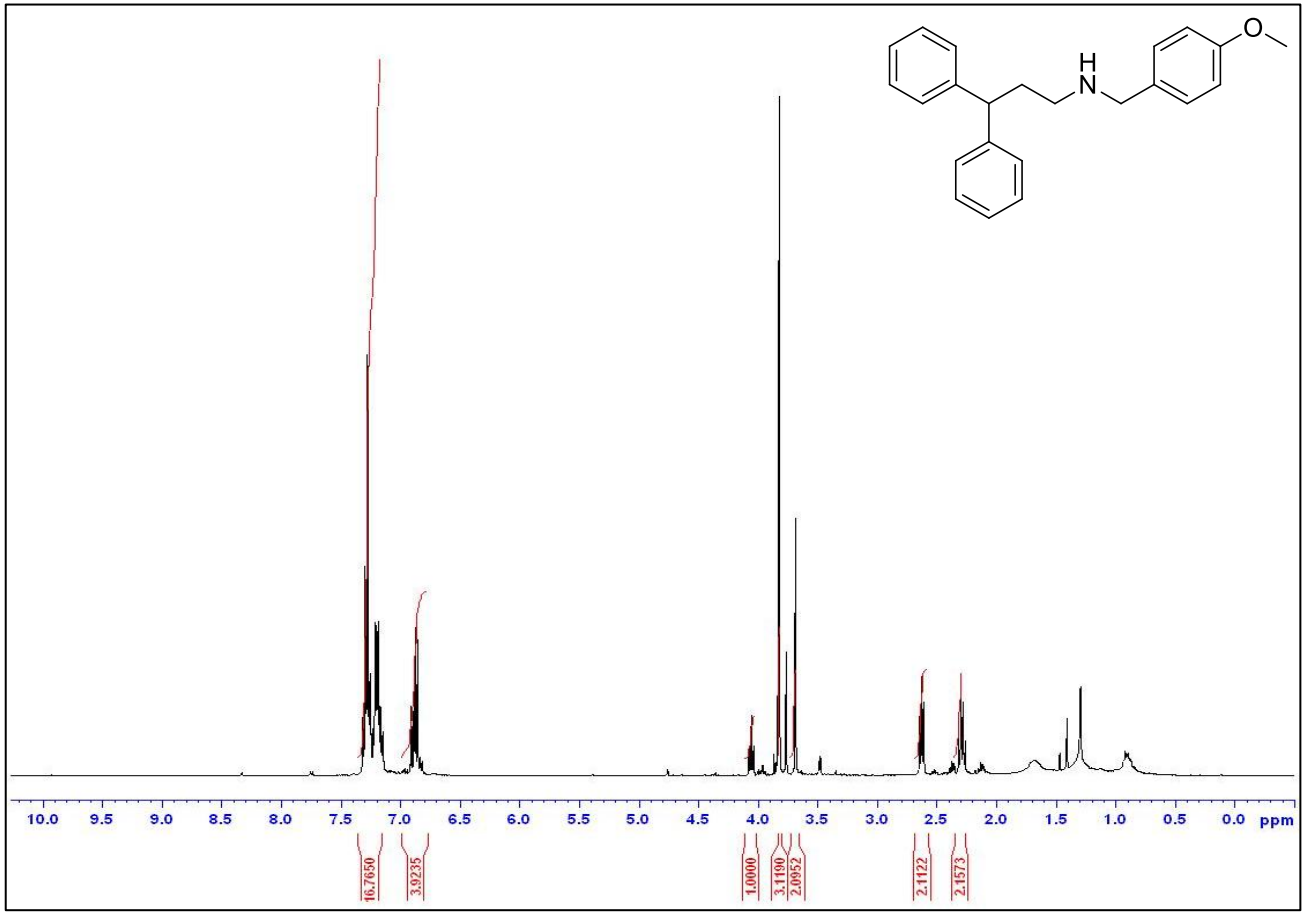
O
H
N
10.0 9.5 9.0 8.5 8.0 7.5 7.0 6.5 6.0 5.5 5.0 4.5 4.0 3.5 3.0 2.5 2.0 1.5 1.0 0.5 0.0 ppm
16.7650
3.9235
1.0000
3.1190
2.0952
2.1122
2.1573

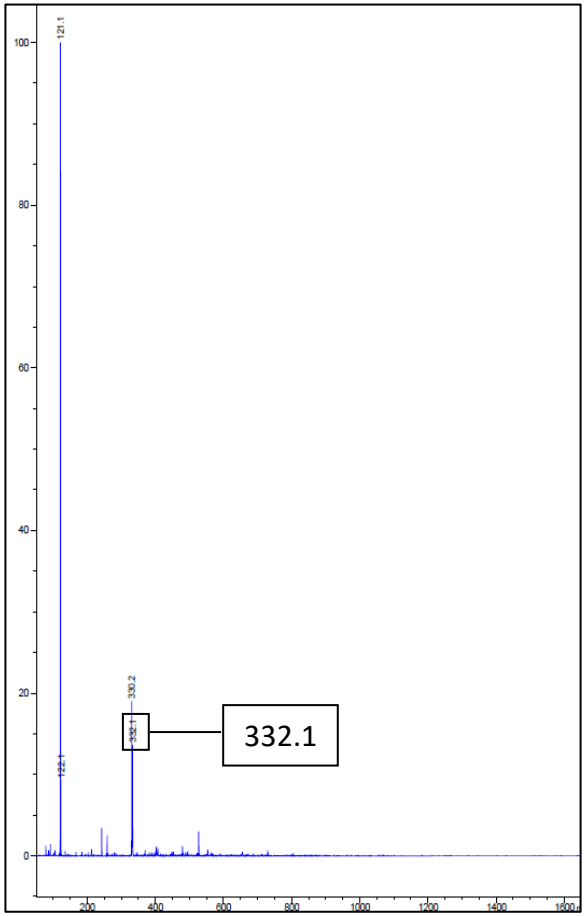
121.1
330.2
332.1
332.1
122.1
100
80
60
40
20
0
200
400
600
800
1000
1200
1400
1600

Compound **3f**

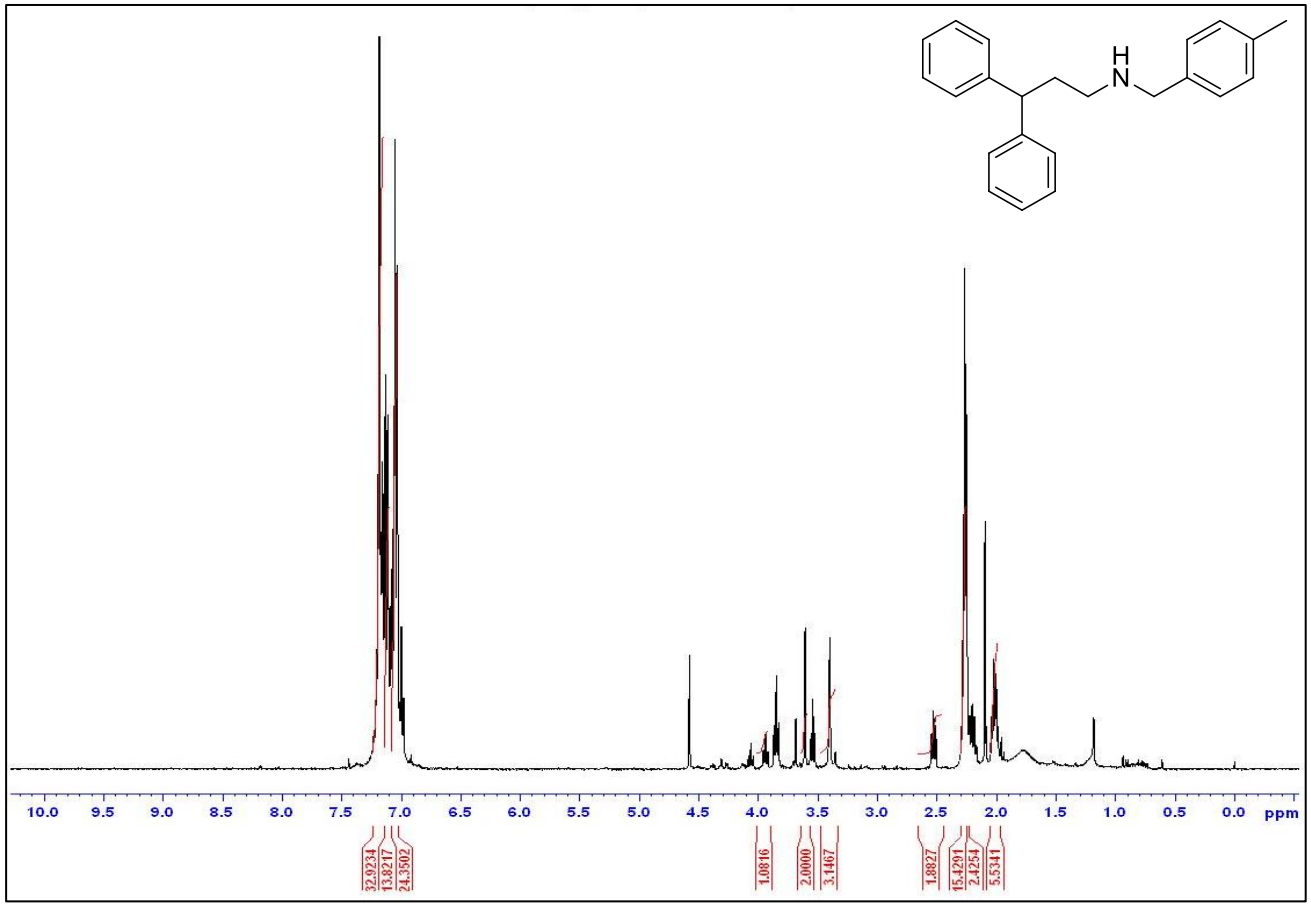
H
N
10.0 9.5 9.0 8.5 8.0 7.5 7.0 6.5 6.0 5.5 5.0 4.5 4.0 3.5 3.0 2.5 2.0 1.5 1.0 0.5 0.0 ppm
2.9234
3.8217
4.3502
1.0816
2.0000
3.1467
1.8827
5.4291
2.4254
5.5341

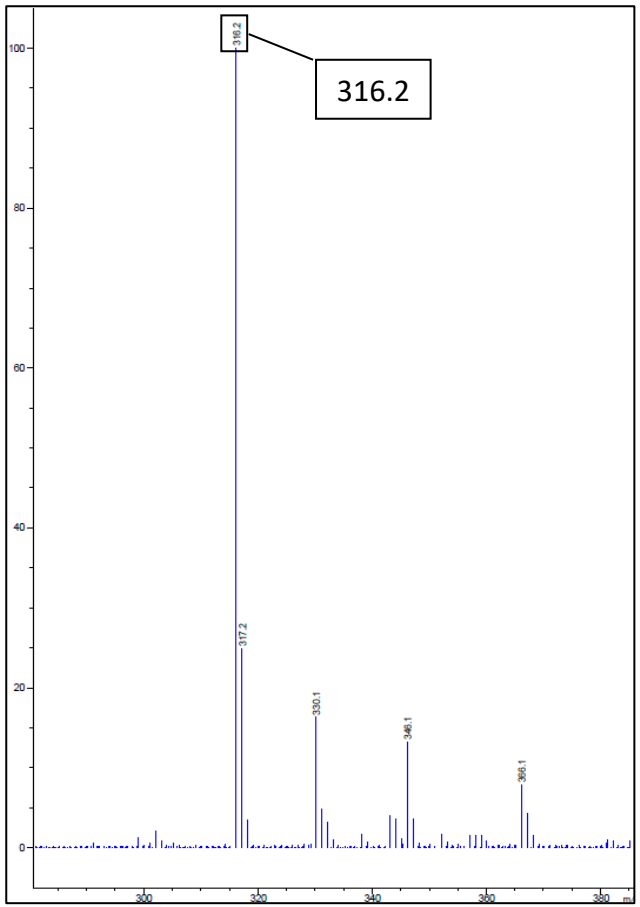
316.2
316.2
317.2
330.1
346.1
366.1
100
80
60
40
20
0
300
320
340
360
380

Compound **3g**

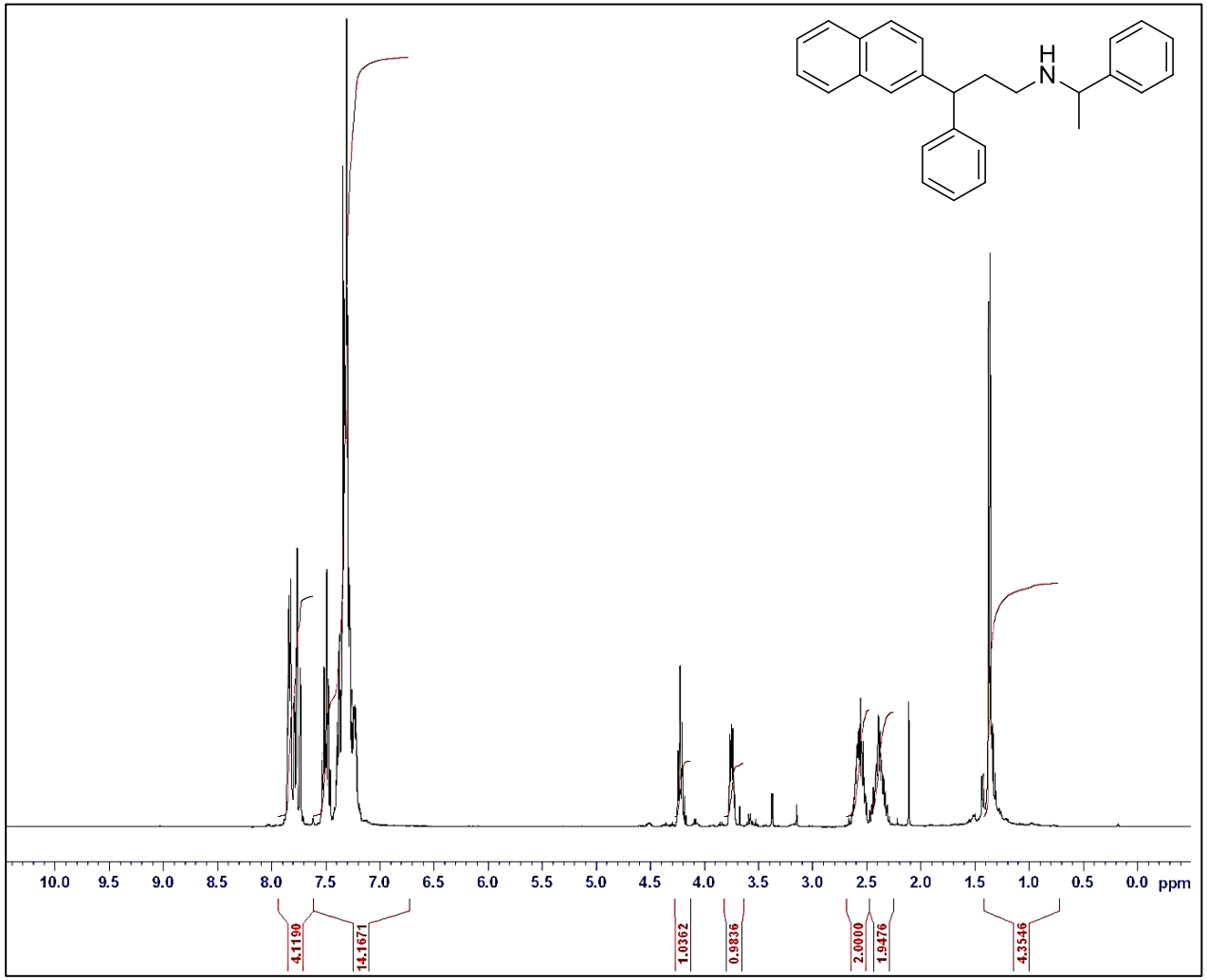
H
N
10.0 9.5 9.0 8.5 8.0 7.5 7.0 6.5 6.0 5.5 5.0 4.5 4.0 3.5 3.0 2.5 2.0 1.5 1.0 0.5 0.0 ppm
4.1190
14.1671
1.0362
0.9836
2.0000
1.9476
4.3546

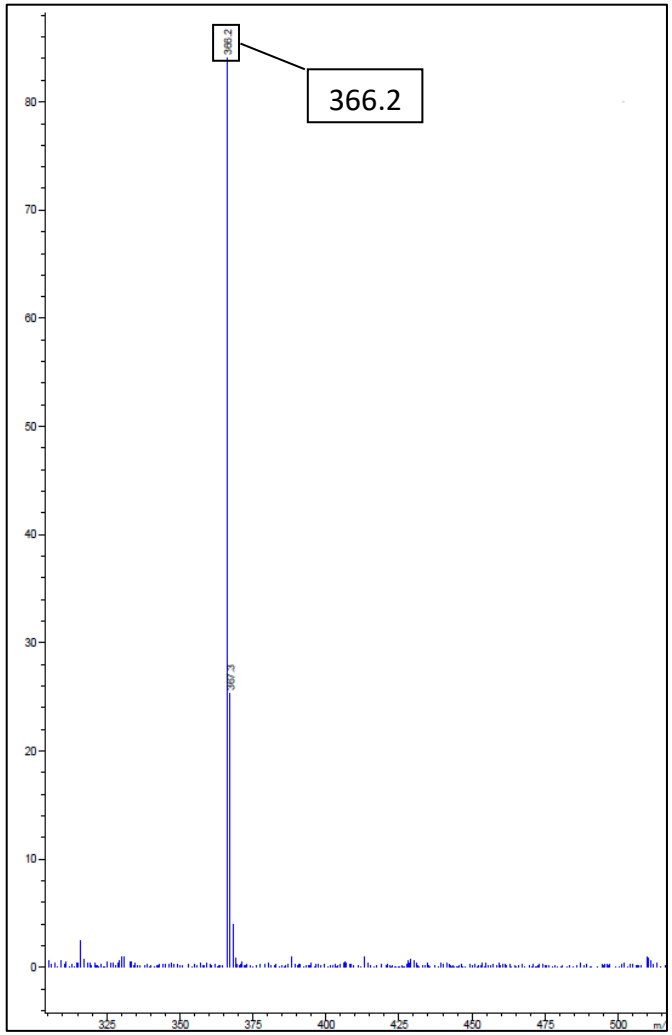
366.2
367.3
80
70
60
50
40
30
20
10
0
325 350 375 400 425 450 475 500 m/

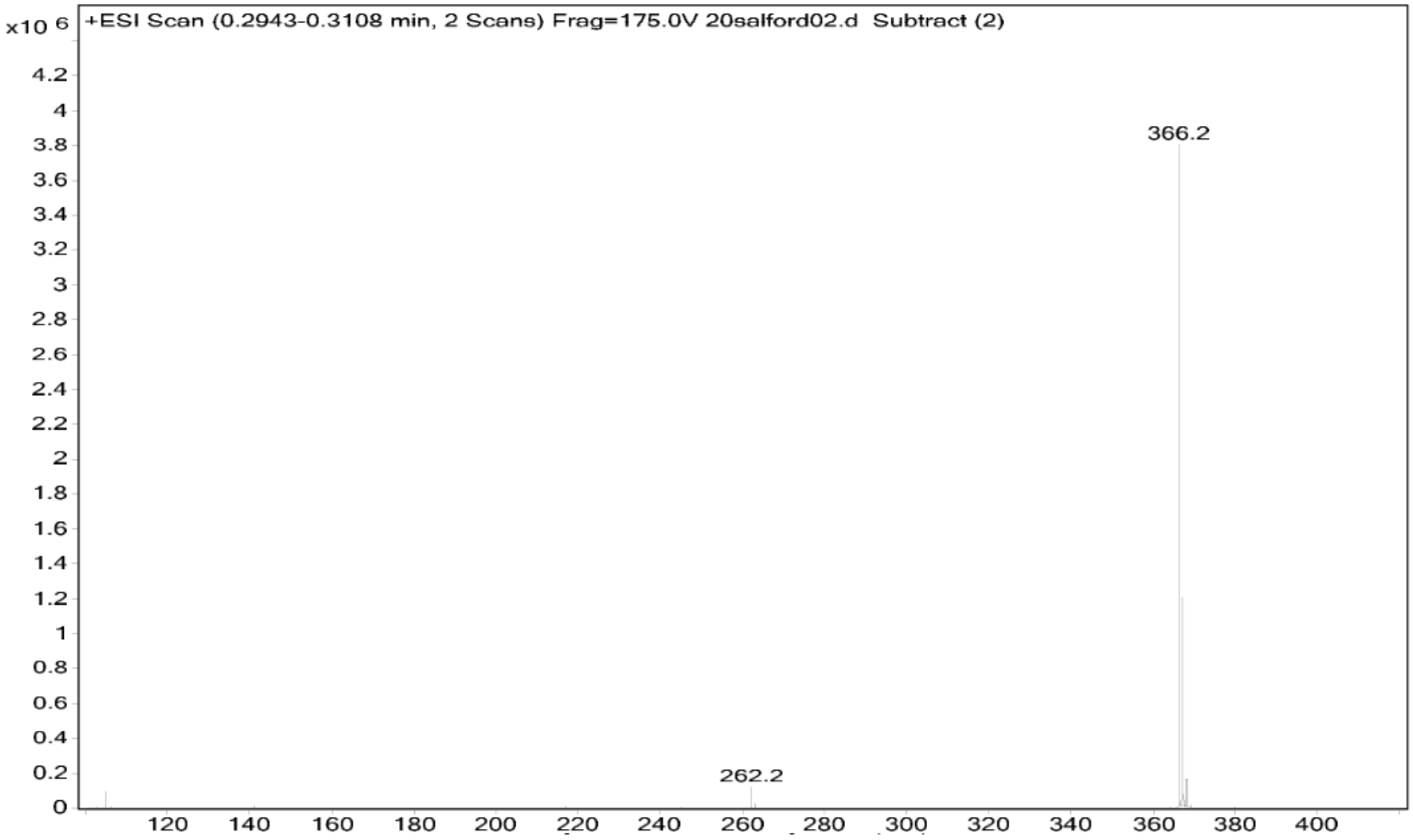
+ESI Scan (0.2943-0.3108 min, 2 Scans) Frag=175.0V 20salford02.d Subtract (2)
x10 6
4.2
4
3.8
3.6
3.4
3.2
3
2.8
2.6
2.4
2.2
2
1.8
1.6
1.4
1.2
1
0.8
0.6
0.4
0.2
0
366.2
262.2
120
140
160
180
200
220
240
260
280
300
320
340
360
380
400

Compound **3h**

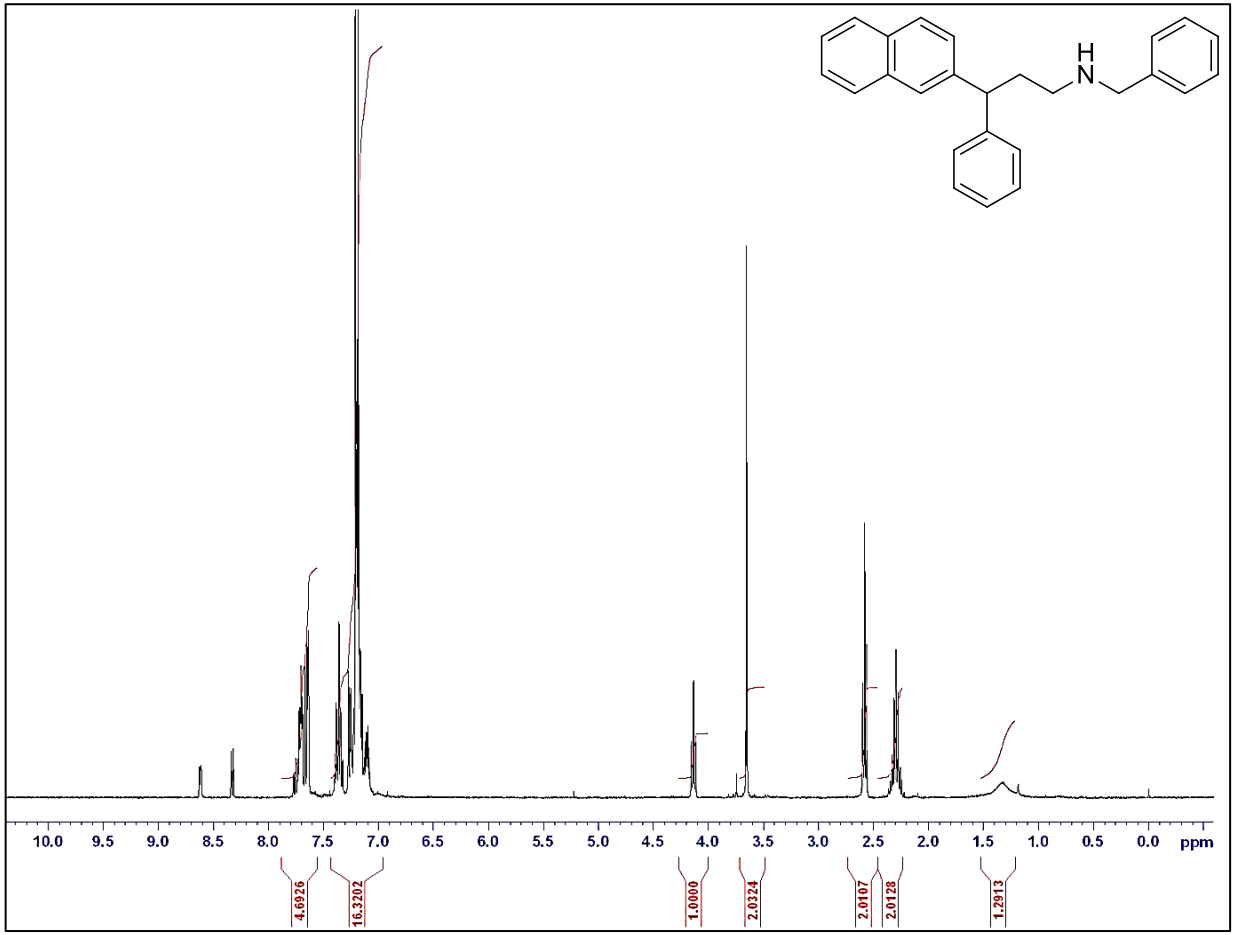
H
N
10.0 9.5 9.0 8.5 8.0 7.5 7.0 6.5 6.0 5.5 5.0 4.5 4.0 3.5 3.0 2.5 2.0 1.5 1.0 0.5 0.0 ppm
4.6926
16.3202
1.0000
2.0324
2.0107
2.0128
1.2913

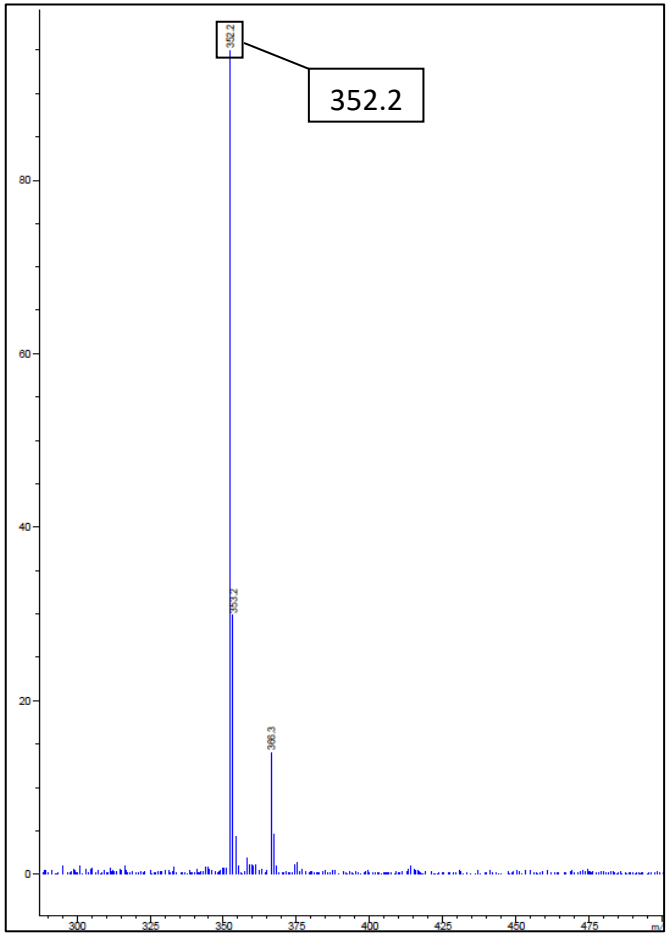
352.2
352.2
353.2
366.3
80
60
40
20
0
300 325 350 375 400 425 450 475

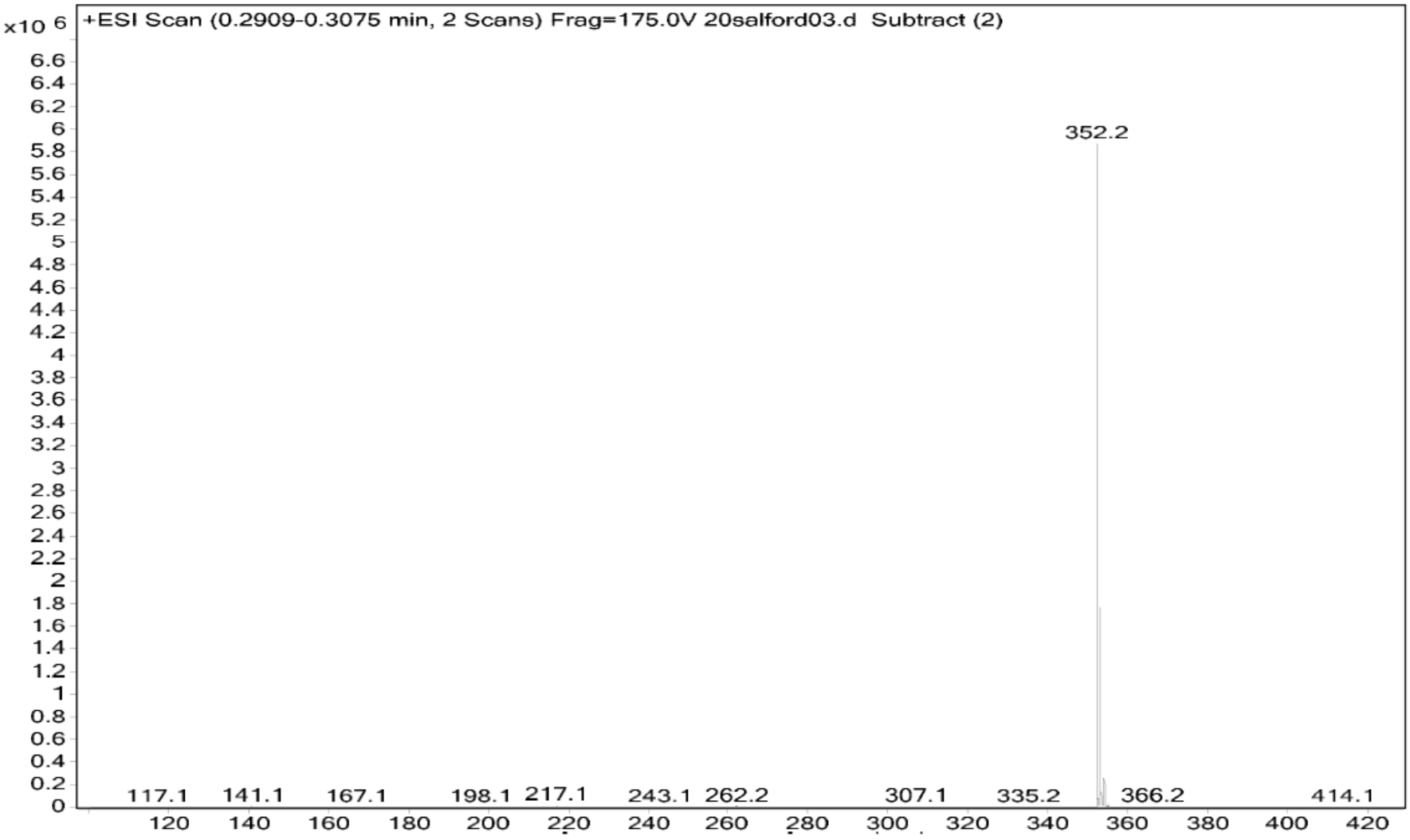
+ESI Scan (0.2909-0.3075 min, 2 Scans) Frag=175.0V 20salford03.d Subtract (2)
x10 6
352.2
117.1
141.1
167.1
198.1
217.1
243.1
262.2
307.1
335.2
366.2
414.1

Compound **3i**

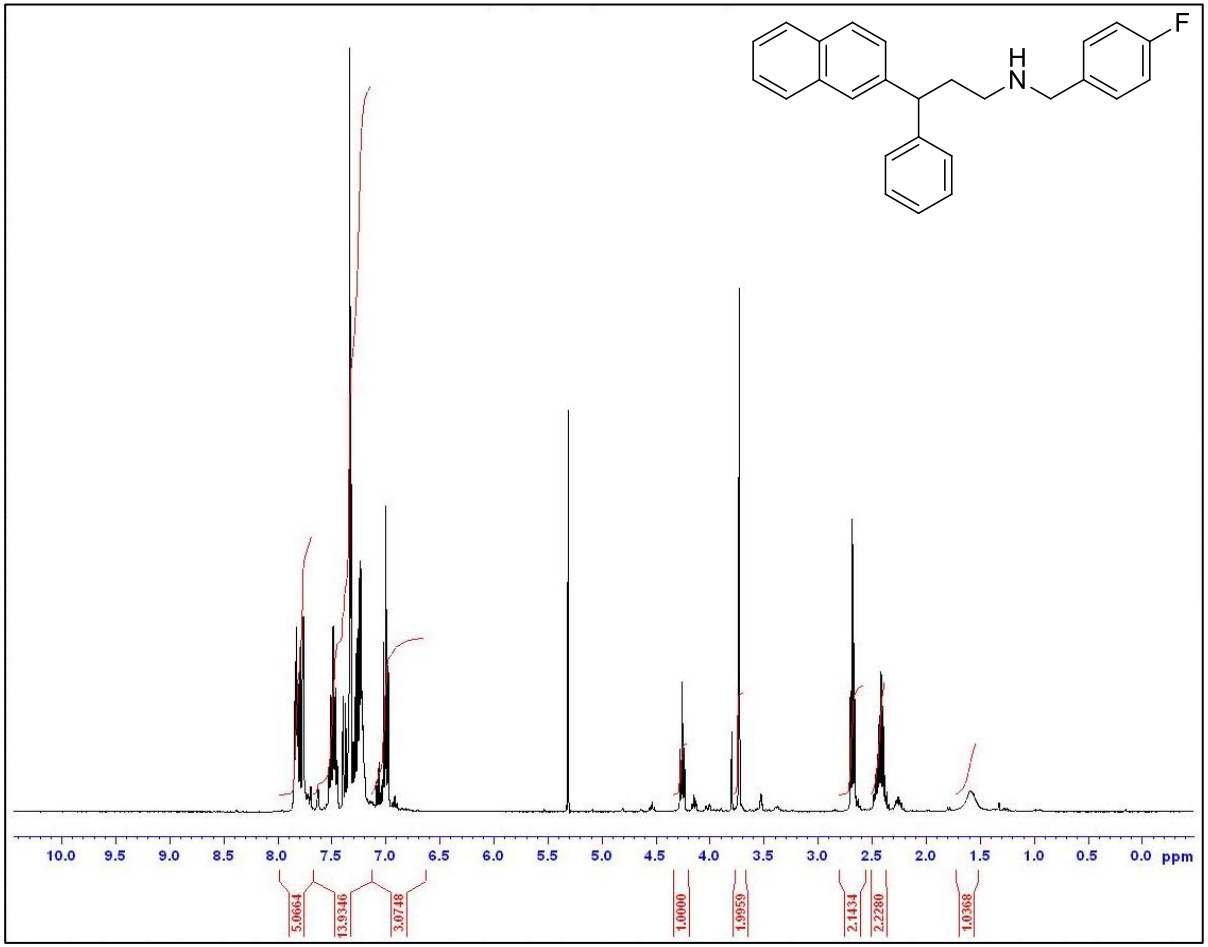
F
H
N
10.0 9.5 9.0 8.5 8.0 7.5 7.0 6.5 6.0 5.5 5.0 4.5 4.0 3.5 3.0 2.5 2.0 1.5 1.0 0.5 0.0 ppm
5.0664
13.9346
3.0748
1.0000
1.9959
2.1434
2.2280
1.0368

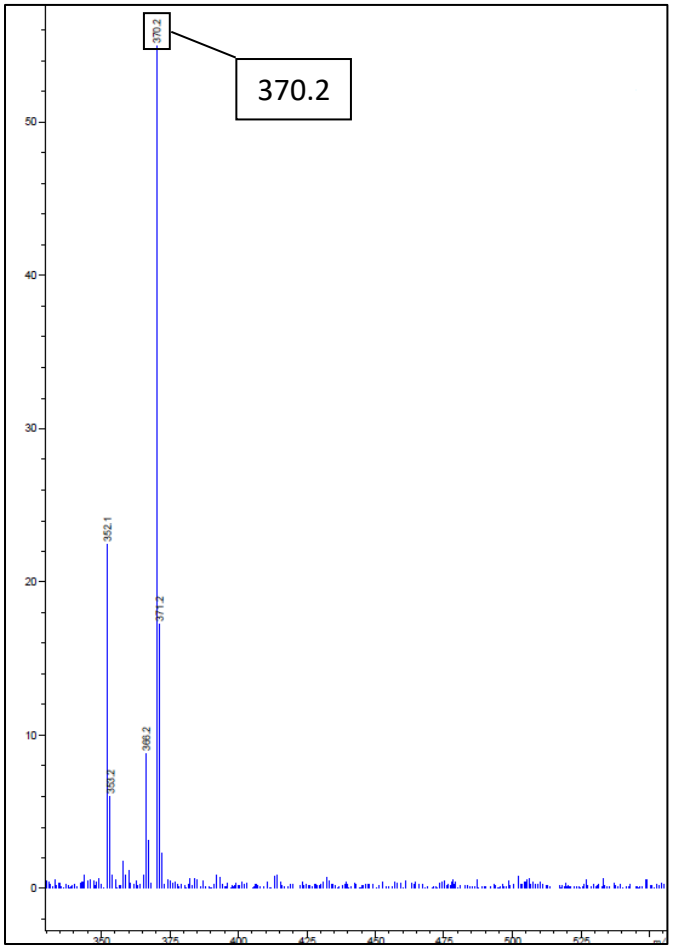
370.2
370.2
352.1
353.2
366.2
371.2
50
40
30
20
10
0

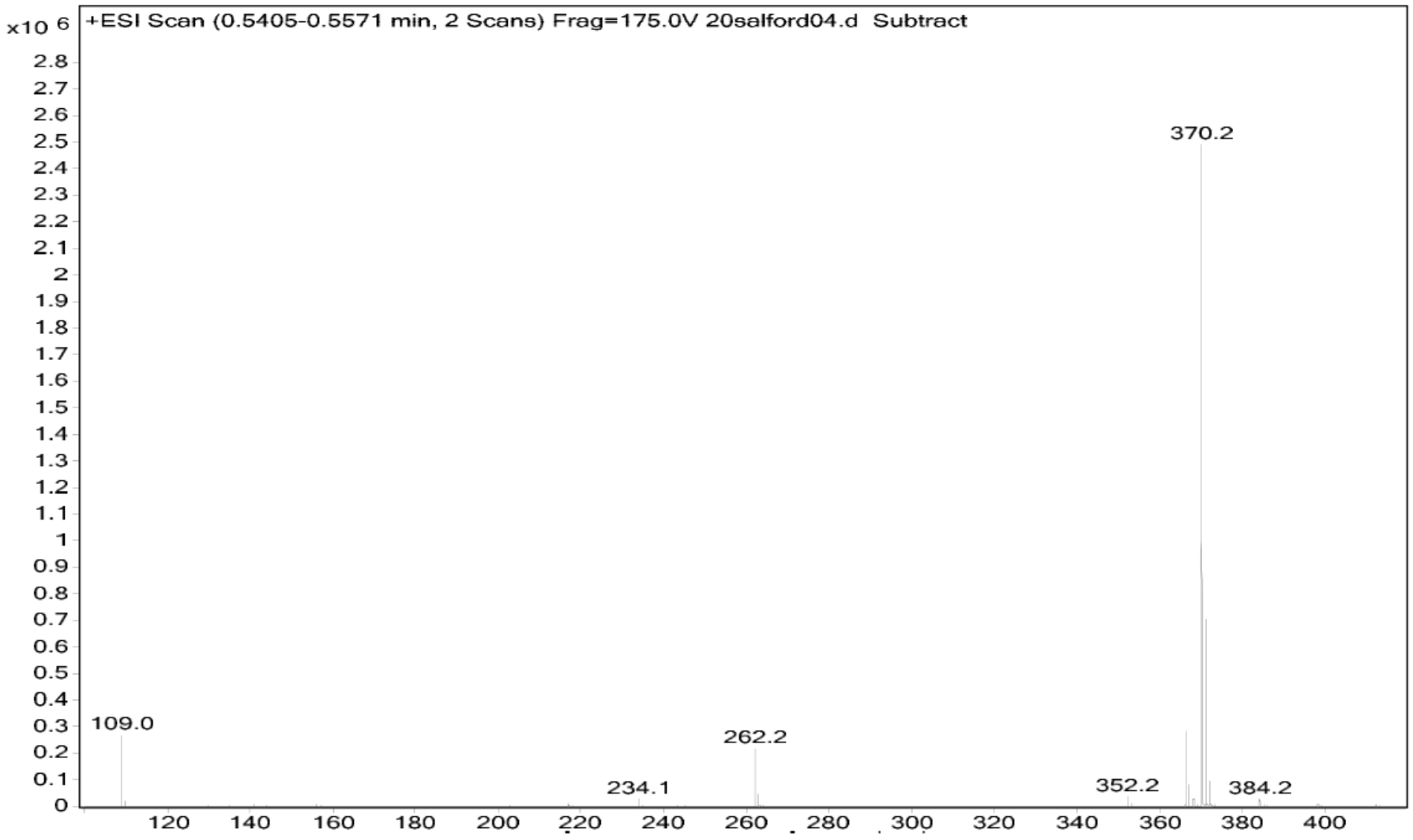
+ESI Scan (0.5405-0.5571 min, 2 Scans) Frag=175.0V 20salford04.d Subtract
x10 6
2.8
2.7
2.6
2.5
2.4
2.3
2.2
2.1
2
1.9
1.8
1.7
1.6
1.5
1.4
1.3
1.2
1.1
1
0.9
0.8
0.7
0.6
0.5
0.4
0.3
0.2
0.1
0
120
140
160
180
200
220
240
260
280
300
320
340
360
380
400
370.2
109.0
262.2
234.1
352.2
384.2

Compound **3j**

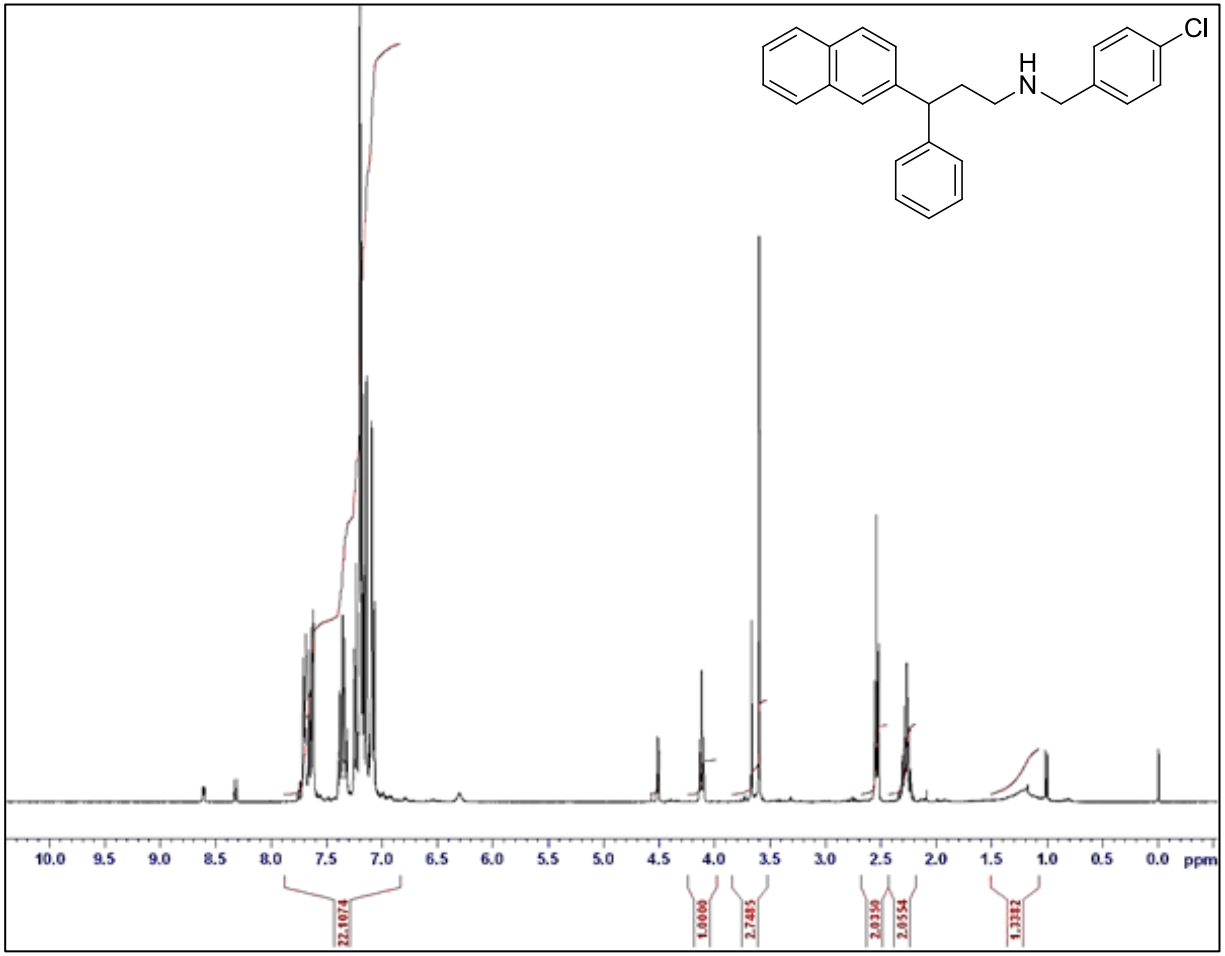
Cl
H
N
10.0 9.5 9.0 8.5 8.0 7.5 7.0 6.5 6.0 5.5 5.0 4.5 4.0 3.5 3.0 2.5 2.0 1.5 1.0 0.5 0.0 ppm
22.1674
1.0000
2.7485
2.0359
2.0554
1.3382

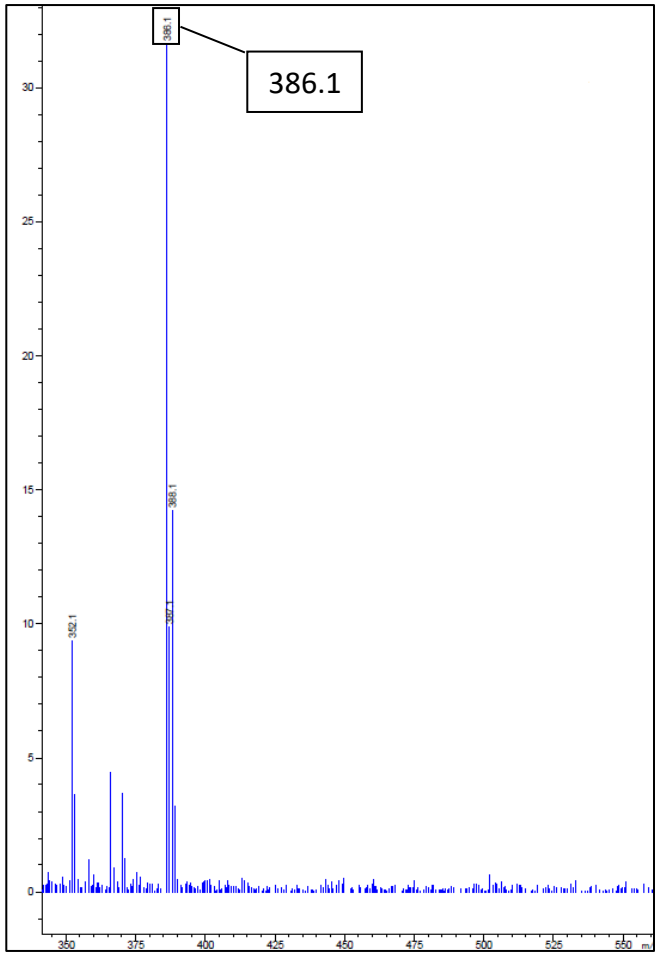
386.1
386.1
386.1
382.1
30
25
20
15
10
5
0
350 375 400 425 450 475 500 525 550 m/z

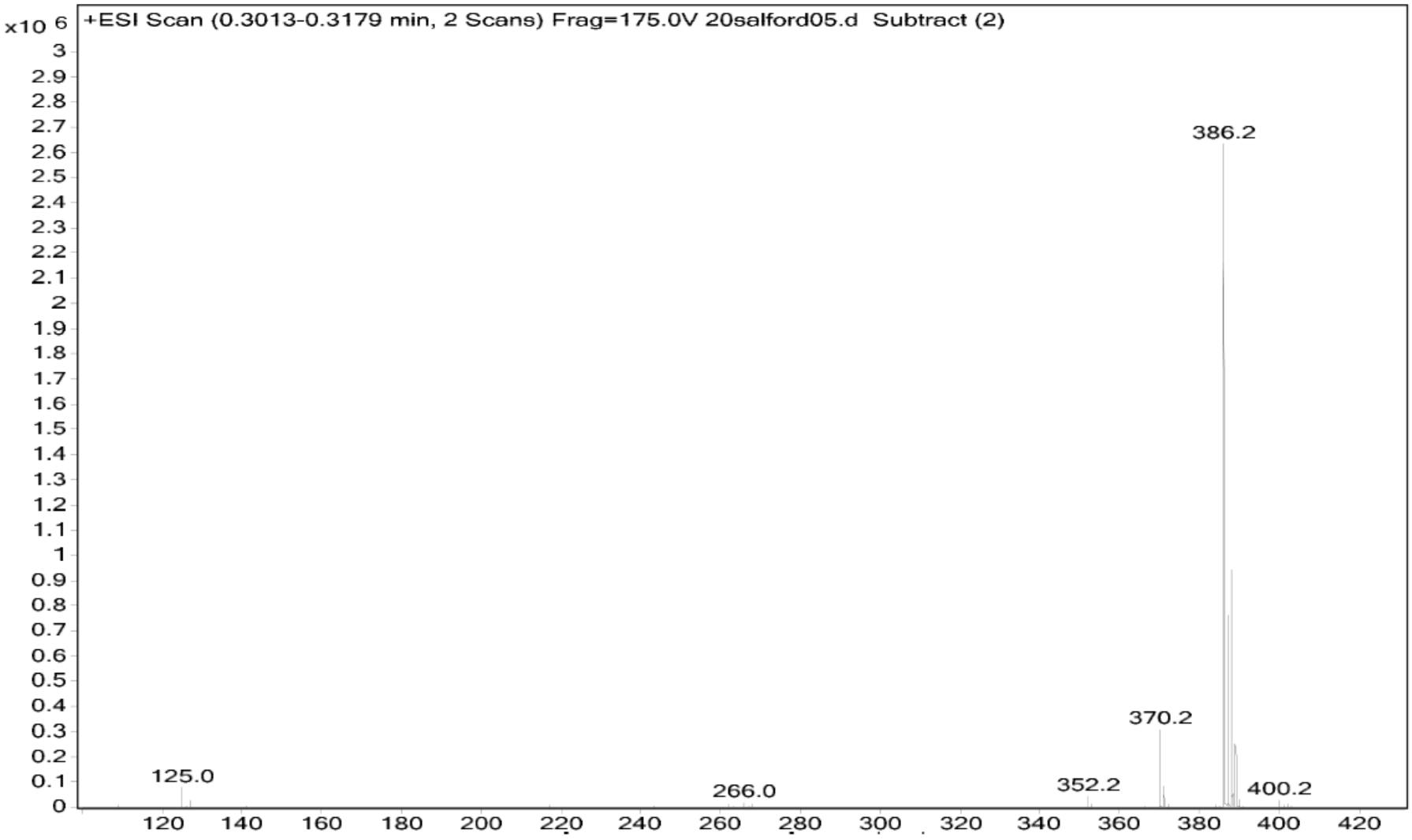
+ESI Scan (0.3013-0.3179 min, 2 Scans) Frag=175.0V 20salford05.d Subtract (2)
x10 6
386.2
370.2
125.0
266.0
352.2
400.2

Compound **3k**

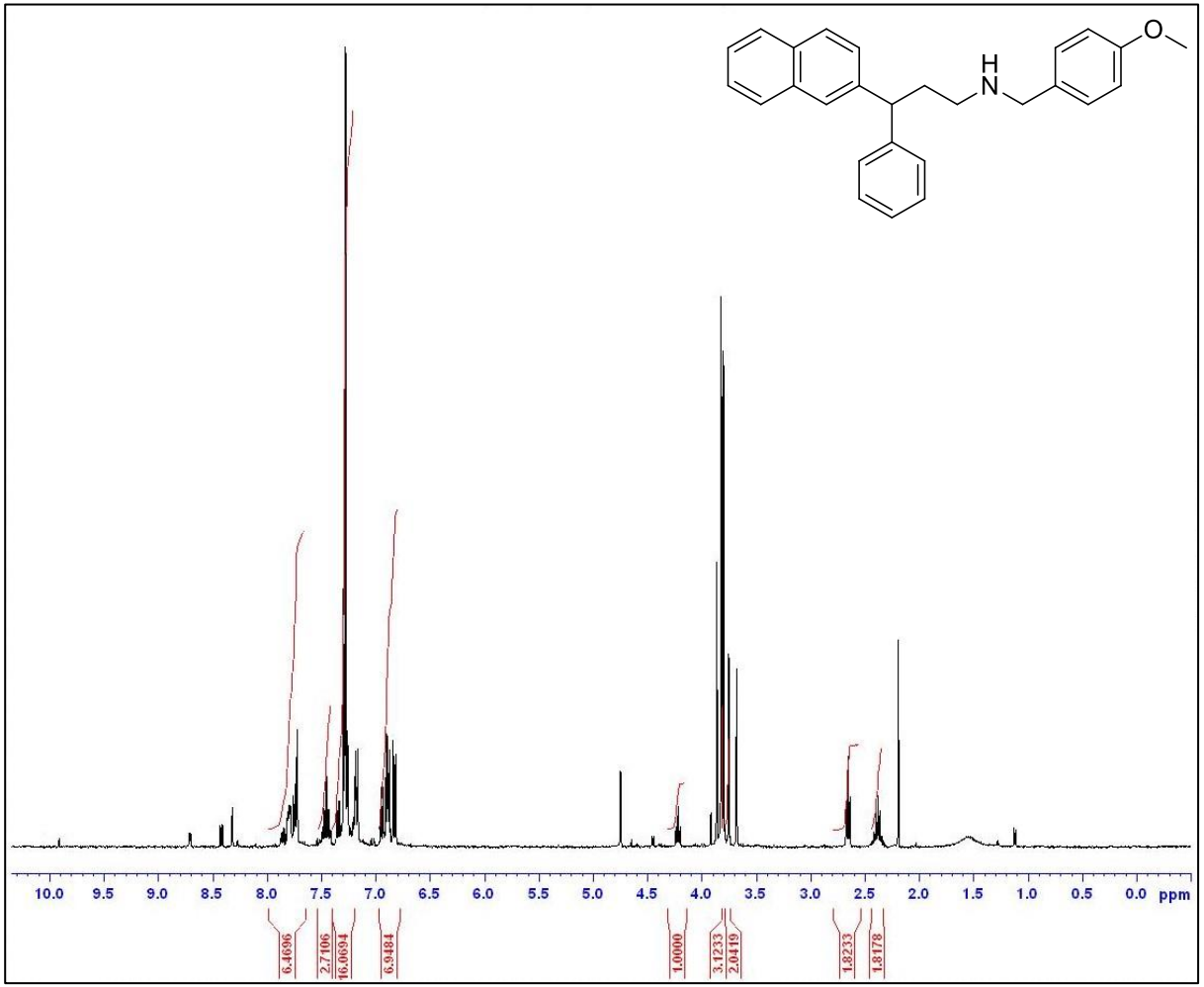
H
N
O
10.0 9.5 9.0 8.5 8.0 7.5 7.0 6.5 6.0 5.5 5.0 4.5 4.0 3.5 3.0 2.5 2.0 1.5 1.0 0.5 0.0 ppm
6.4696
2.7106
16.0694
6.9484
1.0000
3.1233
2.0419
1.8233
1.8178

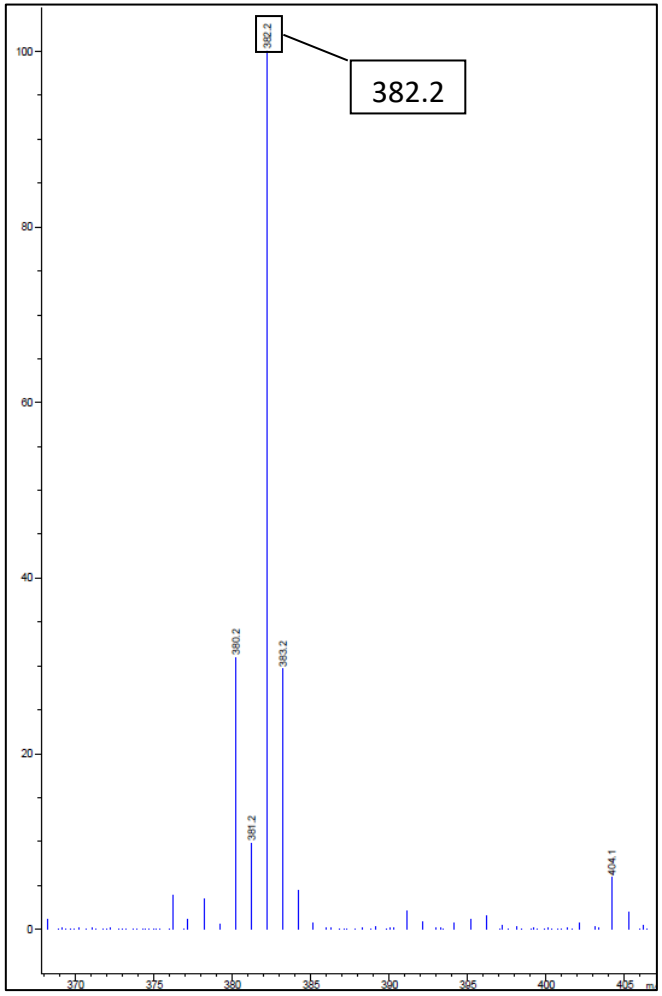
382.2
382.2
380.2
381.2
383.2
404.1
100
80
60
40
20
0
370 375 380 385 390 395 400 405 m/z

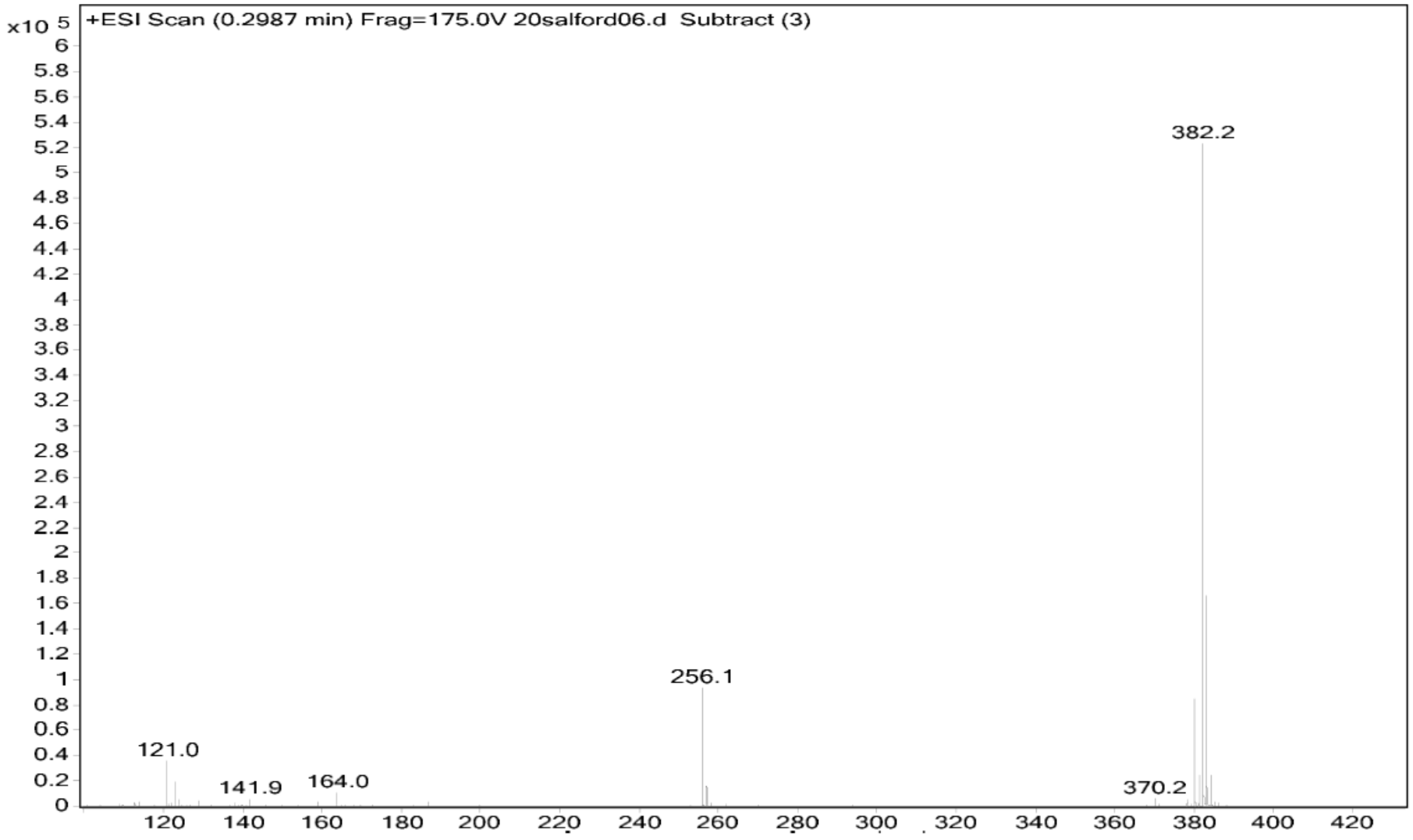
+ESI Scan (0.2987 min) Frag=175.0V 20salford06.d Subtract (3)
x10 5
382.2
256.1
121.0
141.9
164.0
370.2

Compound **3l**

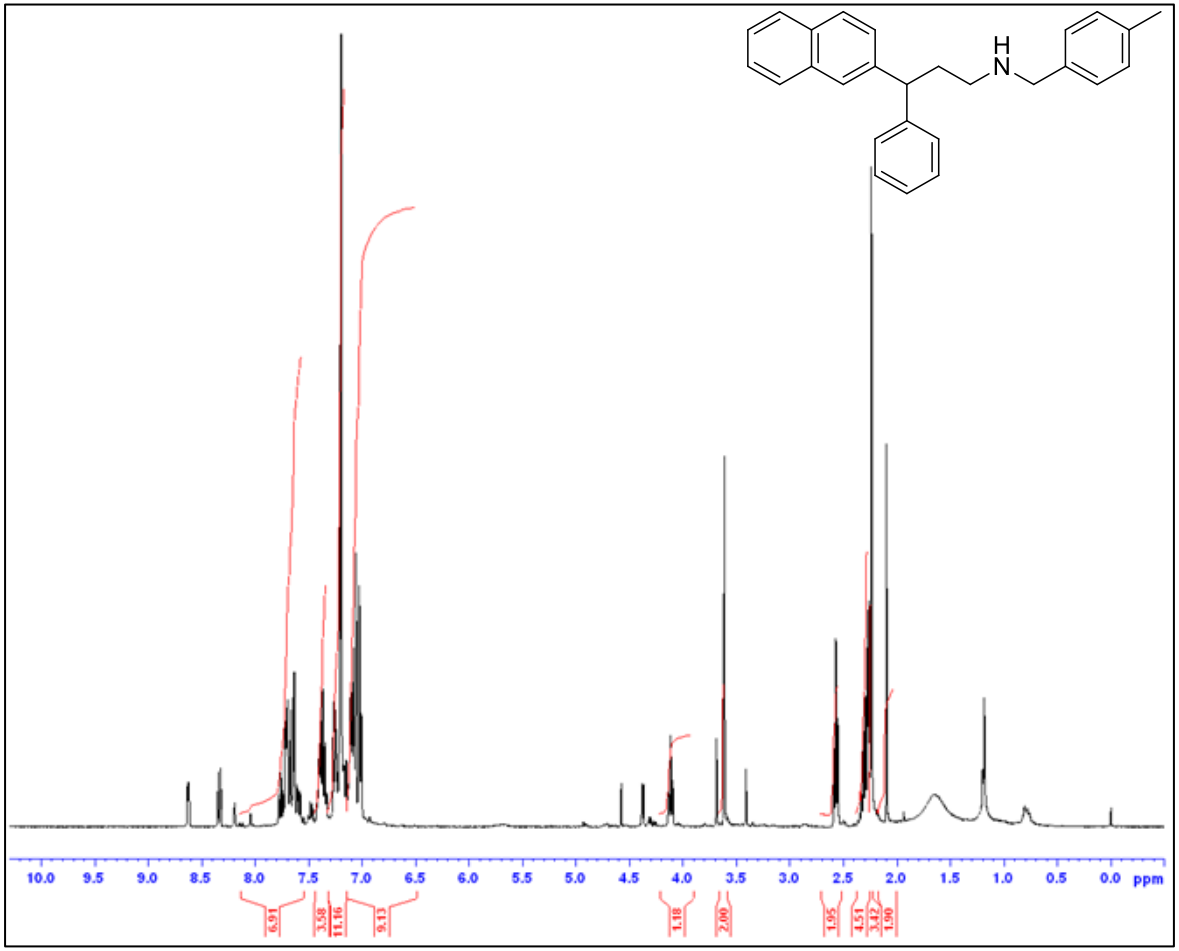
H
N
10.0 9.5 9.0 8.5 8.0 7.5 7.0 6.5 6.0 5.5 5.0 4.5 4.0 3.5 3.0 2.5 2.0 1.5 1.0 0.5 0.0 ppm
6.91
3.58
11.16
3.13
1.18
2.00
1.95
1.51
3.12
1.98

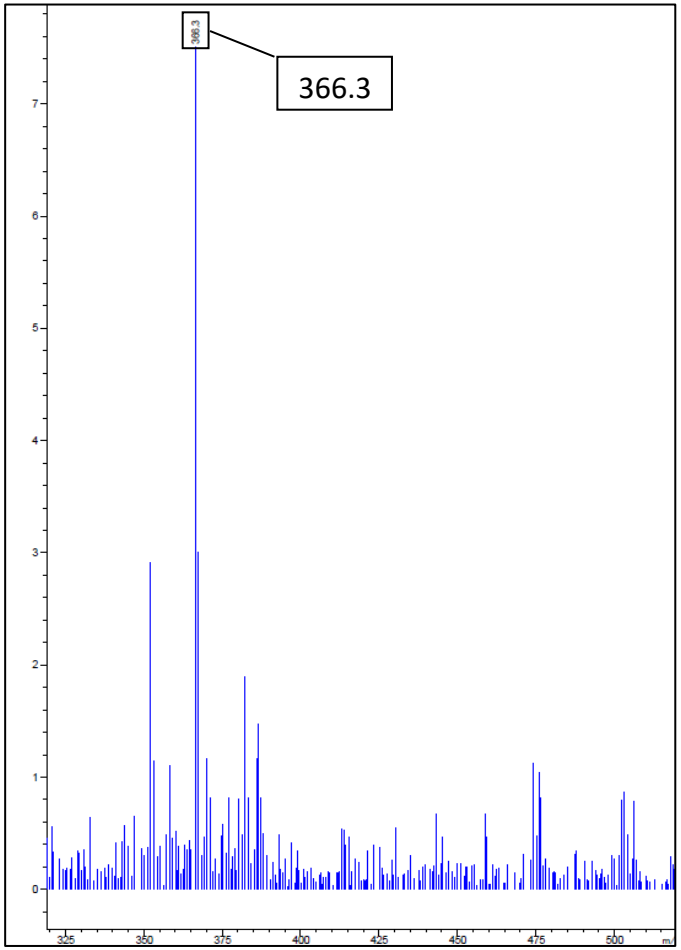
366.3
366.3
325 350 375 400 425 450 475 500 m/z

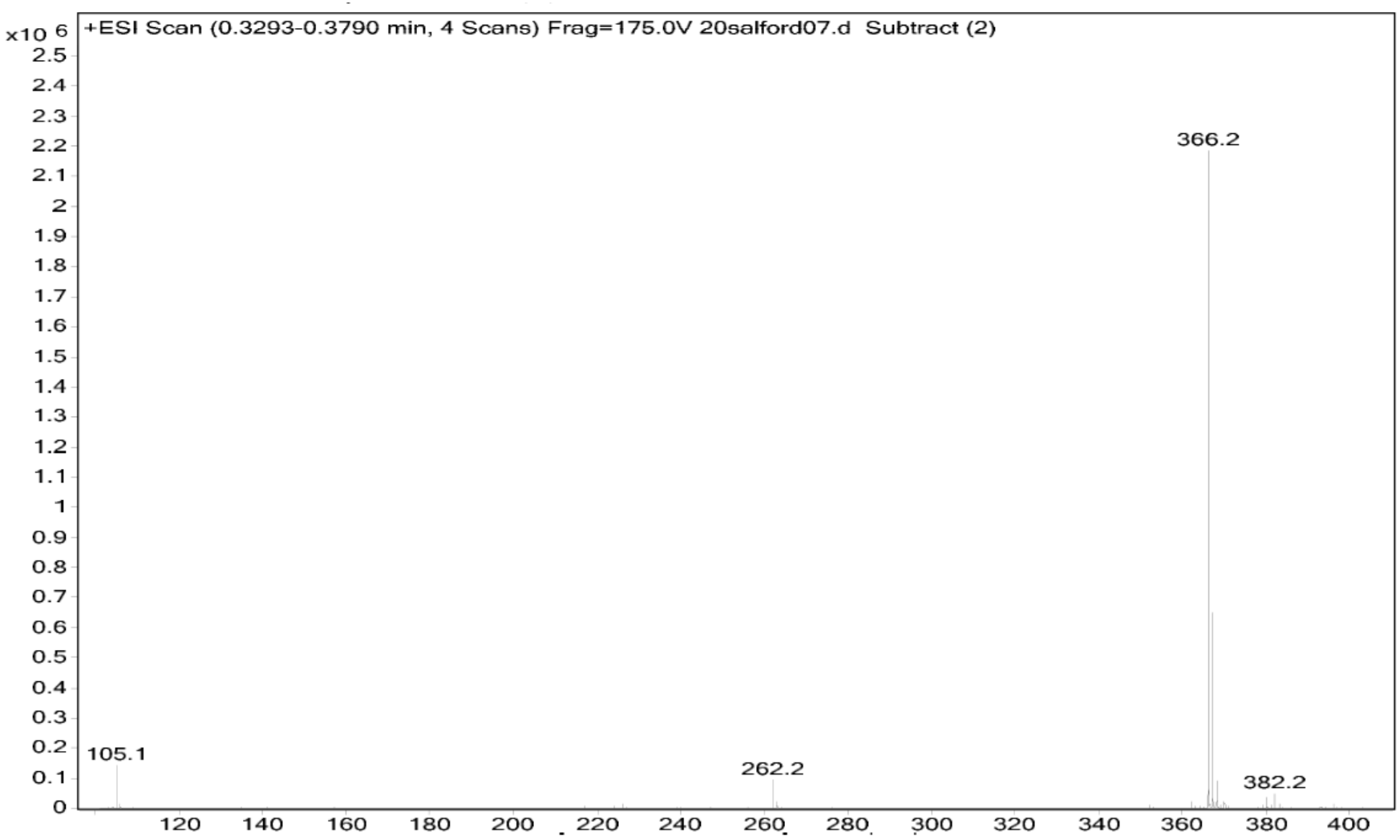
+ESI Scan (0.3293-0.3790 min, 4 Scans) Frag=175.0V 20salford07.d Subtract (2)
x10 6
2.5
2.4
2.3
2.2
2.1
2
1.9
1.8
1.7
1.6
1.5
1.4
1.3
1.2
1.1
1
0.9
0.8
0.7
0.6
0.5
0.4
0.3
0.2
0.1
0
366.2
105.1
262.2
382.2
120
140
160
180
200
220
240
260
280
300
320
340
360
380
400

Appendix II

The dose-response experiments of the synthesised fendiline analogues against the K1 *P. falciparum* parasites can be seen in the graphs below.

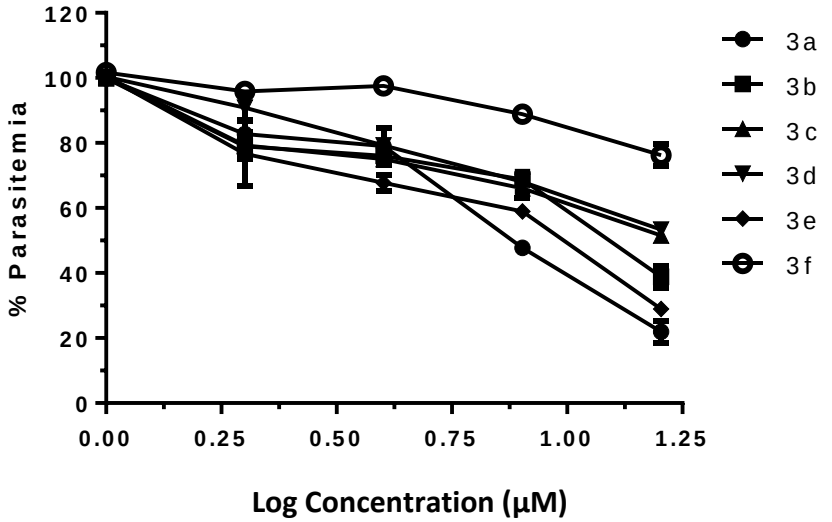

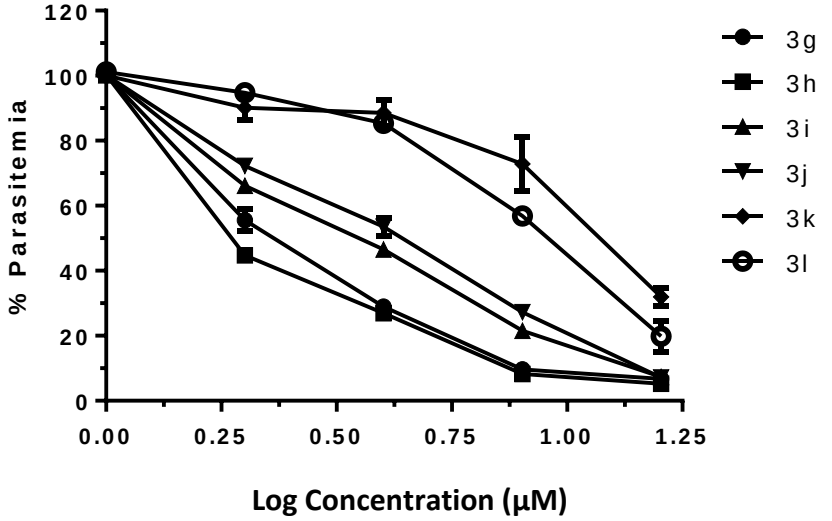

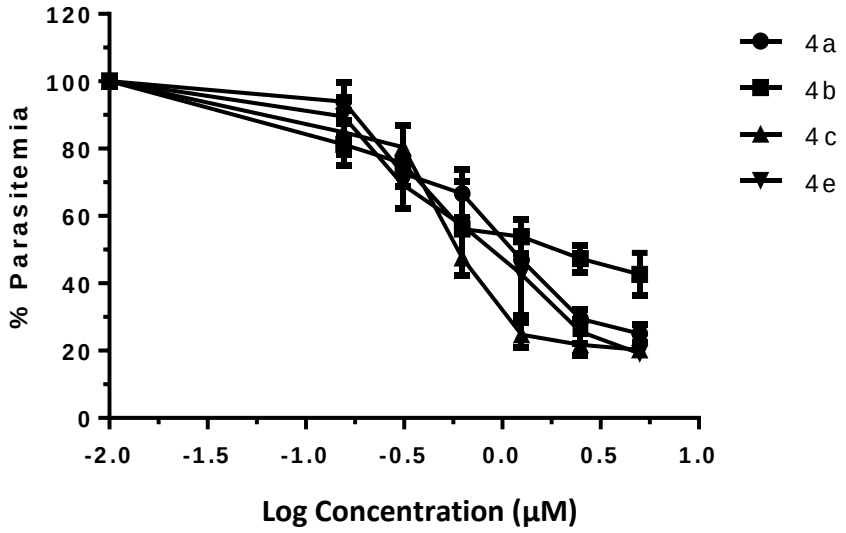
120
100
80
60
40
20
0
% Parasitemia
-2.0
-1.5
-1.0
-0.5
0.0
0.5
1.0
Log Concentration (µM)
4a
4b
4c
4e

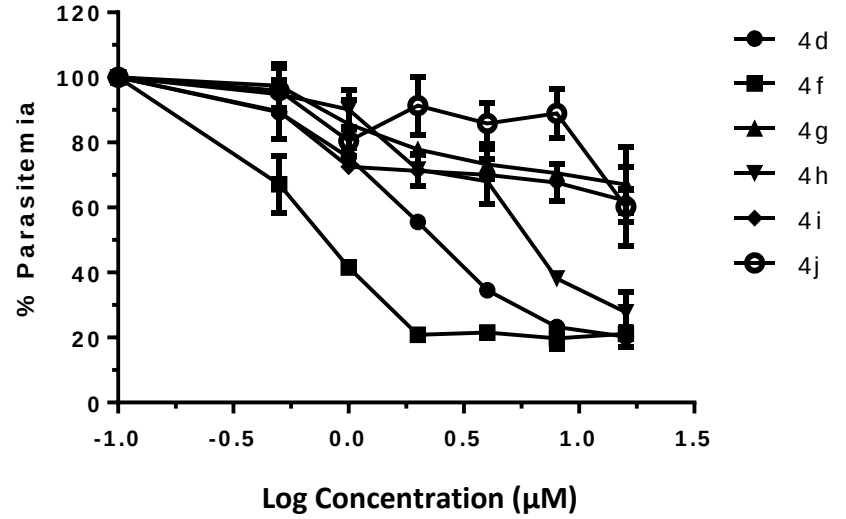
120
100
80
60
40
20
0
% Parasitemia
-1.0
-0.5
0.0
0.5
1.0
1.5
Log Concentration (µM)
4d
4f
4g
4h
4i
4j

Appendix III

The MTT results of the synthesised fendiline analogues against HepG2 cells can be seen in the graphs below.

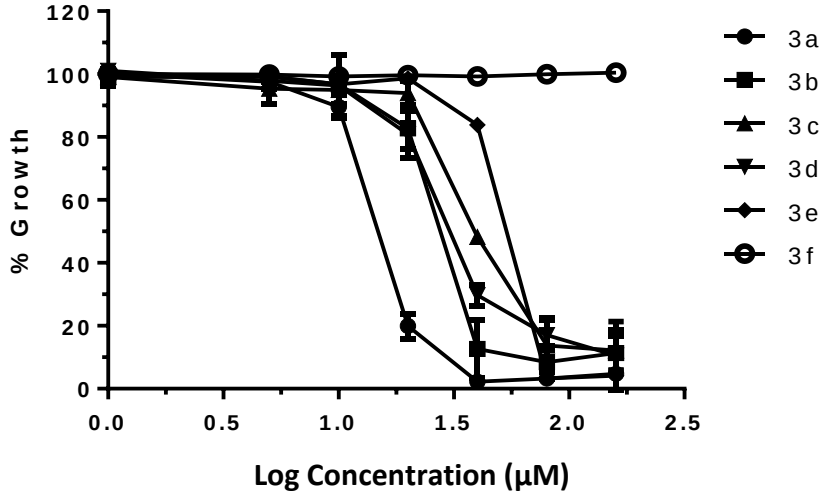

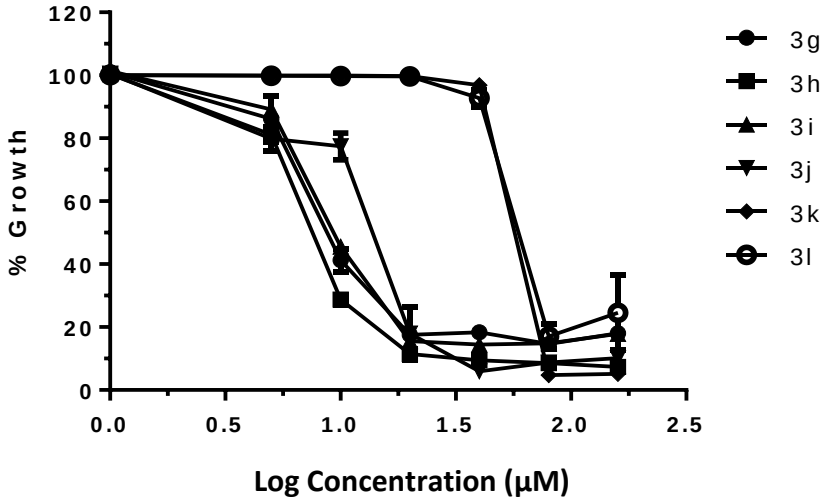

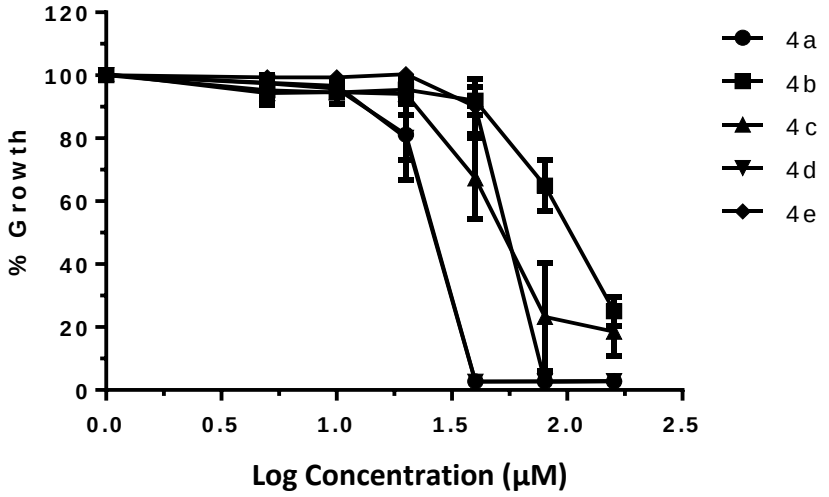
120
100
80
60
40
20
0
% Growth
0.0
0.5
1.0
1.5
2.0
2.5
Log Concentration (µM)
4a
4b
4c
4d
4e

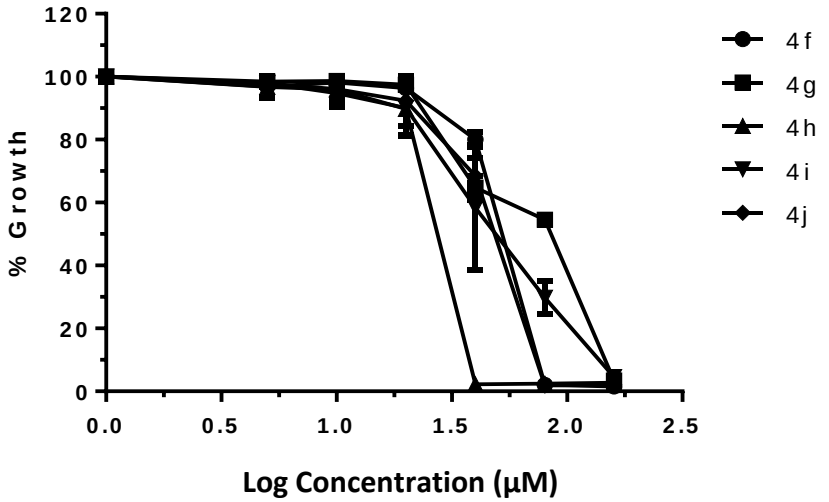
120
100
80
60
40
20
0
% Growth
0.0
0.5
1.0
1.5
2.0
2.5
Log Concentration (µM)
4f
4g
4h
4i
4j

References

Achan, J., Talisuna, A. O., Erhart, A., Yeka, A., Tibenderana, J. K., Baliraine, F. N., … D'Alessandro, U. (2011). Quinine, an old anti-malarial drug in a modern world: role in the treatment of malaria. *Malar J*, *10*, 144. https://doi.org/0.1186/1475-2875-10-144

Abu-Absi, N. R., Zamamiri, A., Kacmar, J., Balogh, S. J., & Srienc, F. (2003). Automated flow cytometry for acquisition of time-dependent population data. *Cytometry A*, *51*(2), 87–96. https://doi.org/10.1002/cyto.a.10016

Adebayo, J. O., & Krettli, A. U. (2011). Potential antimalarials from Nigerian plants: a review. *J Ethnopharmacol*, *133*(2), 289–302. https://doi.org/10.1016/j.jep.2010.11.024

Aditya, N. P., Vathsala, P. G., Vieira, V., Murthy, R. S. R., & Souto, E. B. (2013). Advances in nanomedicines for malaria treatment. *Adv Colloid Interface Sci*, *201–202*, 1–17. https://doi.org/10.1016/j.cis.2013.10.014

Adovelande, J., Bastide, B., Deleze, J., & Schrevel, J. (1993). Cytosolic free calcium in *Plasmodium falciparum*-infected erythrocytes and the effect of verapamil: a cytofluorometric study. *Exp Parasitol*, *76*(3), 247–58.

Adovelande, J., Deleze, J., & Schrevel, J. (1998). Synergy between two calcium channel blockers, verapamil and fantofarone (SR33557), in reversing chloroquine resistance in *Plasmodium falciparum*. *Biochem Pharmacol*, *55*(4), 433–40.

Agarwal, D., Gupta, R. D., & Awasthi, S. K. (2017). Are antimalarial hybrid molecules a close reality or a distant dream? *Antimicrob Agents Chemother*, *61*(5), e00249-17. https://doi.org/10.1128/AAC.00249-17

Akoachere, M., Buchholz, K., Fischer, E., Burhenne, J., Haefeli, W. E., Schirmer, R. H., & Becker, K. (2005). *In vitro* assessment of methylene blue on chloroquine-sensitive and -resistant *Plasmodium falciparum* strains reveals synergistic action with artemisinins. *Antimicrob Agents Chemother*, *49*(11), 4592–7. https://doi.org/10.1128/AAC.49.11.4592-4597.2005

Alister, G. C., Mustaffa, K. M. F., & Pradeep, R. P. (2012). Cytoadherence and severe malaria. *Malays J Med Sci*, 19(2), 5–18.

Alker, A. P., Mwapasa, V., Purfield, A., Rogerson, S. J., Molyneux, M. E., Kamwendo, D. D., … Meshnick, S. R. (2005). Mutations associated with sulfadoxine-pyrimethamine and chlorproguanil resistance in *Plasmodium falciparum* isolates from Blantyre , Malawi. *Antimicrob Agents Chemother*, *49*(9), 3919–21. https://doi.org/10.1128/AAC.49.9.3919-3921.2005

Alleva, L. M., & Kirk, K. (2001). Calcium regulation in the intraerythrocytic malaria parasite *Plasmodium falciparum*. *Mol Biochem Parasitol*, *117*(2), 121–8.

Alonso, P. L., Bassat, Q., Binka, F., Brewer, T., Chandra, R., Culpepper, J., … Rabinovich, R. (2011). A research agenda for malaria eradication: drugs. *PLOS Med*, *8*, e1000402. https://doi.org/10.1371/journal.pmed.1000402

Alves, E., Bartlett, P. J., Garcia, C. R., & Thomas, A. P. (2011). Melatonin and IP_3-induced Ca^{2+} release from intracellular stores in the malaria parasite *Plasmodium falciparum* within infected red blood cells. *J Biol Chem*, *286*(7), 5905–12. https://doi.org/10.1074/jbc.M110.188474

Andrews, K. T., Fisher, G., & Skinner-Adams, T. S. (2014). Drug repurposing and human parasitic protozoan diseases. *Int J Parasitol Drugs Drug Resist*, *4*(2), 95–111. https://doi.org/10.1016/j.ijpddr.2014.02.002

Antony, H. A., & Parija, S. C. (2016). Antimalarial drug resistance: an overview. *Trop Parasitol*, *6*, 30–41. https://doi.org/10.4103/2229-5070.175081

Ariey, F., Witkowski, B., Amaratunga, C., Beghain, J., Langlois, A. C., Khim, N., … Menard, D. (2014). A molecular marker of artemisinin-resistant *Plasmodium falciparum* malaria. *Nature*, *505*(7481), 50–5. https://doi.org/10.1038/nature12876

Arnou, B., Montigny, C., Morth, J. P., Nissen, P., Jaxel, C., Møller, J. V, & Maire, M. le. (2011). The *Plasmodium falciparum* $Ca(^{2+})$-ATPase PfATP6: insensitive to artemisinin, but a potential drug target. *Biochem Soc Trans*, *39*(3), 823–31. https://doi.org/10.1042/BST0390823

Ashley, E., Recht, J., & White, N. (2014). Primaquine: the risks and the benefits. *Malar J*, *13*, 418. https://doi.org/10.1186/1475-2875-13-418

Assinger, A., Volf, I., & Schmid, D. (2015). A novel,rapid method to quantify intraplatelet calcium dynamics by ratiometric flow cytometry. *PLoS ONE*, *10*(4), e0122527. https://doi.org/10.1371/journal.pone.0122527

Autino, B., Corbett, Y., Castelli, F., & Taramelli, D. (2012). Pathogenesis of malaria in tissues and blood. *Mediterr J Hematol Infect Dis*, 4, e2012061. https://doi.org/10.4084/MJHID.2012.061.

Baeder, D. Y., Yu, G., Hozé, N., Rolff, J., & Regoes, R. R. (2016). Antimicrobial combinations: Bliss independence and Loewe additivity derived from mechanistic multi-hit models. *Phil Trans R Soc*, *371*(1695). https://doi.org/10.1098/rstb.2015.0294

Baek, M. C., Jung, B., Kang, H., Lee, H. S., & Bae, J. S. (2015). Novel insight into drug repositioning: Methylthiouracil as a case in point. *Pharmacol Res*, *99*, 185–93. https://doi.org/10.1016/j.phrs.2015.06.008

Bakouh, N., Bellanca, S., Nyboer, B., Moliner Cubel, S., Karim, Z., Sanchez, C. P., … Lanzer, M. (2017). Iron is a substrate of the *Plasmodium falciparum* chloroquine resistance transporter PfCRT in Xenopus oocytes. *J Biol Chem*, *292*(39), 16109–21. https://doi.org/10.1074/jbc.M117.805200

Ballou, R. W., & Vekemans, J. (2017). Malaria Vaccines. In: Plotkin, S. A., Orenstein, W. A., Offit, P. A. & Edwards, K. M. eds. *Plotkin's Vaccines*. Elsevier Inc, 561-66. https://doi.org/10.1016/B978-0-323-35761-6.00035-3

Bangalore, R., Baindur, N., Rutledge, A., Triggle, D. J., & Kass, R. S. (1994). L-type calicum channels: asymmetric intramembrane binding domain revealed by variable length, permanently charged 1,4-dihydropyridines. *Mol Pharm*, *46*(4), 660–6.

Bansal, A., Singh, S., More, K. R., Hans, D., Nangalia, K., Yogavel, M., … Chitnis, C. E. (2013). Characterization of *Plasmodium falciparum* calcium-dependent protein kinase 1 (PFCDPK1) and its role in microneme secretion during erythrocyte invasion. *Journal of Biological Chemistry*, *288*(3), 1590–1602. https://doi.org/10.1074/jbc.M112.411934

Barreaux, P., Barreaux, A. M. G., Sternberg, E. D., Suh, E., Waite, J. L., Whitehead, S. A., & Thomas, M. B. (2017). Priorities for broadening the malaria vector control tool kit. *Trends Parasitol*, *33*(10), 763–74. https://doi.org/10.1016/j.pt.2017.06.003

Barteneva, N. S., Fasler-Kan, E., & Vorobjev, I. A. (2012). Imaging flow cytometry: coping with heterogeneity in biological systems. *J Histochem Cytochem*, *60*(10), 723–33. https://doi.org/10.1369/0022155412453052

Bartoloni, A. & Zammarchi, L. (2012). Clinical aspects of uncomplicated and severe malaria. *Mediterr J Hematol Infect Dis*, 4, e2012026. https://doi.org/10.4084/MJHID.2012.026.

Basco, L. K., & Le Bras, J. (1991). *Plasmodium falciparum*: *in vitro* drug interaction between chloroquine and enantiomers of amlodipine. *Exp Parasitol*, *72*(3), 262–70. https://doi.org/10.1016/0014-4894(91)90145-M

Basco, L. K., & Le Bras, J. (1992). *In vitro* activities of chloroquine in combination with chlorpromazine or prochlorperazine against isolates of *Plasmodium falciparum*. *Antimicrob Agents Chemother*, *36*, 209–13. https://doi.org/10.1128/AAC.36.1.209

Bayer, R., & Mannhold, R. (1987). Fendiline: a review of its basic pharmacological and clinical properties. *Pharmatherapeutica*, *5*(2), 103–36.

Bazanovas, A. N., Evstifeev, A. I., Khaiboullina, S. F., Sadreev II, Skorinkin, A. I., & Kotov, N. V. (2015). Erythrocyte: A systems model of the control of aggregation and deformability. *Biosystems*, *131*, 1–8. https://doi.org/10.1016/j.biosystems.2015.03.003

BD Biosciences. (2015). Multicolor Flow Cytometry - sampledata - bluelaser | BD Biosciences-Europe. Retrieved January 6, 2016 from http://www.bdbiosciences.com/eu/s/multicolorflow/sampledata/bluelaser#search=fitc channel

Bell, A. (2005). Antimalarial drug synergism and antagonism: mechanistic and clinical significance. *FEMS Microbiol Lett*, *253*(2), 171–84. https://doi.org/10.1016/j.femsle.2005.09.035

Bellanca, S., Summers, R. L., Meyrath, M., Dave, A., Nash, M. N., Dittmer, M., … Lanzer, M. (2014). Multiple drugs compete for transport via the *Plasmodium falciparum* chloroquine resistance transporter at distinct but interdependent sites. *J Biol Chem*, *289*(52), 36336–51. https://doi.org/10.1074/jbc.M114.614206

Belson, M. G., Gorman, S. E., Sullivan, K., & Geller, R. J. (2000). Calcium channel blocker ingestions in children. *Am J Emerg Med*, *18*(5), 581–6. https://doi.org/10.1053/ajem.2000.9264

Ben, J. M., Yang, P. S., Bazzazi, H., & Yue, D. T. (2013). Dynamic switching of calmodulin interactions underlies Ca^{2+} regulation of CaV1.3 channels. *Nat Commun*, *4*, 1717. https://doi.org/10.1038/ncomms2727

Benelli, G., & Beier, J. C. (2017). Current vector control challenges in the fight against malaria. *Acta Trop*, *174*, 91–96. https://doi.org/10.1016/j.actatropica.2017.06.028

Beraldo, F. H., Mikoshiba, K., & Garcia, C. R. S. (2007). Human malarial parasite, *Plasmodium falciparum*, displays capacitative calcium entry: 2-aminoethyl diphenylborinate blocks the signal

transduction pathway of melatonin action on the *P. falciparum* cell cycle. *J Pineal R*, *43*(4), 360–4. https://doi.org/10.1111/j.1600-079X.2007.00486

Berchtold, M. W., & Villalobo, A. (2014). The many faces of calmodulin in cell proliferation, programmed cell death, autophagy, and cancer. *Biochim Biophys Acta*, *1843*(2), 398–435. https://doi.org/10.1016/j.bbamcr.2013.10.021

Berridge, M. J., Lipp, P., & Bootman, M. D. (2000). The versatility and universality of calcium signalling. *Nat Rev Mol Cell Biol*, *1*, 11–21. https://doi.org/10.1038/35036035

Bhattacharjee, A. K., Kyle, D. E., Vennerstorm, J. L., & Milhous, W. K. (2002). A 3D QSAR pharmacophore model and quantum chemical structure-activity analysis of chloroquine(CQ)-resistance reversal. *J Chem Inf Comput Sci*, *42*(5), 1212–20. https://doi.org/10.1021/ci0200265

Biagini, G. A., Bray, P. G., Spiller, D. G., White, M. R. H., & Ward, S. A. (2003). The digestive food vacuole of the malaria parasite is a dynamic intracellular Ca^{2+} store. *J Biol Chem*, *278*(30), 27910–5. https://doi.org/10.1074/jbc.M304193200

Biamonte, M. A., Wanner, J., & Le Roch, K. G. (2013). Recent advances in malaria drug discovery. *Bioorg Med Chem Lett*, *23*(10), 2829–43. https://doi.org/10.1016/j.bmcl.2013.03.067

Bitonti, A., Sjoerdsm, A., McCann, P., Kyle, D., Oduola, A., Rossan, R., … Davidson, D. J. (1988). Reversal of chloroquine resistance in malaria parasite *Plasmodium falciparum* by desipramine. *Science*, *242*(4883), 13013.

Bogdanova, A., Makhro, A., Wang, J., Lipp, P., & Kaestner, L. (2013). Calcium in red blood cells-a perilous balance. *Int J Mol Sci*, *14*(5), 9848–72. https://doi.org/10.3390/ijms14059848

Bokhari, M., Carnachan, R. J., Cameron, N. R., & Przyborski, S. A. (2007). Culture of HepG2 liver cells on three dimensional polystyrene scaffolds enhances cell structure and function during toxicological challenge. *J. Anat.*, *211*(4), 567–76. https://doi.org/10.1111/j.1469-7580.2007.00778.x

Bootman, M. D., Rietdorf, K., Collins, T., Walker, S., & Sanderson, M. (2013). Ca^{2+}-sensitive fluorescent dyes and intracellular Ca^{2+} imaging. *Cold Spring Harb Protoc*, *8*(2), 83–99. https://doi.org/10.1101/pdb.top066050

Borch, R. F., Bernstein, M. K., & Durst, H. D. (1971). The cyanohydridoborate anion as a selective reducing agent. *J. Am. Chem. Soc.*, *93*(12), 2897–904. https://doi.org/10.1021/ja00741a013

Borges-Pereira, L., Campos, B. R. K. L., & Garcia, C. R. S. (2014). The GCaMP3 – A GFP-based calcium sensor for imaging calcium dynamics in the human malaria parasite *Plasmodium falciparum*. *MethodsX*, *1*, 151–4. https://doi.org/10.1016/j.mex.2014.08.005

Borle, A. B. (1990). An overview of techniques for the measurement of calcium distribution, calcium fluxes, and cytosolic free calcium in mammalian cells. *Environ Health Perspect*, *84*, 45–56. https://doi.org/10.1289/ehp.908445

Borle, A., & Snowdowne, K. (1986). Measurement of intracellular ionized calcium with aequorin. *Methods Enzymol*, *124*, 90–116.

Boudhar, A., Ng, W., Loh, Y., Chia, N., Tan, M., Nosten, F., … Tan, K. S.-W. (2016). Overcoming chloroquine resistance in malaria: design, synthesis, and structure-activity relationships of novel hybrid compounds. *Antimicrob Agents Chemother*, *60*(5), 3076–89. https://doi.org/10.1128/AAC.02476-15

Brochet, M., Collins, M. O., Smith, T. K., Thompson, E., Sebastian, S., Volkmann, K., … Billker, O. (2014). Phosphoinositide metabolism links cGMP-dependent protein kinase G to essential Ca^{2+} signals at key decision points in the life cycle of malaria parasites. *PLoS Biol*, *12*(3), e1001806. https://doi.org/10.1371/journal.pbio.1001806

Brochet, M., & Billker, O. (2016). Calcium signalling in malaria parasites. *Mol Microbiol*, *100*(3), 397–408. https://doi.org/10.1111/mmi.13324

Bulusu, K. C., Guha, R., Mason, D. J., Lewis, R. P. I., Muratov, E., Motamedi, Y. K., … Bender, A. (2016). Modelling of compound combination effects and applications to efficacy and toxicity: state-of-the-art , challenges and perspectives. *Drug Discov Today*, *21*(2), 225–38. https://doi.org/10.1016/j.drudis.2015.09.003

Burgess, S. J., Selzer, A., Kelly, J. X., Smilkstein, M. J., Riscoe, M. K., & Peyton, D. H. (2006). A chloroquine-like molecule designed to reverse resistance in *Plasmodium falciparum*. *J Med Chem*, *49*(18), 5623–25. https://doi.org/10.1021/jm060399n

Burrows, J. N., Hooft van Huijsduijnen, R., Möhrle, J. J., Oeuvray, C., & Wells, T. N. (2013). Designing the next generation of medicines for malaria control and eradication. *Malar J*, *12,* 187. https://doi.org/10.1186/1475-2875-12-187

Camacho, P. (2003). Malaria parasites solve the problem of a low calcium environment. *J Cell Biol*, *161*, 17–9. https://doi.org/10.1083/jcb.200303116

Campo, J. J., Aponte, J. J., Nhabomba, A. J., Sacarla, J., Angulo-Barturen, I., Jiménez-Díaz, M. B., … Dobaño, C. (2011). Feasibility of flow cytometry for measurements of *Plasmodium falciparum* parasite burden in studies in areas of malaria endemicity by use of bidimensional assessment of YOYO-1 and autofluorescence. *J Clin Microb*, *49*(3), 968–74. https://doi.org/10.1128/JCM.01961-10

Canfield, C. J., Pudney, M., & Gutteridge, W. E. (1995). Interactions of atovaquone with other antimalarial drugs against *Plasmodium falciparum in vitro*. *Exp Parasitol, 80*(3), 373-81. https://doi.org/10.1006/expr.1995.1049

Carvalho, B. O., Lopes, S. C., Nogueira, P. A., Orlandi, P. P., Bargieri, D. Y., Blanco, Y. C., … Costa, F. T. (2010). On the Cytoadhesion of *Plasmodium vivax* – Infected Erythrocytes. *J Infect Dis*, 202(4), 638–47. https://doi.org/10.1086/654815.

Castelli, F., Odolini, S., Autino, B., Foca, E., & Russo, R. (2010). Malaria prophylaxis: a comprehensive review. *Pharmaceuticals (Basel)*, *3*(10), 3212–3239. https://doi.org/10.3390/ph3103212

Catterall, W. a, Perez-Reyes, E., Snutch, T. P., & Striessnig, J. (2005). International Union of Pharmacology. XLVIII. Nomenclature and structure-function relationships of voltage-gated calcium channels. *Pharmacol Rev*, *57*(4), 411–25. https://doi.org/10.1124/pr.57.4.5.

Chakraborty, A. (2016). Understanding the biology of the *Plasmodium falciparum* apicoplast; an excellent target for antimalarial drug development. *Life Sciences*, *158*, 104–10. https://doi.org/10.1016/j.lfs.2016.06.030

Chandra, K. S., & Ramesh, G. (2013). The fourth-generation calcium channel blocker: cilnidipine. *IHJ*, *65*(6), 691–5. https://doi.org/10.1016/j.ihj.2013.11.001

Chen, K. (2012). A pharmacognostic and chemical study of ma huang (Ephedra vulgaris var. Helvetica). 1925. *J Am Pharm Assoc*, *14*(3), 406-12. https://doi.org/10.1331/JAPhA.2012.12519

Chen, Q., Schlichtherle, M. & Wahlgren, M. (2000). Molecular aspects of severe malaria. *Clin Microbiol Rev*, 13(3), 439–50. https://doi.org/10.1128/CMR.13.3.439-450.2000.

Cheng, J., Wang, J., Lo, Y., Chou, K., Lee, K., Liu, C., … Jan, C. (2001). Effects of the antianginal drug fendiline on Ca^{2+} movement in hepatoma cells. *Hum Exp Toxicol*, *20*(7), 359-64. https://doi.org/10.1191/096032701680350523

Cheng, Q., Kyle, D. E., & Gatton, M. L. (2012). Artemisinin resistance in *Plasmodium falciparum*: A process linked to dormancy? *Int J Parasitol Drugs Drug Resist*, *2*, 249–55. https://doi.org/10.1016/j.ijpddr.2012.01.001

Chia, W. N., Lee, Y. Q., & Tan, K. S.-W. (2017). Imaging flow cytometry for the screening of compounds that disrupt the *Plasmodium falciparum* digestive vacuole. *Methods*, *112*, 211–20. https://doi.org/10.1016/j.ymeth.2016.07.002

Chiba, T., Yamanaka, M., Takagi, S., Shimizu, K., Takahashi, M., Shirai, K., & Takahara, A. (2015). Cardio-ankle vascular index (CAVI) differentiates pharmacological properties of vasodilators nicardipine and nitroglycerin in anesthetized rabbits. *J Pharmacol Sci, 128*(4), 185-92. https://doi.org/10.1016/j.jphs.2015.07.002

Chou, T. (2006). Theoretical basis , experimental design, and computerized simulation of synergism and antagonism in drug combination studies. *Pharmacol Rev*, *58*(3), 621–81. https://doi.org/10.1124/pr.58.3.10.

Chou, T. C. (2010). Drug combination studies and their synergy quantification using the Chou-Talalay method. *Cancer Res*, *70*(2), 440–6. https://doi.org/10.1158/0008-5472.can-09-1947

Christel, C., & Lee, A. (2012). Ca^{2+}-dependent modulation of voltage-gated Ca^{2+} channels. *Biochem Biophys Acta*, *1820*(8), 1243–52. https://doi.org/10.1016/j.bbagen.2011.12.012

Clapham, D. E. (2007). Calcium signaling. *Cell*, *131*(6), 1047–58. https://doi.org/10.1016/j.cell.2007.11.028

Clayden, J., Greeves, N., Warren, S., & Wothers, P. (2001). *Organic chemistry*. Oxford: Oxford University Press.

Co, E. M., Dennull, R. A., Reinbold, D. D., Waters, N. C., & Johnson, J. D. (2009). Assessment of malaria *in vitro* drug combination screening and mixed-strain infections using the malaria Sybr green I-based fluorescence assay. *Antimicrob Agents Chemother*, *53*(6), 2557–63. https://doi.org/10.1128/aac.01370-08

Cobo, F. (2014). Current status of malaria. In: *Imported Infectious Diseases: The Developed Countries*. Elsevier. 61–90.

Cohen, A., Suzanne, P., Lancelot, J. C., Verhaeghe, P., Lesnard, A., Basmaciyan, L., … Azas, N. (2015). Discovery of new thienopyrimidinone derivatives displaying antimalarial properties toward both

erythrocytic and hepatic stages of *Plasmodium*. *Eur J Med Chem*, *95*, 16–28. https://doi.org/10.1016/j.ejmech.2015.03.011

Corbett, A., Williams, G., & Ballard, C. (2013). Drug repositioning: An opportunity to develop novel treatments for Alzheimer's disease. *Pharmaceuticals*, *6*(10), 1304–21. https://doi.org/10.3390/ph6101304

Crandall, I., Charuk, J., & Kain, K. C. (2000). Nonylphenolethoxylates as malarial chloroquine resistance reversal agents. *Antimicrob Agents Chemother*, *44*(9), 2431–4. https://doi.org/10.1128/AAC.44.9.2431-2434.2000

D 'alessandro, U., Hill, J., Tarning, J., Pell, C., Webster, J., Gutman, J., & Sevene, E. (2018). Treatment of uncomplicated and severe malaria during pregnancy. *Lancet Infect Dis*, *2*(18). https://doi.org/10.1016/S1473-3099(18)30065-3

Danker, T., & Möller, C. (2014). Early identification of hERG liability in drug discovery programs by automated patch clamp. *Front Pharmacol*, *5*(203). https://doi.org/10.3389/fphar.2014.00203

da Silva, R., & Hochman, G. (2011). A method called Pinotti: medicated salt, malaria, and international health (1952-1960). *Hist Cienc Saude Manguinhos*, *18*(2), 519–543.

Davey, D. G., & Robertson, G. I. (1957). Experiments with antimalarial drugs in man. IV. An experiment to investigate the prophylactic value of proguanil against a strain of *Plasmodium falciparum* known to be resistant to therapeutic treatment. *Trans R Soc Trop Med Hyg*, *51*(5), 463–6.

Delfino, R. T., Instituto Militar de Engenharia Brazil, R. de J., Santos-Filho, O. A., Instituto Militar de Engenharia Brazil, R. de J., Figueroa-Villar, J. D., & Instituto Militar de Engenharia Brazil, R. de J. (2002). Type 2 antifolates in the chemotherapy of falciparum malaria. *J Braz Chem Soc*, *13*(6), 727–41. https://doi.org/10.1590/S0103-50532002000600003

Deloron, P., Bertin, G., Briand, V., Massougbodji, A., & Cot, M. (2010). Sulfadoxine/Pyrimethamine Intermittent Preventive Treatment for Malaria during Pregnancy. *Emerg Infect Dis*, *16*(11), 1666–70. https://doi.org/10.3201/eid1611.101064

Delves, M., Plouffe, D., Scheurer, C., Meister, S., Wittlin, S., Winzeler, E. A., … Leroy, D. (2012). The activities of current antimalarial drugs on the life cycle stages of *Plasmodium*: A comparative study with human and rodent parasites. *PLoS Med*, *9*(2), e1001169. https://doi.org/10.1371/journal.pmed.1001169

Desai, S. A., McCleskey, E. W., Schlesinger, P. H., & Krogstad, D. J. (1996). A novel pathway for Ca++ entry into *Plasmodium falciparum*-infected blood cells. *Am J Trop Med Hyg*, *54*(5), 464–70.

Desgrouas, C., Dormoi, J., Chapus, C., Ollivier, E., Parzy, D., & Taudon, N. (2014). *In vitro* and *in vivo* combination of cepharanthine with anti-malarial drugs. *Malar J*, *13*(90). https://doi.org/10.1186/1475-2875-13-90

Djimde, A., Doumbo, O. K., Cortese, J. F., Kayentao, K., Doumbo, S., Diourte, Y., … Plowe, C. V. (2001). A molecular marker for chloroquine-resistant falciparum malaria. *N Engl J Med*, *344*(4), 257–63. https://doi.org/10.1056/nejm200101253440403

Docampo, R., & Moreno, S. N. J. (2013). Calcium in malaria parasites. In P. G. Kremsner & S. Krishna (Eds.), *Encyclopedia of Malaria*. New York: Springer. https://doi.org/10.1007/978-1-4614-8757-9_54-1

Drew, R. D., & Beeson, J. G. (2015). PfRH5 as a candidate vaccine for *Plasmodium falciparum* malaria. *Trends Parasitol*, *31*(3), 87–88. https://doi.org/10.1016/j.pt.2015.02.001

Dunachie, S., Berthoud, T., Hill, A. V, & Fletcher, H. A. (2015). Transcriptional changes induced by candidate malaria vaccines and correlation with protection against malaria in a human challenge model. *Vaccine, 33*(40), 5321-31. https://doi.org/10.1016/j.vaccine.2015.07.087

Duraisingh, M. T., & Cowman, A. F. (2005). Contribution of the pfmdr1 gene to antimalarial drug-resistance. *Acta Trop*, *94*(3), 181–90. https://doi.org/10.1016/j.actatropica.2005.04.008

Dvorin, J. D., Martyn, D. C., Patel, S. D., Grimley, J. S., Collins, C. R., Hopp, C. S., … Duraisingh, M. T. (2010). A plant-like kinase in *Plasmodium falciparum* regulates parasite egress from erythrocytes. *Science*, *328*(5980), 910–2. https://doi.org/10.1126/science.1188191

Eastman, R. T., & Fidock, D. A. (2009). Artemisinin-based combination therapies: a vital tool in efforts to eliminate malaria. *Nat Rev Microbiol*, *7*(12), 864–74. https://doi.org/10.1038/nrmicro2239

Eastman, R. T., Khine, P., Huang, R., Thomas, C. J., & Su, X. (2016). *Pf*CRT and *Pf*MDR1 modulate interactions of artemisinin derivatives and ion channel blockers. *Sci Rep*, *6*, 25379. https://doi.org/10.1038/srep25379

Ekins, S., Williams, A. J., Krasowski, M. D., & Freundlich, J. S. (2011). *In silico* repositioning of approved drugs for rare and neglected diseases. *Drug Discov Today*, *16*(7–8), 298–310. https://doi.org/10.1016/j.drudis.2011.02.016

Eksi, S., & Williamson, K. C. (2011). Protein targeting to the parasitophorous vacuole membrane of *Plasmodium falciparum*. *Eukaryot Cell*, *10*(6), 744–52. https://doi.org/10.1128/ec.00008-11

Elandalloussi, L. M., & Smith, P. J. (2002). Preparation of pure and intact *Plasmodium falciparum* plasma membrane vesicles and partial characterisation of the plasma membrane ATPase. *Malaria J*, *1*, 6. https://doi.org/10.1186/1475-2875-1-6

El Hage, S., Ane, M., Stigliani, J. L., Marjorie, M., Vial, H., Baziard-Mouysset, G., & Payard, M. (2009). Synthesis and antimalarial activity of new atovaquone derivatives. *Eur J Med Chem*, *44*(11), 4778–82. https://doi.org/10.1016/j.ejmech.2009.07.021

Engel, L. W., & Straus, S. E. (2002). Development of therapeutics: opportunities within complementary and alternative medicine. *Nat Rev Drug Discov*, *1*(3), 229–37. https://doi.org/10.1038/nrd750

Enomoto, M., Kawazu, S., Kawai, S., Furuyama, W., Ikegami, T., Watanabe, J., & Mikoshiba, K. (2012). Blockage of spontaneous Ca^{2+} oscillation causes cell death in intraerythrocitic *Plasmodium falciparum. PLoS One*, *7*(7), e39499. https://doi.org/10.1371/journal.pone.0039499

Ertel, E. A., Campbell, K. P., Harpold, M. M., Hofmann, F., Mori, Y., Perez-Reyes, E., … Catterall, W. A. (2000). Nomenclature of voltage-gated calcium channels. *Neuron*, *25*(3), 533–5. https://doi.org/10.1080/13518040701205365

Eugene-Ezebilo, D. N., & Ezebilo, E. E. (2014). Malaria infection in children in tropical rainforest: assessments by women of Ugbowo Community in Benin City, Nigeria. *Asian Pac J Trop Med*, *7S1*, S97–S103. https://doi.org/10.1016/s1995-7645(14)60212-1

Fan, J. S., & Palade, P. (2002). Effects of FPL 64176 on Ca transients in voltage-clamped rat venticular myocytes. *Br J Pharmacol*, *135*(6), 1495–504. https://doi.org/10.1038/sj.bjp.0704598

Fan, Y. L., Cheng, X. W., Wu, J. B., Liu, M., Zhang, F. Z., Xu, Z., & Feng, L. S. (2018). Antiplasmodial and antimalarial activities of quinolone derivatives: An overview. *Eur J Med Chem*, *146*, 1–14. https://doi.org/10.1016/j.ejmech.2018.01.039

Farrow, R. E., Green, J., Katsimitsoulia, Z., Taylor, W. R., Holder, A. A., & Molloy, J. E. (2011). The mechanism of erythrocyte invasion by the malarial parasite, *Plasmodium falciparum*. *Semin Cell Dev Biol*, *22*(9), 953–60. https://doi.org/10.1016/j.semcdb.2011.09.022

Fatih, F. A., Siner, A., Ahmed, A., Woon, L. C., Craig, A. G., Singh, B., Krishna, S., & Cox-Singh, J. (2012). Cytoadherence and virulence - The case of *Plasmodium knowlesi* malaria. *Malaria J*, 11, 33. https://doi.org/10.1186/1475-2875-11-33.

FDA. (2018). The drug development process - Step 3: clinical research. Retrieved February 6, 2018, from http://www.fda.gov/ForPatients/Approvals/Drugs/ucm405622.htm

Feng, J. Y., Ly, J. K., Myrick, F., Goodman, D., White, K. L., Svarovskaia, E. S., … Miller, M. D. (2009). The triple combination of tenofovir, emtricitabine and efavirenz shows synergistic anti-HIV-1 activity *in vitro*: a mechanism of action study. *Retrovirology*, *6*, 44. https://doi.org/10.1186/1742-4690-6-44

Fenichel, R. R., Malik, M., Antzelevitch, C., Sanguinetti, M. C., Roden, D. M., Priori, S. G., … Cantilena, L. (2004). Drug-induced Torsade de Pointes and implications for drug development. *J Cardiovasc Electrophysiol*, *15*(4), 475–95. https://doi.org/10.1046/j.1540-8167.2004.03534.x

Fernando, S. D., Rodrigo, C., & Rajapakse, S. (2011a). Chemoprophylaxis in malaria: drugs, evidence of efficacy and costs. *Asian Pac J Trop Med*, *4*(4), 330–6. https://doi.org/10.1016/s1995-7645(11)60098-9

Fernando, S. D., Rodrigo, C., & Rajapakse, S. (2011b). Primaquine in vivax malaria: an update and review on management issues. *Malar J*, *10*, 351. https://doi.org/10.1186/1475-2875-10-351

Ficker, E., Kuryshev, Y. A., Dennis, A. T., Obejero-Paz, C., Wang, L., Hawryluk, P., … Brown, A. M. (2004). Mechanisms of arsenic-induced prolongation of cardiac repolarization. *Mol Pharmacol*, *66*, 33–44. https://doi.org/10.1124/mol.66.1.33

Fivelman, Q. L., Adagu, I. S., & Warhurst, D. C. (2004). Modified fixed-ratio isobologram method for studying *in vitro* interactions between atovaquone and proguanil or dihydroartemisinin against drug-resistant strains of *Plasmodium falciparum*. *Antimicrob Agents Chemother*, *48*(11), 4097–102. https://doi.org/10.1128/AAC.48.11.4097-4102.2004

Fivelman, Q. L., Butcher, G. A., Adagu, I. S., Warhurst, D. C., & Pasvol, G. (2002). Malarone treatment failure and *in vitro* confirmation of resistance of *Plasmodium falciparum* isolate from Lagos, Nigeria. *Malar J*, *1*. https://doi.org/10.1186/1475-2875-1-1

Flannery, E. L., Chatterjee, A. K., & Winzeler, E. A. (2013). Antimalarial drug discovery: approaches and progress towards new medicines. *Nat. Rev. Microbiol*, *11*(12), 849–62. https://doi.org/10.1038/nrmicro3138

Fleckenstein, A. (1983). History of calcium antagonists. *Circ Res*, *52*(2 Pt 2), 13-6.

Flynn, J. T., & Pasko, D. A. (2000). Calcium channel blockers: Pharmacology and place in therapy of pediatric hypertension. *Pediatr Nephrol*, *15*(3–4), 302–16. https://doi.org/10.1007/s004670000480

Fong, K. Y., Sandlin, R. D., & Wright, D. W. (2015). Identification of beta-hematin inhibitors in the MMV Malaria Box. *Int J Parasitol Drugs Drug Resist*, *5*(3), 84–91. https://doi.org/10.1016/j.ijpddr.2015.05.003

Foucquier, J., & Guedj, M. (2015). Analysis of drug combinations: current methodological landscape. *Pharmacol Res Perspect.*, *3*(3), e00149. https://doi.org/10.1002/prp2.149

Furuyama, W., Enomoto, M., Mossaad, E., Kawai, S., Mikoshiba, K., & Kawazu, S. (2014). An interplay between 2 signaling pathways: melatonin-cAMP and IP3-Ca2+ signaling pathways control intraerythrocytic development of the malaria parasite *Plasmodium falciparum*. *Biochem Biophys Res Commun*, *446*, 125–31. https://doi.org/10.1016/j.bbrc.2014.02.070

Gamo, F. J. (2014). Antimalarial drug resistance: new treatments options for *Plasmodium*. *Drug Discov Today*, *11*, 81–8. https://doi.org/10.1016/j.ddtec.2014.03.002

Garcia, C. R., Dluzewski, A. R., Catalani, L. H., Burting, R., Hoyland, J., & Mason, W. T. (1996). Calcium homeostasis in intraerythrocytic malaria parasites. *Eur J Cell Biol*, *71*(4), 409–13.

Gazarini, M. L., & Garcia, C. R. S. (2004). The malaria parasite mitochondrion senses cytosolic Ca^{2+} fluctuations. *Biochem Biophys Res Commun*, *321*, 138–44. https://doi.org/10.1016/j.bbrc.2004.06.141

Gazarini, M. L., Thomas, A. P., Pozzan, T., & Garcia, C. R. (2003). Calcium signaling in a low calcium environment: how the intracellular malaria parasite solves the problem. *J Cell Biol*, *161*, 103–10. https://doi.org/10.1083/jcb.200212130

Gbotosho, G., Happi, C., Sijuade, A., Ogundahunsi, O., Sowunmi, A., & Oduola, A. (2008). Comparative study of interactions between chloroquine and chlorpheniramine or promethazine. *Ann Trop Med Parsitol*, *102*, 3–9. https://doi.org/10.1179/136485908X252179

Gelb, M. H. (2007). Drug discovery for malaria: a very challenging and timely endeavor. *Curr Opin Chem Biol*, *11*(4), 440–5. https://doi.org/10.1016/j.cbpa.2007.05.038

Gellis, A., Primas, N., Hutter, S., Lanzada, G., Remusat, V., Verhaeghe, P., … Azas, N. (2016). Looking for new antiplasmodial quinazolines: DMAP-catalyzed synthesis of 4-benzyloxy- and 4-aryloxy-2-trichloromethylquinazolines and their *in vitro* evaluation toward *Plasmodium falciparum*. *Eur J Med Chem*, *119*, 34–44. https://doi.org/10.1016/j.ejmech.2016.04.059

Giao, P. T., Binh, T. Q., Kager, P. A., Long, H. P., Van Thang, N., Van Nam, N., & de Vries, P. J. (2001). Artemisinin for treatment of uncomplicated falciparum malaria: is there a place for monotherapy? *Am J Trop Med Hyg*, *65*(6), 690–5.

Greenwood, B. M. (2008). Control to elimination: implications for malaria research. *Trends Parasitol*, *24*(10), 449–454. https://doi.org/10.1016/j.pt.2008.07.002

Gregson, A., & Plowe, C. V. (2005). Mechanisms of resistance of malaria parasites to antifolates. *Pharmacol Rev*, *57*, 117–45. https://doi.org/10.1124/pr.57.1.4

Grienberger, C., & Konnerth, A. (2012). Imaging calcium in neurons. *Neuron*, *73*(5), 862–85. https://doi.org/10.1016/j.neuron.2012.02.011

Grimberg, B. T. (2011). Methodology and application of flow cytometry for investigation of human malaria parasites. *J Immunol Methods*, *367*(1–2), 1–16. https://doi.org/10.1016/j.jim.2011.01.015

Grimberg, B., Erickson, J., Sramkoski, R., Jacobberger, J., & Zimmerman, P. A. (2008). Monitoring *Plasmodium falciparum* growth and development by UV flow cytometry using an optimized Hoechst-thiazole orange staining strategy. *Cytometry A*, *73*(6), 546–54. https://doi.org/10.1002/cyto.a.20541.

Gorka, A. P., Jacobs, L. M., & Roepe, P. D. (2013). Cytostatic versus cytocidal profiling of quinoline drug combinations via modified fixed-ratio isobologram analysis. *Malar J*, *12*(332). https://doi.org/10.1186/1475-2875-12-332

Grynkiewicz, G., Poenie, M., & Tsien, R. Y. (1985). A new generation of Ca^{2+} indicators with greatly impoved fluorescence properties. *J Biol Chem*, *260*(6), 3440–50.

Guiguemde, W. A., Shelat, A. A., Garcia-Bustos, J. F., Diagana, T. T., Gamo, F. J., & Guy, R. K. (2012). Global phenotypic screening for antimalarials. *Chem Biol*, *19*, 116–29. https://doi.org/10.1016/j.chembiol.2012.01.004

Guo, Z. (2016). Artemisinin anti-malarial drugs in China. *Acta Pharmaceutica Sinica B*, *6*(2), 115–24. https://doi.org/10.1016/j.apsb.2016.01.008

Guth, B. D., & Rast, G. (2010). Dealing with hERG liabilities early: Diverse approaches to an important goal in drug development. *Br J Pharmacol*, *159*, 22–4. https://doi.org/10.1111/j.1476-5381.2009.00265

Haldar, K. & Mohandas, N. (2009). Malaria, erythrocytic infection, and anemia. *Hematology Am Soc of Hematol Educ Program*, 2009, 87–93. https://doi.org/10.1182/asheducation-2009.1.87.

Harasym, T. O., Liboiron, B. D., & D, M. L. (2010). Drug ratio-dependent antagonism: a new category of multidrug resistance and strategies for its circumvention. *Methods Mol Biol.*, *596*, 291–323. https://doi.org/10.1007/978-1-60761-416-6_13

Harvey, K. L., Gilson, P. R., & Crabb, B. S. (2012). A model for the progression of receptor-ligand interactions during erythrocyte invasion by *Plasmodium falciparum*. *Int J Parasitol*, *42*(6), 567–73. https://doi.org/10.1016/j.ijpara.2012.02.011

Hemingway, J., Shretta, R., Wells, T. N. C., Bell, D., Djimdé, A. A., Achee, N., & Qi, G. (2016). Tools and strategies for malaria control and elimination: what do we need to achieve a grand convergence in malaria? *PLoS Biology*, *14*(3), 1–14. https://doi.org/10.1371/journal.pbio.1002380

Henneberger, R., Birch, D., Bergquist, P., Walter, M., & Anitori, R. P. (2011). The fluorescent dyes TO-PRO-3 and TOTO-3 iodide allow detection of microbial cells in soil samples without interference from background fluorescence. *Biotechniques*, *51*(3), 190–2. https://doi.org/10.2144/000113736

Hetterich, N., Lauterbach, E., Stürer, A., Weilemann, L. S., & Lauterbach, M. (2014). Toxicity of antihypertensives in unintentional poisoning of young children. *J Emerg Med*, *47*(2), 155–62. https://doi.org/10.1016/j.jemermed.2014.02.006

Hidaka, H., & Hartshorne, D. J. (1985). *Calmodulin antagonists and cellular physiology*. Florida: Academic Press, Inc.

Hoeflich, K. P., & Ikura, M. (2002). Calmodulin in action: diversity in target recognition and activation mechanisms. *Cell*, *108*(6), 739–42.

Holder, J. C., Goodman, E. D., Kikushima, K., Gatti, M., Marziale, A. N., & Stoltz, B. M. (2015). Synthesis of diverse β-quaternary ketones via palladium-catalyzed asymmetric conjugate addition of arylboronic acids to cyclic enones. *Tetrahedron*, *71*(35), 1–12. https://doi.org/10.1016/j.tet.2014.11.048

Hong, S. C. (2013). Malaria: an early indicator of later disease and work level. *J Health Econ*, *32*(3), 612–632. https://doi.org/10.1016/j.jhealeco.2013.03.004

Huang, X., & Aslanian, R. G. (2012). *Case studies in modern drug discovery and development*. John Wiley & Sons.

Hughes, J. P., Rees, S., Kalindjian, S. B., & Philpott, K. L. (2011). Principles of early drug discovery. *Br J Pharmacol*, *162*(6), 1239–49. https://doi.org/10.1111/j.1476-5381.2010.01127.x

Ismail, H. M., Barton, V., Phanchana, M., Charoensutthivarakul, S., Wong, M. H. L., Hemingway, J., … Ward, S. A. (2016). Artemisinin activity-based probes identify multiple molecular targets within the asexual stage of the malaria parasites *Plasmodium falciparum* 3D7. *Proc Natl Acad Sci U S A*, *113*(8), 2080–5. https://doi.org/10.1073/pnas.1600459113

Iqbal, M. S., Siddiqui, A. A., Alam, A., Goyal, M., Banerjee, C., Sarkar, S., … Bandyopadhyay, U. (2016). Expression, purification and characterization of *Plasmodium falciparum* vacuolar protein sorting 29. *Protein Expr Purif*, *120*, 7–15. https://doi.org/10.1016/j.pep.2015.12.004

Jaeger, S., Igea, A., Arroyo, R., Alcalde, V., Canovas, B., Orozco, M., … Aloy, P. (2017). Quantification of pathway cross-talk reveals novel synergistic drug combinations for breast cancer. *Cancer Res*, *77*(2), 459–69. https://doi.org/10.1158/0008-5472.CAN-16-0097

Jambou, R., Martinelli, A., Pinto, J., Gribaldo, S., Legrand, E., Niang, M., … Cravo, P. (2010). Geographic structuring of the *Plasmodium falciparum* sarco(endo)plasmic reticulum Ca^{2+} ATPase (PfSERCA) gene diversity. *PLoS ONE*, *5*(2), e9424. https://doi.org/10.1371/journal.pone.0009424

Jean, S., Zapata-Jenks, M. A., Farley, J. M., Tracy, E., & Mayer, D. C. (2014). *Plasmodium falciparum* double C2 domain protein, *Pf*DOC2, binds to calcium when associated with membranes. *Exp Parasitol*, *144*, 91–5. https://doi.org/10.1016/j.exppara.2014.06.015

Jin, G., & Wong, S. T. (2014). Toward better drug repositioning: prioritizing and integrating existing methods into efficient pipelines. *Drug Discov Today*, *19*(5), 637–44. https://doi.org/10.1016/j.drudis.2013.11.005

Johansen, L. M., Dewald, L. E., Shoemaker, C. J., Hoffstrom, B. G., Lear-rooney, C. M., Stossel, A., … Olinger, G. G. (2015). A screen of approved drugs and molecular probes identifies therapeutics with anti-Ebola virus activity. *Sci Transl Med*, *7*(290), 290ra89. https://doi.org/10.1126/scitranslmed.aaa5597

Johnson, J. D., Dennull, R. A., Gerena, L., Lopez-Sanchez, M., Roncal, N. E., & Waters, N. C. (2007). Assessment and continued validation of the malaria SYBR green I-based fluorescence assay for use in malaria drug screening. *Antimicrob Agents Chemother*, *51*(6), 1926–33. https://doi.org/10.1128/aac.01607-06

Jones, C. O., & Williams, H. A. (2004). The social burden of malaria: what are we measuring? *Am J Trop Med Hyg*, *71*(2 Suppl), 156–61.

Jones, R. A., Panda, S. S., & Hall, C. D. (2015). Quinine conjugates and quinine analogues as potential antimalarial agents. *Eur J Med Chem*, *97*, 335–55. https://doi.org/10.1016/j.ejmech.2015.02.002

Juge, N., Moriyama, S., Miyaji, T., Kawakami, M., Iwai, H., Fukui, T., … Moriyama, Y. (2015). *Plasmodium falciparum* chloroquine resistance transporter is a H^+-coupled polyspecific nutrient and drug exporter. *Proc Natl Acad Sci U S A*, *112*(11), 3356–61. https://doi.org/10.1073/pnas.1417102112

Kai, O. K. & Roberts, D. J. (2008). The pathophysiology of malarial anaemia: Where have all the red cells gone? *BMC Med*, 6, 24. https://doi.org/10.1186/1741-7015-6-24.

Kamal, T., Green, T. N., Morel-Kopp, M. C., Ward, C. M., McGregor, A. L., McGlashan, S. R., … Kalev-Zylinska, M. L. (2015). Inhibition of glutamate regulated calcium entry into leukemic megakaryoblasts reduces cell proliferation and supports differentiation. *Cell Signal*, *27*(9), 1860–72. https://doi.org/10.1016/j.cellsig.2015.05.004

Karl, S., Wong, R. P., St Pierre, T. G., & Davis, T. M. (2009). A comparative study of a flow-cytometry-based assessment of *in vitro Plasmodium falciparum* drug sensitivity. *Malar J*, *8*, 294. https://doi.org/10.1186/1475-2875-8-294

Karpf, M. (2011). *From milligrams to tons: the importance of synthesis and process research in the development of new drugs*. In: Shioiri, T., Izawa, K. & Konoike, T. Eds. *Pharmaceutical Process Chemistry*. Weinheim: Wiley-VCH Verlag GmBH & Co. https://doi.org/10.1002/9783527633678.ch1

Karunamoorthi, K. (2014). Malaria vaccine: a future hope to curtail the global malaria burden. *Int J Prev Med*, *5*(5), 529–538.

Kate, L., Gokarna, V., Borhade, V., Prabhu, P., Deshpande, V., Pathak, S., … Patravale, V. (2016). Bioavailability enhancement of atovaquone using hot melt extrusion technology. *Eur J Pharm Sci*, *86*, 103–14. https://doi.org/http://dx.doi.org/10.1016/j.ejps.2016.03.005

Kato, K., Sudo, A., Kobayashi, K., Tohya, Y., & Akashi, H. (2008). Characterization of *Plasmodium falciparum* protein kinase 2. *Mol Biochem Parasitol*, *162*, 87–95. https://doi.org/10.1016/j.molbiopara.2008.07.007

Katzung, B. G., Masters, S. B., & Trevor, A. J. (2012). *Basic and clinical pharmacology*. 12th ed. New York: McGraw-Hill Medical.

Kenakin, T. (2014). *A pharmacology primer: techniques for more effective and strategic drug discovery.* 4th ed, Elsevier, San Diego. https://doi.org/10.1016/B978-0-12-407663-1.00011-9

Kimura, M., Yamaguchi, Y., Takada, S., & Tanabe, K. (1993). Cloning of a $Ca^{(2+)}$-ATPase gene of *Plasmodium falciparum* and comparison with vertebrate $Ca^{(2+)}$-ATPases. *J Cell Sci*, *104*(Pt 4), 1129–36.

Kirk, K. (2001). Membrane transport in the malaria-infected erythrocyte. *Physiol Rev*, *81*(2), 495–537.

Klonis, N., Creek, D. J., & Tilley, L. (2013). Iron and heme metabolism in *Plasmodium falciparum* and the mechanism of action of artemisinins. *Curr Opin Microbiol*, *16*(6), 722–27. https://doi.org/10.1016/j.mib.2013.07.005

Klonis, N., Crespo-Ortiz, M. P., Bottova, I., Abu-Bakar, N., Kenny, S., Rosenthal, P. J., & Tilley, L. (2011). Artemisinin activity against *Plasmodium falciparum* requires hemoglobin uptake and digestion. *Proc Natl Acad Sci U S A*, *108*(28), 11405–10. https://doi.org/10.1073/pnas.1104063108

Kotturi, M. F., Carlow, D. a, Lee, J. C., Ziltener, H. J., & Jefferies, W. a. (2003). Identification and functional characterization of voltage-dependent calcium channels in T lymphocytes. *J Biol Chem*, *278*(47), 46949–60. https://doi.org/10.1074/jbc.M309268200

Kramer, I. M. (2015). Intracellular calcium. In: Audet, J. Ed. *Signal transduction.* 3rd ed. Academic Press, London. https://doi.org/10.1002/9781118675410

Kreitzer, A. C., Gee, K. R., Archer, E. A., & Regehr, W. G. (2000). Monitoring presynaptic calcium dynamics in projection fibers by *in vivo* loading of a novel calcium indicator. *Neuron*, *27*, 25–32. https://doi.org/10.1016/S0896-6273(00)00006-4

Krishna, S., Uhlemann, A. C., & Haynes, R. K. (2004). Artemisinins: mechanisms of action and potential for resistance. *Drug Resist Updat*, *7*(4–5), 233–44. https://doi.org/10.1016/j.drup.2004.07.001

Krudsood, S., Wilairatana, P., Tangpukdee, N., Chalermrut, K., Srivilairit, S., Thanachartwet, V., … Looareesuwan, S. (2006). Safety and tolerability of elubaquine (bulaquine, CDRI 80/53) for treatment of *Plasmidium vivax* malaria in Thailand. *Korean J Parasitol*, *44*(3), 221–8. https://doi.org/10.3347/kjp.2006.44.3.221

Krungkrai, J., Imprasittichai, W., Otjungreed, S., Pongsabut, S., & Krungkrai, S. (2010). Artemisinin resistance or tolerance in human malaria patients, *Asian Pac J Trop Dis, 3*(9), 748–53. https://doi.org/10.1016/S1995-7645(10)60180-0

Kublin, J. G., Dzinjalamala, F. K., Kamwendo, D. D., Malkin, E. M., Cortese, J. F., Martino, L. M., … Plowe, C. V. (2002). Molecular markers for failure of sulfadoxine-pyrimethamine and chlorproguanil-dapsone treatment of *Plasmodium falciparum* malaria. *J Infec Dis*, *185*(3), 380–8. https://doi.org/10.1086/338566

Kuhlmann, F. M., & Fleckenstein, J. M. (2017). Antiparasitic agents. In: Cohen, J., Powderly, W. G. & Opal, S. M. eds. *Infectious Diseases*. Elsevier, London. https://doi.org/10.1016/B978-0-7020-6285-8.00157-X

Kyle, D. E., Oduola, A. M. J., Martin, S. K., & Milhous, W. K. (1990). *Plasmodium falciparum*: Modulation by calcium antagonists of resistance to chloroquine, desethylchloroquine, quinine, and quinidine *in vitro*. *Trans R Soc Trop Med Hyg*, *84*(4), 474–8. https://doi.org/10.1016/0035-9203(90)90004-X

Lakshmanan, V., Bray, P. G., Verdier-Pinard, D., Johnson, D. J., Horrocks, P., Muhle, R. A., … Fidock, D. A. (2005). A critical role for PfCRT K76T in *Plasmodium falciparum* verapamil-reversible chloroquine resistance. *EMBO J, 24*(13), 2294–305. https://doi.org/10.1038/sj.emboj.7600681

Lane, C. F. (1975). Sodium cyanoborohydride - a highly selective reducing agent for organic functional groups. *Synthesis*, *1975*(3), 135–46. https://doi.org/10.1055/s-1975-23685

Lang, T., & Greenwood, B. (2003). The development of lapdap, an affordable new treatment for malaria. *Lancet Infect Dis*, *3*(3), 162–8. https://doi.org/10.1016/S1473-3099(03)00547-4

Le Manach, C., Scheurer, C., Sax, S., Schleiferböck, S., Cabrera, D. G., Younis, Y., … Wittlin, S. (2013). Fast *in vitro* methods to determine the speed of action and the stage-specificity of anti-malarials in *Plasmodium falciparum*. *Malar J*, *12*, 424–8. https://doi.org/10.1186/1475-2875-12-424

Leroy, D., Campo, B., Ding, X. C., Burrows, J. N., & Cherbuin, S. (2014). Defining the biology component of the drug discovery strategy for malaria eradication. *Trends Parasitol*, *30*(10), 478–490. https://doi.org/10.1016/j.pt.2014.07.004

Leybaert, L., Sneyd, J., & Sanderson, M. J. (1998). A simple method for high temporal resolution calcium imaging with dual excitation dyes. *Biophys J*, *75*(4), 2025–9. https://doi.org/10.1016/S0006-3495(98)77644-1

Li, Y. (2012). Qinghaosu (artemisinin): Chemistry and pharmacology. *Acta Pharmacol Sin*, *33*(9), 1141–6. https://doi.org/10.1038/aps.2012.104

Lin, M. C., & Jan, C. R. (2002). The anti-anginal drug fendiline elevates cytosolic Ca($^{2+}$) in rabbit corneal epithelial cells. *Life Sci*, *71*(9), 1071–9.

Litwack, G. (2008). *Folic Acid and Folates.* 1st ed. Academic Press.

Liu, C. (2017). Discovery and development of artemisinin and related compounds. *Chinese Herbal Medicines*, *9*(2), 101–14. https://doi.org/10.1016/S1674-6384(17)60084-4

Lo, Y., Cheng, J., Wang, J., & Lee, K. (2001). Fendiline-induced Ca^{2+} movement in A10 smooth muscle cells. *Chin J Physiol*, *44*(1), 19–24.

Lock, J. T., Parker, I., & Smith, I. (2015). A comparison of fluorescent Ca^{2+} indicators for imaging local Ca^{2+} signals in cultured cells. *Cell Calcium*, *58*(6), 638–48. https://doi.org/10.1016/j.ceca.2015.10.003

Looger, L. L., & Griesbeck, O. (2012). Genetically encoded neural activity indicators. *Curr Opin Neurobiol*, *22*, 18–23. https://doi.org/10.1016/j.conb.2011.10.024

Lotharius, J., Gamo-Benito, F. J., Angulo-Barturen, I., Clark, J., Connelly, M., Ferrer-Bazaga, S., … Wells, T. (2014). Repositioning: the fast track to new anti-malarial medicines? *Malar J*, *13*, 143. https://doi.org/10.1186/1475-2875-13-143

Lourido, S., & Moreno, S. N. (2015). The calcium signaling toolkit of the Apicomplexan parasites *Toxoplasma gondii* and *Plasmodium* spp. *Cell Calcium*, *57*(3), 186–93. https://doi.org/10.1016/j.ceca.2014.12.010

Lu, X., & Lin, S. (2005). Pd (II)-Bipyridine catalyzed conjugate addition of arylboronic acid to α,β-unsaturated carbonyl compounds. *J Org Chem*, *70*(23), 9651–3. https://doi.org/10.1021/jo051561h

Luckhoff, A., Bohnert, M., & Busse, R. (1991). Effects of the calmodulin antagonists fendiline and calmidazolium on aggregation, secretion of ATP, and internal calcium in washed human platelets. *Naunyn Schmiedebergs Arch Pharmacol*, *343*(1), 96–101.

Mahmoudi, N., de Julián-Ortiz, J.-V., Ciceron, L., Gálvez, J., Mazier, D., Danis, M., … García-Domenech, R. (2006). Identification of new antimalarial drugs by linear discriminant analysis and topological virtual screening. *J Antimicrob Chemother*, *57*(3), 489–97. https://doi.org/10.1093/jac/dki470

Makhro, A., Hänggi, P., Goede, J. S., Wang, J., Brüggemann, A., Gassmann, M., … Bogdanova, A. (2013). *N*-methyl-*D*-aspartate receptors in human erythroid precursor cells and in circulating red blood cells contribute to the intracellular calcium regulation. *Am J Physiol Cell Physiol*, *305*(11), C1123-38. https://doi.org/10.1152/ajpcell.00031.2013

Makhro, A., Kaestner, L., & Bogdanova, A. (2017). NMDA receptor activity in circulating red blood cells: methods of detection. *Methods Mol Biol.*, *1677*, 265–82. https://doi.org/10.1007/978-1-4939-7321-7_15

Marcus, B. (2009). *Malaria* (*deadly disease and epidemics)*. 2nd ed. Chelsea House Pub.

Martin, S., Oduola, A., & Milhous, W. (1987). Reversal of chloroquine resistance in *Plasmodium falciparum* by verapamil. *Science*, *235*(4791), 899–901. https://doi.org/10.1126/science.3544220

Martiney, J. A., Cerami, A., & Slater, A. F. G. (1995). Verapamil reversal of chloroquine resistance in the malaria parasite *Plasmodium falciparum* is specific for resistant parasites and independent of the weak base effect. *J Biol Chem*, *270*(38), 22393–8. https://doi.org/10.1074/jbc.270.38.22393

Mata-Cantero, L., Lafuente, M. J., Sanz, L., & Rodriguez, M. S. (2014). Magnetic isolation of *Plasmodium falciparum* schizonts iRBCs to generate a high parasitaemia and synchronized *in vitro* culture. *Malaria J*, *13*, 112. https://doi.org/10.1186/1475-2875-13-112

Matthews, H., Deakin, J., Rajab, M., Idris-usman, M., & Nirmalan, N. J. (2017). Investigating antimalarial drug interactions of emetine dihydrochloride hydrate using CalcuSyn-based

interactivity calculations. *PLoS ONE*, *12*(3), e0173303. https://doi.org/10.1371/journal.pone.0173303

Matthews, H., Usman-Idris, M., Khan, F., Read, M., & Nirmalan, N. (2013). Drug repositioning as a route to anti-malarial drug discovery: preliminary investigation of the *in vitro* anti-malarial efficacy of emetine dihydrochloride hydrate. *Malar J*, *12*, 359. https://doi.org/10.1186/1475-2875-12-359

Matthews, H. (2015). *Fast tracking antimalarial drug discovery through repositioning*. PhD thesis. University of Salford.

Medhi, B., Patyar, S., Rao, R. S., Byrav Ds, P., & Prakash, A. (2009). Pharmacokinetic and toxicological profile of artemisinin compounds: An update. *Pharmacology*, *84*(6), 323–32. https://doi.org/10.1159/000252658

Meldolesi, J. (2004). The development of Ca^{2+} indicators: A breakthrough in pharmacological research. *Trends Pharmacol Sci*, *25*(4), 172–4. https://doi.org/10.1016/j.tips.2004.02.004

Meletiadis, J., Pournaras, S., Roilides, E., & Walsh, T. J. (2010). Defining fractional inhibitory concentration index cutoffs for additive interactions based on self-drug additive combinations, Monte Carlo simulation analysis, and *in vitro-in vivo* correlation data for antifungal drug combinations against *Aspergillus fumi*. *Antimicrob Agents Chemother*, *54*(2), 602–9. https://doi.org/10.1128/AAC.00999-09

Menezes, C. M., Kirchgatter, K., Di Santi, S. M., Savalli, C., Monteiro, F. G., Paula, G. A., & Ferreira, E. I. (2003). *In vitro* evaluation of verapamil and other modulating agents in Brazilian chloroquine-resistant *Plasmodium falciparum* isolates. *Rev Soc Bras Med Trop*, *36*(1), 5–9.

Miao, J., & Cui, L. (2011). Rapid isolation of single malaria parasite-infected red blood cells by cell sorting. *Nature Protocols*, *6*(2), 140–6. https://doi.org/10.1038/nprot.2010.185.

Michiels, C. F., Van Hove, C. E., Martinet, W., De Meyer, G. R., & Fransen, P. (2014). L-type Ca^{2+} channel blockers inhibit the window contraction of mouse aorta segments with high affinity. *Eur J Pharmacol*, *738*, 170–8. https://doi.org/10.1016/j.ejphar.2014.05.036

Milardi, D., & Pappalardo, M. (2015). Molecular dynamics: new advances in drug discovery. *Eur J Med Chem*, *91*, 1–3. https://doi.org/10.1016/j.ejmech.2014.10.078

Mishra, M., Mishra, V. K., Kashaw, V., Iyer, A. K., & Kashaw, S. K. (2017). Comprehensive review on various strategies for antimalarial drug discovery. *Eur J Med Chem*, *125*, 1300–20. https://doi.org/10.1016/j.ejmech.2016.11.025

Miyawaki, A., Llopis, J., Heim, R., McCaffery, J. M., Adams, J. A., Ikura, M., & Tsien, R. Y. (1997). Fluorescent indicators for Ca^{2+} based on green fluorescent proteins and calmodulin. *Nature*, *388*(6645), 882–7.

Mojab, F. (2012). Antimalarial natural products: a review. *Avicenna J Phytomed, 2*(2), 52–62.

Moorthy, V., Reed, Z., Smith, P. G., & Efficacy, W. H. O. S. G. on M. of M. V. (2007). Measurement of malaria vaccine efficacy in phase III trials: report of a WHO consultation. *Vaccine, 25*(28), 5115–23. https://doi.org/10.1016/j.vaccine.2007.01.085

Moreno, S. N. J., Ayong, L., & Pace, D. A. (2011). Calcium storage and function in apicomplexan parasites. *Essays Biochem*, *51*, 97–110. https://doi.org/10.1042/bse0510097

Moreno, S. N. J., & Docampo, R. (2003). Calcium regulation in protozoan parasites. *Curr Opin Microbiol*, *6*(4), 359–64. https://doi.org/10.1016/S1369-5274(03)00091-2

Mott, B. T., Eastman, R. T., Guha, R., Sherlach, K. S., Siriwardana, A., Shinn, P., … Thomas, C. J. (2015). High-throughput matrix screening identifies synergistic and antagonistic antimalarial drug combinations. *Sci Rep.*, *5*, 13891. https://doi.org/10.1038/srep13891

Mu, J., Ferdig, M., Feng, X., Joy, D., Duan, J., Furuya, T., … Su, X. (2003). Multiple transporters associated with malaria parasite responses to chloroquine and quinine. *Mol Microbiol*, *49*(4), 977–89.

Müller, I. B., & Hyde, J. E. (2010). Antimalarial drugs: modes of action and mechanisms of parasite resistance. *Future Microbiol*, *5*(12), 166–8. https://doi.org/10.2217/fmb.10.136

Müller, I. B., & Hyde, J. E. (2013). Folate metabolism in human malaria parasites--75 years on. *Mol Biochem Parasitol*, *188*, 63–77. https://doi.org/10.1016/j.molbiopara.2013.02.008

Mushtaque, M., & Shahjahan. (2015). Reemergence of chloroquine (CQ) analogs as multi-targeting antimalarial agents: A review. *Eur J Med Chem, 90*, 280–95. https://doi.org/10.1016/j.ejmech.2014.11.022

Myint, H. Y., Berman, J., Walker, L., Pybus, B., Melendez, V., Baird, J. K., & Ohrt, C. (2011). Review: Improving the therapeutic index of 8-aminoquinolines by the use of drug combinations: review

of the literature and proposal for future investigations. *Am J Trop Med Hyg*, *85*(6), 1010–4. https://doi.org/10.4269/ajtmh.2011.11-0498

Nathan, S., Pepine, C. J., & Bakris, G. L. (2005). Calcium antagonists: effects on cardio-renal risk in hypertensive patients. *Hypertension*, *46*(4), 637–42. https://doi.org/10.1161/01.HYP.0000184541.24700.c7

Nawrath, H., Klein, G., Rupp, J., Wegener, J. W., & Shainberg, A. (1998). Open State Block by Fendiline of L-Type Ca++ Channels in Ventricular Myocytes from Rat Heart. *J Pharmacol Exp Ther*, *285*(2), 546–52.

Ndong, I. C., Reenen, M. V, Boakye, D. A., Mbacham, W. F., & Grobler, A. F. (2015). Trends in malaria case management following changes in the treatment policy to artemisinin combination therapy at the Mbakong Health Centre, Cameroon 2006-2012: A retrospective study. *Acta Trop*, *150*, 100–6. https://doi.org/10.1016/j.actatropica.2015.06.014

Nelson, D. L., & Cox, M. M. (2008). *Lehninger Principles of Biochemistry.* 5th ed. New York: W. H. Freeman and Company.

Newman, D. J., & Cragg, G. M. (2016). Natural products as sources of new drugs from 1981 to 2014. *J Nat Prod*, *79*(3), 629–61. https://doi.org/10.1021/acs.jnatprod.5b01055

Noedl, H. (2009). ABC - antibiotics-based combinations for the treatment of severe malaria? *Trends Parasitol*, *25*(12), 540–4. https://doi.org/10.1016/j.pt.2009.09.001

Nogawa, H., & Kawai, T. (2014). hERG trafficking inhibition in drug-induced lethal cardiac arrhythmia. *Eur J Pharmacol*, *741*, 336–9. https://doi.org/10.1016/j.ejphar.2014.06.044

Noori, S., Hassan, Z. M., Rezaei, B., Rustaiyan, A., Habibi, Z., & Fallahian, F. (2008). Artemisinin can inhibit the calmodulin-mediated activation of phosphodiesterase in comparison with Cyclosporin A. *Int Immunopharmacol*, *8*(13–14), 1744–7. https://doi.org/10.1016/j.intimp.2008.08.012

Noori, S., Hassan, Z. M., Taghikhani, M., Rezaei, B., & Habibi, Z. (2010). Dihydroartemisinin can inhibit calmodulin, calmodulin-dependent phosphodiesterase activity and stimulate cellular immune responses. *Int Immunopharmacol*, *10*(2), 213–7. https://doi.org/10.1016/j.intimp.2009.11.002

Nunomura, W., Takakuwa, Y., Parra, M., Conboy, J. G., & Mohandas, N. (2000). Ca^{2+}-dependent and Ca^{2+}-independent calmodulin binding sites in erythrocyte protein 4.1. *J Biol Chem*, *275*(9), 6360–7. https://doi.org/10.1074/jbc.275.9.6360

Nyunt, M. H., Hlaing, T., Oo, H. W., Tin-Oo, L. L., Phway, H. P., Wang, B., … Han, E. T. (2015). Molecular assessment of artemisinin resistance markers, polymorphisms in the k13 propeller, and a multidrug-resistance gene in the eastern and western border areas of Myanmar. *Clin Infect Dis*, *60*(8), 1208–15. https://doi.org/10.1093/cid/ciu1160

Nzila, A. (2006a). Inhibitors of *de novo* folate enzymes in *Plasmodium falciparum. Drug Discov Today*, *11*(19–20), 939–44. https://doi.org/10.1016/j.drudis.2006.08.003

Nzila, A. (2006b). The past, present and future of antifolates in the treatment of *Plasmodium falciparum* infection. *J Antimicrob Chemother*, *57*(6), 1043–54. https://doi.org/10.1093/jac/dkl104

Nzila, A., Ma, Z., & Chibale, K. (2011). Drug repositioning in the treatment of malaria and TB. *Future Med Chem*, *3*(11), 1413–26. https://doi.org/10.4155/fmc.11.95

Nzila, A., Ward, S. A, Marsh, K., Sims, P. F. G., & Hyde, J. E. (2005). Comparative folate metabolism in humans and malaria parasites (part I): pointers for malaria treatment from cancer chemotherapy. *Trends Parasitol*, *21*(6), 292–8. https://doi.org/10.1016/j.pt.2005.04.002.

Obonyo, C. O., & Juma, E. A. (2012). Clindamycin plus quinine for treating uncomplicated falciparum malaria: a systematic review and meta-analysis. *Malar J*, *11,* 2. https://doi.org/10.1186/1475-2875-11-2

Oduola, A. M., Sowunmi, A., Milhous, W. K., Brewer, T. G., Kyle, D. E., Gerena, L., … Schuster, B. G. (1998). *In vitro* and *in vivo* reversal of chloroquine resistance in *Plasmodium falciparum* with promethazine. *Am J Trop Med Hyg, 58*(5), 625-9.

Oduola, O. O., Happi, T. C., Gbotosho, G. O., Ogundahunsi, O. A. T., Falade, C. O., Akinboye, D. O., … Oduola, A. M. J. (2004). *Plasmodium berghei*: efficacy and safety of combinations of chloroquine and promethazine in chloroquine resistant infections in gravid mice. *Afr J Med Sci*, *33*, 77–81.

Ohrt, C., Willingmyre, G. D., Lee, P., Milhous, W., & Knirsch, C. (2002). Assessment of azithromycin in combination with other antimalarial drugs against *Plasmodium falciparum in vitro*. *Antimicrob Agents Chemother*, *46*(8), 2518–24. https://doi.org/10.1128/AAC.46.8.2518

Ojurongbe, O., Ogungbamigbe, T. O., Fagbenro-Beyioku, A. F., Fendel, R., Kremsner, P. G., & Kun, J. F. (2007). Rapid detection of *Pf*crt and *Pf*mdr1 mutations in *Plasmodium falciparum* isolates by FRET and *in vivo* response to chloroquine among children from Osogbo, Nigeria. *Malar J*, *11*(6), 41. https://doi.org/10.1186/1475-2875-6-41

Oliva, C. F., Vreysen, M. J., Dupe, S., Lees, R. S., Gilles, J. R., Gouagna, L. C., & Chhem, R. (2014). Current status and future challenges for controlling malaria with the sterile insect technique: technical and social perspectives. *Acta Trop*, *132 Suppl*, S130-9. https://doi.org/10.1016/j.actatropica.2013.11.019

Olliaro, P. L., Haynes, R. K., Meunier, B., & Yuthavong, Y. (2001). Possible modes of action of the artemisinin-type compounds. *Trends Parasitol*, *17*(3), 122–6.

Olson, K. R., Erdman, A. R., Woolf, A. D., Scharman, E. J., Christianson, G., Caravati, E. M., … Troutman, W. G. (2005). Calcium channel blocker ingestion: an evidence-based consensus guideline for out-of-hospital management. *Clinical Toxicology*, *43*(7), 797–822. https://doi.org/10.1080/15563650500357404

Ortega, C., Ortolano, S., & Carafoli, E. (2007). The plasma membrane calcium pump, *41*, 179–97. https://doi.org/10.1016/S0167-7306(06)41007-3

Otoguro, K., Ishiyama, A., Ui, H., Kobayashi, M., Manabe, C., Yan, G., … Omura, S. (2002). *In vitro* and *in vivo* antimalarial activities of the monoglycoside polyether antibiotic, K-41 against drug resistant strains of *Plasmodia*. *J Antibiot*, *55*(9), 832–4.

Ovadje, L., & Nriagu, J. (2011). Malaria as an environmental disease. In *Encyclopedia of Environmental Health* (pp. 558–67). https://doi.org/10.1016/B978-0-444-52272-6.00735-2

Pace, D. A., McKnight, C. A., Liu, J., Jimenez, V., & Moreno, S. N. J. (2014). Calcium entry in *Toxoplasma gondii* and its enhancing effect of invasion-linked traits. *J Biol Chem*, *289*(28), 19637–47. https://doi.org/10.1074/jbc.M114.565390

Paloque, L., Ramadani, A. P., Mercereau-Puijalon, O., Augereau, J. M., & Benoit-Vical, F. (2016). *Plasmodium falciparum*: multifaceted resistance to artemisinins. *Malar J*, *15*, 149. https://doi.org/10.1186/s12936-016-1206-9

Pandey, K., Ferreira, P. E., Ishikawa, T., Nagai, T., Kaneko, O., & Yahata, K. (2016). Ca^{2+} monitoring in *Plasmodium falciparum* using the yellow cameleon-Nano biosensor. *Scientific Reports*, *6*, 23454. https://doi.org/10.1038/srep23454

Paredes, R. M., Etzler, J. C., Watts, L. T., & Lechleiter, J. D. (2009). Chemical calcium indicators. *Methods*, *46*(3), 143–51. https://doi.org/10.1016/j.ymeth.2008.09.025

Patel, S., & Docampo, R. (2010). Acidic calcium stores open for business: expanding the potential for intracelluar Ca^{2+} signaling. *Trends Cell Biol*, *20*(5), 277–86. https://doi.org/10.1016/j.tcb.2010.02.003.

Patrick, G. L. (2015). *An introduction to drug synthesis.* 1st ed. Oxford University Press.

Payne, D. (1988). Did medicated salt hasten the spread of chloroquine resistance in *Plasmodium falciparum? Parasitol Today*, *4*(4), 112–5.

Pereira, M. R., Henrich, P. P., Sidhu, A. B. S., Johnson, D., Hardink, J., Van Deusen, J., … Fidock, D. A. (2011). *In vivo* and *in vitro* antimalarial properties of azithromycin-chloroquine combinations that include the resistance reversal agent amlodipine. *Antimicrob Agents Chemother*, *55*(7), 3115–24. https://doi.org/10.1128/AAC.01566-10

Perlmann, K., & Troye-Blomberg, M. (2002). *Malaria Immunolog*. Basel: Karger Medical and Scientific Publishers.

Persechini, A., Lynch, J. A., & Romoser, V. A. (1997). Novel fluorescent indicator proteins for monitoring free intracellular Ca^{2+}. *Cell Calcium*, *22*(3), 209–16. https://doi.org/10.1016/S0143-4160(97)90014-2

Peters, J. U., Hert, J., Bissantz, C., Hillebrecht, A., Gerebtzoff, G., Bendels, S., … Kansy, M. (2012). Can we discover pharmacological promiscuity early in the drug discovery process? *Drug Discov Today*, *17*(7–8), 325–35. https://doi.org/10.1016/j.drudis.2012.01.001

Peyton, D. H. (2012). Reversed Chloroquine Molecules as a Strategy to Overcome Resistance in Malaria. *Curr Top Med Chem.*, *12*(5), 400–7. https://doi.org/10.2174/156802612799362968

Phillips, R. E. & Pasvol, G. (1992). Anaemia of *Plasmodium falciparum* malaria. *Baillieres Clin Haematol*, 5(2), 315–30.

Pinder, M., Jawara, M., Jarju, L. B., Salami, K., Jeffries, D., Adiamoh, M., … Lindsay, S. W. (2015). Efficacy of indoor residual spraying with dichlorodiphenyltrichloroethane against malaria in Gambian communities with high usage of long-lasting insecticidal mosquito nets: a cluster-randomised controlled trial. *Lancet*, *385*(9976), 1436–1446. https://doi.org/10.1016/s0140-6736(14)61007-2

Plowe, C. V. (2009). The evolution of drug-resistant malaria. *Trans R Soc Trop Med Hyg*, *103*, S11-14. https://doi.org/10.1016/j.trstmh.2008.11.002

Ploypradith, P. (2004). Development of artemisinin and its structurally simplified trioxane derivatives as antimalarial drugs. *Acta Trop*, *89*(3), 329–42.

Pollack, H. (1928). Micrurgical Studies in Cell Physiology: Vi. Calcium Ions in Living Protoplasm. *J Gen Physiol*, *11*(5), 539–45. https://doi.org/10.1085/jgp.11.5.539

Pollard, C. E., Abi Gerges, N., Bridgland-Taylor, M. H., Easter, A., Hammond, T. G., & Valentin, J. P. (2010). An introduction to QT interval prolongation and non-clinical approaches to assessing and reducing risk. *Br J Pharmacol*, *159*, 12–21. https://doi.org/10.1111/j.1476-5381.2009.00207

Pradines, B., Alibert-Franco, S., Houdoin, C., Mosnier, J., Santelli-Rouvier, C., Papa, V., … Parzy, D. (2002a). *In vitro* reversal of chloroquine resistance in *Plasmodium falciparum* with dihydroethanoanthracene derivatives. *Am J Trop Med Hyg*, *66*(6), 661–6.

Pradines, B., Alibert, S., Houdoin, C., Santelli-Rouvier, C., Mosnier, J., Fusai, T., … Parzy, D. (2002b). *In vitro* increase in chloroquine accumulation induced by dihydroethano- and ethenoanthracene derivatives in *Plasmodium falciparum*-parasitized erythrocytes. *Antimicrob Agents Chemother*, *46*(7), 2061–8. https://doi.org/10.1128/AAC.46.7.2061-2068.2002

Preiser, P., Kaviratne, M., Khan, S., Bannister, L., & Jarra, W. (2000). The apical organelles of malaria merozoites: host cell selection, invasion, host immunity and immune evasion. *Microbes Infect*, *2*(12), 1461–77.

Priest, B. T., Bell, I. M., & Garcia, M. L. (2008). Role of hERG potassium channel assays in drug development. *Channels (Austin)*, *2*(2), 87–93. https://doi.org/10.4161/chan.2.2.6004

Prole, D. L., & Taylor, C. W. (2011). Identification of intracellular and plasma membrane calcium channel homologues in pathogenic parasites. *PLoS ONE*, *6*(10), e26218. https://doi.org/10.1371/journal.pone.0026218

Pronker, E. S., Weenen, T. C., Commandeur, H. R., Osterhaus, A. D., & Claassen, H. J. (2011). The gold industry standard for risk and cost of drug and vaccine development revisited. *Vaccine*, *29*(35), 5846–9. https://doi.org/10.1016/j.vaccine.2011.06.051

Proschak, E. (2013). Reconsidering the drug discovery pipeline for designed multitarget drugs. *Drug Discov Today*, *18*(23–24), 1129–30. https://doi.org/10.1016/j.drudis.2013.08.019

Przygodzki, T., Sokal, A., & Bryszewska, M. (2005). Calcium ionophore A23187 action on cardiac myocytes is accompanied by enhanced production of reactive oxygen species. *Biochim Biophys Acta*, *1740*(3), 481–8. https://doi.org/10.1016/j.bbadis.2005.03.009

Pulcini, S., Staines, H. M., Lee, A. H., Shafik, S. H., Bouyer, G., Moore, C. M., … Krishna, S. (2015). Mutations in the *Plasmodium falciparum* chloroquine resistance transporter, *Pf*CRT, enlarge the parasite's food vacuole and alter drug sensitivities. *Sci Rep*, *5*, 14552. https://doi.org/10.1038/srep14552

Quinzii, C., & Hirano, M. (2010). Coenzyme Q and Mitochondrial Disease. *Dev Disabil Res Rev*, *16*(2), 183–8. https://doi.org/10.1002/ddrr.108

Rahman, N. N. (1997). Evaluation of the sensitivity *in vitro* of *Plasmodium falciparum* and *in vivo* of *Plasmodium chabaudi* malaria to various drugs and their combinations. *Med J Malaysia*, *52*(4), 390-8.

Raj, D. K., Mu, J., Jiang, H., Kabat, J., Singh, S., Sullivan, M., … Su, X. Z. (2009). Disruption of a *Plasmodium falciparum* multidrug resistance-associated protein (*Pf*MRP) alters its fitness and transport of antimalarial drugs and glutathione. *J Biol Chem*, *284*(12), 7687–96. https://doi.org/10.1074/jbc.M806944200

Rajamani, S., Eckhardt, L. L., Valdivia, C. R., Klemens, C. A., Gillman, B. M., Anderson, C. L., … January, C. T. (2006). Drug-induced long QT syndrome: hERG K^+ channel block and disruption of protein trafficking by fluoxetine and norfluoxetine. *Br J Pharmacol*, *149*(5), 481–9. https://doi.org/10.1038/sj.bjp.0706892

Ramos Júnior, W. M., Sardinha, J. F., Costa, M. R., Santana, M. S., Alecrim, M. G., & Lacerda, M. V. (2010). Clinical aspects of hemolysis in patients with *P. vivax* malaria treated with primaquine, in the Brazilian Amazon. *Braz J Infect Dis*, *14*(4), 410–2.

Rampe, D., & Lacerda, A. E. (1991). A new site for the activation of cardiac calcium channels defined by the nondihydropyridine FPL 64176. *J Pharmacol Exp Ther*, *259*(3), 982–7.

Rathod, P. K., McErlean, T., & Lee, P. C. (1997). Variations in frequencies of drug resistance in *Plasmodium falciparum*. *Proc Natl Acad Sci U S A*, *94*(17), 9389–93. https://doi.org/10.1073/pnas.94.17.9389

Read, M. & Hyde, J. E. (1993). Simple *in vitro* cultivation of the malaria parasite *Plasmodium falciparum* (erythrocytic stages) suitable for large scale preparations. *Methods Mol Biol,* 21, 43-55. https://doi.org/10.1385/0-89603-239-6:43

Reimão, J. Q., Mesquita, J. T., Ferreira, D. D., & Tempone, A. G. (2016). Investigation of calcium channel blockers as antiprotozoal agents and their interference in the metabolism of *Leishmania (L.) infantum. Evid Based Complement Alternat Med*, *2016*, 1523691. https://doi.org/10.1155/2016/1523691

Rick, N. G. (2009). *Drugs; From Discovery to Approval* (2nd ed.). New Jersey: John Wiley & Sons.

Ridley, D. B. (2017). Priorities for the priority review voucher. *Am J Trop Med Hyg, 96*, 14-15. https://doi.org/10.4269/ajtmh.16-0600

Riffel, A, Medina, L. F., Stefani, V., Santos, R. C., Bizani, D., & Brandelli, A. (2002). *In vitro* antimicrobial activity of a new series of 1,4-naphthoquinones. *Braz J Med Biol Res*, *35*(7), 811–8.

Ritz, B., Rhodes, S. L., Qian, L., Schernhammer, E., Olsen, J., & Friis, S. (2010). L-type calcium channel blockers and Parkinson's disease in Denmark. *Ann Neurol*, *67*(5), 600–6. https://doi.org/10.1002/ana.21937

Robson, K. J., Gamble, Y., & Acharya, K. R. (1993). Molecular modelling of malaria calmodulin suggests that it is not a suitable target for novel antimalarials. *Philos Trans R Soc Lond B Biol Sci*, *340*(1291), 39–53. https://doi.org/10.1098/rstb.1993.0047

Rohrbach, P., Friedrich, O., Hentschel, J., Plattner, H., Fink, R. H., & Lanzer, M. (2005). Quantitative calcium measurements in subcellular compartments of *Plasmodium falciparum*-infected erythrocytes. *J Biol Chem*, *280*(30), 27960–9. https://doi.org/10.1074/jbc.M500777200

Rohrbach, P., Sanchez, C. P., Hayton, K., Friedrich, O., Patel, J., Sidhu, A. B. S., … Lanzer, M. (2006). Genetic linkage of *pfmdr1* with food vacuolar solute import in *Plasmodium falciparum*. *EMBO J*, *25*(13), 3000–11. https://doi.org/10.1038/sj.emboj.7601203

Romero, P. J., & Romero, E. A. (1999). The role of calcium metabolism in human red blood cell ageing: a proposal. *Blood Cells Mol Dis*, *25*, 9–19. https://doi.org/10.1006/bcmd.1999.0222

Romero, P. J., Romero, E. A., Mateu, D., Hernandez, C., & Fernandez, I. (2006). Voltage-dependent calcium channels in young and old human red cells. *Cell Biochem Biophys*, *46*(3), 265–76. https://doi.org/10.1385/cbb:46:3:265

Rosenthal, P. J. (2003). Antimalarial drug discovery: old and new approaches. *J Exp Biol*, *206*(Pt 21), 3735–44.

Rossington, S. (2004). *The development of enantioselective methodology involving chiral base systems*. PhD Thesis. University of Salford.

Rotmann, A., Sanchez, C., Guiguemde, A., Rohrbach, P., Dave, A., Bakouh, N., … Lanzer, M. (2010). PfCHA is a mitochondrial divalent cation/H+ antiporter in *Plasmodium falciparum*. *Mol Microbiol*, *76*(6), 1591–606. https://doi.org/10.1111/j.1365-2958.2010.07187.x

RTS/S Clinical Trials Partnership. (2015). Efficacy and safety of RTS,S/AS01 malaria vaccine with or without a booster dose in infants and children in Africa: final results of a phase 3, individually randomised, controlled trial. *Lancet*, *386*(9988), 31–45. https://doi.org/10.1016/s0140-6736(15)60721-8

Sadava, D., Hillis, D. M., Heller, H. C., & Berenbaum, M. R. (2011). *Life; the science of biology*. W. H. Freeman and Company.

Sahney, S. (2006). A review of calcium channel antagonists in the treatment of pediatric hypertension. *Paediatr Drugs*, *8*(6), 357–73.

Said, S., Jeffes, E. W. B., & Weinstein, G. D. (1997). Methotrexate. *Clinics in Dermatology*, *15*(5), 781–97. https://doi.org/10.1016/S0738-081X(97)00014-X

Saifi, M. A., Beg, T., Harrath, A. H., Altayalan, F. S. H., & Al Quraishy, S. (2013). Antimalarial drugs: mode of action and status of resistance. *Afr J Pharm Pharmacol*, *7*(5), 148–56. https://doi.org/10.5897/AJPPX12.015

Salcedo-Sora, J. E., & Ward, S. A. (2013). The folate metabolic network of Falciparum malaria. *Mol Biochem Parasitol*, *188*, 51–62. https://doi.org/10.1016/j.molbiopara.2013.02.003

Samantaray, S., Correia, J., Garelnabi, M., Voelz, K., May, R., & Hall, R. (2016). Novel cell-based *in vitro* screen to identify small-molecule inhibitors against intracellular replication of *Cryptococcus neoformans* in macrophages. *Int J Antimicrob Agents*, *48*, 69–77. https://doi.org/10.1016/j.ijantimicag.2016.04.018

Sanguinetti, M. C., Jiang, C., Curran, M. E., & Keating, M. T. (1995). A mechanistic link between an inherited and an acquired cardiac arrhythmia: *HERG* encodes the I_{Kr} potassium channel. *Cell*, *81*(2), 299–307. https://doi.org/10.1016/0092-8674(95)90340-2

Satheesh, N. J., & Büsselberg, D. (2015). The role of intracellular calcium for the development and treatment of neuroblastoma. *Cancers (Basel)*, *7*(2), 828–48. https://doi.org/10.3390/cancers7020811

Saucerman, J. J., & Bers, D. M. (2012). Calmodulin binding proteins provide domains of local Ca^{2+} signaling in cardiac myocytes. *J Mol Cell Cardiol*, *52*(2), 312–6. https://doi.org/10.1016/j.yjmcc.2011.06.005

Saxena, S., Pant, N., Jain, D. C., & Bhakuni, R. S. (2003). Antimalarial agents from plant sources. *Curr Sci, 85*(9), 1314-29.

Sanz, L. M., Crespo, B., De-Cozar, C., Ding, X. C., Llergo, J. L., Burrows, J. N., … Gamo, F. J. (2012). *P. falciparum in vitro* killing rates allow to discriminate between different antimalarial mode-of-action. *PLoS ONE*, *7*(2), e30949. https://doi.org/10.1371/journal.pone.0030949

Scheibel, L. W., Colombani, P. M., Hess, A. D., Aikawa, M., Atkinson, C. T., & Milhous, W. K. (1987). Calcium and calmodulin antagonists inhibit human malaria parasites (*Plasmodium falciparum*): implications for drug design. *Proc Natl Acad Sci U S A*, *84*(20), 7310–4.

Severini, C., & Menegon, M. (2015). Resistance to antimalarial drugs: an endless world war against *Plasmodium* that we risk losing. *J Glob Antimicrob Resist*, *3*(2), 58–63. https://doi.org/10.1016/j.jgar.2015.02.002

Shimomura, O., & Johnson, F. H. (1969). Properties of the bioluminescent protein aequorin. *Biochemistry*, *8*(10), 3991–7. https://doi.org/10.1021/bi00838a015

Sherlach, K. S., & Roepe, P. D. (2014). Drug resistance associated membrane proteins. *Front Physiol*, *5*(108). https://doi.org/10.3389/fphys.2014.00108

Silver, R. A., Whitaker, M., & Bolsover, S. R. (1992). Intracellular ion imaging using fluorescent dyes - artifacts and limits to resolution. *Pflugers Arch*, *420*(5–6), 595–602. https://doi.org/10.1007/BF00374639

Silverman, R. B., & Holladay, M. W. (2014). *The organic chemistry of drug design and drug action.* 3rd ed. Academic Press. Retrieved May 26, 2016, <http://store.elsevier.com/The-Organic-Chemistry-of-Drug-Design-and-Drug-Action/Richard-B_-Silverman/isbn-9780123820310/>.

Singh, B., & Daneshvar, C. (2013). Human infections and detection of *Plasmodium knowlesi*. *Clin Microbiol Rev*, *26*(2), 165–84. https://doi.org/10.1128/CMR.00079-12

Siregar, J. E., Kurisu, G., Kobayashi, T., Matsuzaki, M., Sakamoto, K., Mi-ichi, F., … Kita, K. (2015). Direct evidence for the atovaquone action on the *Plasmodium* cytochrome bc_1 complex. *Parasitol Int*, *64*(3), 295–300. https://doi.org/10.1016/j.parint.2014.09.011

Slater, L. M., Murray, S. L., Wetzel, M. W., Wisdom, R. M., & DuVall, E. M. (1982). Verapamil restoration of daunorubicin responsiveness in daunorubicin- resistant Ehrlich ascites carcinoma. *J Clin Invest*, *70*(5), 1131–4.

Smilkstein, M., Sriwilaijaroen, N., Kelly, J. X., Wilairat, P., & Riscoe, M. (2004). Simple and inexpensive fluorescence-based technique for high-throughput antimalarial drug screening. *Antimicrob Agents Chemother*, *48*(5), 1803–6.

Smith, C. G. (1992). *The Process of New Drug Discovery and Development*. CRC Press LLC.

Smith, P., Blunt, N., Wiltshire, M., Hoy, T., Teesdale-Spittle, P., Craven, M., … Patterson, L. (2000). Characteristics of a novel deep red/infrared fluorescent cell-permeant DNA probe, DRAQ5, in intact human cells analyzed by flow cytometry, confocal and multiphoton microscopy. *Cytometry*, *40*(4), 280–91.

Smyth, J. T., Hwang, S. Y., Tomita, T., DeHaven, W. I., Mercer, J. C., & Putney, J. W. (2010). Activation and regulation of store-operated calcium entry. *J Cell Mol Med*, *14*(10), 2337–49. https://doi.org/10.1111/j.1582-4934.2010.01168.x

Sowunmi, A., Oduola, A., Ogundahunsi, O., Falade, C., Gbotosho, G., & Salako, L. (1997). Enhanced efficacy of chloroquine-chlorpheniramine combination in acute uncomplicated falciparum malaria in children. *Trans R Soc Trop Med Hyg*, *91*, 63–7. https://doi.org/https://doi.org/10.1016/S0035-9203 (97)90399-0.

Strickland, G. T., & Hoffman, S. L. (1994). Strategies for the control of malaria. *Science & Medicine, 1*(3), 24-33.

Striessnig, J., Pinggera, A., Kaur, G., Bock, G., & Tuluc, P. (2014). L-type Ca^{2+} channels in heart and brain. *Wiley Interdiscip Rev Membr Transp Signal.*, *3*(2), 15–38. https://doi.org/10.1002/wmts.102

Sun, W., Sanderson, P., & Zheng, W. (2016). Drug combination therapy increases successful drug repositioning. *Drug Discov Today*, *21*(7), 1189–95. https://doi.org/10.1016/j.drudis.2016.05.015

Sun, W., Tanaka, T. Q., Magle, C. T., Huang, W., Southall, N., Huang, R., … Zheng, W. (2014). Chemical signatures and new drug targets for gametocytocidal drug development. *Sci Rep.*, *4*, 3743. https://doi.org/10.1038/srep03743

Sut, C., Tariket, S., Chou, M. L., Garraud, O., Laradi, S., Hamzeh-Cognasse, H., … Cognasse, F. (2017). Duration of red blood cell storage and inflammatory marker generation. *Blood Transfus*, *15*(2), 145–52. https://doi.org/10.2450/2017.0343-16

Sutherland, C. J. (2016). Persistent parasitism: the adaptive biology of Malariae and Ovale malaria. *Trends Parasitol*, *32*(10), 808–19. https://doi.org/10.1016/j.pt.2016.07.001

Sutherland, C. J., Laundy, M., Price, N., Burke, M., Fivelman, Q. L., Pasvol, G., … Chiodini, P. L. (2008). Mutations in the *Plasmodium falciparum* cytochrome b gene are associated with delayed parasite recrudescence in malaria patients treated with atovaquone-proguanil. *Malar J*, *7*, 20. https://doi.org/10.1186/1475-2875-7-240

Swulius, M. T., & Waxham, M. N. (2008). Ca^{2+}/Calmodulin-dependent Protein Kinases. *Cell Mol Life Sci*, *65*(17), 2637–57. https://doi.org/10.1007/s00018-008-8086-2

Tahar, R., Vivas, L., Basco, L., Thompson, E., Ibrahim, H., Boyer, J., & Nepveu, F. (2011). Indolone-N-oxide derivatives: *In vitro* activity against fresh clinical isolates of *Plasmodium falciparum*, stage specificity and *in vitro* interactions with established antimalarial drugs. *J Antimicrob Chemother*, *66*(11), 2566–72. https://doi.org/10.1093/jac/dkr320

Takamatsu, A., Ohkawara, B., Ito, M., Masuda, A., Sakai, T., Ishiguro, N., & Ohno, K. (2014). Verapamil protects against cartilage degradation in osteoarthritis by inhibiting Wnt/β-catenin signaling. *PLoS ONE, 9*(3), e92699. https://doi.org/10.1371/journal.pone.0092699

Takken, W., & Knols, B. G. (2009). Malaria vector control: current and future strategies. *Trends Parasitol*, *25*(3), 101–104. https://doi.org/10.1016/j.pt.2008.12.002

Talawanich, Y., Kamchonwongpaisan, S., Sirawaraporn, W., & Yuthavong, Y. (2015). Use of bacterial surrogates as a tool to explore antimalarial drug interaction: synergism between inhibitors of malarial dihydrofolate reductase and dihydropteroate synthase. *Acta Trop*, *149*, 64–9. https://doi.org/10.1016/j.actatropica.2015.05.011

Tallarida, R. J. (2012). Revisiting the isobole and related quantitative methods for assessing drug synergism. *J Pharmacol Exp Ther*, *342*, 2–8. https://doi.org/10.1124/jpet.112.193474

Talisuna, A. O., Noor, A. M., Okui, A. P., & Snow, R. W. (2015). The past, present and future use of epidemiological intelligence to plan malaria vector control and parasite prevention in Uganda. *Malar J*, *14*, 158. https://doi.org/info:pmid/25888989

Tan, K. R., Magill, A. J., Parise, M. E., & Arguin, P. M. (2011). Doxycycline for malaria chemoprophylaxis and treatment: report from the CDC expert meeting on malaria chemoprophylaxis. *Am J Trop Med Hyg*, *84*(4), 517–31. https://doi.org/10.4269/ajtmh.2011.10-0285

Tanabe, K., Izumo, A., Kato, M., Miki, A., & Doi, S. (1989). Stage-dependent inhibition of *Plasmodium falciparum* by potent Ca^{2+} and calmodulin modulators. *J Protozool*, *36*(2), 139–43.

Tanabe, K., Mikkelsen, R. B., & Wallach, F. H. (1982). Calcium transport of *Plasmodium chabaudi*-infected erythrocytes. *J Cell Biol*, *93*(3), 680–4.

Tang, L., Gamal El-Din, T. M., Swanson, T. M., Pryde, D. C., Scheuer, T., Zheng, N., & Caterrall, W. A. (2016). Structural basis for inhibition of a voltage-gated Ca^{2+} channel by Ca^{2+} antagonist drugs. *Nature*, *537*(7618), 117–21.

Terunuma, M., Vargas, K. J., Wilkins, M. E., Ramírez, O. A., Jaureguiberry-Bravo, M., Pangalos, M. N., … Couve, A. (2010). Prolonged activation of NMDA receptors promotes dephosphorylation and alters postendocytic sorting of GABAB receptors. *Proc Natl Acad Sci U S A*, *107*(31), 13918–23. https://doi.org/10.1073/pnas.1000853107

Tres Cantos Open Lab Foundation (2014). *Our Approach.* [ONLINE] Available at: http://www.openlabfoundation.org/ourapproach.html. [Accessed 5 June 2018].

Thomas, S. L., Egee, S., Lapaix, F., Kaestner, L., Staines, H. M., & Ellory, J. C. (2001). Malaria parasite *Plasmodium gallinaceum* up-regulates host red blood cell channels. *FEBS Lett*, *500*(1–2), 45–51.

Thomé, R., Lopes, S. C. P., Costa, F. T. M., & Verinaud, L. (2013). Chloroquine: Modes of action of an undervalued drug. *Immunol Lett*, *153*(1–2), 50–7. https://doi.org/10.1016/j.imlet.2013.07.004

Tilley, L., Straimer, J., Gnädig, N. F., Ralph, S. A., & Fidock, D. A. (2016). Artemisinin action and resistance in *Plasmodium falciparum*. *Trends Parasitol*, *32*(9), 682-96. https://doi.org/10.1016/j.pt.2016.05.010

Toutenhoofd, S. L., Foletti, D., Wicki, R., Rhyner, J. A., Garcia, F., Tolon, R., & Strehler, E. E. (1998). Characterization of the human CALM2 calmodulin gene and comparison of the transcriptional activity of CALM1, CALM2 and CALM3. *Cell Calcium*, *23*(5), 323–38.

Trampuz, A., Jereb, M., Muzlovic, I., & Prabhu, R. M. (2003). Clinical review: severe malaria. *Crit Care*, 7(4), 315–23. https://doi.org/10.1186/cc2183.

Tran, C. V, & Saier, M. H. J. (2004). The principal chloroquine resistance protein of *Plasmodium falciparum* is a member of the drug/metabolite transporter superfamily. *Microbiology*, *150* (Pt 1), 1-3. https://doi.org/10.1099/mic.0.26818-0

Tripathi, O., Schreibmayer, W., & Tritthart, H. A. (1993). Fendiline inhibits L-type calcium channels in guinea-pig ventricular myocytes: a whole-cell patch-clamp study. *Br J Pharmacol*, *108*(4), 865–9.

Tripathy, S., & Roy, S. (2014). A review of age-old antimalarial drug to combat malaria: efficacy up-gradation by nanotechnology based drug delivery. *Asian Pac J Trop Med*, *7*(9), 673–9. https://doi.org/10.1016/S1995-7645(14)60115-2

Tsien, R. Y. (1981). A non-disruptive technique for loading calcium buffers and indicators into cells. *Nature*, *290*(5806), 527–8. https://doi.org/10.1038/290527a0

Tsien, R. Y., & Barrett, C. F. (2005). A brief history of calcium channel discovery. In: Zamponi, G. W. Ed. *Voltage-gated calcium channels*. Boston, MA: Springer US.

Tsien, R. Y., Pozzan, T., & Rink, T. J. (1982). Calcium homeostasis in intact lymphocytes: cytoplasmatic free calcium monitored with a new, intracellularly trapped fluorescent indicator. *J Cell Biol*, *94*(2), 325–34.

Tsuruo, T., Lida, H., Tsukagoshi, S., & Sakurai, Y. (1981). Overcoming of vincristine resistance in p388 leukemia *in vivo* and *in vitro* through enhanced cytotoxicity of vincristine and vinblastine by verapamil. *Cancer Res*, *41*(5), 1967–72. https://doi.org/10.1007/s10853-010-4262-5

Tuikue, N. N., Moussilliou, A., Lavstsen, T., Kamaliddin, C., Jensen, A. T. R., Mama, A., … Deloron, P. (2017). Parasites Causing Cerebral *Falciparum* Malaria Bind Multiple Endothelial Receptors and Express EPCR and ICAM-1-Binding PfEMP1. *J Infect Dis*, 215(12), 1918–25. https://doi.org/10.1093/infdis/jix230

Tun, K. M., Imwong, M., Lwin, K. M., Win, A. A., Hlaing, T. M., Hlaing, T., … Woodrow, C. J. (2015). Spread of artemisinin-resistant *Plasmodium falciparum* in Myanmar: a cross-sectional survey of the K13 molecular marker. *Lancet Infect Dis*, *15*(4), 415–21. https://doi.org/10.1016/s1473-3099(15)70032-0

Urscher, M., Alisch, R., & Deponte, M. (2011). The glyoxalase system of malaria parasites--implications for cell biology and general glyoxalase research. *Semin Cell Dev Biol*, *22*(3), 262–70. https://doi.org/10.1016/j.semcdb.2011.02.003

Uyemura, S. A., Luo, S., Moreno, S. N. J., & Docampo, R. (2000). Oxidative phosphorylation, Ca(2+) transport, and fatty acid-induced uncoupling in malaria parasites mitochondria. *J Biol Chem*, *275*(13), 9709–15.

van den Berg, H., Zaim, M., Yadav, R. S., Soares, A., Ameneshewa, B., Mnzava, A., … Ejov, M. (2012). Global trends in the use of insecticides to control vector-borne diseases. *Environ Health Perspect.*, *120*(4), 577–82. https://doi.org/10.1289/ehp.1104340

van der Hoeven, D., Cho, K. J., Ma, X., Chigurupati, S., Parton, R. G., & Hancock, J. F. (2013). Fendiline inhibits K-Ras plasma membrane localization and blocks K-Ras signal transmission. *Mol Cell Biol*, *33*(2), 237–51. https://doi.org/10.1128/mcb.00884-12

Van Dyk, J. C., Bouwman, H., Barnhoorn, I. E., & Bornman, M. S. (2010). DDT contamination from indoor residual spraying for malaria control. *Sci Total Environ*, *408*(13), 2745–2752. https://doi.org/10.1016/j.scitotenv.2010.03.002

van Schalkwyk, D. A., & Egan, T. J. (2006). Quinoline-resistance reversing agents for the malaria parasite *Plasmodium falciparum*. *Drug Resist Updat*, *9*(4–5), 211–26. https://doi.org/10.1016/j.drup.2006.09.002

Vetter, S. W., & Leclerc, E. (2003). Novel aspects of calmodulin target recognition and activation. *Eur J Biochem*, *270*(3), 404–14.

Vines, A., McBean, G. J., & Blanco-Fernández, A. (2010). A flow-cytometric method for continuous measurement of intracellular Ca^{2+} concentration. *Cytometry A*, *77*(11), 1091–7. https://doi.org/10.1002/cyto.a.20974

Vivas, L., Rattray, L., Stewart, L., Bongard, E., Robinson, B. L., Peters, W., & Croft, S. L. (2008). Anti-malarial efficacy of pyronaridine and artesunate in combination *in vitro* and *in vivo*. *Acta Trop*, *105*(3), 222–8. https://doi.org/10.1016/j.actatropica.2007.12.005

Voigt, R. M., Riddle, J. L., & Napier, T. C. (2014). Effect of fendiline on the maintenance and expression of methamphetamine-induced conditioned place preference in Sprague-Dawley rats. *Psychopharmacology (Berl)*, *231*(9), 2019–29. https://doi.org/10.1007/s00213-013-3347-7

Wahlgren, M., & Perlmann, P. (2003). *Malaria: molecular and clinical aspects*. CRC Press.

Walker, N. F., Nadjm, B., & Whitty, C. J. M. (2018). Malaria. *Medicine*, *46*, 52–58. https://doi.org/10.1016/j.mpmed.2017.10.012

Waller, D. G., & Sampson, A. P. (2018). Chemotherapy of infections. In: *Medical pharmacology and therapeutics.* 5th ed. Elsevier, 581-629. https://doi.org/10.1016/B978-0-7020-7167-6.00051-8

Wang, J., Xu, C., Lun, Z. R., & Meshnick, S. R. (2017). Unpacking "Artemisinin Resistance." *Trends Pharmacol Sci*, *38*(6), 506–11. https://doi.org/10.1016/j.tips.2017.03.007

Wang, J., Zhang, C. J., Chia, W. N., Loh, C. C. Y., Li, Z., Lee, Y. M., … Lin, Q. (2015). Haem-activated promiscuous targeting of artemisinin in *Plasmodium falciparum*. *Nat Commun*, *6*, 10111. https://doi.org/10.1038/ncomms10111

Ward, G. E., Miller, L. H., & Dvorak, J. A. (1993). The origin of parasitophorous vacuole membrane lipids in malaria-infected erythrocytes. *J Cell Sci*, *106*, 237–48.

Ward, P., Equinet, L., Packer, J., & Doerig, C. (2004). Protein kinases of the human malaria parasite *Plasmodium falciparum*: the kinome of a divergent eukaryote. *BMC Genomics*, *5*, 79. https://doi.org/10.1186/1471-2164-5-79

Warsame, M., Wernsdorfer, W. H., & Björkman, A. (1992). Lack of effect of desipramine on the response falciparum malaria to chloroquine of patients with. *Trans R Soc Trop Med Hyg*, *86*(3), 235–6.

Wells, T. N. C., Huijsduijnen, R. H. Van, & Voorhis, W. C. Van. (2015). Malaria medicines: a glass half full? *Nat Rev Drug Discov*, *14*(6), 424–42. https://doi.org/10.1038/nrd4573

Wernsdorfer, W. H. (1994). Epidemiology of drug resistance in malaria. *Acta Trop*, *56*(2–3), 143–56.

Whitaker, M. (2010). Genetically-encoded probes for measurement of intracellular calcium. *Methods Cell Biol*, *99*, 153–82. https://doi.org/10.1016/B978-0-12-374841-6.00006-2

WHO. (2014). WHO | Factsheet on the World Malaria Report 2014. *WHO*. https://doi.org//entity/malaria/media/world_malaria_report_2014/en/index.html

WHO. (2015). *World Malaria Report 2015.* Retrieved from http://apps.who.int/iris/bitstream/10665/200018/1/9789241565158_eng.pdf?ua=1

WHO. (2017a). *Malaria vector control policy recommendations and their applicability to product evaluation*. Retrieved from http://apps.who.int/iris/bitstream/10665/255337/1/WHO-HTM-GMP-2017.12-eng.pdf?ua=1

WHO. (2017b). Update on the RTS,S Malaria Vaccine Implementation Programme. Retrieved from http://www.who.int/malaria/mpac/mpac-oct2017-rtss-implementation-update-session4.pdf

WHO. (2017c). *World Malaria Report 2017*. Retrieved from http://apps.who.int/iris/bitstream/10665/259492/1/9789241565523-eng.pdf?ua=1

WHO. (2018). Overview of malaria treatment. Retrieved February 5, 2018, from http://www.who.int/malaria/areas/treatment/overview/en/

Whyte, I., Buckley, N., & Dawson, A. (2016). Calcium channel blockers. *Medicine*, *44*(3), 148–50. https://doi.org/10.1016/j.mpmed.2015.12.029

Wilkinson, J. A., Rossington, S. B., Leonard, J., & Hussain, N. (2004). Asymmetric alkylation of diarylmethane derivatives. Improved results using methoxyethoxy substituent. *Tetrahedron Lett*, *45*(28), 5481–3. https://doi.org/10.1016/j.tetlet.2004.05.058

Wilkinson, J., Foretia, D., Rossington, S., Heagerty, A., Leonard, J., Hussain, N., & Austin, C. (2007a). 2'-hydroxy-fendiline analogues as potent relaxers of isolated arteries. *Eur J Pharmacol*, *561*(1–3), 160–3. https://doi.org/10.1016/j.ejphar.2007.01.039

Wilkinson, J., Rossington, S., Coe, N. A., Hirst, N., McGown, A. T., Leonard, J., & Hussain, N. (2007b). Synthesis and evaluation of 2'-Substituted fendiline analogues as antileukemics. *Lett Drug Des Discov*, *4*(4), 246–83. https://doi.org/info:doi/10.2174/157018007784620068

Wilkinson, J., Rossington, S., Ducki, S., Leonard, J., & Hussain, N. (2006). Asymmetric alkylation of diarylmethane derivatives. *Tetrahedron*, *62*(8), 1833–44. https://doi.org/10.1016/j.tet.2005.11.044

Williams, M. (2011). Qualitative pharmacology in a quantitative world: diminishing value in the drug discovery process. *Curr Opin Pharmacol*, *11*(5), 496–500. https://doi.org/10.1016/j.coph.2011.04.002

Wirjanata, G., Handayuni, I., Prayoga, P., Leonardo, L., Apriyanti, D., Trianty, L., … Marfurt, J. (2017). *Plasmodium falciparum* and *Plasmodium vivax* demonstrate contrasting chloroquine resistant reversal phenotypes. *Antimicrob Agents Chemother*, *61*(8), e00355-17. https://doi.org/10.1128/AAC.00355-17

Withers-Martinez, C., Strath, M., Hackett, F., Haire, L. F., Howell, S. A., Walker, P. A., … Blackman, M. J. (2014). The malaria parasite egress protease SUB1 is a calcium-dependent redox switch subtilisin. *Nat Commun*, *5*, 3726. https://doi.org/doi:10.1038/ncomms4726

Witkowski, T. X. (2011). Intellectual property and other legal aspects of drug repurposing, *8*(3–4), 139–43. https://doi.org/10.1016/j.ddstr.2011.06.007

Wu, J., Shan, F., Wu, G., Li, Y., Ding, J., & Xiao, D. (2001). Synthesis and cytotoxicity of artemisinin derivatives containing cyanoarylmethyl group. *Eur J Med Chem*, *36*(5), 469–79.

Ye, Z., & Van Dyke, K. (1994). Reversal of chloroquine resistance in falciparum malaria by some calcium channel inhibitors and optical isomers is independent of calcium channel blockade. *Drug Chem Toxicol*, *17*(2), 149–62.

Ye, Z., Van Dyke, K., & Rossan, R. N. (2013). Effective treatment with a tetrandrine/chloroquine combination for chloroquine-resistant falciparum malaria in *Aotus* monkeys. *Malar J*, *12*, 117. https://doi.org/10.1186/1475-2875-12-117

Yeh, P. J., Hegreness, M. J., Aiden, A. P., & Kishony, R. (2009). Drug interactions and the evolution of antibiotic resistance. *Nat Rev Microbiol*, *7*(6), 460–6. https://doi.org/10.1038/nrmicro2133.

Yin, N., Ma, W., Pei, J., Ouyang, Q., Tang, C. & Lai, L. (2014). Synergistic and antagonistic drug combinations depend on network topology. *PLoS One, 9*(4), e93960. https://doi.org/10.1371/journal.pone.0093960.

Yu, G., Baeder, D. Y., Regoes, R. R., & Rolff, J. (2015). Combination effects of antimicrobial peptides. *Antimicrob Agents Chemother*, *60*(3), 1717–24. https://doi.org/10.1128/AAC.02434-15

Yuan, R., & Lin, Y. (2000). Traditional Chinese medicine: an approach to scientific proof and clinical validation. *Pharmacol Ther*, *86*(2), 191–8.

Yuthavong, Y. (2002). Basis for antifolate action and resistance in malaria. *Microbes Infect*, *4*(2), 175–82.

Zhang, K., Yang, B., & Li, B. (2014). Translational toxicology and rescue strategies of the hERG channel dysfunction: biochemical and molecular mechanistic aspects. *Acta Pharmacol Sin*, *35*(12), 1473–84. https://doi.org/10.1038/aps.2014.101

Zhang, C. J., Wang, J., Zhang, J., Lee, Y. M., Feng, G., Lim, T. K., … Liu, B. (2016). Mechanism-guided design and synthesis of a mitochondria-targeting artemisinin analogue with enhanced anticancer activity. *Angew Chem Int Ed Engl*, *55*(44), 13770–4. https://doi.org/10.1002/ange.201607303

Zhao, Y., Kappes, B., Yang, J., & Franklin, R. M. (1992). Molecular cloning, stage-specific expression and cellular distribution of a putative protein kinase from *Plasmodium falciparum*. *Eur J Biochem*, *207*, 305–13. https://doi.org/10.1111/j.1432-1033.1992.tb17051

Zhao, L., Au, J. L. S., & Wientjes, M. G. (2010). Comparison of methods for evaluating drug-drug interaction. *Front Biosci (Elite Ed)*, *1*(2), 241–9. https://doi.org/10.1038/jid.2014.371

Zhou, Y., Li, W., & Xiao, Y. (2016). Profiling of multiple targets of artemisinin activated by hemin in cancer cell proteome. *ACS Chem Biol*, *11*(4), 882–8. https://doi.org/10.1021/acschembio.5b01043

Zhu, S., Zhang, Q., Gudise, C., Meng, L., Wei, L., Smith, E., & Kong, Y. (2007). Synthesis and evaluation of naphthyridine compounds as antimalarial agents. *Bioorg Med Chem Lett*, *17*(22), 6101–6. https://doi.org/10.1016/j.bmcl.2007.09.044

Zimmermann, G. R., Lehár, J., & Keith, C. T. (2007). Multi-target therapeutics: when the whole is greater than the sum of the parts. *Drug Discov Today*, *12*(1–2), 34–42. https://doi.org/10.1016/j.drudis.2006.11.008

Zipprer, E. M., Neggers, M., Kushwaha, A., Rayavara, K., & Desai, S. A. (2014). A kinetic fluorescence assay reveals unusual features of Ca^{++} uptake in *Plasmodium falciparum*-infected erythrocytes. *Malar J*, *13*(1), 184. https://doi.org/10.1186/1475-2875-13-184